DETERMINATION OF GAS EFFECTIVE DIFFUSIVITIES IN POROUS SOLIDS, DISPERSION COEFFICIENTS IN PACKED BEDS AND MOLECULAR DIFFUSIVITY OF BINARY SYSTEMS

by

Brian Richard Davis

D.L.C., Loughborough College, 1956
M.A.Sc., University of British Columbia, 1963

A Thesis Submitted In Partial Fulfilment of
The Requirements For the Degree Of

Doctor of Philosophy

in the Department

of

Chemical Engineering

We accept this Thesis as conforming to the

required standard

THE UNIVERSITY OF BRITISH COLUMBIA

December, 1965

In presenting this thesis in partial fulfilment of the requirements for an advanced degree at the University of British Columbia, I agree that the Library shall make it freely available for reference and study. I further agree that permission for extensive copying of this thesis for scholarly purposes may be granted by the Head of my Department or by his representatives. It is understood that copying or publication of this thesis for financial gain shall not be allowed without my written permission.

Department of Chemical Engineering

The University of British Columbia
Vancouver 8, Canada

Date 4/January/1966

The University of British Columbia

FACULTY OF GRADUATE STUDIES

PROGRAMME OF THE

FINAL ORAL EXAMINATION

FOR THE DEGREE OF

DOCTOR OF PHILOSOPHY

of

BRIAN RICHARD DAVIS

Diploma, Loughborough College of Advanced Technology, UK. 1956

M.A.Sc., The University of British Columbia, 1962

December 21, 1965 AT 10:00 A.M.

IN ROOM 207, CHEMICAL ENGINEERING

COMMITTEE IN CHARGE

Chairman: I. McT. Cowan

R. M. R. Branion
S. D. Cavers
N. Epstein
J. Lielmezs
K. L. Pinder
D. A. Ratkowsky
J.R.Sams

External Examiner: G. L. Osberg
National Research Council
Ottawa

Research Supervisor: D. S. Scott

ABSTRACT

SECTION I

AN EXPERIMENTAL METHOD FOR THE MEASUREMENT OF EFFECTIVE GAS DIFFUSIVITIES IN POROUS PELLETS, AND THE LONGITUDINAL DISPERSION COEFFICIENT IN PACKED BEDS

Present methods of measurement of effective diffusivities are not generally adaptable to the pellets in a packed bed, for example a catalytic reactor. An unsteady state pulse method has been developed employing simple gas chromatographic rate theory.

The method is generally applicable to pellet sizes down to about 2mm. With homogeneous pellets reasonable agreement was obtained on comparison of effective diffusivities measured by a steady state method. For anisotropic solids the unsteady state diffusivity can be quite different from the steady state value due to differences in diffusion path.

Pulse dispersions measured in beds of non porous pellets have revealed a laminar flow regime where the dispersion coefficient is dependent on the square of the velocity. This regime was reported for flow in straight pipes but has not previously been demonstrated in packed beds.

SECTION II

DEVELOPMENT OF AN UNSTEADY STATE FLOW METHOD FOR MEASURING BINARY GAS DIFFUSION COEFFICIENTS

Effusion measurements of one gas from a packed bed of known geometry (porosity and tortuosity) into a second flowing gas have been evaluated as a versatile technique for the determination of binary gas diffusion coefficients.

The molecular diffusivities measured ($\pm$ 10%) approached the scatter encountered by other methods ($\pm$ 5%) and satisfactory results ($\pm$ 3%) are envisaged by optimising parameters in the method.

GRADUATE STUDIES

Field of Study: Diffusion and Kinetics

Chemical Engineering Reactor Design	D. S. Scott
Industrial Kinetics and Catalysis	D. S. Scott
Mass, Heat and Momentum Transfer	S. D. Cavers
Chemical Kinetics	E. A. Ogryzlo D. G. L. James
Gas Adsorption and Solvent Extraction	D. S. Scott S. D. Cavers

Other Studies

Chemical Engineering Thermodynamics	P. L. Silveston
Analogue Computers	E. V. Bohn
Mathematical Operations in Chemical Engineering	N. Epstein
Fortran Programming	H. Dempster
Differential Equations	S. A. Jennings
Industrial Relations	N. A. Hall
Industrial Organisation	J. P. Van Gigch

PUBLICATIONS

DAVIS, B. R. and D. S. SCOTT, 1964.
Rate of isomerisation of cyclopropane in a flow reactor.
Ind. & Eng. Chem. Fundementals, 3, 20-23.

ABSTRACT

SECTION I

AN EXPERIMENTAL METHOD FOR THE MEASUREMENT OF EFFECTIVE GAS DIFFUSIVITIES IN POROUS PELLETS, AND THE LOGITUDINAL DISPERSION COEFFICIENT IN PACKED BEDS

Present methods for measuring effective diffusivities in small porous particles are not applicable to assemblages of such pellets, for example, as in catalytic reactors, and require special techniques or apparatus. A pulse technique has been developed which can successfully yield a reasonable value of the diffusivity by analysis of pulse dispersion in terms of simple chromatographic rate theory. A non-adsorbing pulse gas is necessary, and hydrogen is nearly ideal. Because of the high molecular diffusivity of hydrogen the smallest size of particle which can be tested with this gas is about 2 mm diameter. The unsteady state pulse effective diffusivity measurement which should be more realistic for catalytic studies was compared with a conventional steady state method and good agreement obtained in a spherical isotropic pellet (4%); however, as may be expected agreement was poor with anisotropic pellets.

A regime was found in a study of beds of non porous pellets where the dispersion coefficient is proportional to the square of the velocity. This regime is reported for pipes but has not been realized as a separate regime in packed beds. This dispersion data is compared with the limited data of other workers although the ranges of experimental conditions do not overlap.

SECTION II

DEVELOPMENT OF AN UNSTEADY STATE FLOW METHOD FOR MEASURING BINARY GAS DIFFUSION COEFFICIENTS

Effusion of one gas from a packed bed of known geometry into a second flowing gas has been evaluated as a versatile technique for determination of binary gas diffusion coefficients having few limitations of pressure, temperature and analysis method. Optimization of experimental parameters should yield satisfactory results (± 3%).

SECTION 1

EXPERIMENTAL MEASUREMENT OF EFFECTIVE GAS DIFFUSIVITIES IN POROUS PELLETS AND DISPERSION COEFFICIENTS IN PACKED BEDS

SECTION II

DEVELOPMENT OF AN UNSTEADY STATE FLOW METHOD FOR MEASURING BINARY GAS DIFFUSION COEFFICIENTS

TABLES

SECTION I

SECTION II

APPENDICES

FIGURES

SECTION I

SECTION II

APPENDIX I

ACKNOWLEDGEMENT

Thanks are extended to Dr. Forsythe and the faculty and staff of the University of British Columbia, chemical engineering department. Particularly the author wishes to thank Dr. Epstein for his help in Dr. Scott's absence and Mr. E. R. Rudischer and Mr. J. Baranowski for their assistance and co-operation.

The author is indebted to Dr. Scott for his direction and support and is grateful for financial assistance extended by the National Research Council.

INTRODUCTION

A. THIELE MODULUS

The rate of reaction in a porous solid catalyst can be limited by the rate at which reactants and products can diffuse in and out of the solid. Thiele (1) quantitatively described this effect with a mathematical treatment which is applied to a simple case of an infinite slab in the derivation below. In Fig. 1.1 a single pore of radius r and length L is shown. A first order gas phase reaction with rate = k C_A moles/(sec)(cm^2) is assumed to be taking place isothermally on the pore walls, and a constant concentration C_{AO} moles/cm^3 is maintained at each face of the slab at the pore mouth. A material balance around the element dx yields,

$$-D \frac{dC_A}{dx} \pi r^2 - (-D)\left[\frac{dC_A}{dx} + \frac{d_2C_A}{dx^2} \delta x \right]\pi r^2 - kC_A \; 2\pi r \; \delta x = 0 \qquad (1.1)$$

which may be simplified to,

$$\frac{d_2C_A}{dx^2} = \frac{2k}{rD} C_A \qquad (1.2)$$

The boundary conditions, $C_A = C_{AO}$ at x = 0, and $dC_A/dx = 0$ when x = L, may be applied to the solution of (1.2) to give the concentration in the pore,

$$C_A = C_{AO} \frac{\cosh\left[h\left(1 - \frac{x}{L}\right)\right]}{\cosh h} \qquad (1.3)$$

where $h = L\sqrt{\frac{2k}{Dr}}$, commonly known as the Thiele modulus.

The rate of reaction is given by the rate of diffusion of A into the pore mouth, which in turn is given by,

$$\text{rate/pore} = -D \left(\frac{dC_A}{dx} \right)_{x=0} \pi r^2 \qquad (1.4)$$

$$= \frac{D\, C_{AO}}{L} h \tanh (h) \; \pi r^2$$

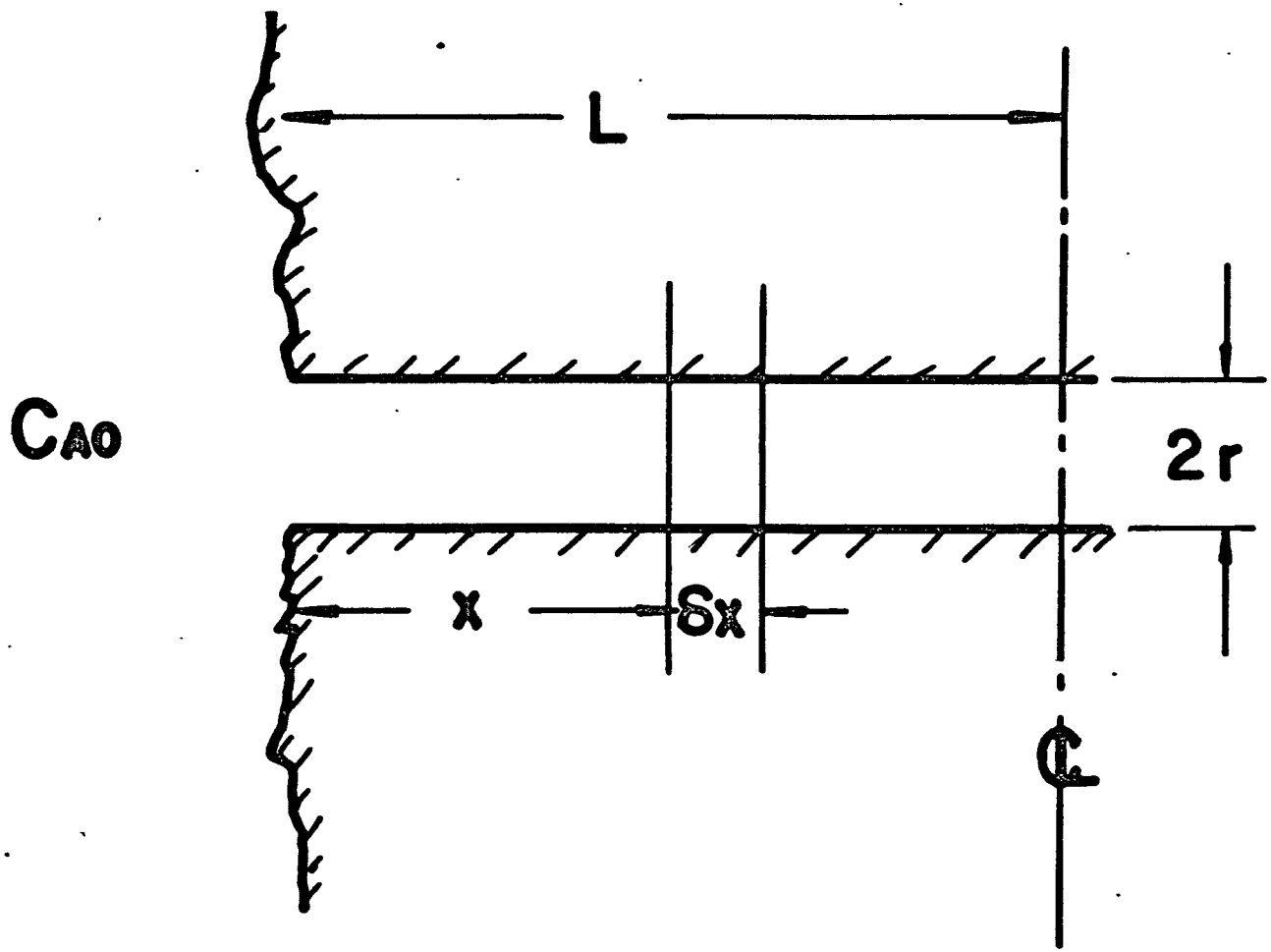

Figure 1.1

Pore Model For Derivation Of Effectiveness Factor

If the whole pore contains gas at the surface concentration, C_{AO}, the rate of reaction will be a maximum, given by $k.C_{AO} \cdot 2\pi rL$ moles/sec. The ratio of the rate given by equation (1.4) and this maximum rate is defined as the effectiveness factor, E.

$$\frac{\text{rate/pore}}{\text{maximum rate}} = E = \frac{rD}{2kL^2} \quad h \quad \tanh \quad h = \frac{\tanh \quad h}{h} \tag{1.5}$$

The effectiveness factor is a function of the Thiele modulus only, and can be used to calculate the rate of reaction when diffusional resistances are controlling.

$$\text{rate of reaction/pore} = k\ C_{AO}\ 2\pi r\ L\ E \tag{1.6}$$

Additional equations can be derived for other orders of reaction, (2) other assumed pore geometries (3), or for cases where the stoichiometry does not allow equimolar counter diffusion to occur (1)(4).

In practical cases it is very difficult to define accurately the pore geometry of a porous solid, and rate constants are more commonly based upon unit mass of catalyst. It is convenient mathematically to treat the porous solid as a homogeneous medium having an effective diffusivity, rather than attempting to use the true interstitial diffusivity together with the void fraction and suitable assumptions about the pore geometry.

B. DIFFUSION MECHANISMS

There are two basic gas transport processes which occur in porous solids, and which obey Fick's laws of diffusion, namely, molecular or bulk diffusion which occurs through intermolecular collisions, and Knudsen diffusion, which depends only upon wall collisions. In addition, a phenomenon known as "surface diffusion" can take place, but this is not a well understood process. Surface diffusion is believed to result from multilayers of gas molecules condensed to a liquid-like state, which flow from the areas with several layers to those of lower surface concentration. This process results in diffusion rates much larger than those possible by collision mechanisms.

Gases above their critical temperature are less likely to display this phenomenon, because of the reduction in surface adsorption under these conditions.

Molecular Diffusion in Pores

This mode of diffusion predominates when the ratio of the pore radius to mean free path is greater than about 10. Fick's law, or the one dimensional flux equation for steady-state molecular diffusion in a two component mixture takes the form,

$$N_A = - D_B \frac{d\ C_A}{dx} + (N_A + N_B) \frac{C_A}{\rho_m} \tag{1.7}$$

where the last term accounts for bulk flows which may be caused by non-equimolar counter diffusion rates of the two gases with respect to stationary coordinates. In order to apply the equation to a porous structure the flux is taken per total unit area of solid and pore, rather than unit area of pore only,

$$N_A{}^1 = N_A \epsilon_p = - \left[\frac{D_B \epsilon_p}{\lambda}\right] \frac{dC_A}{dx} + (N_A{}^1 + N_B{}^1) \frac{C_A}{\rho_m} \tag{1.8}$$

where λ is the "tortuosity" which corrects for the fact that the pore length is greater than the geometric length of the structure. The terms which are grouped with the diffusivity form the definition of an "effective diffusivity" which will be discussed later.

Fick's second law which describes the unsteady state diffusion process is usually expressed as,

$$\frac{\partial C_A}{\partial t} = D_B \frac{\partial 2\ C_A}{\partial x^2} \tag{1.9}$$

In a porous solid, introducing the concept of an effective diffusivity, this equation should be modified as shown below:

In unit area of a porous infinite slab, a mass balance over the element δx when no chemical reaction is occurring and allowing for a net bulk flow gives the rate of change of gas content in terms of the effective diffusivity, D_E, as,

$$\epsilon_P \frac{\partial C_A}{\partial t} \delta x = + D_E \left(\frac{\partial_2 C_A}{\partial x^2} \right) \delta x - \frac{\partial (u C_A)}{\partial x} \delta x \qquad (1.10)$$

where u is the superficial bulk velocity.

Simplication of 1.10 gives,

$$\frac{\partial C_A}{\partial t} = + \frac{D_E}{\epsilon_P} \frac{\partial_2 C_A}{\partial x^2} - \frac{1}{\epsilon_P} \frac{\partial (u C_A)}{\partial x} \qquad (1.11)$$

For equimolal counter diffusion, this reduces to the usual form of Fick's second law, that is, equation (1.9) except that the molecular diffusion coefficient is replaced by the effective diffusion coefficient divided by the porosity.

If equimolar counterdiffusion occurs then equation (1.8) for the steady state reduces to

$$N_A^1 = - D_E \frac{d C_A}{dx} \qquad (1.12)$$

The binary molecular diffusion coefficient of a gas is proportional to the absolute temperature to about the 1.7 power, and inversely proportional to the pressure.

Knudsen Diffusion

This mechanism predominates when the mean free path of the gas molecules is greater than the pore radius, and because wall collisions contribute primarily to the process in these circumstances, the diffusion coefficient is independent of the presence of other gases. Bulk flow is not distinguishable from diffusion in this case, and so Fick's law in the form of equation (1.12) applies.

The Knudsen diffusion coefficient in cylindrical straight pores is given by,

$$D_K = 2/3\ r\ \bar{v} \tag{1.13}$$

where $\bar{v}$ is the average velocity of the gas molecules, and r the pore radius. In consequence, the value of this coefficient is independent of pressure, and proportional to the square root of the temperature.

Intermediate or Mixed Diffusion Coefficient

In the intermediate range between molecular and Knudsen diffusion there is a region where both the above diffusion mechanisms occur. The ratio of pore radius to mean free path lies approximately between the following limits in the intermediate zone:

Knudsen		Intermediate		Molecular
0.1	$<$	$\frac{r}{\bar{\lambda}}$	$<$	10

By assuming round capillaries, rigid sphere kinetics and diffuse molecular reflection from the walls, Scott and Dullien (5) derived the following relationship for the flux in a binary gas mixture in the intermediate region.

$$N_A = -\frac{P}{RT}\frac{dy_A}{dx}\left[\frac{1}{\frac{1 - jy_A}{D_B} + \frac{1}{D_{KA}}}\right] \tag{1.14}$$

where $j = 1 + N_A/N_B$, and y_A is the mole fraction of A.

If the term in brackets is considered as the diffusion coefficient, it is obvious that in this region the coefficient is dependent upon the concentration and flux. A diffusion coefficient defined by an equation of the form of (1.12) and measured in this region is not valid for use in the Thiele modulus as defined previously, as the stoichiometry of the chemical reaction imposes a flux ratio which is unlikely to be the same as the flux ratio obtained in an independent non-reactive determination.

Effective Diffusion Coefficient

An effective diffusion coefficient is defined in equation (1.8) for molecular diffusion where two factors are used to modify the true or interstitial diffusivity. The porosity, or void fraction, is a fairly easily defined and measured absolute quantity, and in a granular bed may be of the range of 0.3 to 0.5. However, the tortuosity is a derived quantity, and is therefore usually a less well-defined property, especially in non-uniform pore structures. Although a value of around 1.5 might be expected from simple pore models, it can vary from 1 to 100 when calculated from experimental results. Thus, a typical simple structure may have an effective diffusivity about 4 times less than the interstitial value.

The large range of tortuosity values can be attributed to two sources. First, the pores are not necessarily open-ended and so the mass transfer may be only occurring in a limited number of passages. Second, the pore radius is liable to vary along the length of the pore, and it has been shown (6) (7) that the rate of diffusion is smaller through a pore of varying radius than it is through a cylindrical pore of equivalent volume to surface ratio.

The effective diffusivity can serve as a simple correction to the diffusion mechanism so that the diffusion equation describes the transport behaviour in a uniform porous structure. On the other hand, porous structures can be so haphazard that any of the mechanisms described may occur at the same time in series or in parallel in the same solid. The use of an effective diffusivity in this case amounts to forcing the behaviour observed to fit one of the diffusion equations, and so the result cannot be used to predict the diffusive behaviour under other conditions.

C. EXPERIMENTAL ESTIMATION OF THE EFFECTIVE DIFFUSIVITY

Prediction

The basis for the prediction of the effective diffusivity has been briefly outlined in the previous paragraph, and clearly rests on some physical idealization of the pore structure. Prediction methods based upon porosity and experimental tortuosity values are often not too satisfactory due to the non-uniform nature of many porous solids. However, a variety of catalyst pellets can be approximated by the "pile of bricks" structure which yields a model consisting of a honeycomb of connected passages. This approach has been described in detail by Wheeler (2), with rules for predicting the effective diffusion coefficient defined by this model.

Other simple pore models include unconnected parallel cylindrical pores (8) (9), and pores with "ink bottle" capacities (10) which are used to explain the hysteresis in certain adsorption-desorption curves.

Possibly of more general application to the problems involved in catalytic kinetics is the bidisperse pore structure model proposed by Wakao and Smith (11) and Mingle and Smith (12). In the latter paper, a concept of larger macro pores in series with micro pores is used. In the former, three parallel mechanisms are considered; first, diffusion through the macro pores between the basic particles from which the pellet is pressed, second, diffusion in the micro pores of the basic particle, and finally, series diffusion from micropores to macro pores or vice versa. The model does not require empirical constants, or assumptions regarding the mode of diffusion in any of the pores, but porosities and a pore size frequency distribution function are required in addition to tortuosity values.

Steady State Experimental Method for Measurement of Diffusion in Solids

In this method, a cylindrical catalyst pellet is fitted into a tube and two test gases of known composition are passed continuously across the ends. The two exit streams are analyzed, and from an appropriate solution of the diffusion equation the effective diffusivity can be computed (13) (5).

This method has also been used to obtain molecular diffusivities (14), because calibration of the porous pellet by a gas pair of known diffusivity allows calculation of the diffusivities of other gas pairs by making the assumption that the tortuosity is independent of the gas system. As a technique for measuring molecular diffusivities it has the advantage that it is a flow method, and so analysis in situ is not required. On the other hand, care must be taken that a narrow pore size distribution exists and that Knudsen diffusion does not occur.

When used as a method for measuring the effective diffusivity in porous pellets one must be sure that the correct diffusion equation has been used (e.g. eqn. (1.8) or (1.12)). The method can be applied to the mixed diffusion range if measurements are made at varying total pressures. However, it has the limitation of being tedious if a representative average value is needed, because each pellet must be tested separately, and cracks and fissures have an overwhelming influence on the result. The technique is not convenient for use with other than cylindrical shapes, and therefore other shapes must be machined to cylinders. If the pellet is not isotropic, this procedure may result in a faulty value of the diffusion coefficient.

The result obtained by the steady state method in a bidisperse pellet weighs the diffusivity in favour of the larger pores, but in the chemical reaction case most of the conversion takes place in the micro pores. This bias is frequently not serious as the micropores are generally short, and so a micropore effectiveness factor of unity is common (11). Hence, the diffusional resistance to reaction is in the macropores, and the steady state effective diffusivity value may be quite adequate.

Chemical Reaction Method

It is obviously possible to carry out a chemical reaction of known kinetic behaviour at constant conditions using successively smaller sizes of pellet until the reaction rate becomes constant, indicating that an effectiveness factor of unity has been reached. From these effectiveness factors the Thiele modulus, and hence effective diffusion coefficients, can be calculated providing the kinetic behaviour is not complex. This method is not easy to apply experimentally, and is subject to many errors.

Unsteady State Methods

A typical procedure for measuring the molecular diffusivity of a gas (Loschmidt method) consists of flushing two cylinders with the test gases, and then bringing them together at time zero with the lighter gas on top. One or both of the cylinders is removed at a given time, and the total contents analyzed. The diffusion coefficient is then calculated from the solution derived from Fick's second law (equation (1.9)). It is difficult to achieve accuracy in this experiment due to the tendency for eddies to be created either when the cylinders are fitted together or by the action of temperature gradients.

For porous pellets the analog of the above experiment cannot be readily applied due to the rapidity of the diffusion process in gases. For example, if a one cm. diameter pellet of typical pore structure is initially bathed in one gas, and at time zero the surface is flushed with another gas, then 98.8% of the first gas in the pellet is removed by diffusion in 10 seconds if the diffusivity D_E/E_P is 0.01 cm^2/sec. (See Appendix III for details of this calculation.) Thus, it is obvious that some means to extend the time scale in experiments with small pellets would be very desirable.

Currie (6) has developed a non-flow apparatus of this type which can be used only at normal temperatures and pressures for measuring diffusivities in soils and other granular beds. Only rather complex frequency response techniques, discussed below, are presently available for the measurement of effective diffusion coefficients by transient response methods.

Frequency Response and Pulse Methods

McHenry and Wilhelm (15) have described a method for measuring the eddy diffusivity in packed beds, and this apparatus has been used also by Deissler and Wilhelm (16) to measure both the effective diffusivity and the eddy diffusivity in packed beds. The method is based on frequency response techniques using a concentration sine wave generated in the feed to the bed, with amplitudes and phase angles recorded at the entrance and exit of a test section.

In the same way, Van Deemter, Zuiderweg and Klinkenberg (17) have applied the delta function (that is, an ideal pulse) to packed beds in the form of gas chromatography columns and ion exchange beds. Hougen (18)

has pointed out that there is no real difference between the results obtained by a delta function or by a frequency response method.

In the work of Van Deemter et al the dispersion effects due to molecular diffusivity, eddy diffusivity and a mass transfer coefficient are each found, on the basis of the theory developed, to have a different velocity dependence, which allows separation of the influence of each factor on the delta function. The mass transfer coefficient can be derived in terms of the effective diffusivity of the porous pellet, and hence, if this quantity can be evaluated, an effective diffusion coefficient may be calculated from it. The theory on which this approached is based is dealt with more fully in succeeding sections.

Comparison of Various Methods

In porous solids there is a basic difference between the application of diffusion coefficients to the steady state and the unsteady state. This difference is the result of the capacitance effects which manifest themselves in the unsteady state. In other words, the time of diffusion from a porous solid containing dead end pores would be much greater than the effective diffusivity measured by a steady state method would indicate. This effect is allowed for in equation (1.11) because instead of the effective diffusivity alone, the effective diffusivity divided by a capacitance term (the porosity) is utilized. Similarly, if adsorption occurs on the surface of the solid then the volume of gas adsorbed must be added to the porous volume or porosity in the divisor. (This last statement regarding adsorption assumes that the adsorption process is effectively at equilibrium and that the isotherm is linear, otherwise the simple diffusion equation would no longer hold.) With the correct diffusion equation, there should be no

basic difference between effective diffusivity in an isotropic solid determined by a steady state or unsteady state method.

If bulk diffusion is the transport mechanism there is no difficulty in correctly defining the effective coefficient for either the steady state or unsteady state methods. However, this is not true when Knudsen diffusion predominates. Consider a simple model of dead end pores of equal length in parallel in which Knudsen diffusion is taking place. The total composition of each pore (after a step change in surface concentration) will vary according to its radius. Initially, the large pores will yield the major flux, but after a time the lower flux in the smaller pores will result in larger concentration gradients, which will eventually result in the flux from the smaller pores equalling or exceeding that from the larger pores. Hence, an unsteady state experiment in the Knudsen regime may yield a diffusivity which varies with time.

An interesting aspect of this latter conclusion arises because the majority of a solid-surface catalyzed chemical reaction occurs in the smaller pores (due to the large surface area), and if these pores are long then they may not be fully effective. The steady state method is insensitive to the resistance which may occur in dead end pores, while the unsteady state method is potentially capable of allowing for this resistance. The unsteady state method will give a diffusivity which is some average value of all pore resistances, and the ability of this value to describe the rate of a diffusion limited chemical reaction may depend upon the weighting by the experimental procedure or the experimenter. For example, most unsteady state methods involve an initial period before readings are taken in order to allow the application to the data of simple solutions of the diffusion equation applicable at longer times. Thus, in this case, the

diffusivity obtained from such experiments may be expected to be weighted in favour of the small pores if Knudsen diffusion predominates.

D. OBJECTIVES OF THE PRESENT WORK

On the basis of the foregoing comparison of methods for obtaining a value of the effective diffusivity, it is apparent that, in most cases, a diffusion coefficient obtained from an unsteady-state experiment in which all the pores contribute to the diffusional process may well be a better value for use in chemically reacting systems. In many instances, steady-state experiments may also give suitable values, but this cannot be assumed without considerable knowledge of the particular porous structure.

It would be useful to develop a method using a pulse technique, which would avoid most of the experimental difficulties of frequency-response measurements, while giving the advantages of an unsteady-state method and which could be applied to a representative sample of pellets without requiring special shaping. It might be possible to make use of such a technique to follow changes in catalyst diffusional behaviour with age. Recent advances in the theory of transport processes in chromatographic columns suggest that it might be possible to interpret pulse dispersion results in such a way as to yield an effective diffusion coefficient.

The primary objective of the present work was to attempt the development of a pulse method as a means of measuring effective diffusivities of gases in porous pellets, a technique not previously reported. A secondary objective was to be the investigation of the use of unsteady state flow methods for measuring the binary diffusion coefficient of gases. The flow methods possess the advantage of allowing analysis outside the apparatus, by any convenient means. Further, the use of a porous bed of unit tortuosity would also allow such a measurement to give absolute values of the

diffusion coefficient without any calibration being necessary. Freedom from convective effects would aid in making possible measurements at widely varying temperatures and pressures, as does the freedom in choice of concentration measurement.

II

THEORY

A. DERIVATION OF VAN DEEMTER EQUATION

Height Equivalent to a Theoretical Plate

The performance of a chromatograph column is generally measured in terms of a "height equivalent to a theoretical plate" (HETP). In a gas chromatograph column a narrow band of sample gas is injected into a stream of carrier gas which passes through the column to a detecting device. The components of the sample have differing retention times in the column depending upon the properties of the gas component and the liquid stationary phase in the column. It is obvious that a column which results in a broadening of the pulse is detrimental to the separation desired, and the height equivalent to a theoretical plate (HETP) which is defined below is a measure of the degree of longitudinal dispersion.

The HETP is obtained by postulating that the mechanism of pulse broadening is caused by equilibration of the stationary material in a given plate with the mobile gas phase which then passes on to the next plate.

A linear absorption isotherm $WC_n = C_{Ln}$ (where C_n = mobile phase concentration, C_{Ln} = stationary phase concentration) is assumed and a material balance around the nth plate (see Figure 1.2) with an increment of gas flow dU yields,

$$dU(C_{n-1} - C_n) = (V + Wv)dC_n \qquad (1.15)$$

from which is obtained,

$$\frac{dC_n}{dU} = \frac{C_{n-1} - C_n}{V + Wv} \qquad (1.16)$$

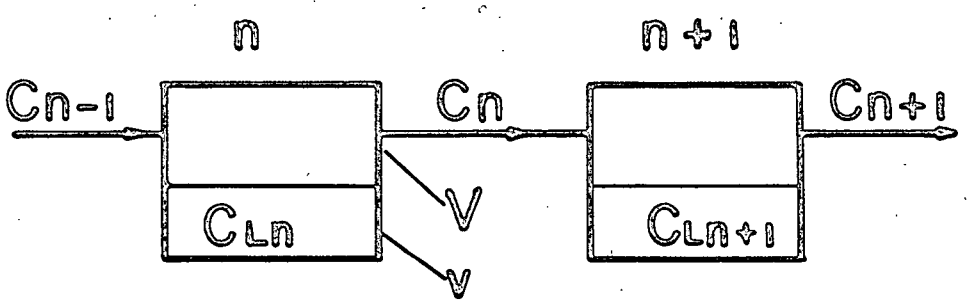

Figure 1.2

Model For Derivation Of Plate Theory

where V = volume of mobile phase in plate and v = volume of plate stationary phase.

Assume that all the pulse gas is initially in stage 1 yielding an initial gas concentration C'. Applying n = 1 to equation (1.16), $C_n = C_1$, and $C_{n-1} = 0$,

$$\frac{-dC_1}{C_1} = \frac{dU}{V_p} \tag{1.17}$$

where V_p = Volume of plate = (V + Wv). On integration, (1.17) gives,

$$C_1 = K \exp\left(-\frac{U}{V_p}\right) \tag{1.18}$$

When $U = 0$, $C_1 = C'$, and therefore $K = C'$ in (1.18). Hence,

$$C_1 = C' \exp\left(- \frac{U}{V_p} \right) \tag{1.19}$$

Now applying the above result to equation (1.16) with $n = 2$,

$$\frac{dC_2}{dU} + \frac{C_2}{V_p} = \frac{C'}{V_p} \exp\left(- \frac{U}{V_p} \right) \tag{1.20}$$

Equation (1.20) can be solved by use of the integrating factor, $\exp\left(+ \frac{U}{V_p} \right)$

$$C_2 \exp\left(\frac{U}{V} \right) = \frac{C'}{V_p} \exp - \frac{U}{V_p} + \frac{U}{V_p} \, dU = C' \frac{U}{V_p} + K \tag{1.21}$$

When $U = 0$, $C_2 = 0$, and so $K = 0$, yielding the result,

$$C_2 = C' \frac{U}{V_p} \exp\left(- \frac{U}{V_p} \right) \tag{1.22}$$

Hence by continuing this process to the nth stage

$$C_n = \frac{C' \, U^{n-1}}{(n-1)! \, V_p^{n-1}} \exp\left(- \frac{U}{V_p} \right) \tag{1.23}$$

This is a Poisson distribution function, and for a large number of plates this distribution approaches a Gaussian or normal distribution. The mean of the above distribution is $\frac{U}{V_p}$ and the variance is $\frac{U}{V_p}$ (that is, $\sigma = \sqrt{\frac{U}{V_p}}$ so that the $(\text{Mean})^2/(\text{standard deviation})^2 = \left(\frac{U}{V_p}\right)^2 / \frac{U}{V_p} = \frac{U}{V_p}$

Now U is the total volume of gas which has flowed, and V_p is the volume of a theoretical plate, so that when the mean approaches the end of the column the $(\text{mean})^2/\sigma^2$ = no. of theoretical plates.

By definition, therefore,

$$\text{HETP} = L \left(\frac{\sigma}{\text{mean}} \right)^2 \tag{1.24}$$

where L is the column length.

Measurement of HETP

For a large number of stages the output can be assumed to be a Gaussian distribution, and the mean and variance may be read directly from the record of the output at the end of the column by using the properties of the Gaussian distribution shown in Figure1.3. This representation is not strictly correct, in that the output is Gaussian with respect to position in the column, while the recorded profile at the end of a column is with respect to time. However, if the time of purge of the pulse is small relative to the time of the mean, the error in reading this time distribution compared to the distance distribution is negligible.

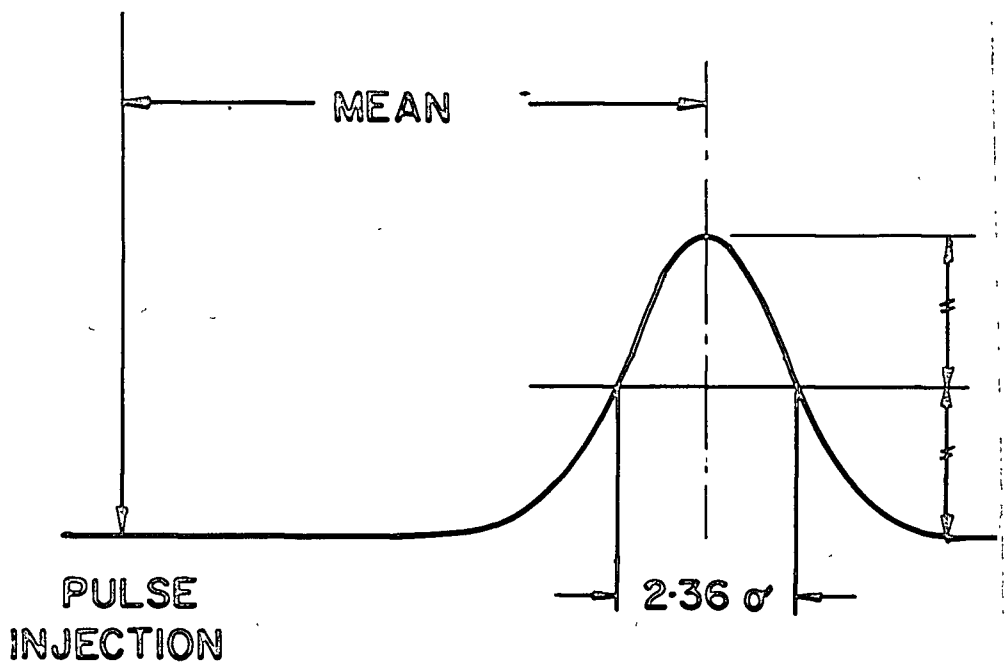

Figure 1.3

Gaussian Distribution Properties

Inasmuch as 90% of a normal distribution lies between 4σ limits, then the time of purge which is approximately 4 σ, must be ≪ mean to achieve a Gaussian distribution. If now both sides of this inequality are squared and multiplied by L, on rearranging

$$\frac{16\ L\sigma^2}{\text{mean}^2} \ll L \quad \text{or} \quad L \gg 16\ \text{HETP}$$

Hence, a column must contain much more than 16 plates to satisfy an assumption of a Gaussian distribution in the output record.

Input Pulse Distribution

The derivation of the HETP assumed that all the pulse is in the first stage at the start, however, it is obvious that if the pulse extended over several stages an effect would be noticed in the output. It has been shown by Van Deemter (17) that the effect of the initial distribution can be ignored if,

$$\frac{A_s}{V_p\sqrt{n}} < 0.5 \qquad (1.25)$$

where A_s is the volume of gas in the initial pulse and n is the number of theoretical plates.

Rate Theory

The theoretical plate model does not attempt to explain the rate processes occurring in a chromatograph column, but relies on the fact that the sum of several distributions tend to approach a normal Gaussian distribution, having a mean made up of the sum of the independent means, and having a variance made up of the sum of the independent variances (19).

One obvious mechanism which occurs to cause a pulse to broaden is molecular diffusion in the mobile phase. Longitudinal diffusion in the

stationary phase can generally be ignored as the stationary phase is discontinuous in a packed bed, and, in addition, the diffusion coefficient is small in this phase.

There is a group of little understood processes which cause a pulse to disperse due to the flow pattern in the packed bed. Fortunately, in a deep bed these aberrations are of a statistical nature which tend to result in a Gaussian distribution as obtained for molecular diffusion, so that they can be grouped together in a term described as the eddy diffusivity. In the work of Van Deemter et al (17) the eddy diffusivity (below a particle Reynolds number of 1) is considered to be caused by the difference in flow paths between particles. These concepts are discussed in the following sections.

A pulse broadening mechanism analogous to the theoretical plate mechanism described earlier can also occur in the chromatograph column. If a resistance exists preventing equilibrium between the mobile and stationary phase, then the degree of pulse broadening caused by the capacitance of the stationary phase is increased due to the fact that although less material enters the stationary phase the time taken to get out again causes the pulse to broaden more than would be the case for the equilibrium situation.

Lapidus and Amundson (2) have derived an expression based on a diffusion model to describe the concentration profile for the conditions where a pulse gas passes through a packed bed containing a stationary phase with a linear absorption isotherm between the gas and stationary phase. The pulse is not assumed to be in equilibrium with the stationary phase, due to a resistance defined by a mass transfer coefficient, α. Longitudinal diffusion including molecular and eddy contributions is

characterized by a dispersion coefficient, D_L, and is assumed to occur in the mobile phase, but not in the stationary phase. The model is shown in Figure 1.4.

A material balance around the element δx yields

$$F_1 \frac{\partial C_1}{\partial t} = F_2 D_L \frac{\partial_2 C_1}{\partial x^2} - F_1 U \frac{\partial C_1}{\partial x} + \alpha (WC_2 - C_1) \qquad (1.26)$$

$$F_2 \frac{\partial C_2}{\partial t} = \alpha (C_1 - WC_2) \qquad (1.27)$$

Where W is the equilibrium constant between the mobile and stationary phases. If the stationary phase is a porous solid W can be replaced by $\frac{1}{\epsilon_p}$.

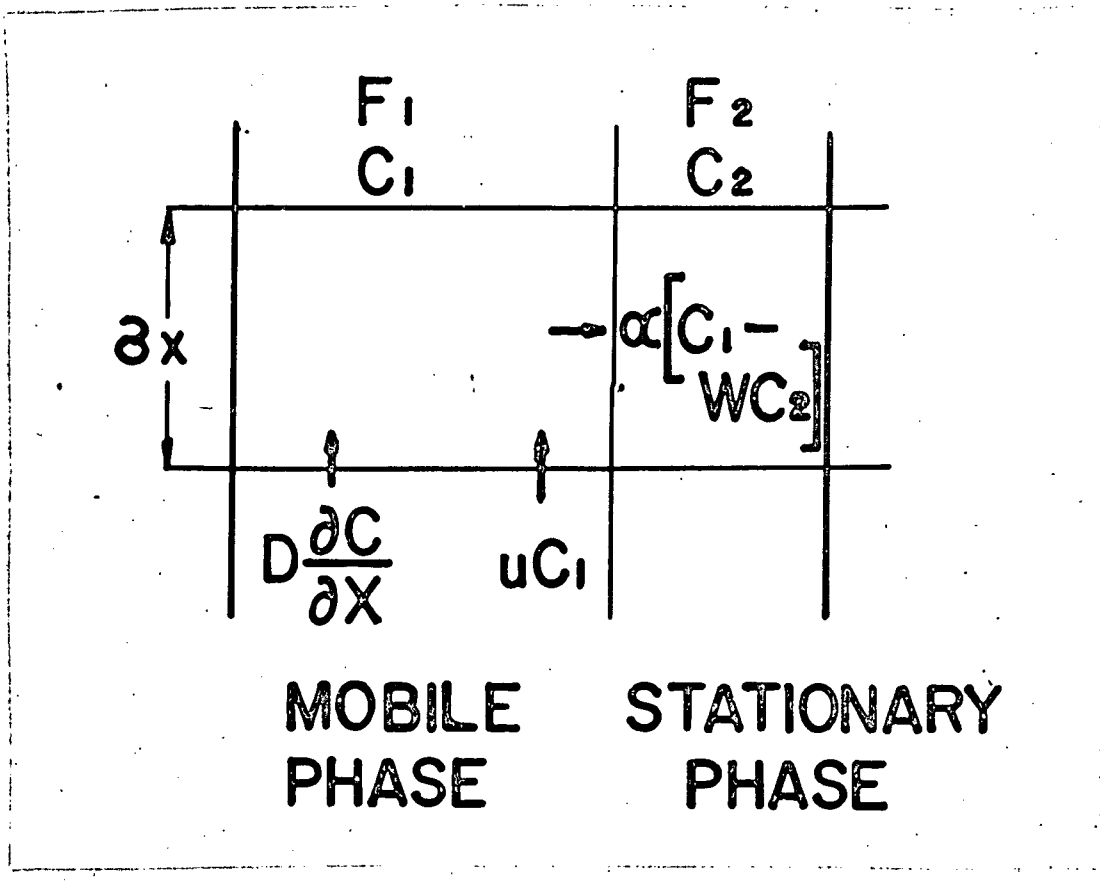

Figure 1.4

Mathematical Model for the Column

For a small pulse injection time, t_o, and an initial pulse concentration C_o, Lapidus and Amundson (20) obtained the following solution to the above equations,

$$\frac{C_1}{C} = \frac{x\, t_o}{2t\sqrt{\pi D_L t}} \exp\left(\frac{-(x - ut)^2}{4 D_L t} - \frac{\alpha t}{F_1} \right) + \int \frac{x\, t_o}{2t^1\sqrt{\pi D_L t^1}} \exp\left(- \frac{(x-ut^1)^2}{4 D_L t^1} \right) X \; F(t^1)\, dt^1 \qquad (1.28)$$

where

$$F(t)^1 = \left(\frac{2\, Wt^1}{F_1 F_2 (t-t^1)} \right)^{1/2} \exp\left(\frac{\alpha W}{F_2} (t - t^1) - \frac{\alpha t^1}{F_1} \right) I_1 \left(2\sqrt{\frac{2\, Wt^1 (t-t^1)}{F_1 F_2}} \right) \qquad (1.29)$$

where t is time, t_o, time of initial pulse with concentration C_o, x is distance along the column, and I_1 is the hyperbolic Bessel function.

It has been shown by Van Deemter et al (17) that the above solution can be reduced to a Gaussian distribution under certain conditions. These conditions are that the height of a transfer unit $\frac{F_1 u}{\alpha} \ll L$, the height of the bed, and the longitudinal mixing stage $\frac{2\, D_L}{u} \ll L$. Essentially, these requirements state that the column must contain a large number of theoretical plates, in which case the concentration profile reduces to,

$$\frac{C_1}{C_o} = \frac{\beta t_o}{\sqrt{2\pi(\sigma_1^2 + \sigma_2^2)}} \exp\left(\frac{L/u - \beta t}{2\,(\sigma_1^2 + \sigma_2^2)} \right)$$

where

$$\frac{1}{\beta} = 1 + \frac{F_2}{F_1} W, \quad \sigma_1^2 = \frac{2\, D_L L}{u^3} \quad \text{and} \quad \sigma_2^2 = \frac{2\, \beta^2 F_2^2 L}{F_1 W^2 u} \qquad (1.30)$$

This is a Gaussian distribution with mean L/u or Bt and variance $\sigma_1^2 + \sigma_2^2$. As mentioned above, the variance of a Gaussian distribution is composed of the sum of the individual variances, so equating the ratio $\frac{\sigma^2}{\text{mean}^2}$ for the above solution yields the following which can be combined with the HETP derivation of equation (1.24).

$$\frac{\sigma_1^2 + \sigma_2^2}{(L/u)^2} = \frac{2\,D_L L}{u^3}\left(\frac{u^2}{L^2}\right) + \left(\frac{1}{1 + \frac{F_2}{F_1 W}}\right)^2 \frac{2\,F_2^2 L}{\alpha F_1 W^2 u}\left(\frac{u^2}{L^2}\right) = \frac{\sigma^2}{\text{mean}^2} \qquad (1.31)$$

$$= \frac{2\,D_L}{u} + \left(\frac{1}{1 + \frac{WF_1}{F_2}}\right)^2 \frac{2\,F_1 u}{\alpha} = \frac{\sigma^2}{\text{mean}^2} \times L = \text{HETP} \qquad (1.32)$$

The diffusivity D_L in equation (1.32) refers to any axial mixing mechanism which occurs in the mobile phase, so that it can be called a dispersion coefficient, including the eddy diffusivity. It was pointed out by Van Deemter that in the laminar region the eddy diffusivity in a packed bed is probably created by the difference in flow patterns in the bed. A perfectly uniform bed thus conceivably has no eddy term.

The molecular diffusivity corrected for the path lengthening in a packed bed by a tortuosity factor, and the eddy diffusivity D_L* are commonly assumed to be additive, so that the dispersion coefficient D_L is given by, $D_L = \frac{D_B}{\lambda} + D_L^*$ (1.33)

where D_L* depends on the axial dispersion caused by the flow patterns. This assumption is discussed by Klinkenberg and Sjenitzer (19) and they concluded that this approach is justifiable if the theory adequately describes the results. The abundant work on gas chromatography appears to lend support to the assumption of additivity of coefficients. At high flow rates, the molecular dispersion becomes negligible compared to the turbulent dispersion, so that the overall dispersion is the same as the flow dispersion and can be called the eddy diffusivity.

At low flow rates, e.g. particle Reynolds numbers 1, the eddy diffusivity can be represented according to Van Deemter et al by the expression $D_L^* = u\,d_p$. Thus equation (1.32), after introducing the

concept of additive coefficients stated in (1.33), takes the form,

$$HETP = 2\gamma d_p + \frac{2 D_B}{\lambda u} + \left[\frac{1}{1 + \frac{WF_1}{F_2}}\right]^2 \frac{2 F_1 u}{\alpha} \qquad (1.34)$$

The quantity γ is reported to decrease with larger diameter pellets, having a value of about 8 for 200 mesh, and practically zero for 30 mesh, particles.

Mass Transfer Coefficient and Effective Diffusivity

Diffusional resistance to mass transfer from the mobile phase to the interior of the pellets (stationary phase) is made up of two parts, the first being due to resistance in the mobile phase and the second to the resistance within the pellets. The solution of Lapidus and Amundsen (2) used by Van Deemter et al (17) (equation 1.28) treats the resistance in terms of a mass.transfer coefficient.

Van Deemter et al treated the two resistances as separate mass transfer coefficients which could be combined by the resistances-in-series rule. (A mass transfer coefficient is really a conductance rather than a resistance hence the reciprocals are the additive property.)

$$\frac{1}{\alpha} = \frac{1}{\alpha_1} + \frac{W}{\alpha_2} = \frac{1}{k_1 A_p} + \frac{W}{k_2 A_p} \qquad (1.35)$$

Where α_1 is the mobile phase coefficient/unit vol. of bed, α_2 is the stationary phase coefficient and α is the overall coefficient with k_1 and k_2 being the corresponding surface mass transfer coefficients. W is the partition coefficient, which is necessary in gas chromatography because the diffusion in the stationary phase occurs in a liquid and the liquid-phase concentration gradients are expressed in terms of equivalent equilibrium gas phase concentrations in order to make equation (1.35)

consistent. In diffusion in porous solids, the effective diffusivity is defined on the basis of the interstitial gas concentrations and so the partition coefficient becomes a quantity relating interstitial concentrations to stationary phase concentrations, that is $\frac{1}{\epsilon_p}$, where ϵ_p is the pellet porosity.

External Mass Transfer Coefficient

Based on the work of Ergun (21) Van Deemter et al suggested the use of the following correlation for the mass transfer coefficient in the mobile phase,

$$k_1 = \frac{25}{6} \frac{D_B}{F_1} A_p \text{ cm. /sec.} \tag{1.36}$$

Where k_1 is the mass transfer coefficient per unit area and A_p is the surface area per unit volume of bed,

$$\alpha_1 = A_p k_1 \quad \text{sec.}^{-1} \tag{1.37}$$

In a bed of spherical particles of diameter d_p, the surface area per unit volume, A_p, is given by the following, if the bed porosity is F_1,

$$A_p = 6(1 - F_1)/d_p \tag{1.38}$$

Internal Mass Transfer Coefficient

In this work it is desired to obtain the effective diffusivity in the porous pellet, and so it is necessary to find a relationship between the mass transfer coefficient, $\alpha_2 = k_2 A_p$, and the effective diffusivity. Such an expression was given by Van Deemter et al without derivation, but it can be obtained in a pellet of radius R as shown below.

Let

$$D_E \left(\frac{\partial C}{\partial r} \right)_{r=R} = k_2 (C_s - C_{avg}) \tag{1.39}$$

where C_s and C_{avg} are the surface and average concentrations in the pellet respectively.

Crank (22) (page 233) has obtained solutions of the diffusion equation for a spherical pellet of radius R which give the concentration C_A at any radius r and time t when the surface concentration changes stepwise from 0 to C_s,

$$C_A = C_s + \frac{2\,RC_s}{\pi r} \sum_{n=1}^{\infty} \frac{(-1)^n}{n} \sin\left(\frac{n\pi r}{R}\right) \exp\left(-\frac{D_E n^2 \pi^2 t}{R^2}\right) \tag{1.40}$$

Similarly the average concentration is given by:

$$C_{avg} = C_s - \frac{6\,C_s}{\pi^2} \sum_{n=1}^{\infty} \frac{1}{n^2} \exp\left(-\frac{D_E\, n^2 \pi^2\, t}{R^2}\right) \tag{1.41}$$

If t is large then only the first terms of the series solutions need be considered. This amounts to suggesting that C_s approaches C_{avg} and in view of the rapidity of gas diffusion as demonstrated in the example given in the introduction, this assumption would appear to be reasonable.

From (1.40),

$$\frac{C_A}{C_s} - 1 = \frac{C_A - C_s}{C_s} = \frac{-2\,R}{\pi r} \sin\left(\frac{\pi r}{R}\right) \exp\left(-\frac{D_E\,\pi^2 t}{R^2}\right) \tag{1.42}$$

From (1.41),

$$\frac{C_{avg}}{C_s} - 1 = \frac{C_{avg} - C_s}{C_s} = -\frac{6}{\pi^2} \exp\left(-\frac{D_E\,\pi^2 t}{R^2}\right) \tag{1.43}$$

Divide (1.42 by (1.43)

$$\frac{C_A - C_s}{C_{avg} - C_s} = \frac{2\,R\,\pi}{6\,r} \sin\frac{\pi r}{R} = \frac{C_s - C_A}{C_s - C_{avg}} \tag{1.44}$$

Let $\frac{C_s - C}{\Delta r} = \left(\frac{\partial C}{\partial r}\right)_{r = R}$, then substitute in equation (1.39)

$$D_E \frac{R\pi}{3r} \sin\frac{\pi r}{R} \frac{C_s - C_{avg}}{\Delta r} = k_2 (C_s - C_{avg})$$

Taking the limit as $\Delta r \rightarrow 0$

$$\text{limit}\left[-\frac{D_E \pi^2}{3k_2} \left[\frac{\sin\frac{\pi r}{R}}{\frac{\pi r}{R}}\right] \frac{1}{\Delta r} = 1\right] \tag{1.45}$$

or $\frac{2\pi^2 D_E}{k_2 d_p} = 1$ where $d_p = 2R$

therefore $k_2 = \frac{2}{3}\pi^2 \frac{D_E}{d_p}$ (1.46)

The mass transfer per unit volume of bed α_2 is obtained by multiplying k_2 by the surface area per unit volume A_p given by equation (1.36).

The two mass transfer coefficients could be combined using equation (1.35). However, at this stage, the conditions of the present work differs from that of Van Deemter et al. If k_1 is large compared to k_2, then when the inverse is summed in equation (1.35), k_1 may be ignored. The expression for k_1 suggested by Van Deemter et al applies only to the laminar flow region, but in the turbulent region the value will be greater rather than less, and so if reason can be found to neglect k_1 in the laminar region, it need not be considered in evaluating mass transfer in the turbulent flow region.

If we assume the effective diffusivity in the porous pellet is 1/5 of the molecular diffusivity as suggested in the introduction, and assume a bed porosity of 0.4, then the ratio of k_1/k_2 from equations (1.36) and (1.45) is around 28. Thus, at most, the resistance outside the pellet makes a 3% contribution and can be ignored.

The derivation for k_2 was made on the assumption of a step change in the surface concentration, but in this work a Gaussian curve is expected to describe the surface concentration. It would be desirable to have a derivation applicable to other surface functions, or at least to the Gaussian function. An attempt to obtain an alternate expression for k_2 using a ramp surface function could not be made to reduce to the expression of (1.46), because the exponential functions would not cancel

out as is the case in the step yielding equation (1.44). Thus, a further degree of approximation results from using (1.46), but it is probable that an experimental constant other than $2/3\pi^2$ can be found which would yield a satisfactory diffusivity from a pulse experiment.

Van Deemter's Equation

The expression for the mass transfer coefficient can now be substituted in equation (1.34). Ignoring k_1, and combining (1.35) (1.38) and (1.46)

$$\alpha = 2/3\pi^2 \frac{D_E}{d_p} \quad 6 \frac{(1 - F_1)}{d_p} \tag{1.47}$$

Substituting (1.47) into (1.34),

$$\text{HETP} = 2\gamma d_p + 2\frac{D_B}{\lambda u} + \left[\frac{1}{1 + \frac{WF_1}{F_2}}\right]^2 \frac{2F_1 d_p^2 u}{4\pi^2 D_E (1-F_1)} \tag{1.48}$$

Making the substitutions,

$$F_1 = \epsilon_B$$

$$F_2 = 1 - F_1 = (1 - \epsilon_B)$$

$$W = \frac{1}{\epsilon_p}$$

$$\text{HETP} = 2\gamma d_p + 2\frac{D_B}{\lambda u} + \left[\frac{1}{1 + \frac{\epsilon_B}{\epsilon_p(1 - \epsilon_B)}}\right]^2 \frac{2\epsilon_B d_p^2 u}{4\pi^2 D_E(1 - \epsilon_B)} \tag{1.49}$$

This is the equation derived by Van Deemter et al (17) and it may be observed to be of the general form

$$\text{HETP} = A + B/u + Cu \tag{1.50}$$

where A, B and C would be constants for a given packed bed and a given system.

A sketch of the behaviour of this equation is shown in Figure 1.5 indicating the physical significance of the constants A, B and C.

The magnitude of the A term, which may be called the eddy diffusivity term, depends largely on the value of γ. As pointed out by Van Deemter et al, γ is expected to be quite small for large packing sizes, e.g. 30 mesh diameter or larger. Therefore, it is likely that the eddy diffusivity term may not seriously mask the other terms.

At low flow rates, the quantity B/u, or molecular diffusivity term, may be expected to dominate, while at high flow rates the effective diffusivity, or Cu, term will predominate.

The effective diffusivity, or Cu term, is of primary interest and so this term will be considered in more detail. It was mentioned earlier that a lower mass transfer coefficient or effective diffusivity causes the pulse to broaden, and in the effective diffusivity term a lower effective diffusivity does indeed result in a larger HETP, which is a measure of the amount of pulse dissipation. Similarly, a non porous pellet will have zero porosity (ϵ_p), and so the pellet capacity term becomes zero. This implies that for a bed of non porous pellets the following equation should apply:

$$HETP = A + B/u$$

The influence of the bed porosity ϵ_B on the magnitude of the effective diffusivity term is very small over the range of porosities commonly found in random pellet packings. On the other hand, the pellet diameter which has an exponent of 2 has a strong influence on the value of the effective diffusivity term, and suggests that this term will be much more easily evaluated for larger pellets.

Typical Values of the Effective Diffusivity Term (C)

In Table 1.I following, some values of the effective diffusivity term are calculated for some typical porous pellet properties and dimensions,

and for a range of possible effective diffusivities. The velocities where the molecular diffusion term equals the effective diffusivity term in equation (1.49) (i.e. the minimum shown in Figure 1.5) are also calculated. for an effective diffusivity of 0.01 cm^2/sec, an assumed molecular diffusion coefficient of 0.2 cm^2/sec, and a tortuosity factor of 1.33. It can easily be shown that,

$$u_{min} = \left[\frac{2\, D_B}{\dfrac{1}{1 + \dfrac{\epsilon_B}{\epsilon_p(1-\epsilon_B)}} \quad \dfrac{\epsilon_B\, d_p^{\,2}}{2^{\,2}\, D_E(1 - \epsilon_B)}} \right]^{1/2} = \frac{B}{C}^{\;1/2}$$

Because the velocity at the minimum is proportional to $1/d_p$ the particle Reynolds number, $d_p u \rho / \mu$, at each of the minima obtained for different particle sizes will be the same, and has a value of around 6 if a value of 1/6 is taken for the kinematic viscosity.

TABLE 1.I

THE EFFECT OF PELLET DIAMETER AND EFFECTIVE DIFFUSIVITY ON THE EFFECTIVE DIFFUSIVITY TERM (C) IN EQUATION (1.50) ($\epsilon_B = 0.4$, $\epsilon_p = 0.33$)

d_p cms. / Eff.Diff.	1	.5	.25	.1
.1 cm^2/sec	.0375	.00938	.00235	.000375
.01 "	.375	.0938	.0235	.00375
.001 "	3.75	.938	.235	.0375
Velocity at minimum from $u_{min} = \left(\frac{B}{C}\right)^{1/2}$ cm/sec	.895	1.79	3.16	8.95

From the first three lines of calculations in Table 1.I, it is obvious that for high effective diffusivities and small pellet diameters a pulse dispersion method may break down because the effective diffusion

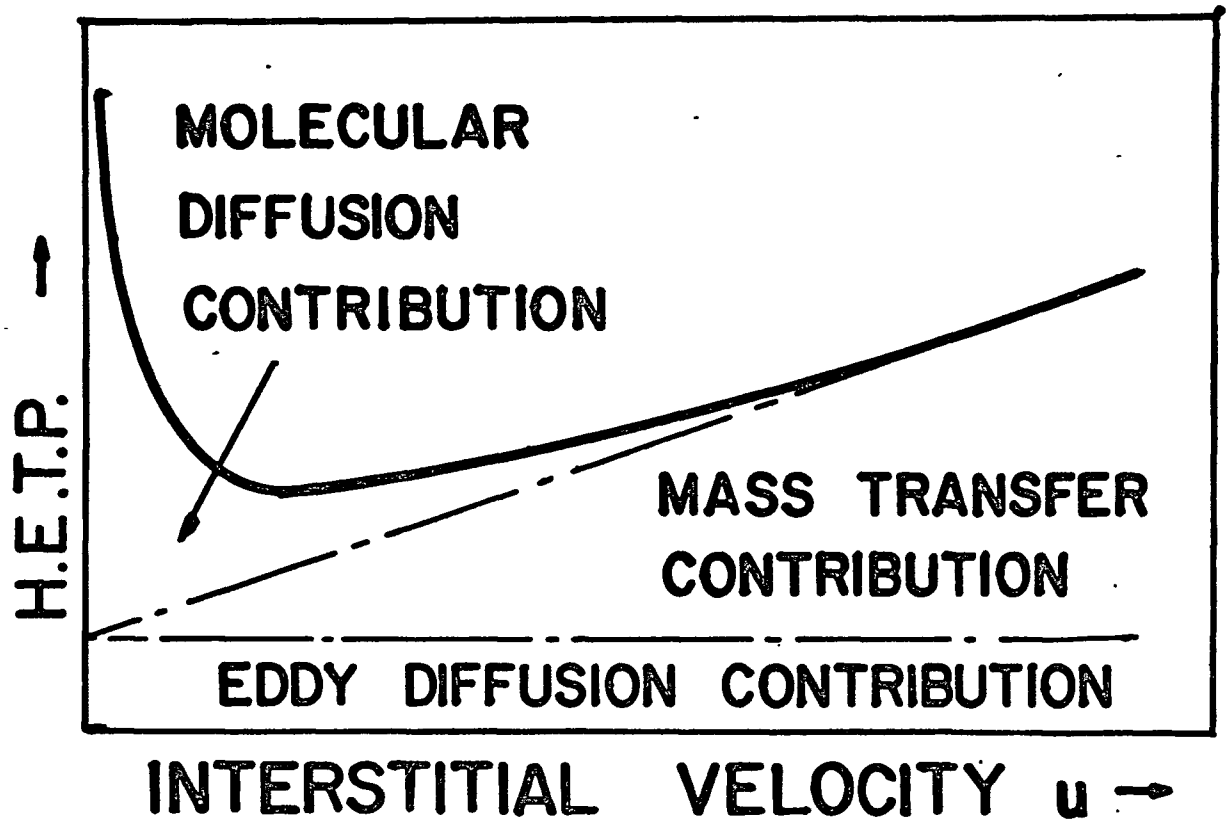

Figure 1.5

Typical Plot of HETP Vs. Velocity (Equation 1.50)

term becomes too small with respect to the other terms unless extremely high flow rates can be used. For example, assuming the figures given above, the constant B = .15 and A = d_p if the quantity $2\gamma = 1$ is used. At very high flow rates, the description of eddy diffusivity suggested by Van Deemter et al (17) would not be expected to hold. However, if the "perfect mixer" model (discussed in the following section) applies, as suggested by McHenry and Wilhelm (15), then the eddy diffusivity D_L^* is given by $D_L^* = 1/2\ ud_p$ for superficial Reynolds numbers from about 10 to 400. This expression compares favorably with that suggested by Van Deemter et al ($D_L^* = \gamma\ ud_p$). However, the constant given as 1/2 actually varied with Reynolds number from 1/1.8 to 1/2.2 in McHenry and Wilhelm's experimental work, and this drift would tend to cause errors in determining the effective diffusivity term in equation (1.50) if pellets with high diffusivity and small diameter were used.

As mentioned earlier, the velocities at the bottom of the Table 1.I show the location of the minimum in Figure 1.5, and correspond to a constant particle Reynolds number of about 6 which is well above the flow range considered by Van Deemter et al. Nevertheless, it is apparent that if the effective diffusivity term is to be maximised relative to the other terms, higher flow rates and Reynolds numbers must be used.

<u>Least Square Error fit of data to Van Deemter Equation</u>

Consider an equation of the type

$$H = A + B/u + Cu \qquad (1.51a)$$

Given an adequate number of experimental points relating H to u for a given packing bed and gas system, the best values of the constants A, B and C can be determined by a "least squares error" fit.

Three simultaneous equations involving A, B and C can be obtained in the usual way, that is,

1. Sum all the n data points:

$$nA + B\sum\frac{1}{u} + C\sum u = \sum H \tag{1.51b}$$

2. Multiply by the coefficient of B:

$$A\sum\frac{1}{u} + B\sum\frac{1}{u}^{2} + nC = \sum\frac{H}{u} \tag{1.51c}$$

3. Multiply by the coefficient of C:

$$A\sum u + nB + C\sum u^{2} = \sum Hu \tag{1.51d}$$

Eliminating A and B from (1.51b), (1.51c), and (1.51d)

$$C = \frac{\left(\dfrac{\sum(H) - \dfrac{n\sum(Hu)}{\sum u}}{\sum\left(\frac{1}{u}\right) - \dfrac{n^2}{\sum u}}\right) - \left(\dfrac{\sum H - \dfrac{n\sum\left(\frac{H}{u}\right)}{\sum\left(\frac{1}{u}\right)}}{\sum(1/u) - \dfrac{n\sum(1/u)^2}{\sum(1/u)}}\right)}{\left(\dfrac{\sum(u) - \dfrac{n\sum(u)^2}{\sum u}}{\sum\left(\frac{1}{u}\right) - \dfrac{n^2}{\sum u}}\right) - \left(\dfrac{\sum u - \dfrac{n^2}{\sum\left(\frac{1}{u}\right)}}{\sum\left(\frac{1}{u}\right) - \dfrac{n\sum\left(\frac{1}{u}\right)^2}{\sum\left(\frac{1}{u}\right)}}\right)} \tag{1.51e}$$

Hence,

$$B = \frac{\sum H - \dfrac{n\sum\left(\frac{H}{u}\right)}{\sum\left(\frac{1}{u}\right)} - C\left(\sum u - \dfrac{n^2}{\sum\left(\frac{1}{u}\right)}\right)}{\sum\left(\frac{1}{u}\right) - \dfrac{n\sum\left(\frac{1}{u}\right)^2}{\sum\left(\frac{1}{u}\right)}} \tag{1.51f}$$

$$A = \frac{\sum H - C\sum u - B\sum\frac{1}{u}}{n} \tag{1.51g}$$

B. LONGITUDINAL DISPERSION COEFFICIENTS

There are two models generally used to describe the longitudinal dispersion in packed beds of non porous solids. The dispersed plug flow model superimposes co-ordinates moving at the average stream velocity, u, on the appropriate solution of the diffusion equation. Thus, the variation of axial concentration profile C with time t and axial distance x of a quantity M per unit area of gas with diffusivity D_L, initially on a plane

at x = 0 is given by (22)

$$C_A = \frac{M}{2\sqrt{\pi D_L t}} \quad \exp\left(\frac{-x^2}{2(2D_L t)}\right) \tag{1.52}$$

which is a Gaussian distribution with mean 0 and variance 2 $D_L t$.

With plug flow at a velocity u this becomes

$$C_A = \frac{M}{\sqrt{2\pi \; 2D_L t}} \quad \exp\left(-\frac{(L - ut)^2}{2(2D_L t)}\right) \tag{1.53}$$

with mean L and variance 2 $D_L t$.

A second model is the "perfect mixers in series" which can be developed by applying the theoretical plate derivation described earlier, again yielding a Poisson distribution, with a mean of $\frac{U}{V_L}$ and variance $\frac{U}{V_L}$, where U is the volume of gas which has passed through, and V_L the volume of each mixer. The number of perfect mixers in series is equivalent to the number of stages and is given by U/V_L as before.

Equating the ratio $\frac{(\text{mean})^2}{\text{variance}}$ = number of mixers, N, for both models,

$$\frac{\left(\frac{U^2}{V_L}\right)}{\left(\frac{U}{V_L}\right)} = N = \frac{L^2}{2\,D_L t} = \frac{uL}{2\,D_L} \tag{1.54}$$

If one mixer is assumed to correspond to each layer of particles, then the number of mixers = L/d_p, and therefore,

$$D_L = 1/2\ u\ d_p \tag{1.55}$$

The only work, (apart from a few data points in the laminar flow regime obtained by Carberry and Bretton (23)) which has been carried out with gases for the purpose of investigating dispersion models in packed beds has been done by McHenry and Wilhelm (15), using a frequency response technique. They found that over a particle Reynolds number

(based on superficial velocity) range of 10-400 the above relationship held reasonably well.

Other factors which influence the axial dispersion coefficient are buoyancy effects which may be expected when flow rates approach laminar conditions, and wall effects which Hiby (24) has shown greatly increase the apparent dispersion coefficient.

Velocity Profile Contribution

Taylor (25) has separated the velocity profile contribution to the dispersion coefficient in pipe flow. Taylor found that four dispersion regimes exist in pipe flow. The first is due to molecular diffusion which predominates at low flow rates. As the velocity increases the parabolic profile contributes to the longitudinal dispersion of a pulse, but the molecular diffusivity is able to largely remove the radial concentration profiles. This yields an eddy diffusivity,

$$D_L^* = K \frac{u^2 R^2}{D_B} \tag{1.56}$$

where u is the mean velocity, D_B the molecular diffusivity, and R is the pipe radius. It may be noted that high molecular diffusivity gases reduce the eddy diffusivity in this region. The constant K is $\frac{1}{48}$ for pipes, but Aris (26) has shown that the constant depends upon the geometry of the system. The range of application of the above regime is described by Turner (27) as,

$$\frac{7\, D_B}{R} \ll u < \frac{4\, D_B\, L^1}{R^2} \tag{1.57}$$

where L^1 is the length of test section containing most of the pulse. Within the above limits the molecular diffusivity contribution is negligible so $D_L^* = D_L$. Since a Gaussian distribution is assumed we can say that 95% of the pulse exists in four standard deviations.

If L' is defined as 4σ then,

$$L' = 4\sqrt{2D_L t}$$

Substituting for D_L from (1.56) and setting $t = \frac{L}{u}$, where L is the length of column (or mean), the upper limit becomes,

$$u \ll 2\ 16^2\ K_1\ \frac{L.D_B}{R^2}$$

For pipes $K_1 = \frac{1}{48}$ giving an upper limit of

$$u \ll 10\ \frac{LD_B}{R^2}$$

Turner (27) in his derivation obtained $5\ LD/R^2$ for the R.H.S. of (1.58), apparently because of the omission of a factor of 2 in defining L . The residence time is introduced if the velocity is replaced by $\frac{L}{t}$ then,

$$\frac{L}{t} = u \ll 10\ \frac{LD_B}{R^2} \quad \text{or } t \gg \frac{R^2}{10\ D_B} \tag{1.58}$$

In other words, a pulse must be allowed to flow for some finite time after the injection before the eddy diffusivity is defined by equation (1.56). If the dispersion is measured very shortly after injection (a time less than $R^2/10\ D_B$), then the eddy diffusivity is given by some undefined function. This latter function does not include the molecular diffusivity, and so resembles the function for the turbulent regime.

Longitudinal dispersion in the turbulent flow regime in pipes has been dealt with by Taylor by use of the universal velocity profile. This approach yielded

$$D_L^* = 7.14\ Ru\sqrt{f} \tag{1.59}$$

where f is the Fanning friction factor.

The application of the Taylor derivation to packed beds has been somewhat limited, although Bischoff and Levenspeil (28) have considered the overall profile in a packed bed. Inasmuch as the velocity profile in packed beds approaches plug flow the contribution of the overall profile to axial dispersion is small.

Saffman (29) has developed a model based on a network of capillaries of length ℓ which are joined in a random manner. Assumptions must be made regarding the length and diameter of the capillaries. Saffman derived the following expression to cover the transition from laminar to an eddy regime and by assumming a capillary length to diameter ratio of 5 the experimental results of Hiby (24) for liquid were fitted

$$D_L = \frac{uL}{6}\left[\mathrm{Log}_e \frac{3}{2}\frac{uL}{D_B} - \frac{17}{12} - \frac{1}{8}\frac{R^2}{\ell^2}\frac{uL}{D_B}\right] + \frac{D_B}{\lambda} + \frac{4}{9}D_B + O\left[\frac{D_B}{\ell u}\right]^2 \quad (1.60)$$

The value of the tortuosity λ obtained by Saffman from this model approaches 3 to 4, considerably higher than the tortuosities normally encountered in beds of spheres.

Saffman's model appears to show the most potential at present in describing the axial mixing in packed beds, but as in Taylor's work on pipes assumptions made concerning the nature of the flow lead to different solutions. Hence, the basic flow mechanism must be understood before one can apply the appropriate solution from the model.

III

APPARATUS

A. DEVELOPMENT

The initial work to test the calculation of effective diffusivities by means of the Van Deemter equation was carried out on an apparatus based on a gas chromatograph as shown in Figure 1.6. A cyclopropane pulse was injected by a chromatograph sample valve into a helium carrier gas and was detected on a GOW MAC model 9238-D thermal conductivity cell. The flow rate was measured with a soap bubble flow meter at the cell outlet, and the detector output was recorded on a Leeds and Northrup -1 to 10 mv recorder. The test section was mounted in a vertical plane, although initially a set of results were taken with a horizontal bed, but the settling of the packing resulted in a channel along the top of the bed. The first vertical apparatus suffered from the following defects:

1. The detector would only operate within a limited gas flow range (about 50 mls/min.).
2. The small ports in the sample injector restricted the flow of gas.
3. No provision existed for adjusting the recorder chart speed, and at the available chart speed the pulse output was not broad enough to make accurate measurements of standard deviations possible.

B. DESCRIPTION OF APPARATUS

The apparatus with which the bulk of the results were taken is shown in Figure 1.7. The shortcomings of the earlier apparatus were eliminated in this set-up by the following modifications:

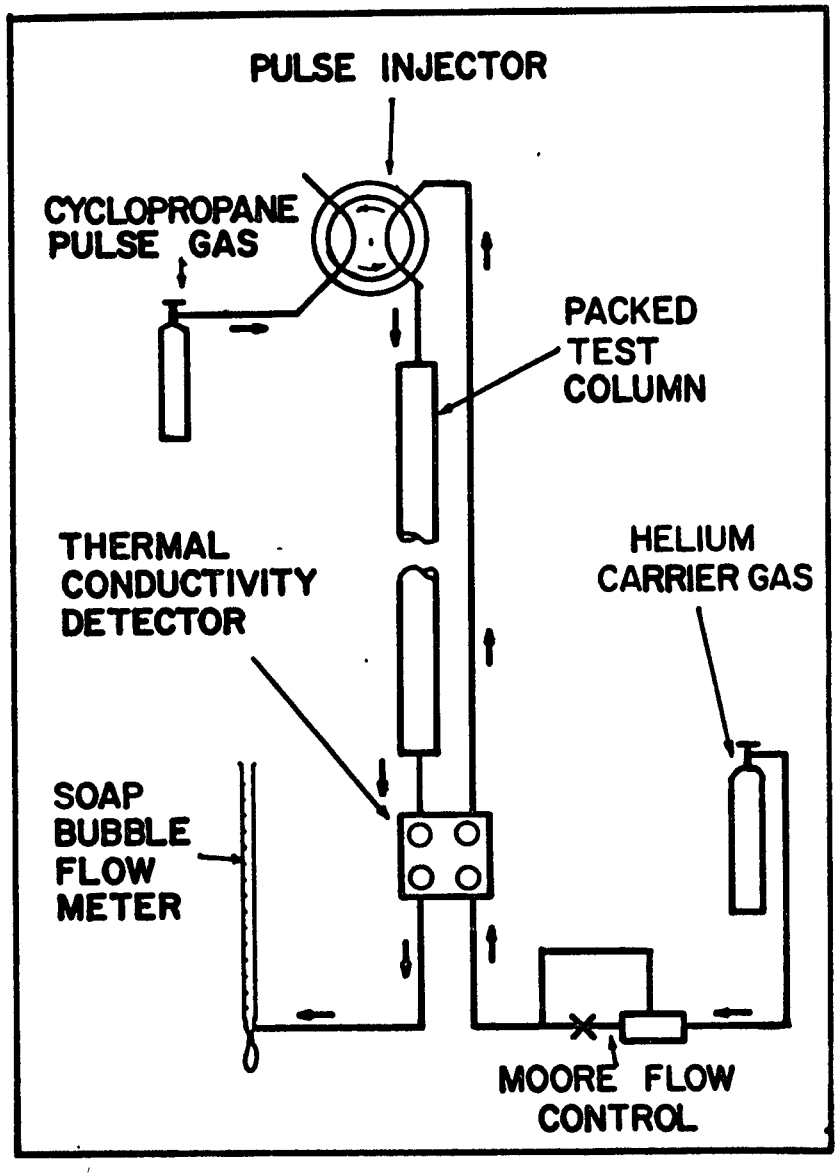

Figure 1.6

Apparatus For Exploratory Tests

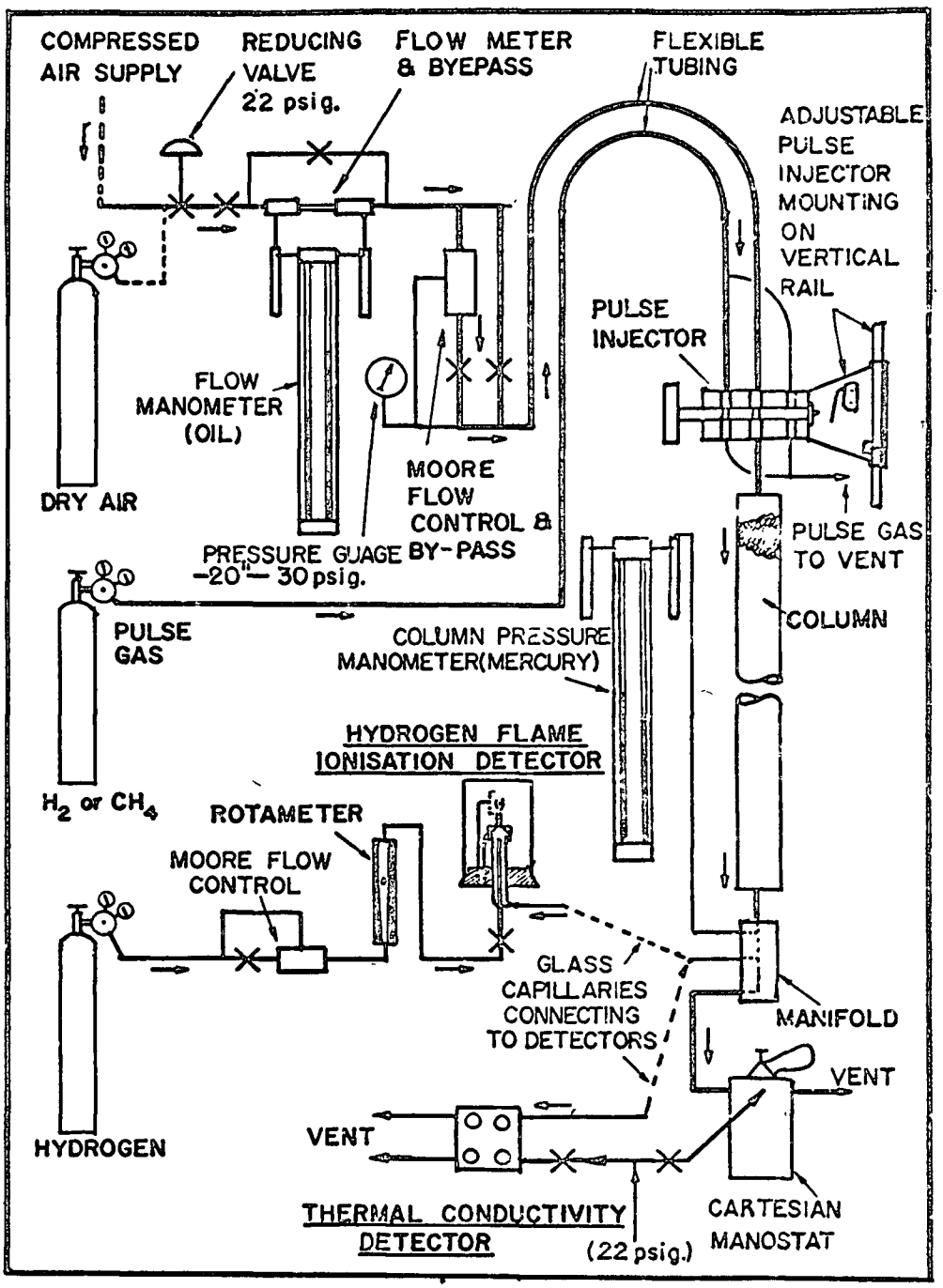

Figure 1.7

Basic Experimental Apparatus

1. A cartesian manostat was fitted on the column exit to maintain a slight positive pressure in the column (1/2 to 2 inches of mercury). This pressure made it possible to direct a side stream through a capillary to supply the detector at a fixed flow rate. At gas flow rates less than the amount needed for the detector the manostat supplied additional gas, thus reversing the flow direction between the manifold and the manostat.
2. A sample or pulse injection valve was constructed having large ports as shown in Figure 1.8. This Figure also shows an experimental pulse injection system which was used to test the effect of varying pulse size.
3. A Bausch and Lomb 0- 10, 100, 1000 mv recorder with chart speed adjustments from 0.05 to 20 inches/min. allowed the pulses to be recorded in such a way that good accuracy could be obtained in measuring the dispersion of the pulse.

The apparatus was set up with the test bed mounted in a vertical plane, and resting on a manifold block at the discharge end. The side stream for the detector was taken from the manifold, and the main column effluent gas discharged through the manostat. A port connected to a mercury manometer indicated the manifold absolute pressure.

Air carrier gas was taken at either 30% RH from the building supply or from a cylinder of dry air. The air passed through a regulator set for 22 psig. downstream pressure, and then to a flow meter consisting of a sp. gr. 1 oil manometer and capillary tube. A series of capillary tubes were calibrated using soap bubble flow meters or a wet test gas meter, so that a wide range of flows could

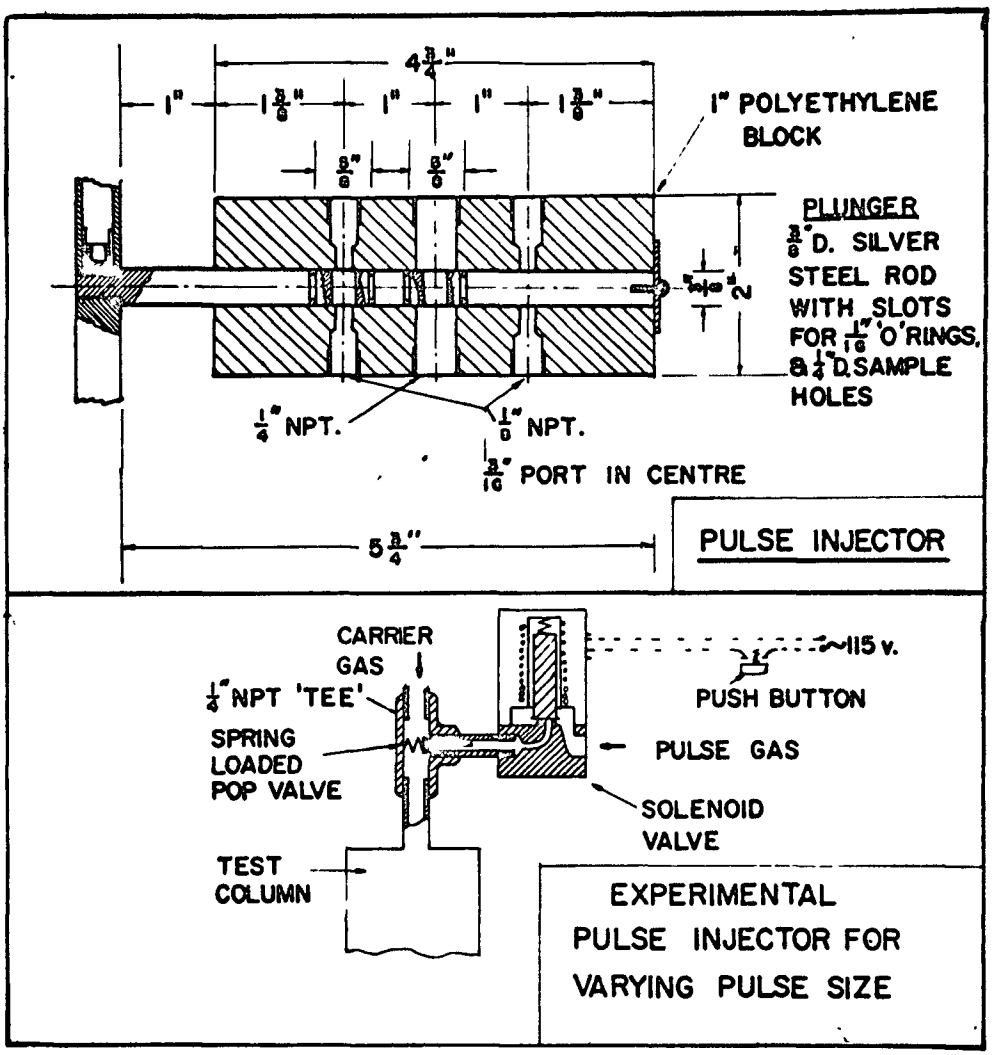

Figure 1.8

Pulse Injectors

be covered. No attempt was made to size the capillaries so that they remained in their linear range. From the flow meter, the carrier gas passed through a Moore Constant Differential gas flow control and by-pass loop to the pulse injector. The pulse injector was mounted on a vertical rail so that it could be adjusted over a six foot range to allow for varying column lengths. Polyethylene tubing was used to supply the carrier gas, as well as the pulse gas to the injector. The flexibility of the polyethylene tubing allowed the injector to be adjusted anywhere on the rail without the need of piping alterations.

A microswitch mounted on the injector was either opened or closed at each movement of the injectors. This action operated an event marker on the recorder to indicate the start of each run.

C. DETECTORS

Hydrogen Flame Ionisation Detector

In equation (1.49), it was evident that lower effective diffusivities increased the magnitude of the C term. To take advantage of this, the hydrogen flame ionisation detector was selected, as it allowed the use of air and hydrocarbons of any convenient molecular weight, as opposed to the need for hydrogen or helium (which have high diffusivities) as one of the gases in thermal conductivity detectors if high precision is desired. In addition, the hydrogen flame detector is linear over a 5 decade range, and the high sensitivity allows the use of extremely small pulse volumes.

The detector was constructed from the circuit described by Harley, Nels, and Pretorius (30) and is shown in Figure 1.9. A power supply was also constructed to supply the detector, however, the AC filament supply was found to create excessive noise in the output so the detector tube was powered from a 6 volt accumulator.

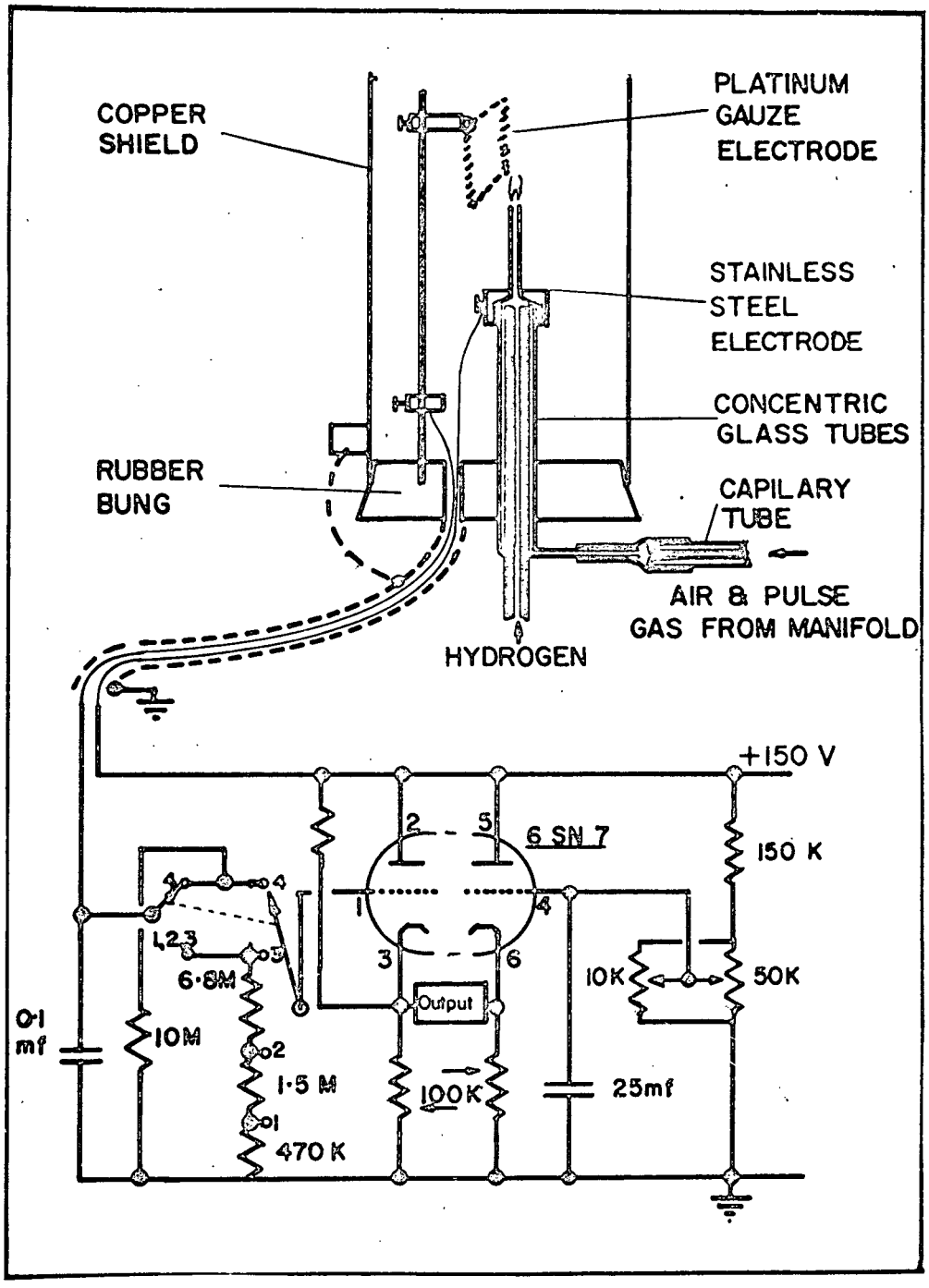

Figure 1.9

Hydrogen Flame Detector

No output could be obtained initially from the circuit as described, and on investigation the voltages on the 6 SN 7 tube were found to be outside the range in which a response could be expected. To correct this problem it was necessary to change the two load resistors from 10 KΩ to 100 KΩ. It is concluded that a misprint has occurred in the original publication. The actual ionisation or combustion chamber was constructed to minimize the holdup time of the primary air containing the traces of pulse gas from the manifold. The air entered through the annular space in the glass tubes and joined with the hydrogen before passing through the stainless steel orifice which formed one electrode. Hydrogen was supplied from a cylinder via a Moore flow controller and a rotameter at a rate of about 150 mls/min. Lower flow rates increased the detector output but in the extreme, the flame became unstable. Air and pulse gas arrived through the capillary at the rate of about 0.7 mls/sec. The volume of the detector air side and supply tubes from the manifold was estimated at 0.2 mls, giving a time lag of about 0.3 seconds.

Initially, the flame orifice was made flush with the metal electrode, but the heat from the flame caused the glassware to crack and so the orifice was modified by adding about 1 1/2" of 1/8 inch stainless steel tube. The whole assembly was held on a rubber bung, thus supplying the insulation for the platinum electrode which was supported by a heavy wire inserted in the rubber. Shielded cable connected the detector to the electrical system, and a grounded copper chimney shielded the flame from draughts.

Other modifications to the reference circuit (also shown in Figure 1.9) included a fourth position on the selector switch with a

10 meg resistance to ground, and a coarse and fine zero setting using 20 K and 50 K variable resistors in parallel. The 10 megohm position was used on all runs.

Fibre glass filters were fitted in the hydrogen tube and the manifold to reduce the noise in the detector caused by dust. The detector still gave occasional characteristic jumps in output, probably caused by dust in the secondary air, but no attempt was made to correct this.

Thermal Conductivity Detector

A "Gow mac" model 9238D tungsten wire thermal conductivity detector was used with the recommended conventional auxiliary circuits. A 6v. battery supplied the current for the detector and the event marker on the recorder. The output to the recorder was fitted to an attenuator having 1, 2, 5, 10, 50, 100 and 500 ratios, but only the 1, 2 and 5 positions were needed in the pulse apparatus.

The reference side of the detector was supplied through a needle valve from the 22 psig air line, and a small bleed maintained. The capillary supplying the measuring side of the detector from the manifold was sized to give approximately 46 mls/min. of air at 1/2" Hg gauge manifold pressure.

IV

EXPERIMENTAL PROCEDURE

A. OUTLINE OF EXPERIMENTAL INVESTIGATION

The experimental work was carried out in three parts to (a) test the applicability of Van Deemter's equation with large pellet diameters and higher flow rates; (b) measure the effective diffusivity in some samples of porous pellets using the pulse method, and (c) compare the effective diffusivity obtained with the pulse experiment to those obtained by an independent method. Part (a) was carried out by injecting methane and hydrogen pulses in beds containing non-porous pellets, while (b) was an obvious extension of (a) to porous pellets. The well-tested steady state method was selected to obtain an independent effective diffusivity value. It was convenient, however, to develop a specific solution of the diffusion equation to fit pellets with curved faces. The details of this section of the work are recorded in Appendix 1.

B. NON POROUS PELLETS IN PULSE APPARATUS

A simple gas chromatograph assembly was used for some early exploratory runs with a cyclopropane pulse in an helium or air carrier gas flowing through beds of 2 mm. glass spheres. These results were discarded due to limitations of the apparatus, which included a limited supply of the 2 mm. glass beads necessitating short beds, as well as the defects already listed.

With the development of the more sophisticated apparatus, a series of runs using methane pulses in air was carried out with various bed diameters and lengths packed with three kinds of non porous pellets: 0.208 cm. No. 9 lead shot, 0.568 cm. glass beads, and 1 cm. diameter ceramic beads.

Because the value of the quantity "C" in equation (1.50), $HETP = A + \frac{B}{u} + Cu$ was not found to be zero in the exploratory work with non porous pellets, runs 50 to 55 were designed to determine the magnitude of this term, and to investigate ways of minimizing it. To check the possibility that this effect was caused by a high velocity "by-pass" flow at the wall, run 50 was made with a 5 cm. diameter column packed with the 0.208 cm. lead shot, and having a maximum particle Reynolds number of 2. Run 50 was different from the other runs in that a higher pressure was used, giving a lower diffusivity. Run 51 was made with a 2.5 cm. column packed with the lead shot to see if particle to tube diameter ratio had much influence on the wall effect. Run 52 duplicated run 50, but used a higher Reynolds number range, and normal column pressure. A run designated 51D was also made on the 2.5 cm. bed, but five doughnut rings were distributed evenly down the column in an attempt to eliminate the wall effect.

Run 53 was made with a 6.27 cm. diameter column packed with the 1 cm. ceramic spheres. The experimental sample injection system using a solenoid valve, which allowed varying pulse sizes, was introduced in this column. Run 54 was made on a 1/4" polyethylene tube packed with 3 mm. glass spheres, and run 55 was made with a 1.2 cm. diameter bed packed with the 1 cm. balls to see if a tube/pellet diameter ratio < 2 could eliminate the wall effect. This latter case has been designated as a "single pellet" bed. In all the foregoing runs, the test system used was a methane pulse in air as a carrier gas.

Following these tests, runs 56 to 62 with porous pellets were carried out. One of the porous pellets, an activated alumina, gave

abnormally low values for the effective diffusivity. Further investigation, which is summarized in Appendix IV, showed that methane was adsorbed to a significant degree on the activated alumina. The need for a non-adsorbing system resulted in further runs using the non porous pellets being carried out with a hydrogen pulse, as well as the methane pulse, in air system. Runs 63 to 66 were carried out with 0.568 cm. glass spheres, both gas systems and two column diameters, including one for a single pellet diameter. Runs 69 to 72 were a similar set of results with the 1 cm. diameter spheres, two column diameters and two gas systems. Runs 69 and 72 using methane are duplicates of runs 53 and 55, but covered a wider range of Reynolds number. Table 1.II summarizes the values of the variables pertaining to each run number.

TABLE 1.II

SUMMARY OF THE PELLET AND TUBE TO PELLET DIAMETER RATIOS COVERED BY THE EXPERIMENTAL RUNS

Pulse Gas	Tube/Pellet Ratio / Pellet Diameter	1	3	6	12	25
Methane	.208 cm.		54*		51 51D	50 52
	.568 cm.	64	65			
	1.0 cm.	72 55		69 53		
Hydrogen	.567 cm.	63	66			
	1.0 cm.	71		70		

*pellet diam. 0.29 cm.

C. POROUS PELLETS IN PULSE APPARATUS

Three samples of porous spherical pellets were acquired for testing. These included 1/8" and 1/4" diameter H151 Alcoa activated alumina pellets, and 1/2" diameter Norton Alundum catalyst supports. The physical characteristics of these pellets are summarized in Appendix III. One of the difficulties experienced in setting experimental conditions was that the activated alumina test pellets could not be adequately dried in the steady state apparatus, as the epoxy resin holding the sample could not stand the necessary drying temperature. In view of this problem, the pulse investigation was attempted on the "wet" pellets, because it was found that the moisture content of the pellets which had been open to the atmosphere was quite stable even though the atmospheric humidity varied from 30% RH to 100% RH. The only problem remaining concerned the true porosity of the wet pellets, but the manufacturer's literature (31) indicated that the water existed as liquid water, and hence could be assumed to have a density of 1. Thus, the porosity could be computed from the dry pellet porosity and the moisture content. The details of these calculations and other confirming experiments with respect to the porosities of the pellets are included in Appendix III.

The pulse technique was first applied using a methane pulse, in run 56, to the 1/4" diameter H151 activated alumna pellets in a four foot long single pellet diameter bed. The pellets were in equilibrium with air at room temperature. Unexpectedly high dispersion of the pulse (HETP) caused some doubt about the number of transfer units, so the bed was lengthened for run 57 by adding two bends and two further four foot lengths to create a trombone configuration. A 20% change in C was found

between the long bed and the short. As shown later in the "Results", the short column was found to contain insufficient transfer units for a Gaussian distribution. In run 58, the same bed as that used in run 57 was employed but the pellets were previously dried. At this stage, the possibility of surface adsorption of methane by the alumina was appreciated, and run 59 was conducted at higher flow rates in the hope that the adsorption was a slow process and would not occur to a significant extent under these conditions.

In run 60, a methane pulse was used in a single pellet diameter trombone bed, which was packed with 1/2" diameter Norton catalyst carrier pellets. In run 61, the use of a hydrogen pulse was tested on the same dry 1/4" diameter H151 activated alumina pellets from runs 58 and 59, while in run 62 the same bed was wetted back to the normal moisture content, and the hydrogen pulse applied again.

Run 73 was carried out on a four foot long by 3/4" diameter bed packed with 1/8" H151 activated alumina pellets and using a hydrogen pulse.

D. INDEPENDENT EFFECTIVE DIFFUSIVITY MEASUREMENT

A conventional steady state method was selected for a second determination of effective diffusivity, but the technique was adapted for use with spherical pellets. This modification consisted of mounting the pellets with epoxy resin in a hole in a plate about 0.75 pellet diameter in thickness. The two spherical caps on each side of the plate were ground off when the resin had dried. The solution for the differential diffusion equation with this geometry is included in Appendix I, along with the results and details of this experiment. Only the 1/4" and 1/2" pellets

were tested. On the basis of the manufacturer's data Knudsen diffusion was expected in the 1/4" alumina pellets, while molecular diffusion was expected in the 1/2" Norton pellets.

The major problem with this part of the investigation was the moisture content of the pellets. The activated alumina could only be dried in situ, but the epoxy resin would not survive the drying temperature. Since the moisture content of the "wet" pellets remained relatively constant, as mentioned previously, it was decided to test the pellets wet and correct the porosity accordingly.

E. PREPARATION OF THE TEST COLUMNS

The packed beds (columns) were constructed from glass tubing with rubber bungs or tubing in the ends. The dimensions of the beds were generally obtained with a metric rule except for small diameter tubes, where a caliper rule was used. The bed porosities were obtained either by weighing the beds full and empty if the pellet density was known, or by addition of water and weighing. For the single pellet diameter beds, the porosity was calculated by counting the number of pellets in a given length of bed, and calculating the pellet volume from the mean pellet diameter.

The mean pellet diameter was measured by placing a known number of pellets in line and measuring the overall length.

For the porous pellet beds, the porosity was calculated as for the single pellet beds above, or from the weight of pellets in the bed with the characteristic data of the pellet. All the columns were then mounted in a vertical plane.

Joints in trombone columns were made with rubber tubing.

F. OPERATION OF PULSE APPARATUS

1. One of the four calibrated flow meter capillaries was selected and fitted.
2. The column was assembled, (after taking the necessary data for the porosity calculations), and fitted to the apparatus.
3. The air supply was turned on with the flow capillary bypass open, and the column pressure was set at a convenient level (usually around 0.5" Hg), using the cartesian manostat.
4. The column was tested for leaks with soap solution.
5. The appropriate detector was started up as described below.
6. The appropriate pulse gas was set to flow at a low bleed rate using the cylinder regulator and valves. The gas was bubbled in water at the exit to estimate the flow.
7. A suitable air flow rate was passed through the column using the flow meter and control. The flow meter manometer reading was recorded.
8. The recorder chart was started at any speed (unless previous experiments suggested a specific chart speed), and a pulse injected. When the pulse was produced, the height of the pulse was adjusted on the attenuators (recorder attenuator for H_2 flow or attenuator box for thermal conductivity detector) and the width noted. Using the initial pulse, the equipment was adjusted to give a convenient peak height (e.g. 0.75 scale), and a pulse width on the chart of at least 1.5 cm.
9. A series of pulses were injected, each at a different gas flow rate, to give about ten results covering the flow range desired.
10. During the course of each run the room temperature, atmospheric pressure and column pressure were recorded.

Hydrogen Flame Detector

1. The detector was connected to the manifold with the correct capillary.
2. Hydrogen flow was started at around 150 mls/min (using rotameter) and the flame was ignited.
3. The power supply was turned on and connected to a 6v battery for filament and event marker.
4. The recorder was turned on and the zero of the recorder and detector adjusted. The selector switch on the detector amplifier was always set at the No. 4 position for all runs.

Thermal Conductivity Detector

1. The manifold was connected with the correct capillary.
2. The reference air bleed was turned on and adjusted to give a slow positive flow (e.g. by bubbling in water).
3. The filament current was adjusted to 100 ma. after connecting to 6v supply along with event marker leads.
4. The recorder was set to zero and the detector to zero signal.

V

RESULTS

A. NON POROUS PELLETS

Treatment of Data for Non Porous Pellets

For each pulse input the primary data consisted of: the flow rate of carrier gas, Q mls/sec, at STP, which is actually recorded as a manometer reading and transformed using the calibration charts in Appendix II to a flow rate, the width of the pulse at half the height (WIDTH) taken from the recorder chart and also the "mean" or distance from the pulse injection to the peak of the pulse (designated TOTAL). These data points are printed (in cm. units) in columns 8, 6 and 7 respectively of the tables of results in Appendix II.

In addition to the above raw data, each table in Appendix II is headed with details of the columns pertinent to the individual run. These include a "Run number" which starts at 50 for the sophisticated apparatus, but a run (No. 1) from the preliminary results obtained on the initial simple apparatus is included. The column length (L), diameter (d_t) and porosity (E_B) are included in the heading along with pellet porosity (E_p) and diameter (d_p), and the carrier gas temperature (T^oK), molecular weight and pressure (P). The pulse gas-carrier diffusivity is also printed for the run temperature and pressure.

The values for the molecular diffusivity of the pulse-carrier gas systems are taken from the following sources:

The diffusivity of hydrogen in air was taken from the experimental results of Currie (6). Currie found a temperature dependence of

diffusivity to the 1.715 power for this system, and this was used to interpolate from the experimental results a diffusivity of 0.755 cm^2/sec at 298°K and 1 atmosphere.

The diffusivity of methane in air was calculated from the Hirschfelder equation using the force constants tabulated in Bird, Stewart and Lightfoot (32). The computation, which is shown in Appendix III, yielded a diffusivity for methane in air of 0.212 cm^2/sec at 298°K and 1 atmosphere.

Values corresponding to the table headings were fed directly to the computer except for the pulse gas-carrier gas diffusivities which were modified to the run temperature and pressure assuming an inverse pressure dependence and a temperature dependence to the 1.7 power.

Provision was included to read in the carrier gas viscosity, but in the computations shown in Appendix II the viscosity value read in has been over-ruled in the program by a viscosity for air computed from the Sutherland equation (33),

$$\mu = 0.01709 \left[\frac{273 + 114}{T + 114} \right] \left(\frac{T}{273} \right)^{2/3} \qquad (1.61)$$

The carrier gas density was calculated assuming the perfect gas law

$$\rho = \frac{\text{Mol. Wt.}}{22400} \; \frac{273}{T} \times P \qquad (1.62)$$

Finally, the hydraulic diameter was calculated from the following equation,

$$h_D = 4 \; \frac{\text{Free Volume}}{\text{Wetted Area}} = \frac{d_T \; \epsilon_B}{\left(\frac{3}{2} \; \frac{d_T}{d_p} \; (1 - \epsilon_B) + 1 \right)} \qquad (1.63)$$

As mentioned earlier the primary data of flow rate at STP, WIDTH (= 2.36o) and TOTAL (mean) are given in columns 8, 6 and 7,

respectively, in Appendix II. From these values and the [illegible] in the heading of each table, the following calculated data are printed.

In column 1 the interstitial velocity was calculated from tube diameter d_T, and the flow rate Q, corrected for temperature T and pressure P.

$$u = Q \frac{T}{273} \frac{1}{P} \left[\frac{1}{\pi d_T^2}\right] \frac{1}{\epsilon_B} \tag{1.64}$$

The HETP was calculated as defined by equation (1.26)

$$HETP = \frac{L\sigma^2}{mean^2} = L \left[\frac{WIDTH}{2.36}\right]^2 \left[\frac{1}{TOTAL}\right]^2 \tag{1.65}$$

Three Reynolds numbers were calculated for comparing the axial dispersion data with data of other workers and are defined as follows: the particle Reynolds number shown in column 4 of the table of results in Appendix II is given by $\frac{u\, d_p \rho}{\mu}$, the superificial Reynolds number shown in column 11, $\frac{u \epsilon_B\, d_p \rho}{\mu}$, and the hydraulic Reynolds number based on the hydraulic diameter, $u\, h_D \rho / \mu$, in column 13.

The dispersion coefficient D_L, was obtained from equation (1.34), which for non porous pellets reduces to,

$$HETP = \frac{2\, D_L}{u} \tag{1.66}$$

so $D_L = HETP \frac{u}{2}$

and this value is printed in column 9 under the heading of "eddy diffusivity". In fact, it is the sum of the molecular and eddy diffusivities as given by equation (1.33).

The number of transfer units (NTU), defined by $\frac{uL}{2D_L}$, must be large for equation (1.30) to be satisfied, however, the values calculated and

recorded in column 5 are based on the molecular diffusivity rather than the dispersion coefficient D_L. Inspection of the term shows that the NTU is smallest at low velocities, and since low velocities imply the existence of the molecular diffusivity regime, the NTU's based on these diffusivities are an adequate test. The use of "long" beds has generally eliminated the NTU as a limiting criterion in this work.

To make possible comparisons between the eddy diffusivity computed from this work and the correlations and results of other workers, the Peclet and Schmidt numbers were also calculated.

The molecular and so-called "eddy" Peclet numbers are recorded in columns 3 and 10, respectively, and were computed from the following definitions,

Molecular Peclet number $\frac{u\, d_p}{D_B}$

Eddy Peclet number $\frac{u\, d_p}{D_L}$

This eddy Peclet number should probably be called the dispersion Peclet number, however, because the eddy diffusivity $D_L{}^*$ has not been separated from the dispersion coefficient D_L in this work the eddy Peclet or dispersion Peclet are interchangeable.

The Schmidt number based on the dispersion coefficient is recorded as the inverse Schmidt number in column 12, that is,

$$\frac{1}{\text{Schmidt}} = D_L \rho / \mu \quad .$$

At the base of each table the least square error fit of the HETP vs. u data to equation (1.50) is computed and the best values of the constants A, B and C are printed out. The span of certain runs was restricted to the eddy diffusion regime, and the scatter of the data points could cause anomalous values of the B, or molecular diffusion, term, which

was a relatively small quantity in this range. To offset this problem a second least squares computation is carried out on the data to fit the equation,

$$HETP' = AA + CCu \qquad (1.67)$$

where $HETP' = HETP - \frac{B}{u}$.

The value of B is set at 2 x .75 x D_B, where 0.75 represents the inverse of the tortuosity $1/\lambda$ in equation (1.49).

From the value of B derived from the three constant equation (1.50), the inverse of the tortuosity has been calculated for each run. Since λ varies from 1 to ∞ as discussed in the introduction, then the inverse ranges from 1 to 0. The usual value expected in a packed bed is about 0.67 to 0.8. The result printed on the computer sheet (Appendix III) is in the nomenclature originated by Van Deemter (17)and so the inverse tortuosity computed from equation 1.49 as $\frac{1}{\lambda} = \frac{2\ D_B}{B}$ is given under the heading GAMMA.

Similarly, the value of the constant characteristic of the eddy diffusivity which has been designated γ is computed from the value of the eddy diffusion term A using equation (1.49), that is $\gamma = A/2d_p$. Van Deemter et al (17) suggest that γ varies from about 8 for 200 mesh particles to about zero, for, say, 1/8 inch particles. The computer has printed the values of γ under the heading LAMDA (from Van Deemter et al.) in Appendix III.

Results for Beds of Non Porous Pellets

Some typical curves of the HETP vs. velocity are shown in Figure 1.10 and 1.11. Figure 1.10 shows the results for run 52 which covered both the molecular and eddy diffusion regimes while Figure 1.11 shows the results for runs 51, 69 and 70. The five straight lines shown

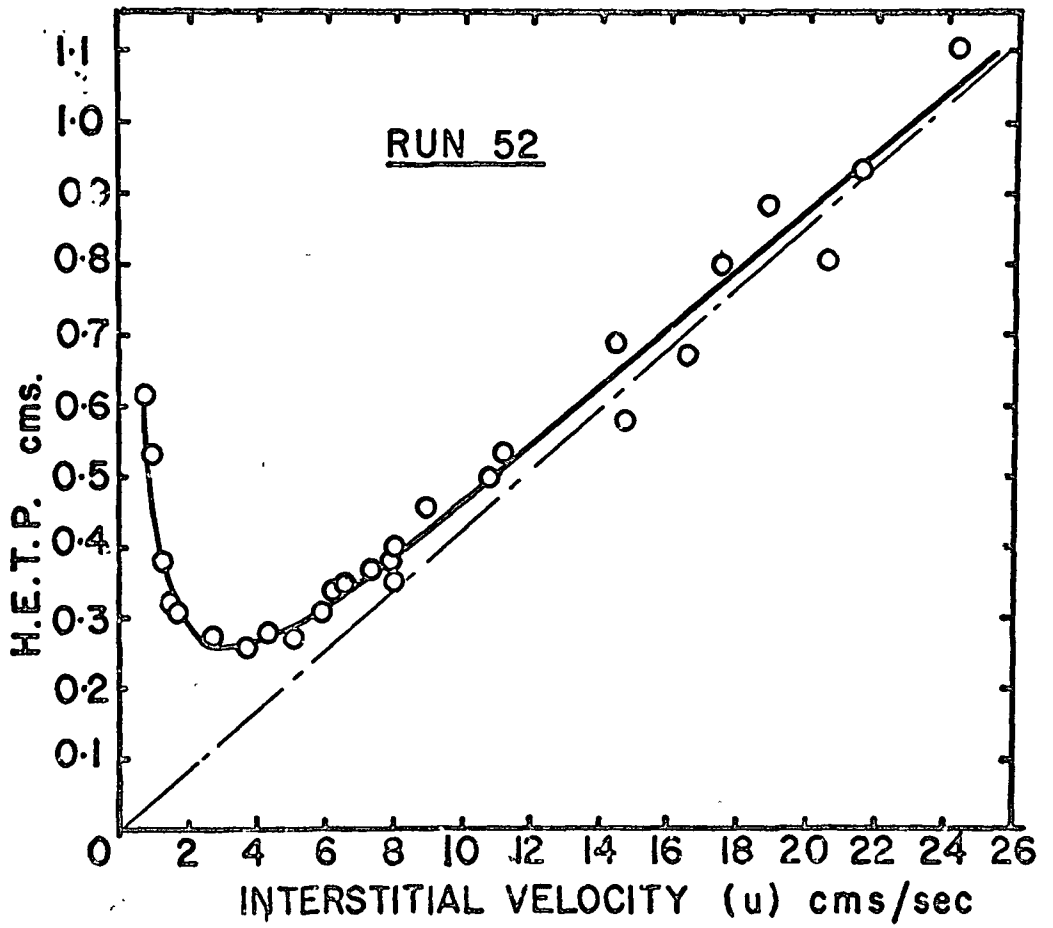

Figure 1.10

HETP Vs. Velocity For Run 52

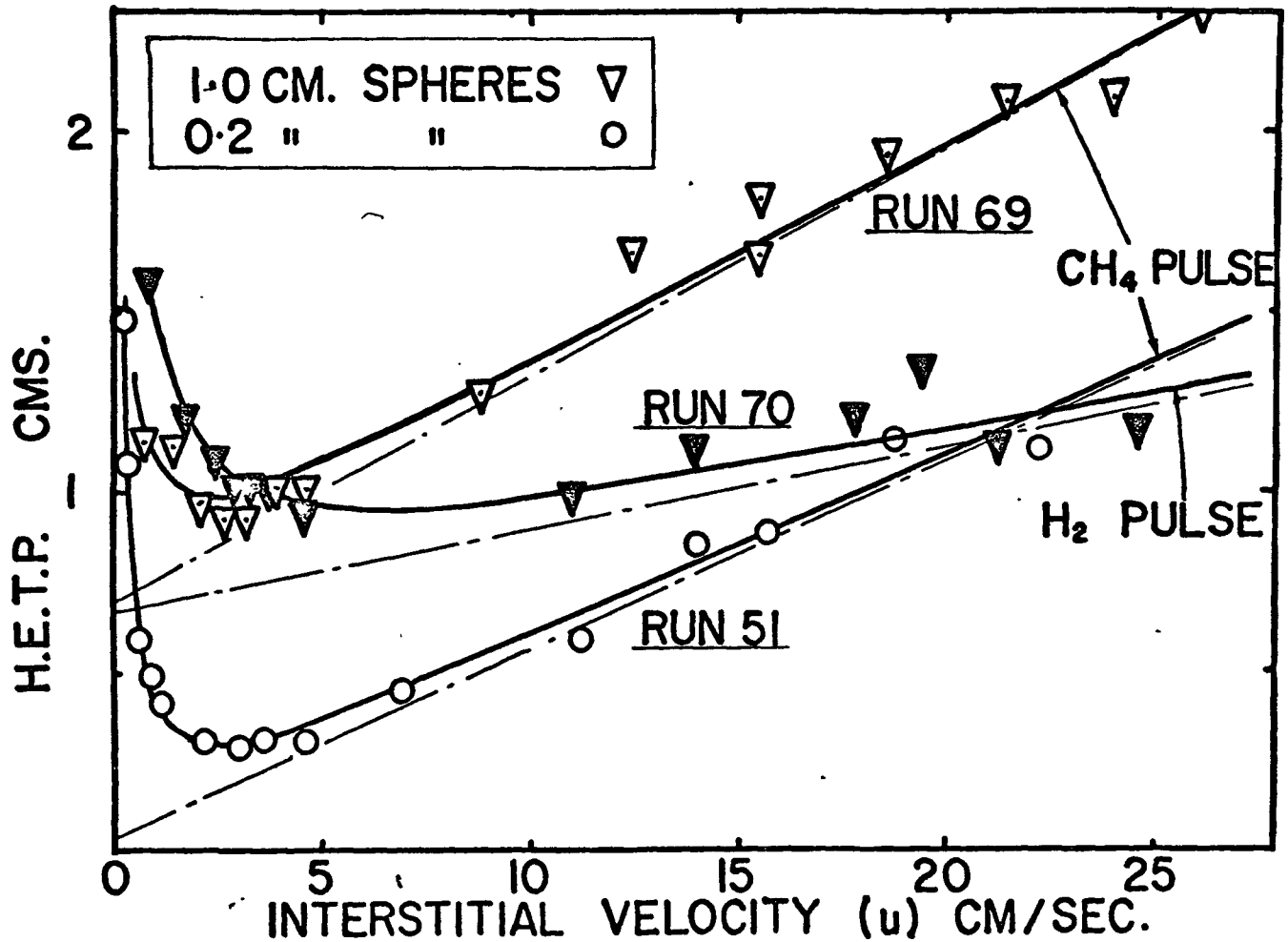

Figure 1.11

HETP Vs. Velocity For Runs 51, 69 and 70.

on the plots represent the equation HETP = A + Cu, using values of A and C determined from applying equation (1.50) to the data. Runs 69 and 70 were made in a bed with a tube to particle diameter ratio of 6 containing the 1 cm. spheres, but a methane pulse was used in run 69 and a hydrogen pulse in run 70. It may be noted that both sets of data have the same intercept, indicating that Van Deemter's definition of the eddy diffusivity given by $D_L^* = \gamma u d_p$ is valid, but a further mechanism which depends on the gas diffusivity and has a velocity exponent of 2 must be added to account for the presence of a "C" term.

Van Deemter et al (17) suggested that the eddy diffusivity term in equation (1.49), $A = 2\gamma d_p$, decreased with increase in pellet diameter, due to the decrease of the coefficient γ. In Figure 1.12 it may be noted that with the larger pellets and generally higher flow rates in this work the trend has been reversed, and "A" increases with pellet diameter. If a straight line is put through the points in Figure 1.12 a slope around unity is obtained, making $\gamma = 1/2$ corresponding to the value obtained by McHenry and Wilhelm (15) with gases at Reynolds numbers greater than 10.

Of the early runs, only run 1, which was carried out on a 134 cm. bed with a cyclopropane pulse in an air carrier gas stream is included in the data. The results of this run together with additional results from initial tests with methane pulses in beds of non porous pellets (runs 50 to 55) are summarized in Table 1.III. The most significant feature of these results is that over a range of pellet diameters from 0.2 cm. to 1 cm., with tube to pellet diameter ratios from 1 to 25, the wall effect or "C" term, which might mask the dispersion effect due to pellet porosity, gave results which varied in value only from 0.04 to 0.08.

In Runs 50 and 52 the C term calculated from tests in the lower Reynolds number range (run 50) is considerably higher than the value obtained in the same column at higher Reynolds numbers (run 52). This suggests that either the wall effect term is not constant or that the exponent of the velocity in the dispersion coefficient is less than 2. The plots of the dispersion coefficient vs. u given in Figure 1.13 would appear to substantiate the latter view.

Comparisons of Runs 51 and 51D demonstrate that artificial mixing devices or wall barriers do not reduce the wall dispersion effect.

No data in the regime in which molecular diffusivity is important were taken in run 51D, so that the comparison is best made using the CC value from run 51D, which was calculated using equation (1.65) as described previously. The value of B found from the results of run 51D represents a molecular diffusivity more than double the normal gas diffusivity (GAMMA = 2.07), demonstrating the failure of equation (1.50) when results in the eddy regime only are used in the least squares evaluation of the three constants A, B and C. Values obtained in run 54 also demonstrate this point.

The large diameter pellets in runs 53 and 55 show a large intercept, or A term, compared to the other runs which show essentially zero intercept. Inasmuch as A is approximately proportional to d_p, this difference is to be expected. It is rather interesting that a bed with a single pellet diameter (run 55) has essentially the same or less slope (i.e. C value) at high Reynolds numbers as the bed six particles in diameter of run 53. This, as well as other results given in Table 1.III, indicate that the dispersion due to the wall effect is not a function of tube diameters.

TABLE 1.III

DISPERSION RESULTS WITH BEDS OF NON POROUS PELLETS

Run	Pellet Diameter	Column Length	Column Diameter	Column to Pellet Diameter Ratio	A	B	C	AA	CC	Range of Reynolds Number
1	0.22	134.6	2.61	11.9	0.13	0.18	0.07			
50	0.208	111.8	5.0	24	-0.07	0.35	0.07	-0.28	-0.150	0.5 - 2.4
51	0.208	118.1	2.6	12.5	0.050	0.31	0.052	0.04	0.053	0.29 - 31.3
51 D	0.208	118.1	2.6	12.5	-0.27	0.87	0.071	-0.037	0.064	2.6 - 32.6
52	0.208	111.8	5.0	24	0.001	0.37	0.041	0.032	0.037	0.8 - 33.0
53	1.03	186.3	6.27	6.1	0.68	0.36	0.071	0.72	0.064	5.0 - 44.0
54	0.297	185.4	0.415	1.4	-0.22	3.88	0.079	0.177	0.069	16.0 - 79.0
55	1.005	121.0	1.15	1.1	0.601	0.16	0.060	0.260	0.122	3.0 - 48.0

Continued...

TABLE 1.III (Continued)

Run	Number of Points	Gamma	Remarks
1	10		
50	9	0.76	
51	15	0.73	
51D	8	2.07	Doughnut rings in column
52	30	0.87	
53	13	0.85	
54	10	9.24	Very small diameter (and hence plate volume) and high flow rates
55	10	0.37	

The experimental pulse injector shown in Figure 1.8 was used in run 53 on the six particle diameter bed containing 1 cm. spheres. Methane pulses are used and the effect of pulse size (as measured by peak height) at a particle Reynolds number of 62.4 is shown in Table 1.IV. Over a 13 fold range different pulse sizes resulted in essentially the same HETP values. It must be pointed out, however, that these values are not included in the data for Run 53. At the time when the data were taken a maximum particle Reynolds number of 35 was employed in the hope that Van Deemter's assumption regarding the eddy diffusivity could be extended to a Reynolds number of 35 without serious error. This limitation was later discarded, and the four points in Table 4 were included with those of Run 53. However, they were found to change seriously the constants of the least square equation (1.50), indicating an inconsistency. Run 60 repeated the conditions of Run 53, but employed the normal pulse injection, and these data were consistent with the results at low flow rates in Run 53, but not with the four points in Table 1.IV. It is concluded that the inconsistency was created by the experimental injector at high flow rates because of the failure of the pop valve in the injector to close cleanly. The requirements suggested by Van Deemter to ensure that the feed pulse size does not influence the exit distribution (equation 1.25) were easily satisfied in this work, particularly with a large diameter column such as that used in Run 53.

TABLE 1.IV

EFFECT OF PULSE SIZE (PEAK HEIGHT) ON HETP
at Particle Reynolds number of 62.4

Run 53 HETP	PEAK HEIGHT
1.65	27.5 units
1.66	59
1.75	56
1.59	19

TABLE 1.V

FURTHER DISPERSION RESULTS WITH BEDS OF NON POROUS PELLETS

Run	Pellet Diameter	Column Length	Column Diameter	Column to Pellet Diameter Ratio	Pulse	A	B	Inverse Tortuosity	C	AA	CC
63	0.568	421.0	0.66	1.16	H_2	0.11	1.88	1.25	0.019	0.51	-0.021
64	0.568	421.0	0.66	1.16	CH_4	-0.06	0.79	1.88	0.081	0.24	0.048
65	0.568	119.5	2.175	3.83	CH_4	0.12	0.37	0.901	0.057	0.18	0.049
66	0.568	119.5	2.175	3.83	H_2	0.12	0.87	0.59	0.027	-0.13	0.059
69	1.03	186.3	6.27	6.1	CH_4	0.70	0.32	0.76	0.063	0.703	0.063
70	1.03	186.3	6.27	6.1	H_2	0.68	0.86	0.57	0.023	0.54	0.030
71	1.005	122.0	1.15	1.1	H_2	0.31	1.14	0.79	0.028	0.34	0.027
72	1.005	122.0	1.15	1.1	CH_4	0.64	0.17	0.41	0.06	0.59	0.062

All Dimensions, cms.

Continued.....

Table 1.V (Continued)

Run	Range of Reynolds Numbers	Number of Points	Remarks
63	6 - 35	10	
64	6 - 33	9	
65	4 - 28	14	
66	0.6-125	20	
69	5 -180	16	
70	7 -130	13	
71	4 -183	14	
72	10 -181	12	

Table 1.V shows the later results with non porous pellets which extends the range of the earlier data, and allows comparison of the hydrogen pulse technique with methane pulse results. Once again the wall dispersion effects (C value) for the methane vary only from 0.057 to 0.081 with pellet sizes from 0.56 to 1.0 cms. For the hydrogen pulses, the value of the C term varied from 0.019 to 0.028 in the same beds. These data confirm the previous conclusions regarding the effects of tube diameter and pellet diameter.

Runs 63 and 64 show high B values (inverse tortuosity), indicating that insufficient data has been obtained in the molecular diffusivity region, and the AA and CC values are probably more meaningful than the A and C terms.

The values of AA and A for all the data are plotted versus pellet diameter in Figure 1.12, which indicates, in spite of considerable scatter, the approximately linear dependence of the packed bed eddy diffusivity on pellet diameter for a wide range of Reynolds numbers, as suggested by Van Deemter. The deviation from linearity could be ascribed to variation of the constant γ in Van Deemter's eddy diffusion expression. However, the data from this work aligns itself well with the typical values of γ quoted by Van Deemter (17), as shown in Table 1.6, except that the trend is reversed with larger pellets, and γ increases with pellet diameter.

TABLE 1.VI

VALUES OF THE EDDY DIFFUSIVITY TERM CONSTANT, $\gamma = \frac{u\, d_p}{D_L^*}$

	Pellet diameters cms.			γ
Van Deemter (17	.003	-	.0074	8
"	.015	-	.025	3
"	.035	-	.083	≈ 0
This work		.2		0.06
		.6		0.13
		1.0		0.37

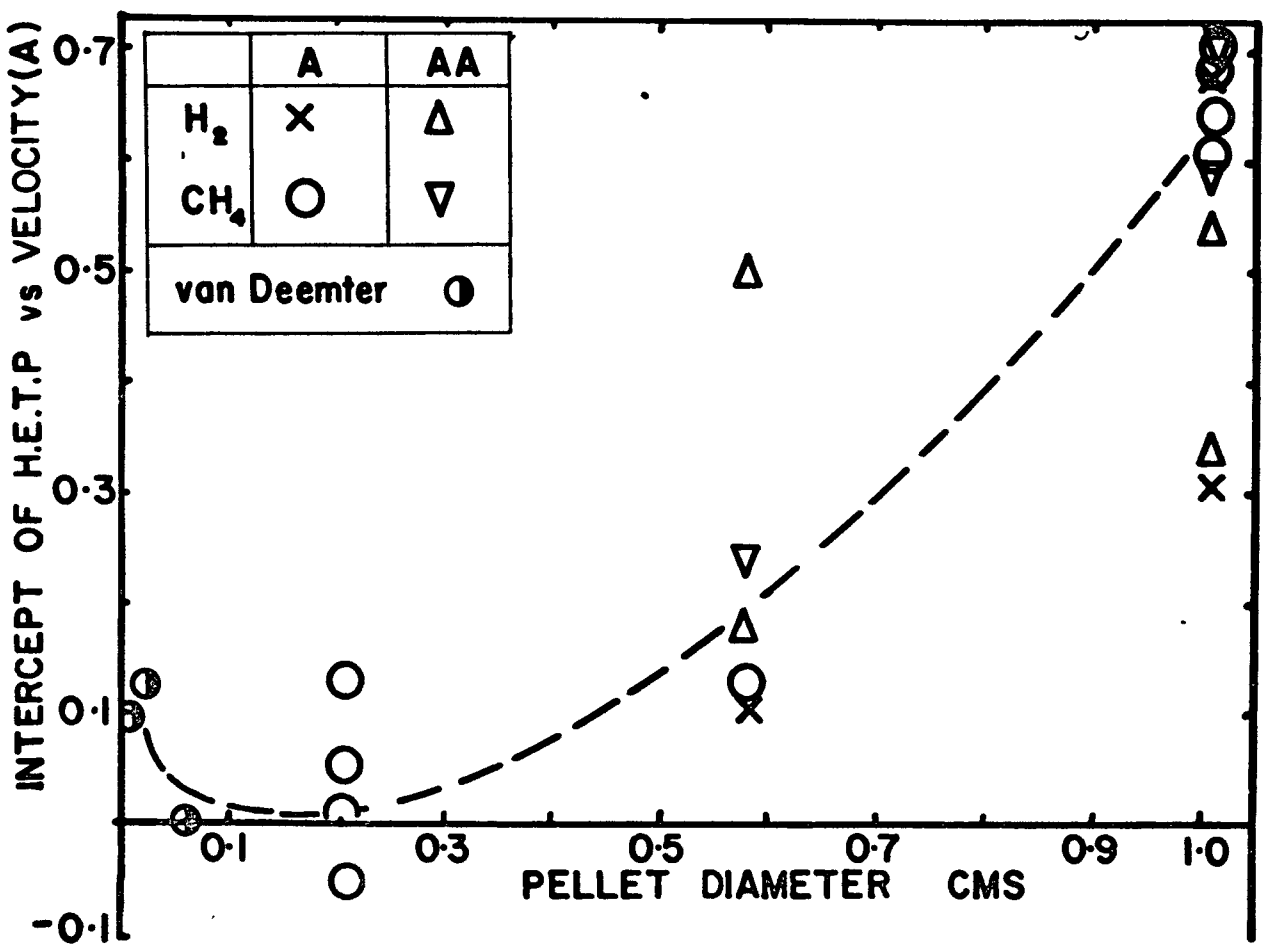

Figure 1.12

Eddy Diffusion Term, A, (Equation 1.50) Vs. Pellet Diameter

B. LONGITUDINAL DISPERSION COEFFICIENT

The data obtained in the beds of non porous pellets were computed as overall dispersion coefficients (that is, eddy plus molecular coefficients) and are compared with the correlations and theories of other workers in Figures 1.13, to 1.17. In Figure 1.13 all the data except those from run 1 are plotted as dispersion coefficients vs. the interstitial velocity (u). The data points form smooth curves but the slopes in the turbulent region vary, showing an exponential velocity dependence of 1.5 for the larger 1 cm pellets, increasing to an exponent of 2 for the smaller packing sizes. At low velocities, the dispersion coefficients approach the value of the molecular diffusivity. In Figures 1.14 - 1.17, the smoothed data from Figure 1.13 has been used, and is shown as a continuous curve with identifying symbols marking the start and finish of the line.

In Figure 1.14 the inverse dispersion Peclet number $\frac{D_L}{ud_p}$ is plotted vs. the superficial Reynolds number $u\epsilon_B d_p \rho/\mu$ to compare the results with those of McHenry and Wilhelm (15) obtained by the frequency response method in a bed of 0.3 cm diameter spheres. The data from this work are not entirely consistent with McHenry and Wilhelm's, but the lack of agreement is probably due to a difference in the Schmidt number since McHenry and Wilhelm used a 50% hydrogen stream while the pulses in this work used only a trace of hydrogen. The Reynolds number above is thus not a complete criterion, particularly in the transition flow regimes as pointed out by Hiby (24). The data of Cairns and Prausnitz (34) for liquids are also included in Figure 1.14. Hiby (24) suggested that at low flow rates (approaching the molecular regime) the inverse dispersion Peclet number is better plotted against the molecular Peclet numbers as shown in Figure 1.15. Unfortunately the molecular Peclet numbers could not be calculated from McHenry and Wilhelms' publication without access to

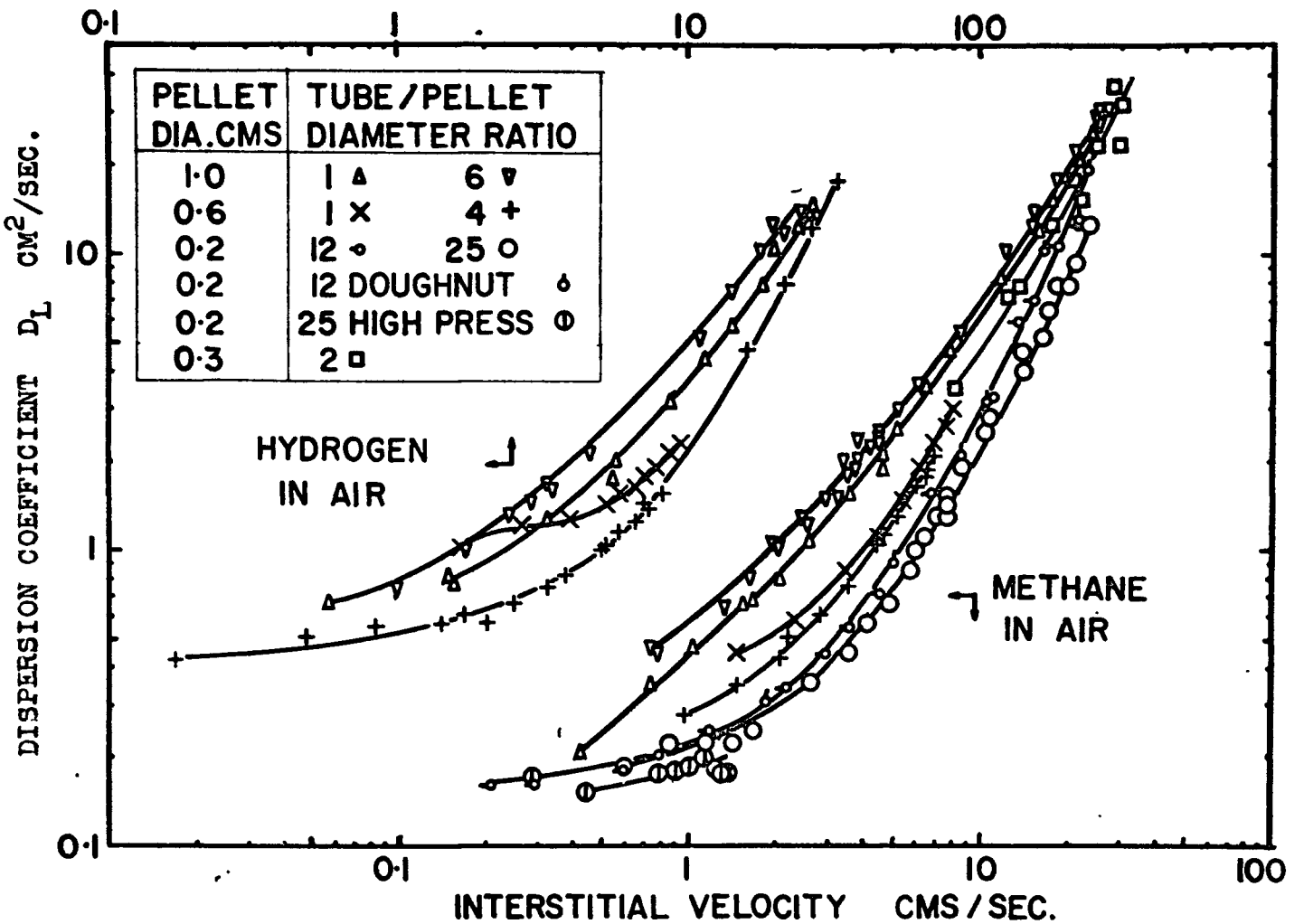

Figure 1.13

Dispersion Coefficient, D_L Vs. Interstitial Velocity, u.

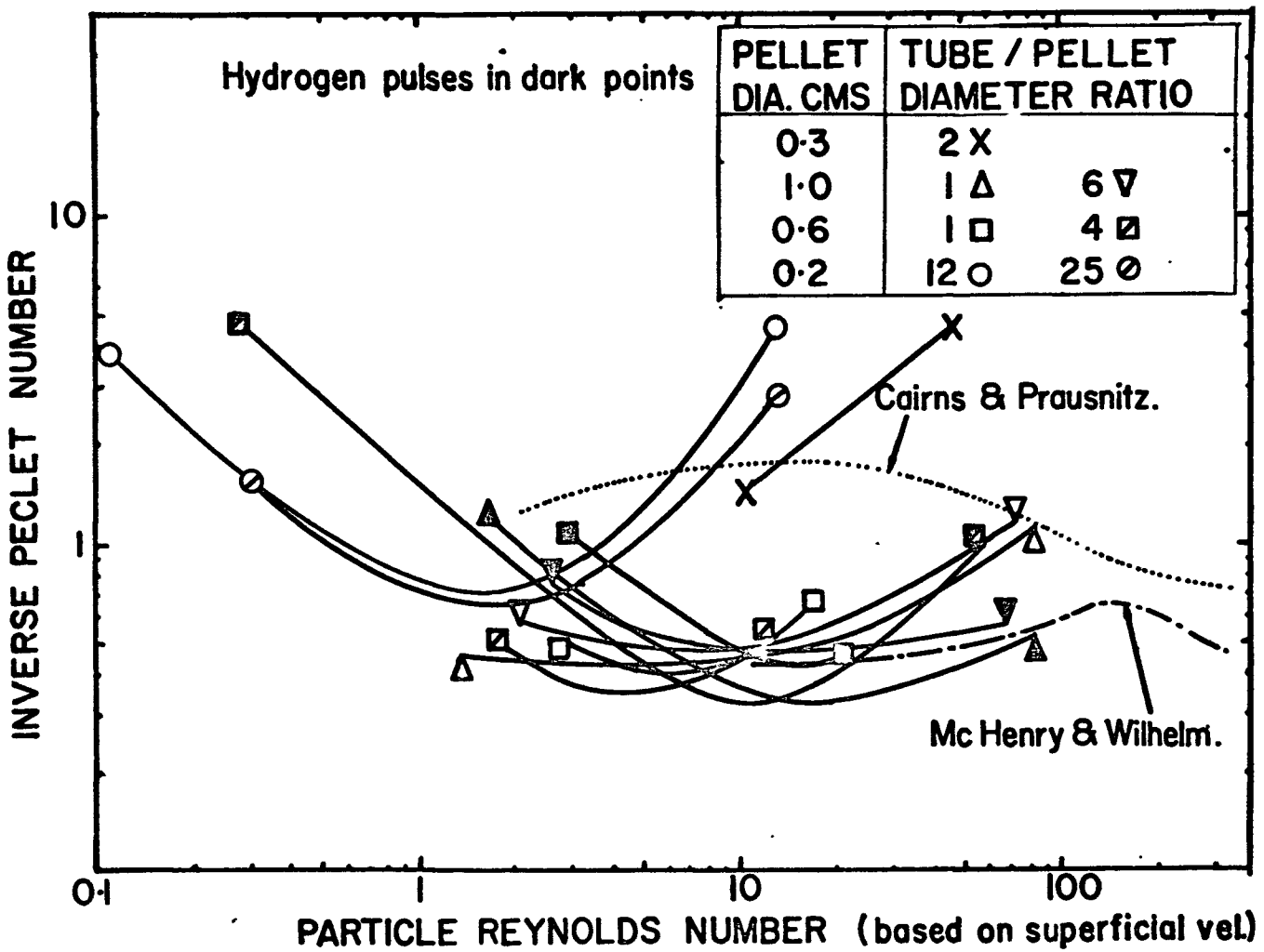

Figure 1.14

Inverse Eddy Peclet Number Vs. Superficial Reynolds Number

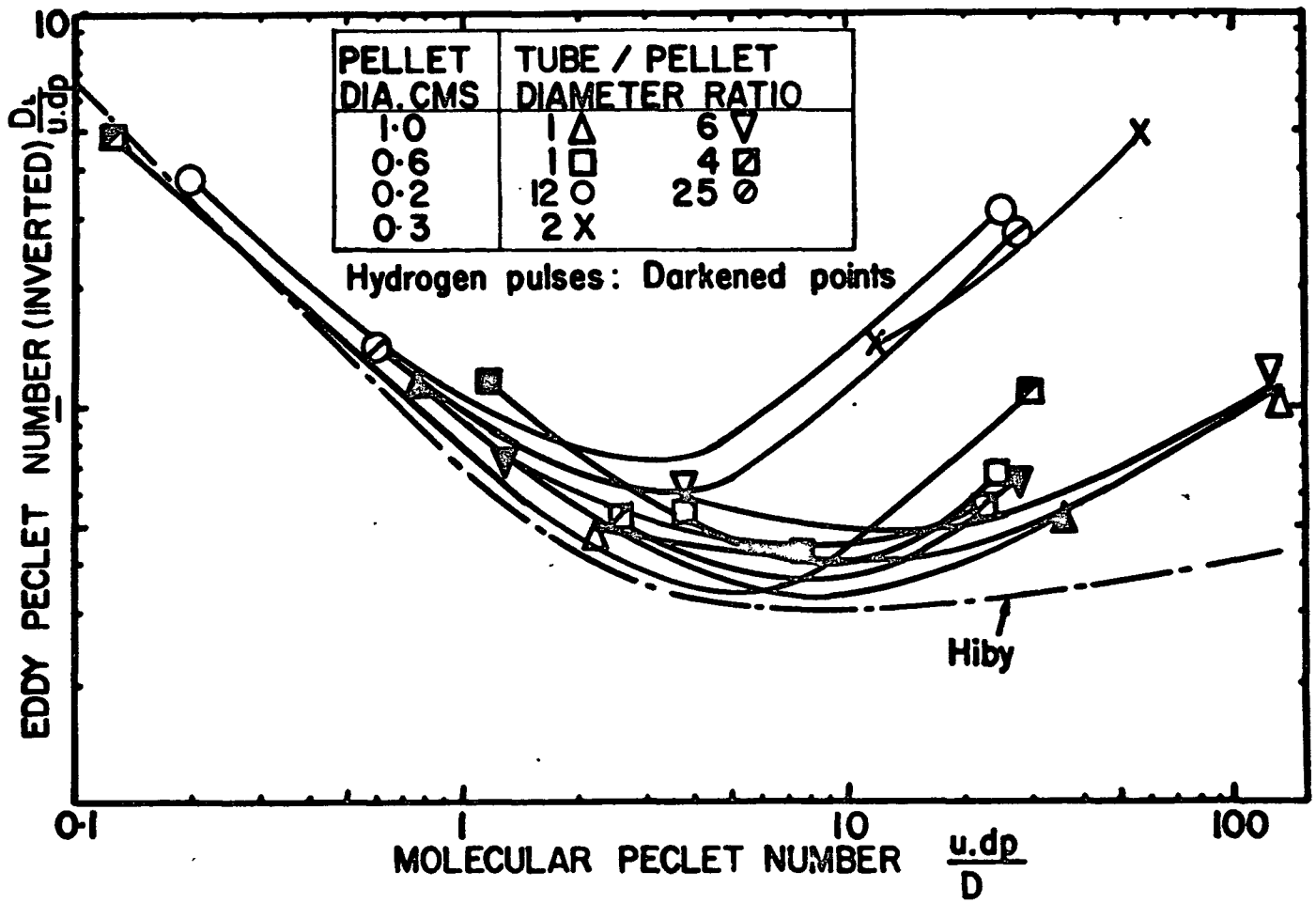

Figure 1.15

Inverse Eddy Peclet Number Vs. Molecular Peclet Number

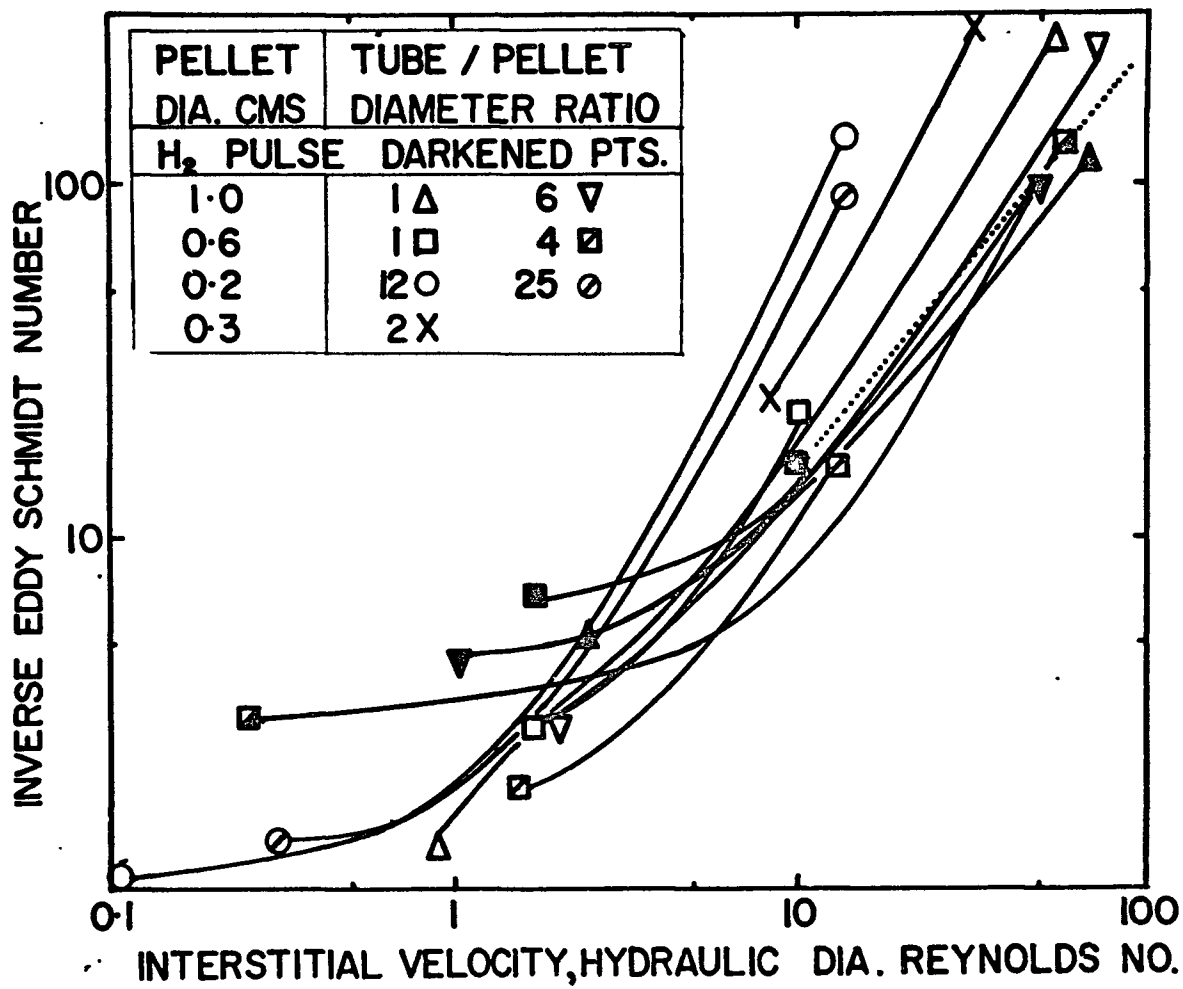

Figure 1.16

Inverse Eddy Schmidt Number Vs. Hydraulic Diameter Reynolds Number

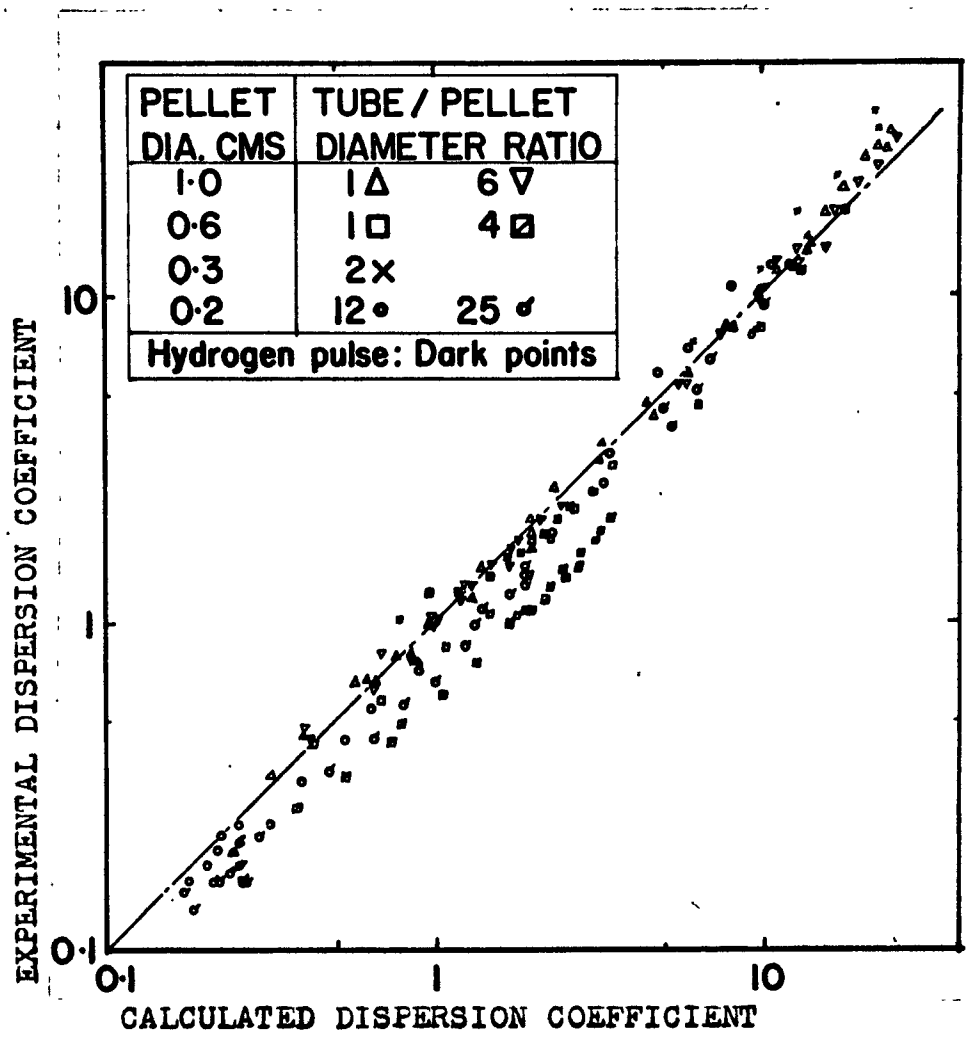

Figure 1.17

Empirical Dispersion Coefficient Correlation

primary data and so a comparison could not be made, but it may be noticed that in Figure 1.15 the results from this work are not so scattered as in the previous illustrations. The data for liquids published by Hiby (24) are also included in Figure 1.15, but the values are lower than the results from this work. This decrease was to be expected because Hiby took pains to eliminate the high porosity wall section, and thus remove the dispersion due to wall effect. It is also significant that Hiby considered the results of McHenry and Wilhelm to show lower values of the eddy diffusivity or dispersion coefficient than would be expected in a bed with wall effects.

In Figure 1.16, the correlation suggested by Bischoff and Levenspiel (28) is examined by plotting the data as inverse dispersion Schmidt number vs. the Reynolds number based on hydraulic diameter. The covergence of the data is no better than in the other plots.

The Saffman model (29) could not be tested because the boundaries of the dispersion regimes in packed beds are not known as they are in the case of dispersion in pipes. However, it would appear that the Saffman model may have the greatest potential in providing a correlation for eddy diffusion in packed beds.

In the absence of a more logical correlation, an empirical correlation has been developed below, which is an extension of the simpler form proposed by Bischoff and Levenspiel (28).

$$D_L = 0.75\, D_B + 0.6\, u\, h_D + \frac{0.02\, u^2\, h_D^{0.6}}{0.75\, D_B + 0.022 u\, h_D} \qquad (1.68)$$

This correlation is plotted in Figure 1.17 as experimental vs. calculated values of axial dispersion coefficient, and although the agreement is not good, the method is sufficiently accurate to allow a correction to be calculated for the "C" term in equation (1.50), which will correct the value of this term in porous pellet tests where any effects of eddy dispersion are not allowed for in the eddy diffusion, or "A", term.

C. POROUS PELLETS

Porous Pellet Samples

The properties of the three porous pellet samples tested are summarized in Table 1.VII. However, there was originally some question about the pellet properties, the details of which are discussed in Appendix III. A knowledge of the pellet porosity is essential for this work, but the manufacturers' data supplied with the pellets seemed to be somewhat inconsistent.

The data on the 1/2" Norton catalyst support pellet were generally satisfactory. However, in the trade literature a 41% porosity was quoted for these pellets. In a private communication, a value of 36-40% was given, and a simple experimental measurement described in Appendix III found a 36% porosity. A value of 38% has thus been accepted as a reasonable average.

With the activated alumina pellets, in addition to the inconsistency of the manufacturer's and supplier's data, the amount of moisture contained in the pellet presented a problem. As discussed earlier, the epoxy resins used to mount the test pellet in the steady state diffusion apparatus

TABLE 1.VII

PROPERTIES OF POROUS PELLET SAMPLES

Manufacturers' Trade Description	Pellet Diameter	Pellet Porosity	Pellet Moisture Content in 60% RH Air	Porosity of Moist Sample	Pore Diameter	Solid Density gm/ml
1/2" Norton Catalyst support SA 203 mixture	1.30 cm.	0.38	negligible	0.38	90% of pores 2-40 microns	3.5
1/4" Alcoa activated alumina H 151	0.597 cm.	0.50	12%	0.31 at 12% wet 0.34 at 10% wet	50 Å	3.2
1/8" Alcoa activated alumina H 151	0.32 cm.	0.50	12%	0.31 at 12% wet	50 Å	3.2

could not stand the drying temperature necessary, and so it was decided to make the diffusion tests on the wet pellets. The moisture content of the wet pellets was found to be stable, and not sensitive to atmospheric humidity, remaining between 10-14% by weight. In addition, the manufacturer's literature (31) suggested that adsorbed water existed in liquid form, so that if the dry pellet porosity could be found, the porosity of the wet pellets could be calculated.

The suppliers quoted a dry pellet porosity of 60-65%, while the manufacturer's literature stated 50%. The moisture content in equilibrium with 60% R.H. air was given as 20-24%, but at no time could more than 15% water actually be found in the pellets. Examination of some of the manufacturer's drying data indicated that after 6 months a 12-15% moisture content was normal. In order to obtain a better value of the dry pellet porosity, special measurements were carried out. One of the experiments for this purpose described in Appendix III involved putting pellets under vacuum and then flooding them with water. This test suggested that the 50% porosity was correct, and this value was later verified more exactly by placing dry pellets in a chromatograph sample loop, and measuring the resulting reduction in sample volume of the loop. Hydrogen gas was used at the sample gas in the loop. This experiment gave a 50% porosity for the dry pellets and yielded 28% and 33% porosities for wet pellets having a 12% moisture content. A porosity of 31% corresponds to a 50% dry porosity in a pellet containing 12% by weight water in the liquid state.

In addition, the alumina pellets are not homogeneous in that they are apparently manufactured by seeding a colloidal solution. Examination of a slice of pellet on a microscope slide showed pores up to 150 microns in the centre core, compared to a pore diameter of 50Å in the

outer shell. These pellets provide an excellent example of an instance in which the steady state method of measuring diffusivities would give a poor result for use in catalysis work, while the unsteady state method would yield an average diffusivity value which would be more likely to be suitable.

Steady State Apparatus Results (Appendix I)

The effective diffusivity of hydrogen and nitrogen in 1/2" Norton SA203 spheres was found to be 0.0667 $cm^2/sec.$ at 23°C and 760.7 mm. Hg.

The effective diffusion coefficient of hydrogen in 1/4" diameter Alcoa H151 activated alumina pellets containing 12% by weight of water was found to be 0.0067 $cm^2/sec.$ at 26°C.

Treatment of Data for Pulse Apparatus

For the porous pellets, the same measurements and computations are recorded in Appendix II as for the non porous pellets, except that the eddy diffusivity calculations in columns 8, and subsequent columns are omitted. Column 3 contains the inverse velocity rather than the molecular Peclet number which was used with the non porous pellet results.

Equation 1.50 was fitted to the data, and the quantity C found thereby was corrected using the differential of the last term of the empirical correlation equation (1.68) to remove the eddy diffusivity contribution as follows,

$$\text{Correction} = \frac{dHETP}{du} = \frac{0.3\ D_B\ h_D^{\ .66}}{(0.75\ D_B + 0.2\ u^*\ h_D)^2} \qquad (1.69)$$

where u* is the mean velocity from all the data points and allows the correction to be made in the middle of the velocity range of interest.

The correction is subtracted from the slope C and the corrected slope C applied in the calculation of the effective diffusivity from equation 1.49 and 1.50 using the form,

$$D_E = \frac{\epsilon_B}{2\, C_{CORR}(1 - \epsilon_B)} \left[\frac{d_p}{\pi \left(1 + \frac{\epsilon_B}{\epsilon_p (1 - \epsilon_B)}\right)} \right]^2 \qquad (1.70)$$

Porous Pellet Results

In Table 1.VIII, runs 56 to 62 were made with 1/4" Activated Alumina pellets, except run 60 which was made with the 1/2" Norton Catalyst support, and run 73 in which the 1/8" Activated Alumina pellets were used. All the results were taken in single pellet diameter beds, except run 73 which used a bed having a 7:1 diameter ratio.

Runs 56 and 57 differ only in the length of column, while in 58 the same bed was used as in 57, except that the pellets were dried. Run 59 was essentially unsatisfactory, but it shows the results of an attempt to eliminate the adsorption effect with extremely high flow rates. Run 61 repeated 58, and 62 repeated 57, except that hydrogen pulses were used. The hydrogen pulse was also used in run 73. Run 60 employed a methane pulse in the single pellet diameter bed packed with the 1/2" Norton Catalyst supports.

The results for porous pellets are summarized in Table 1.VIII. It may be noted that there appears to be an end effect in comparing runs 56 and 57. However, under Table 1.VIII the values of the criterion for Gaussian dispersion, $\frac{F_1 u}{\alpha}$ are given, and for run 56 these are greater than the column length due to the large dispersion caused by the adsorption of the methane pulse. Thus Van Deemter's solution (17) to obtain equation (1.31) would not hold.

The effects of adsorption on a catalyst pellet have been mentioned in section C of the introduction under "Comparison of Methods". The adsorption of methane on dry Alcoa 1/4" Activated Alumina pellets was

TABLE 1.VIII

DISPERSION RESULTS FOR POROUS PELLETS

Run	Pellet	Moisture Content wt., %	Pellet Porosity	Column Length Cm.	Column Diameter Cm.	Pulse Gas	Pellet Diameter	A	B	C
56	1/4" activated Alumina	12	0.31	129	0.66	CH_4	0.597	-0.26	-0.64	1.32
57	1/4" activated Alumina	12	0.31	421	0.66	CH_4	0.597	-0.22	0.58	1.61
58	1/4" activated Alumina	0	0.50	421	0.66	CH_4	0.597	-2.2	4.65	1.699
59	1/4" activated Alumina	0	0.50	421	0.66	CH_4	0.597	68	-592	-0.33
60	1/2" Norton Catalyst Support	-	0.38	420	1.6	CH_4	1.3	0.29	0.50	0.44
61	1/4" activated Alumina	0	0.50	421	0.66	H_2	0.397	0.64	0.87	0.22
62	1/4" activated Alumina	10	0.34	421	0.66	H_2	0.597	0.38	1.5	0.237
73	1/8" activated Alumina	12	0.31	119.4	2.17	H_2	0.32	-0.015	1.43	0.096

Continued.....

Run Number	Height of Transfer Unit $\frac{F_1 u}{\alpha} < L$ at max. velocity
56	166 cm.
60	3.38 cm.
61	20.2 cm.
73	5.38 cm.

TABLE 1.VIII (Continued)

Dispersion Results for Porous Pellets

Run	Slope Correction	Corrected Slope	Diffusivity	Diffusivity Assuming Equilibrium Adsorption	Bed Porosity	Reynolds Range
56	0.061	1.26	0.00085		0.471	3-48
57	0.062	1.54	0.00069		0.471	2-42
58	0.061	1.63	0.0012	0.0045	0.471	2-42
59	0.019	0.31	--		0.471	47-318
60	0.12	0.32	0.0193		0.522	5-33
61	0.019	0.20	0.0102		0.471	3-95
62	0.019	0.22	0.0056		0.471	7-86
73	0.017	0.079	0.0045		0.39	1-19

measured, and the procedure, which involved taking pressure and volume measurements of a gas pellet sample trapped in the leg of a mercury manometer is described in Appendix IV. The results of this experiment, which showed methane adsorbed to the extent of 1.37 mls/ml of pellet, are utilized in run 58 to calculate the effective diffusivity assuming equilibrium of the adsorbed gas in the pulse apparatus. If equilibrium had been attained, then the diffusivity calculated with the increased capacity due to adsorption in the pellet taken into account, should be equivalent to the diffusivity found in run 61 using a hydrogen pulse with dry pellets (after correcting for the different gas system).

In Table 1.IX the diffusivities adjusted to those equivalent to hydrogen diffusion are compared for all the runs. The effective diffusivity with a hydrogen pulse in run 61 lies between the two diffusivities calculated from run 58 with the methane pulse, (a) assuming no adsorption and (b) assuming equilibrium adsorption. This result would indicate that the methane probably does not approach equilibrium adsorption closely in the pulse apparatus.

The values of the constants A and B from equation 1.50 presented in Table 1.VIII would appear to represent a breakdown of the theory and/or an inconsistency with the results from the eddy diffusion runs with non porous pellets, but if the fact that the C terms are extremely large due to the adsorption of methane in runs 56 to 58 is considered, then the A and B terms are negligible, and correction of them has very little influence on the slope, or C, term. For the remaining runs, the C terms are smaller but at the same time the values of the A and B terms are within the expected range.

TABLE 1.IX

COMPARISON OF EXPERIMENTAL EFFECTIVE DIFFUSION COEFFICIENTS

Diffusivities cm^2/sec units

Run	Pulse Gas	Pulse Method Experimental Result	Factor to Convert to Hydrogen or H_2-N_2 Diffusivity	Result as a Hydrogen Diffusion	Assuming Adsorption at Equilibrium	λ from Column 5	Steady State
56	CH_4	0.00085	$\sqrt{\frac{16}{2}}$	0.0024			0.0067
57	CH_4	0.00069	$\sqrt{\frac{16}{2}}$	0.00195		3.02	0.0067
58	CH_4	0.00127	$\sqrt{\frac{16}{2}}$	0.0036	0.017	2.64	
60	CH_4	0.0193	$\frac{0.750}{0.208}$	0.0694		4.14	0.067
61	H_2	0.0102	1	0.0102		0.93	
62	H_2	0.0056	1	0.0056		1.05	0.0067
73	H_2	0.0045	1	0.0045		1.31	0.0067*

*For 1/4" pellets

Interstitial Diffusivities

D_B Nitrogen and Hydrogen = 0.755 $cm^2/sec.$ at 1 atm. and 296°K

D_K Hydrogen in 50 A pores at 296°K = $\frac{2}{3} \times \frac{25}{10^8} \times 1.84500 \times \frac{296}{273}$ = 0.019 $cm^2/sec.$

Comparison of Steady State and Pulse Apparatus Results

In order to compare results, Table 1.IX presents the pulse data converted to the equivalent hydrogen diffusivity (or hydrogen-nitrogen for bulk diffusion). If the results with the 1/2" Norton pellets in run 60 are examined, it is seen that the pulse method agrees with the steady state value within 4%.

Run 62 should give the same diffusivity for hydrogen in the 1/4" Alcoa activated alumina pellets as the steady state apparatus, but the latter result is 20% higher than the pulse result. If the diffusivity in the 1/8" pellets could be expected to be the same as that in the 1/4" size, the steady state result is 52% higher than the result from run 73. In view of the lack of homogeneity of the alumina pellets these results are not surprising.

The pellet tortuosity values calculated from the true interstitial diffusivities and the pellet porosities shown below Table 1.IX also indicate that the Alcoa activated alumina pellets are not homogeneous, as the tortuosities are much lower than would be expected for this type of material. The steady state results should be even more influenced by the macroporous pellet centre or seed because of the removal of part of the microporous shell, and if the tortuosity is calculated from the steady state result an impossible value of 0.88 is obtained. The reason for this anomalous result is because the pore size has been assumed to be 50A in the calculation of the Knudsen diffusion coefficient, when in fact the centre core has some pores up to 150 microns in diameter as measured under a microscope.

VI

DISCUSSION

A. NON POROUS PELLETS

HETP vs. Velocity Results

The HETP vs. velocity curves shown in Figures 1.10 and 1.11 appear to fit Van Deemter's equation (1.50)well. However, a velocity dependent, or Cu term, was not to be expected with non porous pellets on the basis of Van Deemter's analysis. From Figures 1.10 and 1.11, as well as from the results in Tables 1.III and 1.V, the magnitude of this term can be seen to be independent of particle diameter, but inversely proportional to the molecular diffusivity of the gas system. If the Cu term (which is a velocity dependent axial dispersion effect) in non porous pellets is caused by the higher velocity annulus which results from the high packing porosity at the wall, then by analogy with Van Deemter's treatment, the relative velocity between the flow in the wall annulus and in the packing core could create a term which would be inversely proportional to the molecular diffusivity. This reasoning implies that this additional dispersive effect for non porous pellets is caused by a wall effect.

On the other hand, the above model becomes less satisfactory if single pellet diameter beds are considered, so it would appear that another but similar mechanism occurs in single pellet beds, or that the above physical explanation is questionable.

The intercept, or A term, (which is a dispersion due to the mixing effect of the packing) of equation (1.50) depends on pellet diameter at Reynolds numbers less than 1, according to Van Deemter et al (17), and a similar relationship for high Reynolds numbers based on the mixing stage model has been obtained by McHenry and Wilhelm. The results from this

work as shown in Tables 1.III and 1.V, and in Figure 1.12, also show that the intercept A is an approximately linear ($\pm$ 50%) function of the packing diameter for diameters from about 0.2 to 1 cm., and for a wide range of tube: pellet diameter ratios.

Axial Dispersion Coefficient

If the same data as above are considered in terms of the dispersion coefficient (i.e. the data for non porous pellets are not fitted to equation (1.50)) as defined by equation (1.66), then it would appear that the wall effect is not the major contribution to the mixing due to packing geometry.

Figure 1.13 shows that the smaller pellets tend to yield a dispersion coefficient proportional to the square of the velocity which would correspond to the Cu term in equation 1.50, but the larger pellets show a lower exponent of 1.5. Hiby (24) obtained the following empirical correlation for liquids,

$$D_L = 0.67\, D_B + \frac{0.65\,(u\, d_p)^{1.5}}{7\sqrt{D_B} + \sqrt{u\, d_p}}$$

and at low flow rates where $7\sqrt{D_B} > \sqrt{u\, d_p}$ this expression has a velocity exponent to the 1.5 power. In the same work (24), the results of other workers with liquids are summarized. In general, the axial dispersion coefficient found by other workers is a little larger than that obtained by Hiby, who eliminated the wall effect, but Hiby points out that the data of McHenry and Wilhelm, who worked with gas systems, gives the appearance of having the wall effect removed. This effect may be due to the fact that end corrections were applied to the bed data by McHenry and Wilhelm, because in their work relatively short beds were used (1', 2' and 3' long), with only the largest being comparable to the bed lengths in the present work.

In Figure 1.14, it may be seen that the data from this work shows higher dispersion coefficient values than does that of McHenry and Wilhelm (15), so that the data from this work would appear to be consistent with those of Hiby (24).

The use of the hydraulic diameter to describe the system as proposed in Bischoff and Levenspiel's work (28), and as shown in Figure 1.16, does not appear to improve the correlation. The hydraulic diameter would only be expected to account for the wall effect, and if the wall effect is not predominant, as suggested by Hiby, then a major improvement in correlation would not be likely to result.

As mentioned in the "Theory", Saffman's model (29) of a series of interconnected cylindrical capillaries would appear to show the most potential for describing the longitudinal dispersion in a packed bed. Since the results presented here were generally obtained between particle Reynolds numbers of 1 and 100 (i.e. in the intermediate region between laminar and turbulent flow), then it is quite conceivable that a velocity profile mechanism equivalent to that described by Taylor (25) occurs, resulting in regions where the dispersion coefficient is proportional to the squares of the velocity and inversely proportional to the molecular diffusivity.

The upper limit of the region was found to be, from (1.57)

$$u \ll 10\ L\ D_B/R^2$$

where u is the gas velocity, L the tube length, R the radius and D_B the molecular diffusivity.

Let the capillary length be $K_1 d_p$ and radius $K_2 d_p$ in the Saffman model, which should be a reasonable assumption for packings of uniformly sized spheres.

Then,

$$u \ll \frac{10\, K_1 d_p\, D_B}{K_2 d_p^2}$$

$$\text{or} \quad u \ll K_3 \frac{D_B}{d_p}$$

where $K_3 = K_1/K_2$

Thus, the smaller the pellet diameter, (d_p), the larger the right hand side of the above equation.

This model would explain therefore, why the smallest pellets showed a velocity exponent of 2 as compared to 1.5 or 1.7 for the larger pellets. A large molecular diffusivity would also increase the upper limit of the region, and may explain why a maximum is seen in McHenry and Wilhelm's results at a superficial Reynolds number of about 100 in Figure 1.14.

It would appear that at least two mechanisms are operating here; 1.) the velocity dependent dispersion described by equation (1.55) which is caused by the difference in flow paths between adjacent parts of the bed, and which can also be described by the mixing stage theory, and 2.) the effects of velocity profile (equation 1.56) in the individual channels, which yield a velocity exponent of 2 within the flow limits derived by Taylor, given in equation (1.57). Thus, the resultant dispersion coefficient has a velocity exponent between 1 and 2. As pointed out above, a high molecular diffusivity would result in a higher upper limit of significance for the velocity profile range. Nevertheless, McHenry and Wilhelm's results for eddy diffusivity using hydrogen approach a velocity dependence of 1, possibly because although the molecular diffusivity is high, the magnitude of the contribution to the dispersion due to the velocity profile in the capillaries is smaller with higher diffusivity

gases (equation 1.56), and so the mechanism of equation (1.55) would predominate.

In pipes, when the flow becomes turbulent, the profile contribution changes from the velocity squared dependence of equation (1.56) to a function of velocity and friction factor. In this turbulent region, the dispersion coefficient is independent of the molecular diffusivity and the same independence would be expected in a packed bed.

Correlation of the Axial Dispersion Coefficient

As may be seen from Figures 1.13 to 1.16, several attempts were made to obtain a correlation for the dispersion coefficient. In addition to these efforts, dimensional analysis and a least square calculation based on the resulting expression using all the non porous pellet results yielded the following correlation,

$$\frac{D_L}{u\ h_D} = \frac{1}{0.495} \left[\frac{u\ h_D}{D_B}\right]^{0.61} \left[\frac{u^2}{g\ h_D}\right]^{0.24} \left[\frac{\mu}{h_D\ u\ \rho}\right]^{0.41} \qquad (1.70)$$

where μ and ρ are the carrier gas viscosity and density. The above correlation shows an exponent for the hydraulic diameter of nearly unity, and a velocity exponent of 1.67, which is an average of the values shown in Figure 1.13. Equation (1.70) does not provide a particularly good fit to the data, which is not surprising because the velocity exponent is obviously not constant, a fact clearly evident in Figure 1.13. Of the correlations of the above type, that of Hiby recommended for the transition region and shown in Figure 1.15 seems to be most satisfactory, but due to a dependence on the packing diameter squared, the degree of correlation is less satisfactory than that given by equation (1.70).

Bischoff and Levenspiel (28) suggest the following expression, which does have the virtue of allowing for the experimental fact that the

velocity dependence is 2 for small pellets and approaches 1.5 for larger ones. The expression is based on the Taylor transition regime in which velocity profile effects are significant, but the molecular diffusivity is replaced by a radial diffusivity which includes a velocity dependent term.

$$D_L = \frac{D_B}{\lambda} + \left[\frac{K_1 u^2 d_p^2}{\frac{D_B}{\lambda} + K_2 u d_p}\right]$$

Although better than equation (1.70), a further considerable improvement in fit was achieved by reducing the packing diameter exponent from 2 to 1. However, the equation then becomes dimensionally inconsistent.

The correlation finally utilized essentially makes the longitudinal dispersion coefficient a summation of a molecular term, a mixing stage term as suggested from McHenry and Wilhelm's work (15) and a velocity profile term as suggested by Taylor (25) or by Saffman's model (29).

$$D_L = 0.75\, D_B + 0.6\, u\, h_D + \frac{0.02\, u^2\, h_D^{0.6}}{(0.75\, D_B + 0.0212\, u\, h_D)}$$

The above expression is plotted in Figure 1.17 as experimental vs. calculated results.

B. POROUS PELLETS

The effect of gas adsorption on the measured diffusivity presents interesting features of significance in any type of unsteady state diffusion measurement. The method used to measure the degree of adsorption, described in Appendix III, has been developed since this work was done and reported as a technique for determining adsorption isotherms for gases on solids (40). If the amount of gas adsorbed from a methane pulse were close to equilibrium, methods of estimating the diffusivity could still be worked out. Unfortunately, the adsorption is not indicated to be at equilibrium on the alumina pellets in this work, but as the adsorption data were derived for large concentrations (1 atm.) of methane, while the pulse apparatus uses trace concentrations in the presence of air, the state of the

equilibrium cannot really be claimed to be conclusively known.

Inconsistency of Steady State and Pulse Results for Activated Alumina Pellets

The results of runs 62 and 73 with 1/4" and 1/8" activated alumina illustrates the potentially serious errors possible with non homogeneous pelleted materials in measuring the unidirectional diffusion through a part or all of a pellet, as, for example, in the steady state apparatus, when in the actual reaction diffusion occurs towards the centre and out again. There are, of course, other potential reasons for differences in the results from steady state and pulse methods, which have already been discussed.

The pulse method in this work maintains either bulk equimolar counter diffusion or Knudsen diffusion in the pellet so that equation 1.13 is valid no matter what mechanism occurs. In the case of the alumina pellets, the outer shell has a uniform structure with 50°A pores so that Knudsen diffusion occurs, and settles the choice of equation for the steady state apparatus. Thus, the discrepancy between the steady state and pulse apparatus must be caused largely by the macroporous seed which carries a disproportionately large portion of the diffusion flux in the steady state apparatus.

The 1/4" alumina pellets were examined under a microscope and the seed in the centre was seen to be approximately 1/8" across with pores up to 150 microns, as compared to the 50°A pore size in the deposited outer layer. The seed in the 1/8" pellets was not visible by eye and it is possible that these pellets either had an extremely small seed or none at all. This would account for the lower diffusivity of the 1/8" pellets compared to the 1/4" ones.

If the interstitial Knudsen diffusivity is calculated for 50 Å cylindrical pores, the extremely large pores in the seed would account for the tortuosity value of less than unity obtained by the steady state method and given in Table 1.IX. Another factor which could account for the difference in diffusivity values from the pulse and steady state apparatus is that the alumina pellets were prone to break down in annular layers. With caps ground off each side in the steady state apparatus, the strata of these layers are exposed and may represent a low resistance diffusion path through the pellet.

Porosity

One of the critical factors in applying the pulse technique is an accurate knowledge of the pellet porosity. A 1% change in porosity can result in a 4% variation in diffusivity. As a check on the manufacturer's data, an experiment was carried out using a gas chromatograph and a 15' by 1/2" diameter empty tube as a dispersing system. Samples of the 1/8" "wet" alumina pellets were placed in the sample loop of the chromatograph and a hydrogen pulse injected in an air carrier gas. The height of the pulse output compared to the height obtained in the same way from the empty sample loop gave a good measure of the solid volume of the porous pellet. The sample gas of hydrogen had to be diluted with air to keep the detector in the linear range, but it would appear reasonable that if a pulse apparatus was to be utilized, a porosity measuring device of this type would be very useful, so that the porosity of the pellets as tested is measured.

Non Spherical Pellets

There should be no reason why the effective diffusion coefficient of granular pellets of almost any form could not be measured by applying an

appropriate shape factor, and a surface-to-volume pellet diameter as used for effectiveness factor charts (3). A derivation was attempted to express the mass transfer coefficient for cylinders in terms of an effective diffusivity, (as in equation (1.46)) but no simplified approximation could be made, due to the presence of Bessel functions in the solution. Thus, for shapes other than spheres, a constant based on experiment would seem to be required to relate the mass transfer coefficient and effective diffusivity if the simplified form of equation (1.49) is to be preserved.

Methane Pulse

The use of a methane pulse seems to be of little value. The correction to the dispersion measured for a bed of porous pellets which is due to eddy diffusion effects is no higher for hydrogen than the correction term for methane. The desirable amplification of the pellet capacity dispersion term can be achieved by a high velocity, rather than attempting to use a gas of lower molecular diffusivity. The hydrogen flame detector could conceivably have a lower response lag as compared to the thermal lag in a hot wire detector (thermal conductivity), but this does not appear to be a problem in this work.

Errors

The errors in the result caused by the mathematical manipulations are not readily estimated, however, the effects of inaccuracies in the measured values are considered below. The effective diffusivity is given by,

$$D_E = \left[\frac{1}{1 + \frac{\epsilon_B}{\epsilon_p (1 - \epsilon_B)}}\right]^2 \qquad \frac{2\ \epsilon_B\ (d_p)^2}{4\pi^2\ C\ (1 - \epsilon_B)}$$

where C is the term from equation (1.50).

The overall potential error may be estimated by adding the effects of individual errors for a given typical set of values.

In the following table typical variable magnitudes are given along with the estimated error and the effect on the resultant effective diffusivity.

TABLE 1.X
POTENTIAL ERRORS

Variable	Magnitude	Degree of Uncertainty	Percentage error in Effective Diffusivity
C	0.375 cm/sec	± 5%	5%
d_p	1.0	± 2%	4%
ϵ_p	0.33	± 10%	16%
ϵ_B	0.40	± 5%	2%
			27%

It is fairly obvious that more accuracy in the pellet porosity values would radically improve the results, but at the same time it is extremely improbable that all the errors would be in the same sense and yield the above overall error. It should be mentioned that the above error estimates apply to inaccuracies in mean values obtained from a reasonable sample. For example, although the pellet diameters could show 50% variation between individual pellets, the mean of 20 to 40 pellets was not found to vary when a grab sample was taken.

VII

CONCLUSIONS

1. The effective diffusivity of gases in porous pellets can be adequately measured using a hydrogen pulse technique. A 27% random error is conceivable due to errors in the measured variables; however, this can be halved with better methods of measuring the pellet and bed porosities. In addition, a probable error exists from the mathematical derivations. This latter error should be a relatively constant percentage, thus lending itself to elimination by calibration.

2. An eddy diffusion mechanism exists in the transition region between laminar flow and turbulent flow in packed beds such that the axial dispersion coefficient is proportional to the square of the velocity.

VIII

RECOMMENDATIONS

The method for the measurement of the porosity of pellets by injecting a pulse of hydrogen which has been purged from the sample loop of a chromatograph containing the test pellets, should be developed further and incorporated into the pulse apparatus. The main problem to overcome is that of minimizing the interparticle volume by packing in as many pellets as possible.

By extending the flow ranges covered in this work, the range of the region where eddy diffusivity is proportional to the square of the velocity may be determined. The results may then be compared with the results obtained in empty pipes by Taylor (25).

SECTION II

DEVELOPMENT OF AN UNSTEADY STATE FLOW METHOD FOR MEASURING BINARY GAS DIFFUSION COEFFICIENTS

I

INTRODUCTION

The bulk, or molecular diffusion coefficient of binary gas mixtures is not readily measured experimentally. One of the oldest techniques is the Loschmidt method which is based on bringing two cylinders containing the gases (lighter on top) together and measuring concentration variation with time. However, this method is sensitive to convection or thermal eddies.

In Stefan's method the rate of diffusion of a vapour in a vertical glass capillary tube is measured by following the drop in level of a liquid meniscus as evaporation occurs. The open top end of the glass tube is flushed with the second component. This method obviously cannot be used for gases above the critical temperature, and, in practice, is limited to narrow ranges of temperature and pressure.

The longitudinal dispersion coefficient in a straight tube, within the limits described in Section I on Taylor's work (25), is a function of the molecular diffusivity. Thus by measuring the dispersion in a straight tube by a method similar to that described in Section I, the molecular diffusivity may be obtained. Chromatography apparatus can also be used for this type of work. Good results can be obtained, although the apparatus is not simple, and experimental conditions feasibly are limited (35)(36).

The molecular diffusivity at high temperatures has been measured by Walker and Westenberg (37) by a point source technique in which a trace of one gas is fed through a capillary which is mounted in the centre of a tube in which the second gas is flowing. The profile of the trace gas in the bulk stream is measured downstream from the source, and the molecular diffusivity can be calculated using the appropriate solution of the diffusion equation. Very careful experimental technique is required to obtain accurate values by this method, although wide temperature ranges can be covered.

Other methods, such as measurement of diffusion rates through porous barriers, have been employed by numerous workers, but these do not give absolute values, and require calibration, and a correct interpretation of results. In particular, there appears to exist no absolute methods which can be used to give acceptable values of the binary diffusion coefficient over wide ranges of both temperature and pressure, and which will allow some investigation of concentration effects also. The present work is an attempt to develop a measurement technique which will satisfy all these requirements.

An unsteady state flow method similar to the Stefan technique was selected, as offering the possibility of analysis of an effluent stream remote from the diffusion cell by any convenient means and at any necessary conditions. The cell itself could be maintained at any temperature and pressure desired. By varying flowing and cell gas compositions, concentration effects might be studied. However, convection effects in the cell must be absent, and so some form of packing to produce capillary channels would also be a part of the construction.

II

THEORY

A. SIMPLIFIED SOLUTION OF A DIFFUSION EQUATION

It has been shown (6) that for equimolar diffusion in a porous solid Fick's second law of diffusion takes the following form,

$$\frac{\partial C_A}{\partial t} = - \frac{D_E}{\epsilon_B} \frac{\partial_2 C_A}{\partial x^2} \tag{2.1}$$

where D_E is the effective diffusivity, ϵ_B the porosity, C the concentration and t the time. The absence of significant surface adsorption is also implied by the above equation.

The relationship between the effective diffusivity D_E and the true binary diffusion coefficient D_B of the free gas D is given by,

$$D_E = \frac{D_B E_B}{\lambda} \tag{2.2}$$

where λ is the tortuosity with values varying from 1.0 for straight parallel pores to about 100 for a structure containing dead end pores. If D_E from equation (2.2) is substituted into (2.1), then for a bed with tortuosity 1.0 the solution of (2.1) would yield the molecular diffusivity D_B of the gas.

A simple solution of the diffusion equation (2.1) for the model shown in Figure 2.1 is obtained if the assumption is made that the vessel is initially bathed in a gas concentration C_o and then at time zero the plane at x = L is maintained at zero concentration.

Mathematically, the boundary conditions are:

$$x = 0, \quad \frac{\partial C}{\partial x} = 0$$

$$C_A = C_o \text{ for all } x \text{ when } t \leq 0$$

$$C_A = 0 \text{ when } x = L \text{ for } t > 0$$

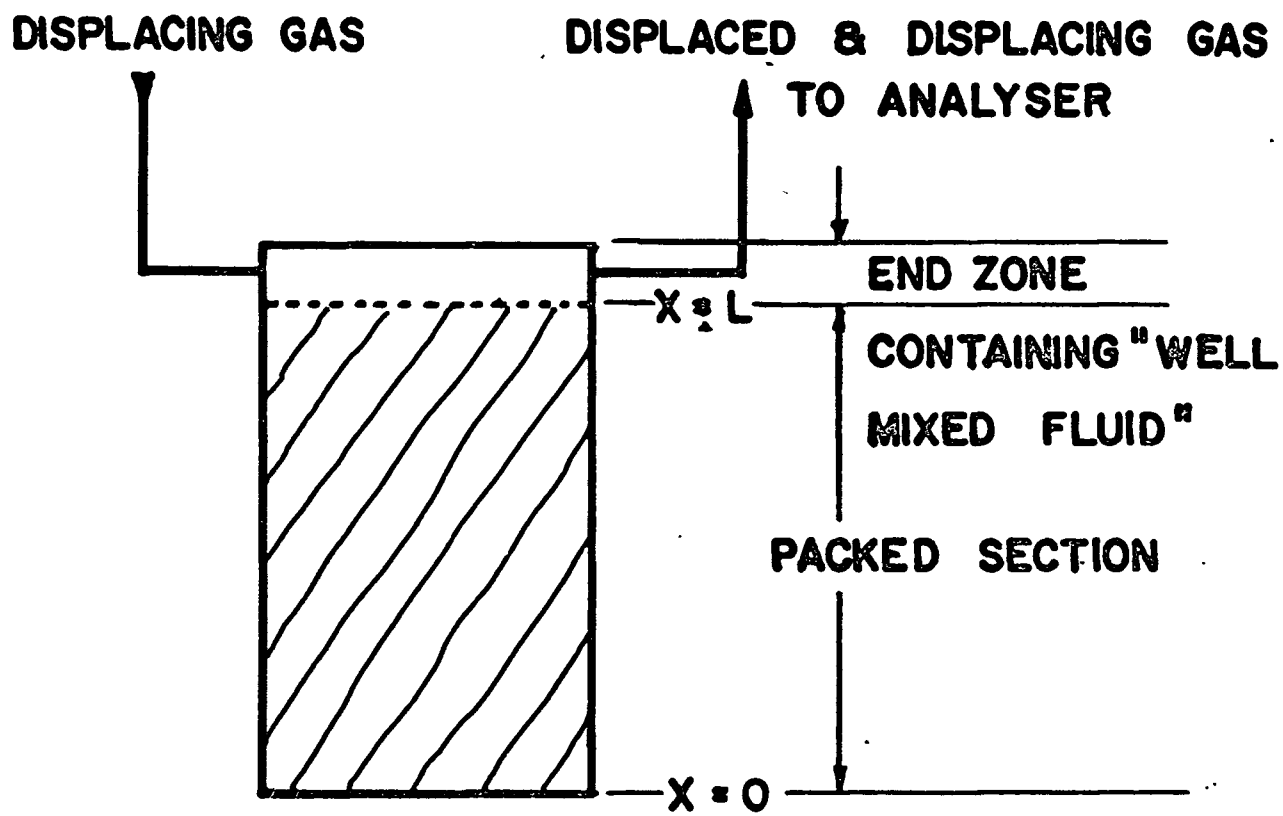

Figure 2.1

Model of The Bed For Proposed Diffusion Experiment

Crank (22) (p. 97) has given the solution of equation (2.1) with these boundary conditions, except that his solution applies from x = -L to +L

$$C_A = \frac{4\,C_o}{\pi}\sum_{n=0}^{\infty} \frac{(-1)^n}{(2n+1)} \exp - \frac{D_E}{B}\,\frac{(2n+1)^2\pi^2 t}{4\,L^2} \cos\frac{(2n+1)\pi x}{2\,L} \qquad (2.3)$$

In order to find the flux from the end of the vessel the above solution must be differentiated with respect to x, and the resulting expression solved to give the concentration gradient at the end (x = L). This gradient may then be applied in conjunction with Fick's first law of diffusion,

$$N_A = - D_E \cdot \frac{dC_A}{dx} \qquad (2.4)$$

where N_A is the flux of gas A in moles/(sec)(cm^2) under conditions of equimolar counter diffusion, which must exist in the model of Figure 2.1.

The series solution for the concentration gradient given by (2.3) when x = L is,

$$\left[\frac{dC_A}{dx}\right]_{x=L} = \frac{2\,C_o}{L}\sum_{n=0}^{\infty} \exp\left[- \frac{D_E}{B}\,\frac{(2n+1)^2\pi^2 t}{4\,L^2}\right] \qquad (2.5)$$

This solution can be simplified by taking into account only times greater than the time when the second term of the series is less than 1% of the first, or in other words,

$$\text{Ln } 0.01 - \frac{D_E}{\epsilon_B}\,\frac{\pi^2 t}{4\,L^2} = - \frac{9\,D_E}{4\,\epsilon_B}\,\frac{\pi^2 t}{L^2} \qquad (2.6)$$

If a molecular diffusivity of 0.75 cm^2/sec (e.g. hydrogen-nitrogen) is assumed, and a diffusion path of unit tortuosity and length of 10 cm., then solving 2.6 gives t = 31 seconds. Similarly if the gas diffusivity is taken as 0.1 cm^2/sec then the time before the second term can be ignored becomes 232 sec.

If now the boundary condition requiring that the end of the bed at x = L should be at zero concentration is achieved by sweeping the end rapidly with a second gas, then the concentration of the displaced gas in the exit stream will be proportional to the flux at the end of the bed. If, in addition, sufficient time as calculated above is allowed to elapse before concentrations are recorded so that the second and higher terms become negligible, then the flux equation from (2.5) reduces to the form,

$$\text{Ln } C_{exit} = \text{Ln } Z - \frac{D_E \pi^2 t}{\epsilon_B \, 4 \, L^2} \qquad (2.7)$$

where Z is a constant including the unwanted terms from the material balance, and from equations 2.4 and 2.5.

$$Z = \frac{A_B \, D_E}{Q} \cdot \frac{2 \, C_o}{L} \qquad (2.8)$$

Q is the displacing gas flow rate in mls/sec., and A_B the area of bed at x = L.

A semi-logarithmic plot of exit concentration vs. time for a constant flow rate should yield a straight line with slope $\frac{D_E}{B} \frac{\pi^2}{4 \, L^2}$. If the bed is packed with parallel tubes the tortuosity should be 1, and the slope of the plot becomes $\frac{D_B \pi^2}{4 \, L^2}$, thus providing a means for measuring the free gas molecular diffusivity without calibration of the apparatus.

B. MORE RIGOROUS SOLUTION

A problem with the above experimental model arises, in that if a displacing gas flow rate high enough to satisfy the boundary condition that $C_A = 0$ at x = L is maintained, then by the time analysis is started the concentration is so small that an extremely sensitive analytical method is required. Possibly this very high gas flow rate could be used

anyway, but a second problem due to turbulence caused by the high velocities entering above the packed section could arise and cause eddies in the diffusion zone.

In order to minimize the displacing gas flow rate, the end zone through which the displacing gas flows must be as small as possible, but too narrow an end zone would result in pressure drops which could cause bulk flow in the diffusion section.

Experimentally, it was not found possible to achieve the boundary conditions described above, but a solution for the diffusion equation with a well mixed fluid at the end of the diffusion zone (i.e. a finite end zone) has been obtained by Carslaw and Jaeger (38) for heat conduction from a solid. Essentially, the solution expressed in terms of the mass diffusion case discussed above is for the following boundary conditions,

$$\frac{dC_A}{dx} = 0 \qquad \text{at } x = 0 \text{ for all } t$$

$$C_A = C_o \qquad \text{for all } Z \text{ at } t = 0$$

and a material balance around the well mixed end zone yields,

$$- D_E A_B \left[\frac{\partial C_A}{\partial x}\right]_{x=L} - Q\, C_{Ao} = \ell A_B \frac{\partial C_{Ao}}{\partial t} \qquad (2.9)$$

where A_B is the area of the end of the bed, ℓ is the height of the end zone, and C_{Ao} is the well-mixed end zone concentration. As before, Q is the gas flow rate, so that the loss of displaced gas from the system is proportional to the concentration in the end zone and also the gas flow rate.

The solution obtained by Carslaw and Jaeger in terms of heat gives the temperature v at time t in the region $0 < x < L$ with initial uniform temperature V, and no heat loss at the plane x = 0. At x = L, contact is assumed with a mass of well stirred fluid M' per unit area of contact, and

specific heat c' which is cooling by a radiation mechanism at H times its temperature. The initial temperature of the fluid is taken as zero. The latter boundary condition is not compatible with the apparatus proposed for this work but this does not influence the solution at large times which is the region of interest in this work.

$$v = 2V \sum_{n=1}^{\infty} \frac{\exp\left[-K\alpha_n^2 t\right]\left[h - k\alpha_n^2\right]\cos\left(\alpha_n x\right)}{\left[L(h - k\alpha_n^2) + \alpha_n^2 (L + k) + h\right]\cos\left(\alpha_n L\right)} \tag{2.10}$$

where $h = H/K'$, $k = \frac{M' c'}{\rho c}$ and α_n are the consecutive roots of

$$\alpha \tan \alpha L = h - k\alpha^2 \tag{2.11}$$

In the above equations, ρ is the density of the bed, with heat capacity c and thermal diffusivity K' cm²/sec. The thermal conductivity is K cals/sec cm² (°K)/cm.

The above solution has been transposed to the equivalent diffusion case, and the tabulation which follows may assist in explaining the diffusion parameters.

	Heat Transfer	Mass Transfer
$v\rho c$	cals/cm³	C_A concentration moles/cm³
ρc	cals/cm³ °K	1.0, unless in a porous bed when equals porosity ϵ_B
K	cm²/sec	$\frac{D_E}{\epsilon_B}$ effective diffusivity cm²/sec or D_B if $\epsilon_B = 1.0$
$K' = K\rho c$	cals/sec cm²(°K/cm)	D_E
H v	cals/sec cm²	Q C_{Ao}/A_B moles/sec cm², where Q is the gas flow rate, cm³/sec, and A_B the bed area, cm²

Other quantities appearing in equation (2.10) when written for the diffusion case are,

$v/V = C/C_o$, where C_o is the initial concentration in the bed.

$$h = \frac{Q}{A_B D_E} \tag{2.12}$$

$$k = \frac{A_B \ell \rho_M}{\epsilon_B \rho_M A_B} = \frac{\ell}{\epsilon_B} \tag{2.13}$$

where ρ_M is the molar density and ℓ is the length of the end zone. Rewriting equation (2.10) and setting x = L yields,

$$C_{Ao} = \frac{2\, C_o \sum_{n=1}^{\infty} (h - k\alpha_n^2) \exp\left[- \frac{D_E}{\epsilon_B}(\alpha_n)^2 t\right]}{L\,(h - k\alpha_n^2)^2 + \alpha_n^2\,(L + k) + h} \tag{2.14}$$

If the time, t, is large then the second term in the series becomes negligible compared to the first, and equation (2.14) becomes,

$$C_{Ao} = \frac{2\, C_o\, (h - k\alpha_1^2) \exp\left[- \frac{D_E}{B}\, \alpha_1^2 t\right]}{L\,(h - k\alpha_1^2)^2 + \alpha_1^2\,(L + k) + h} \tag{2.15}$$

or

$$Ln\,(C_{Ao}) = L_n\,(Z) - \frac{D_E}{\epsilon_B}\, \alpha_1^2\, t \tag{2.16}$$

where $Z = \dfrac{2\, C_o\, (h - k\alpha_1^2)}{L\,(h - k\alpha_1^2) + \alpha_1^2\,(L + k) + h}$

Thus a plot of Ln (C_{Ao}) versus t for large times should yield a straight line of slope $- D_E\alpha_1^2/\epsilon_B$. It is also of interest to note that an absolute value of the concentration is not needed. For example, the peak height of a chromatograph is proportional to the concentration at low concentrations, and so the logarithm of peak heights rather than concentrations may be plotted versus time.

Equation (2.16) must be solved simultaneously with the auxiliary equation (2.11) in order to obtain a diffusion coefficient from a set of exit gas concentration versus time data. Examination of the equations shows that an analytical solution is not possible. In order to obtain a trial and error solution the following iterative procedure was applied using the Newton-Raphson method (39).

The first root of equation (2.11) must lie between $\alpha = 0$ and $\pi/2L$. Selection of an initial value approaching zero could result in a break down of the iterative operation because the second approximation falls outside the zero to $\pi/2$ L range. A further reason for selecting a root close to $\pi/2$ L is apparent, because on substitution of $\alpha = \pi/2$ L back in (2.16) the simplified solution given by (2.7) is obtained. Because the apparatus was designed to approach the simpler boundary conditions, it is reasonable to assume that $\alpha = \pi/2$ L will be close to the actual root. Also, due to the iterative nature of the solutions to (2.16) and (2.11), the time when the second root can be ignored cannot easily be derived, but as the more rigorous solution approaches the simplified solution it is reasonable to suppose that the time calculated from the simpler solution (2.6) and (2.7) is an adequate criterion.

From the assumed value of $\alpha_1 = \pi/2$ L and the slope of the semilogarithmic concentration vs. time plot one gets,

$$\text{Slope} = \frac{D_E}{\epsilon_B} \alpha_1^2 \tag{2.17}$$

and so an initial value of the diffusivity D_E/ϵ_B is obtained. Equations (2.12) and 2.13) may then be substituted in equation (2.11), but since the value of D_E/ϵ_B is an initial approximation, equation (2.11) is corrected by a term for the resulting error, Δ ,

$$\Delta = h - k\alpha_1^2 + \alpha_1 \tan \alpha_1 L \tag{2.18}$$

Differentiating (2.18) with respect to α_1,

$$\frac{d\Delta}{d\alpha_1} = -2k\alpha_1 - \frac{\alpha_1 L}{(\cos \alpha_1 L)^2} - \tan \alpha_1 L \tag{2.19}$$

The second approximation for the first root α_1 can then be obtained from the first approximation, and equations (2.18) and (2.19).

$$\alpha_1 = \alpha_1 \text{ (first approximation)} - \frac{\Delta}{\frac{d\Delta}{d\alpha_1}} \tag{2.20}$$

With the second approximation the process can be repeated from equation (2.17) until a satisfactory result is obtained.

C. COMPUTATION OF SLOPE OF DECAY CURVE WITH A RESIDUAL CONCENTRATION

In cases where the gases are not pure, or where there are dead zones in the apparatus which are not easily purged, a plot of experimental data according to equation (2.7) may yield a curve. A problem was experienced in finding the value of the steady state (or infinite time) concentration which the data should approach with time. This value must be subtracted from the results to yield a straight line. It was found that on a log plot a slight change in the steady state value caused a large change in the slope, and hence uncertainty in the resulting value of the diffusivity.

To eliminate the need for judgment on the part of the experimenter in deciding on a value of the steady state level a least squares solution was prepared for the equation $Y-C = A.e^{-Bt}$ where A, B and C are the constants to be determined, Y represents the concentration (or peak height), and t is the time.

There is reason to question the use of an equation of the above form as it tends to weight the solution in favour of data at short times. However, as there is evidence that the so-called steady state value is dependent on the gas flow rate in this apparatus, weighting in favour of shorter times where the steady state value is negligible would seem to be justifiable. The derivation of the expression for evaluating B is given below.

$$E^2 = \sum \left[Y_i - C - Ae^{-Bt_i} \right]^2 \qquad (2.21)$$

where C represents the value of Y approached at infinite time and A and B are constants of the system when equation (2.16) is fitted to (2.21), with E being the error to be minimized.

Differentiating 2.21 by A, B and C yields.

$$\frac{dE^2}{dA} = \sum 2\left[Y_i - C - Ae^{-Bt_i}\right]\left(-e^{-Bt_i}\right) \tag{2.22}$$

$$\frac{dE^2}{dB} = \sum 2\left[Y_i - C - Ae^{-Bt_i}\right]\left(-At_ie^{-Bt_i}\right) \tag{2.23}$$

$$\frac{dE^2}{dC} = \sum 2\left[Y_i - C - Ae^{-Bt_i}\right]\left(-1\right) \tag{2.24}$$

Setting (2.22), (2.23) and (2.24) equal to zero and eliminating A and C yields the following, where Δ represent the error resulting from assuming an incorrect value of B.

$$\Delta = -\sum Ye^{-Bt}\frac{\sum te^{-Bt}}{u}\sum e^{-Bt} + \sum Ye^{-Bt}\sum te^{-2Bt} + \sum te^{-Bt}\frac{\sum Y\sum e^{-2Bt}}{n}$$
$$-\sum Y\,e^{-Bt}\sum e^{-2Bt} - \sum Y\,e^{-Bt}\frac{\sum te^{-2Bt}}{n} + \sum Yte^{-Bt}\frac{\left(\sum e^{-Bt}\right)^2}{n} \tag{2.25}$$

To apply the Newton-Raphson method (39),

$$\frac{d\Delta}{dB} = \frac{\sum Ye^{-Bt}}{n}\left[\left(\sum te^{-Bt}\right)^2 + \sum e^{-Bt}\sum te^{-Bt}\right] + \sum te^{-Bt}\sum e^{-Bt}\frac{\sum Yte^{-Bt}}{n}$$
$$-2\sum Ye^{-Bt}\sum t^2e^{-2Bt} - \sum te^{-2Bt}\sum Yte^{-Bt} - \frac{2\sum Y\sum te^{-Bt}\sum te^{-2Bt}}{n} +$$
$$\frac{\sum Y\sum e^{-2Bt}\sum t^2e^{-Bt}}{n} + 2\sum Y\,te^{-Bt}\sum te^{-2Bt} + \sum e^{-2Bt}\sum Y\,te^{-2Bt}$$
$$+\frac{2\sum Y\sum e^{-Bt}\sum t^2e^{-2Bt}}{n} + \sum Y\sum te^{-2Bt}\frac{\sum te^{-Bt}}{n} - 2\frac{\sum Y\,te^{-Bt}\sum e^{-Bt}}{n}\sum te^{-Bt}$$
$$-\left(\sum e^{-Bt}\right)^2\frac{\sum Y\,t^2\,e^{-Bt}}{n} \tag{2.26}$$

$$\text{Hence } B_2 \doteq B_1 - \frac{\Delta}{d\Delta} \tag{2.27}$$

In (2.27), B_2 represents a better value of B than the previous assumed value, that is, B_1.

III

APPARATUS

A constant temperature air bath was fitted with the hardware for a gas chromatograph, and a vessel containing the bed for the diffusion measurement. The test vessels were soldered from pieces of brass or copper pipe and were filled to the brim with the packing material. A rubber gasket was used to provide the spacer for the "well mixed end zone" as shown in the sketches in Figure 2.2. Two entrance flow patterns were used in the beds, a tangential entry in the 5 cm. dia. vessel, and a direct sweep across the bed in one direction in the 2.5 cm. cell.

A schematic diagram of the apparatus is shown in Figure 2.2. Moore constant differential flow controllers were used to maintain constant gas flow rates, while a soap bubble meter was used for measurement of the effluent stream flows. In order to reduce the hold up of the apparatus due to valves and fittings, the two gas feed systems were connected to the diffusion cell with 1/4" polyethylene tubing, and switching from one gas to the other was done by disconnecting one tube at the entrance to the constant temperature zone and connecting the second. A bypass valve at the entrance to the constant temperature bath allowed gas to flow directly to the flow meter. The use of 1/8" tubing to connect the test vessel to the chromatograph sample valve provided sufficient resistance to flow to make the bypass valve effective without shut-off valves.

Test gases used in diffusion runs were:

Nitrogen	Prepurified	Matheson Co.	99.9%
Ethane	CP	"	99.0%
Hydrogen	Prepurified	"	99.9%
Butane	CP	"	99%

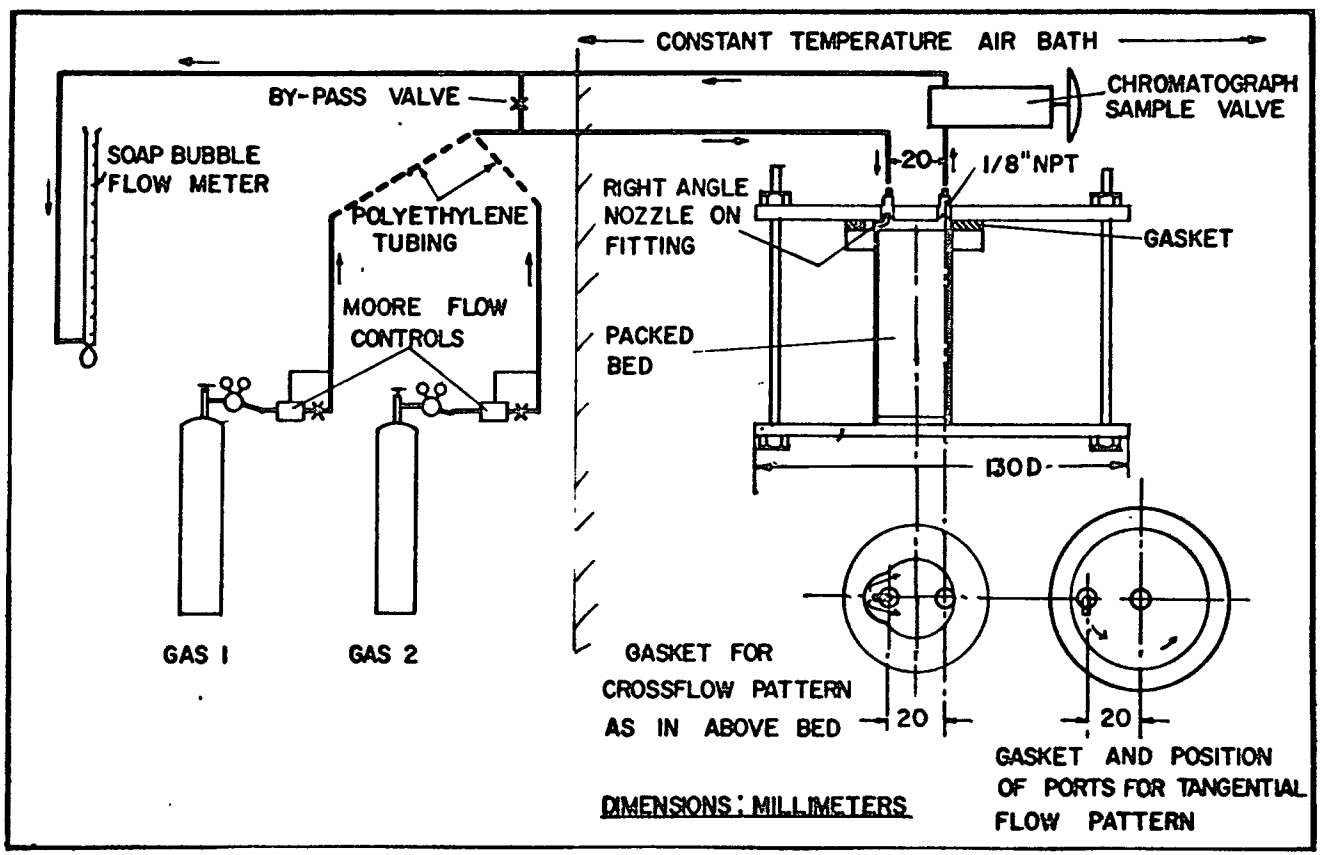

Figure 2.2

Diffusion Apparatus

The details of the packed beds tested are shown in Table 2.I.

The chromatograph columns were packed with 25% Nujol on chromasorb. The separation of nitrogen and ethane was accomplished with a 9' x 1/4" diam. column using a helium carrier. Hydrogen and nitrogen were analyzed on the same column but with a hydrogen carrier so that only nitrogen showed as a peak. Butane and nitrogen were analyzed by an 18" column with helium carrier gas. Ten psig carrier gas pressure was used in the long columns but the short column needed only 2 psig.

IV

PROCEDURE

A. SELECTION OF THE DISPLACED AND DISPLACING GAS

In the selection of displaced and displacing gas from a gas pair two factors must be considered. The tail normally encountered in gas chromatography peaks tends to mask a following peak, and this effect may be particularly serious when the columns are made as short as possible to reduce analysis time. Thus, it was necessary to make the displaced gas the first peak to appear on the chromatograph. The second effect to be considered is that the lighter gas should be placed on top, and if the end zone is also at the top of the bed then this latter requirement is contradictory to the first, as the lighter gases usually tend to appear first in the chromatographic trace.

TABLE 2.I

DIFFUSION CELL PROPERTIES

	Parallel Tube Packing	Porous Solid Packing	Spherical Packing Spheres
Bed Length, cms.	10.0	7.0	7.0
Bed Diameter, cms.	5.0	2.61	2.61
Length of "End Zone", cms.	0.27	0.27	0.27
Porosity	0.52	0.59	0.39
Properties of Packing material	"Kimax" melting point tubes 10 cm. long x 1.2 mm O.D. x 0.8 mm I.D.	Selas 01 Microporous synthetic ceramic average pore size 4.5 Specific surface area 0.577 m^2/cm^3 or 1.10 m^2/cm^3 by B.E.T. Ref. (5)	Borosilicate Glass

Three gas systems were tested on each bed, hydrogen-nitrogen, ethane-nitrogen and butane-nitrogen. The problems described above were overcome for the first pair by using a hydrogen carrier gas so that the hydrogen peak was lost completely. For ethane-nitrogen, it was hoped that because of the identical molecular weights density effects would not be significant, however, this system does represent a more difficult separation if chromatography is used for analysis. If the bed packing is firmly held then obviously an inverted bed can be readily used also with gas chromatography for the analysis. Butane and nitrogen were readily separated in the analysis, providing butane was used as the displacing gas.

B. OPERATION OF EQUIPMENT

To start a run the constant temperature air bath was brought up to its control temperature, (95°F), the carrier gas was put on stream, and a purge of about one ml/sec. of the displaced gas was passed across the bed (by-pass closed). When the bed had been thoroughly purged, a sample of the purge gas was taken.

After purging, the bypass was opened, and the displacing gas line connected and put on stream. The displacing gas was allowed to purge for about 10 minutes while the flow rate was measured on the soap bubble meter and adjusted to the desired range. The stop watch was started at the same time as the bypass valve was closed. Samples were taken and injected into the chromatograph at convenient times, until the displaced gas peak had become too small to give a satisfactory analysis, or until sufficient results had been obtained. In general, the highest concentration

included in a run was about 25% by volume of the displaced gas and calibrations of the chromatograph indicated a linear response up to about 40%. Therefore, absolute values of concentrations were not usually used, but rather peak height readings.

At the end of the run the flow rate was checked. If any discrepancy from the initial value was found, the later measurement was utilized because the Moore flow controls were found to drift for the first few minutes after a setting change. No flow measurements were taken during a run as the soap bubbles caused a visible increase in pressure in the system. The room temperature and atmospheric pressure were recorded for each run, and the temperature of the air bath was checked.

V

RESULTS

A. TREATMENT OF DATA

The raw data, computer program and computed results are recorded in Appendix V for each run. The value of the diffusivity recorded is actually the D_B/λ value which is obtained by this experiment. The diffusivity value is for the temperature of the bed, but is corrected to one atmosphere assuming no pressure drop in the vent lines. The effective diffusivity is computed for the same conditions.

The data for each bed are printed along with the constants and sums for the least mean square line computed from the data. Ten iterations were used for this least square calculation, but 4 or 5 were generally sufficient to obtain four figure accuracy. The number of iterations for the diffusivity calculation was set by a test of the

magnitude of the error, and this number is recorded. Certain data points were rejected as described in the following. These points are recorded, but they were not used by the computer.

The results were calculated by a two-part computer program. A subroutine used the Newton-Raphson (39) iteration described in the "Theory" to compute the least mean square fit of the equation $Y-C = A \exp(-Bt)$ to the data of peak heights (Y) vs. time, (t). Then using the solution of the diffusion equation described in "Theory" (equation 2.16), the main program calculated the diffusivity from the slope of the least squares line with a second Newton-Raphson iteration.

The least squares fit of the equation in the form $Y-C = A \exp(-Bt)$ weighs the line in favour of the small time (large Y) points. Thus, if the first or second point was inconsistent with the rest of the results, the computed slope showed this inconsistency in spite of all the other points. From the plot of Log Y vs. t, points which appeared to be inconsistent when plotted have been discarded before arriving at the values in the following tables.

The residence time of analysis gases in the chromatograph was extremely short for the butane-nitrogen system, with the result that the recorder was not able to follow the sharp narrow peaks. The lag of the recorder caused the peak heights to be non-linear with composition unless small peak heights were used. Thus, computations for the butane-nitrogen system are based on considerably longer times than the minimum for acceptable data indicated in the discussion of theory. Other reasons for rejecting data points are discussed where applicable.

In order to compare the data, the tortuosity of the beds as calculated from each data point offers a convenient parameter. This calculation requires a knowledge of the value of the molecular diffusivity

for each gas pair used, and the values in Table 2.V show that available published results are not reliable beyond ± 5%. Because of this discrepancy the tortuosity only gives a good indication of the consistency of the method, but its absolute value depends upon the value of molecular diffusivity selected. The tortuosity is shown in the following tables, but in Table 2.V the computed value D_B/λ for each set of gas systems and beds are averaged, and then ratioed with the results for the ethane-nitrogen system. These ratios may then be compared with the same ratios of the published experiments and calculated values, and give a comparison less dependent upon experimental error.

B. PARALLEL TUBE PACKING

The first experiments were carried out on a bed packed with 1.2 mm diameter melting point tubes, thus providing a bed with unit tortuosity parallel to the tube bundle. The details of this bed are given in Table 2.I, while the diffusion results are summarized in Table 2.II and shown graphically in Figures 2.3, 2.4 and 2.5 as plots of the log peak heights vs. time. In some of the runs shown a Millipore Type HA filter (80% porosity) was placed over the bed of tubes to prevent eddy currents in the diffusion channels due to the flowing displacing gas. The results shown suggest that such currents are not significant.

An inspection of the tortuosities in Table 2.II shows that the results scatter over a ± 9% range. Turning the bed on its side so that gravity effects became influential increased the diffusivity by 50%. The reason for the scatter can be seen in the run with the hydrogen-nitrogen system at a flow rate of 0.563 ml/sec. Three data points had to be discarded because the recorder automatic standardization operated and thus

TABLE 2.II

RESULTS FOR PARALLEL TUBE BED

Bed Temp. 306°K

Displacing Gas	Displaced Gas	Flow Rate $cm^3/sec.$	Slope sec^{-1}	D_B/λ $cm^2/sec.$	Molecular Diffusivity Used for λ Computation $cm^2/sec.$	Tortuosity λ	Remarks
Nitrogen	Hydrogen	0.510	0.00364	0.551	0.82	1.49	Bed on Side
Hydrogen	Nitrogen	0.544	0.00406	0.715	0.82	1.15	
		0.563	0.00434	0.873	0.82	0.940	
		2.81	0.0115	0.776	0.82	1.05	Millipore
			Average	0.788			
Ethane	Nitrogen	0.485	0.00200	0.135	0.151	1.11	
		1.461	0.00295	0.148	0.151	1.02	Millipore
		2.27	0.00300	0.140	0.151	1.08	Millipore
		2.94	0.00357	0.165	0.151	0.915	
		3.08	0.00329	0.149	0.151	1.015	Millipore
			Average	0.1505			
Nitrogen	Butane	0.460	0.00143	0.0817	0.095	1.16	Millipore
		0.903	0.00158	0.0766	0.095	1.24	Millipore
		2.05	0.00202	0.0905	0.095	1.016	Millipore
			Average	0.084			

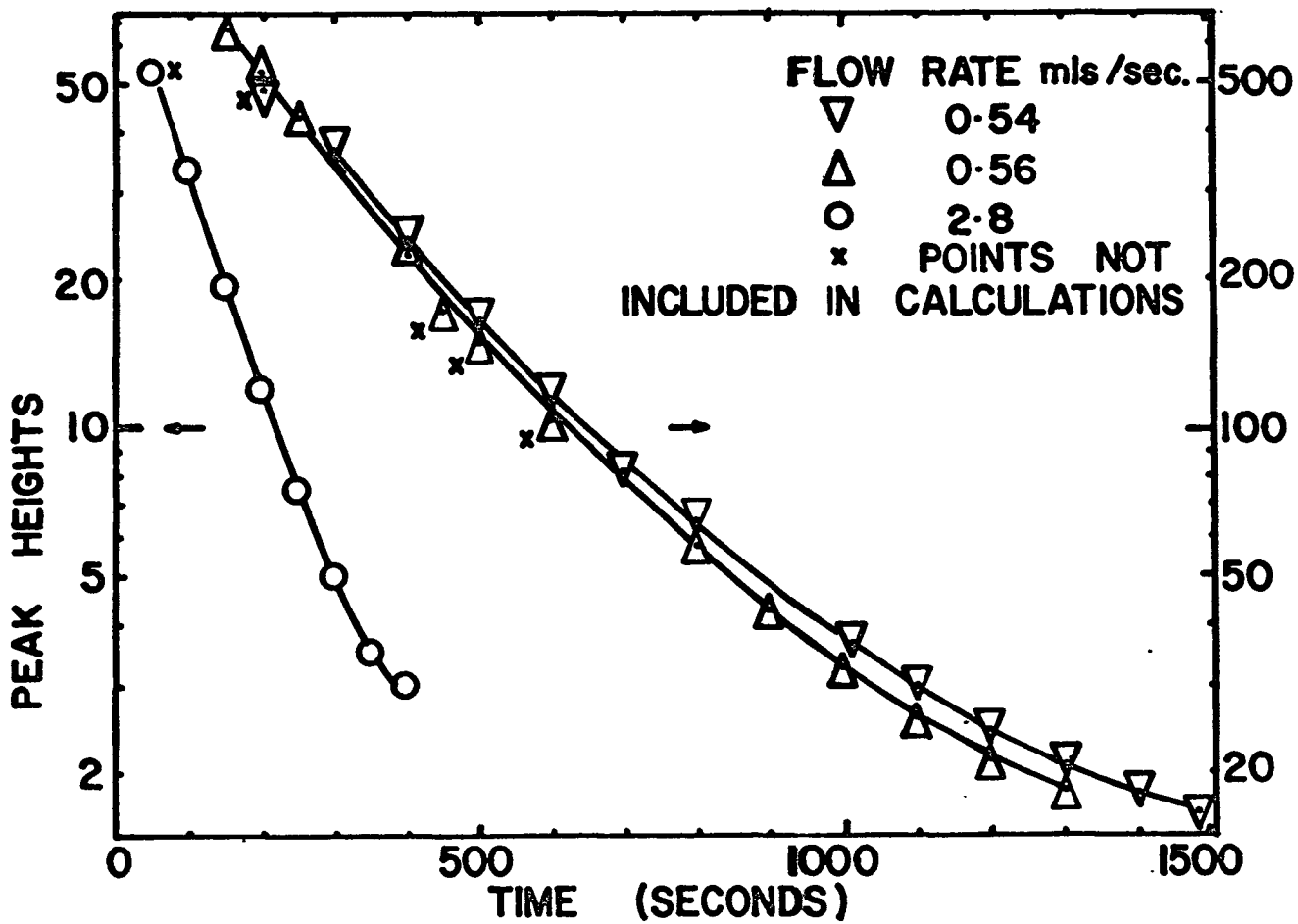

Figure 2.3

Results With Parallel Tube Bed. Hydrogen-Nitrogen

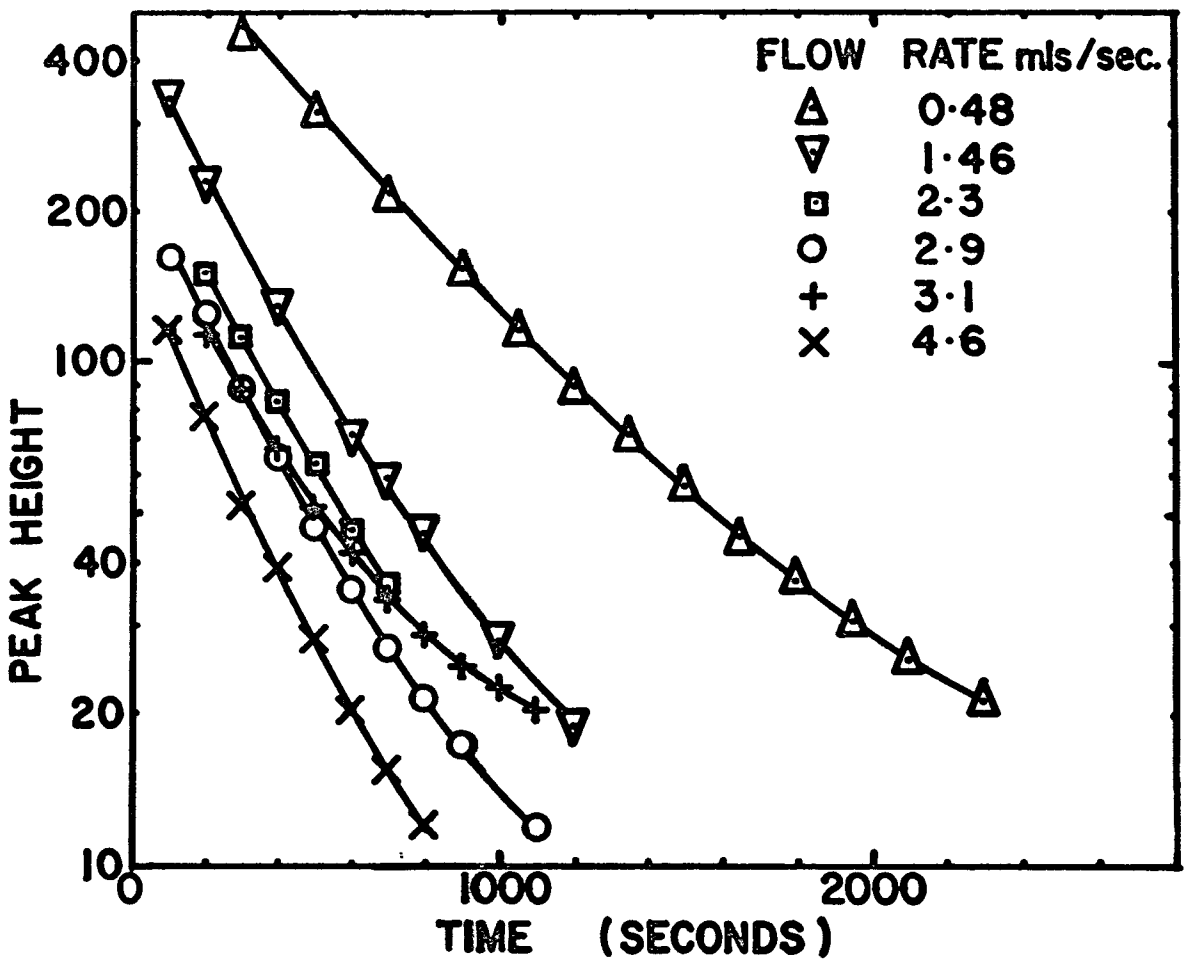

Figure 2.4

Results With Parallel Tube Bed. Ethane-Nitrogen

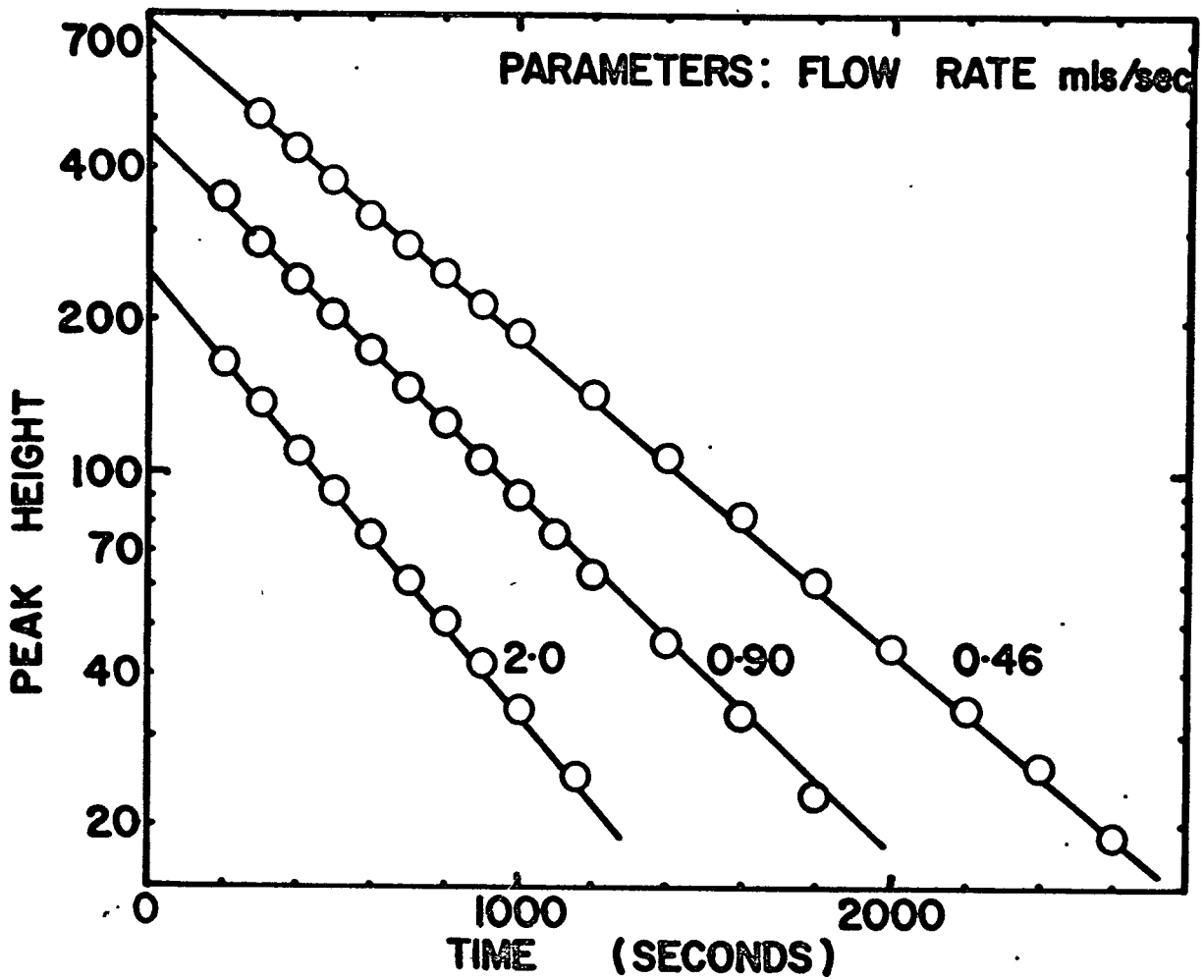

Figure 2.5

Results With Parallel Tube Bed. Butane-Nitrogen

caused a shift in the peak height proportionality with concentration. Removal of these points caused the least square line slope to change from 0.00446 to 0.00434 with a resulting change in the D_B/λ value from 1.008 to 0.873 cm^2/sec. The three discarded points are not in error by more than 4%, yet in a total of 15 points these three cause a 3% variation in the slope, which in turn causes a 15% difference in the diffusivity.

C. POROUS SOLID PACKING

The results of the runs using parallel tubes were initially calculated by hand from slopes obtained by graphical means. The sensitivity of the method to slight errors was not appreciated at the time, and errors were tolerated in the iterative calculation as well as those caused by the uncertainty of placing a straight line through a slightly curved set of points to obtain the slope.

Because it was originally felt that these errors could also be due in some measure to eddy diffusion within the relatively coarse-pored tubular packing, additional experiments were carried out using fine porous solids as a diffusion medium.

A Selas 01 ceramic filter medium solid rod was fitted tightly into a 2.61 cm. diameter vessel thereby halving the former bed diameter, but the pore diameter was also reduced from 0.8 mm (800 microns) to 4.5 microns. The details of this bed are given in Table 2.I, and the results are summarized in Table 2.III.

Because of the smaller diameter end zone, the flow pattern was changed from the former tangential inlet arrangement to one having flow in one direction across the chamber.

TABLE 2.III

RESULTS FOR POROUS SOLID PACKING
Bed Temp. 306°K

Displacing Gas	Displaced Gas	Flow Rate cm^3/sec	Slope $secs^{-1}$	$\frac{D_B}{\lambda} = \frac{D_E}{\epsilon_B}$ cm^2/sec	Molecular Diffusivity cm^2/sec	λ
Hydrogen	Nitrogen	0.562	0.0139	0.565	0.82	1.45
		0.793	0.0159	0.596	0.82	1.37
		0.928	0.0171	0.533	0.82	1.54
		1.25	0.0191	0.538	0.82	1.52
		1.83	0.0245	0.651	0.82	1.26
	Average			0.577		1.43
Ethane	Nitrogen	0.39	0.00450	0.114	0.151	1.34
		0.82	0.00490	0.108	0.151	1.40
		1.32	0.00525	0.112	0.151	1.35
		1.90	0.00523	0.108	0.151	1.39
	Average			0.1105		1.37
n Butane	Nitrogen	0.594	0.00337	0.0747	0.099	1.32
		1.14	0.00380	0.0802	0.099	1.23
		2.06	0.00400	0.0823	0.099	1.20
	Average			.0791		1.25

An examination of the results in Table 2.III. shows that the tortuosities are fairly consistent, with each gas system showing about a ± 5% scatter from the mean. However, the butane-nitrogen system tortuosities are lower than those obtained from the other gases, indicating that a true diffusivity value higher than that used would be appropriate. In order to avoid the "tail effect" mentioned earlier, nitrogen was made the displaced gas. The fact that butane is almost double the density of nitrogen would probably lead to gravity effects and could cause an apparent increase in the diffusivity. The difference between the average tortuosity of the hydrogen-nitrogen and ethane-nitrogen systems is not significant as it

depends upon the assumed value of the diffusivity. For example, if a value of 0.80 cm^2/sec is assumed for the hydrogen-nitrogen diffusivity rather than 0.82 cm^2/sec, both systems give an average tortuosity of 1.37 to 1.38.

The result at high flow rate for the hydrogen containing system is included in the averages. If this result is ignored it would appear that this system is showing about 5% lower diffusivity relative to the ethane system. The average pore diameter of the Selas Bed is 4.5 microns, while the mean free path of hydrogen at NTP is 0.18 microns. It is unlikely that the pore size distribution is so narrow that some percentage of the pores are not smaller than, say, 1.8 , at which pore size the resultant of the mixed Knudsen and bulk diffusion rates could be 5% less than the bulk diffusion alone.

Thus, in spite of the fact that the results look fairly good, use of the Selas 01 bed is questionable with high diffusivity gases at room temperature. Such a packing also suffers from the need to calibrate the bed to find the tortuosity before it can be used on gases of unknown diffusivity.

D. SPHERICAL PACKING

The relationship of porosity to tortuosity has been published (6) for beds of spherical particles, and this provides an obvious means of overcoming the need to calibrate a porous solid type of packing to first determine its tortuosity. The bed vessel was the same as that which held the Selas 01, but it was packed with 42 μ diameter glass spheres. However, the porosity obtained with the spherical packing was considerably less than for the porous solid, and the resulting reduced bed capacity led to a decay curve that rapidly decreased below the range of analysis by chromatography. The hydrogen-nitrogen results were most influenced by this effect.

TABLE 2.IV

RESULTS FOR SPHERICAL PACKING

Bed Temp. 306°K

Displacing Gas	Displaced Gas	Flow Rate cm^3/sec	Slope sec^{-1}	$\frac{D_B=D_E}{\lambda \quad B}$ $cm^2/sec.$	Molecular Diffusivity cm^2/sec	λ
Hydrogen	Nitrogen	0.456	0.0164	0.682	0.82	1.20
		0.832	0.0218	0.687	0.82	1.19
		1.25	0.0242	0.661	0.82	1.24
			Average	0.677		
Ethane	Nitrogen	0.604	0.00524	0.117	0.151	1.29
		0.919	0.00521	0.112	0.151	1.35
		1.36	0.00520	0.109	0.151	1.39
			Average	0.113		
Butane	Nitrogen	0.596	0.00364	0.0795	0.099	1.25
		0.979	0.00370	0.0784	0.099	1.26
		1.24	0.00369	0.0775	0.099	1.28
			Average	0.0785		

The graphical plots of the data in Figures 2.6, 2.7, and 2.8 shows a sharp change of slope at longer times. It is possible that the diffusion flux measured is the resultant of two decay processes, one due to the diffusion from the bed and the other due to diffusion from stagnant portions of the piping. This latter contribution would normally be negligible for a diffusion cell with a sufficiently large capacity. It may be noticed that for the hydrogen data with this bed (Appendix V), the least square computation has shown the decay curve to approach a value higher than the data for larger times. For this reason, the slope and hence the diffusivity (see Table 2.III) is higher for these runs, giving a lower tortuosity.

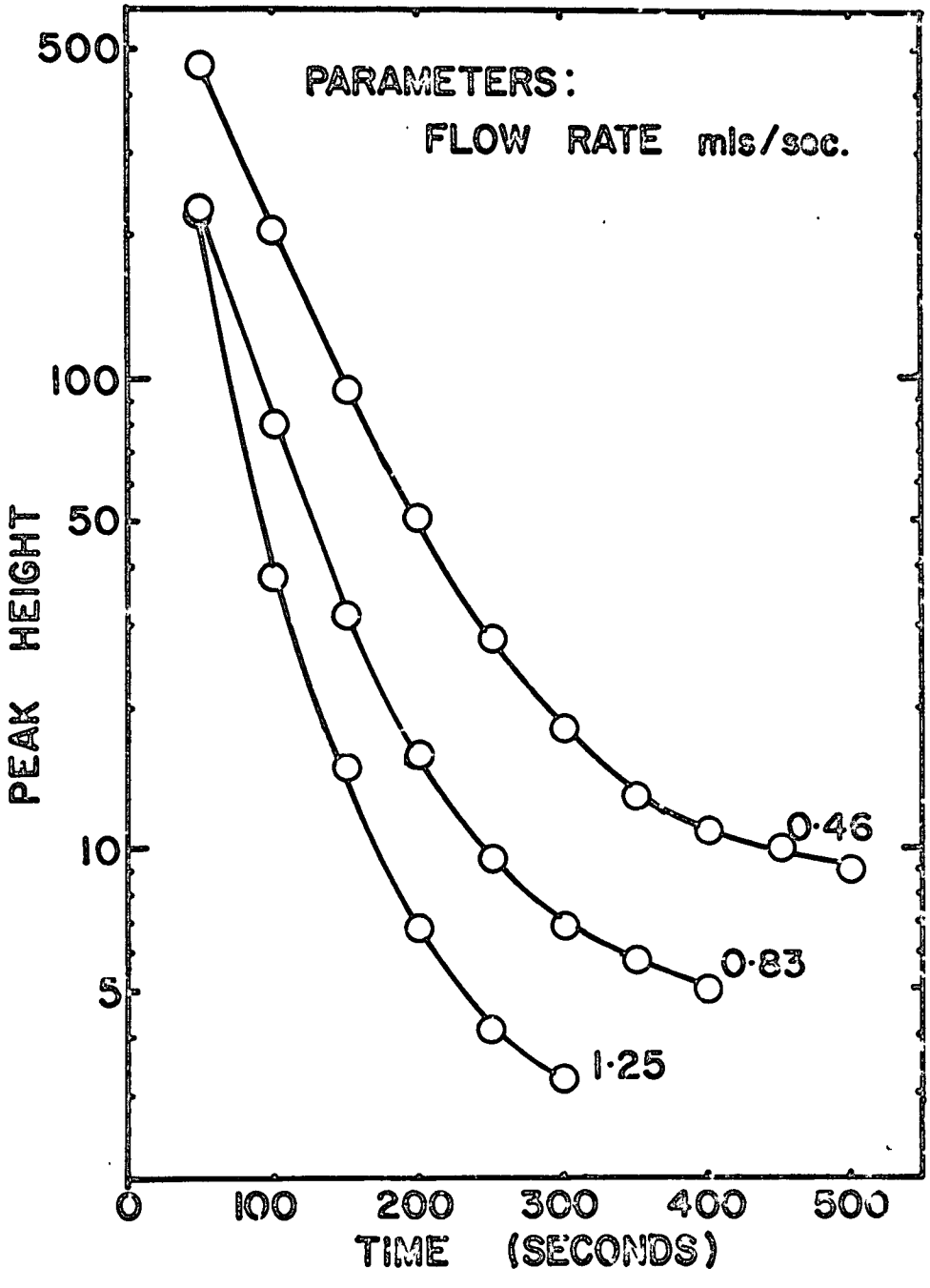

Figure 2.6

Results With Spherical Packing Bed. Hydrogen-Nitrogen

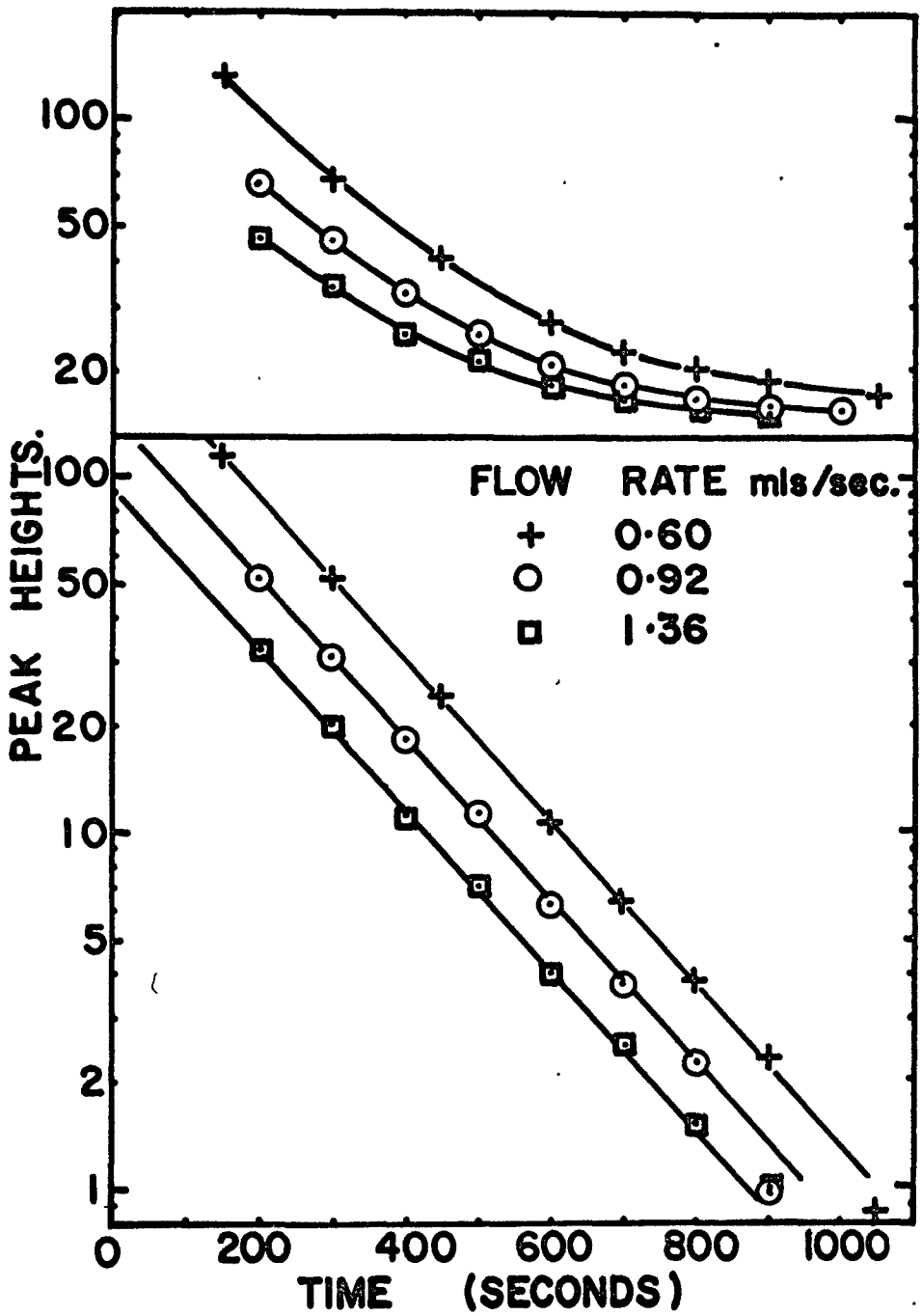

Figure 2.7

Results With Spherical Packing Bed. Ethane-Nitrogen
The lower graph shows the above points after the steady state constant has been subtracted

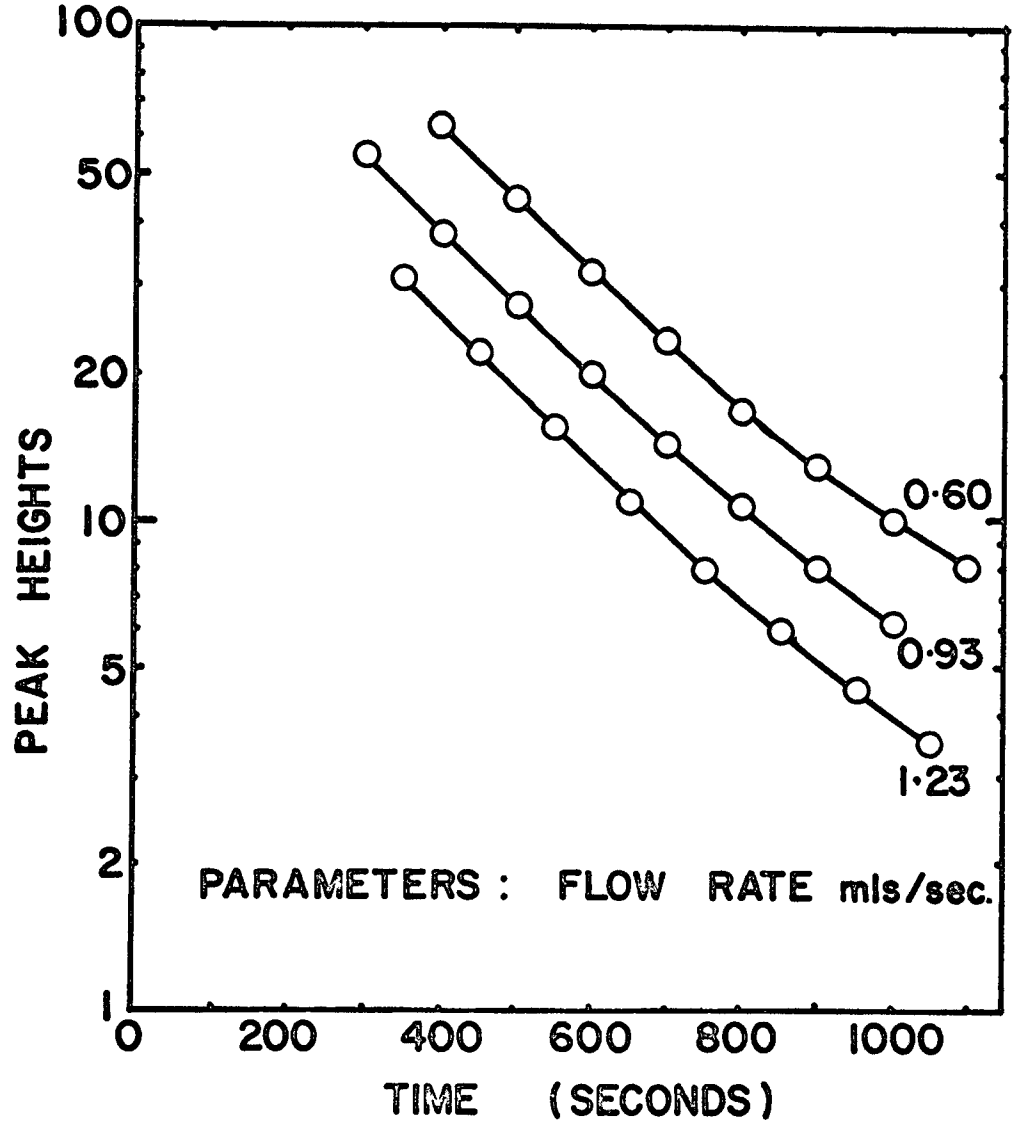

Figure 2.8

Results With Spherical Packing Bed. Butane-Nitrogen

TABLE 2.V

COMPARISON OF RESULTS

PUBLISHED DIFFUSIVITIES REF 40						EXPERIMENTAL RESULTS FROM THIS WORK					
Calculated			Experimental			Melting Point		Selas 01		42 Micron Spheres	
Temp. °K	Diff.	Ratio	Temp. °K	Diff.	Ratio	D_B	Ratio	D_B	Ratio	D_B	Ratio
H_2-N_2											
273.2	0.656		273.2	0.674							
288.2	0.718		288.2	0.743							
293.2	0.739		293.2	0.76							
306*	0.790	5.27		0.814	5.28	0.788	5.24	0.577	5.22	0.677	5.99
C_2H_6-N_2											
298.2	0.144		298.2	0.148							
306*	0.1498	1.0		0.154	1.0	0.1505	1.0	0.1105	1.0	0.113	1.0
nC_4H_{10}-N_2											
298.2	0.0986		298.2	0.0908							
306*	0.1025	0.685		0.0944	0.613	0.084	0.567	0.0791	0.716	0.0785	0.695

*Extrapolated Values

Again the use of the heavier gas as the displacing gas in the butane-nitrogen experiments may have caused the diffusivity to be relatively somewhat higher than that of the ethane-nitrogen system, similar to the effect apparent in Table 2.III also.

IV

DISCUSSION

The overall potential error of the method cannot be estimated by the conventional methods due to the iterative nature of the solution. Nevertheless, the extreme sensitivity of the procedure to errors is indicated by the example in the "Results" section (for the hydrogen-nitrogen system in a bed of parallel tubes) where a 3% change in the slope causes a 15% change in the diffusivity. An understanding of the potential accuracy of the method may be aided by examining the first root of the auxillary equation,

$$\tan \alpha L = \frac{h}{\alpha} - \frac{k}{\alpha} = \frac{Q}{A_B\ D_E \alpha} - \frac{\ell \alpha}{\epsilon_B} = \frac{Q\lambda}{A_B\ D_B\ \epsilon_B \alpha} - \frac{\ell \alpha}{\epsilon_B}$$

If the right hand side (RHS) of the equation is large, then αL approaches $\pi/2$ and α becomes independent of the flow rate (Q), bed porosity (ϵ_B), bed area (A_B), end zone length (ℓ) and gas diffusivity (D_B). Thus in order to reduce the present 10% scatter of the experiments, it would appear to be necessary to achieve a large value of αL, that is to increase h/α, and minimize $k\alpha$.

Both h and k are inversely proportional to the porosity, so if $h/\alpha \gg k\alpha$, a porosity decrease will increase the RHS, however, the reduction of bed capacity which results, decreases the time available for

analysis of effluent concentrations. It is noticeable that the results from the low porosity 42 micron bed are less scattered.

The term h increases as the bed area decreases, but experimentally, reduction of the area has the same limitations as a decrease of the porosity, except that the benefits do not depend upon the relative magnitude of h and k.

The gas diffusivity has the same influence as the bed area, and so high diffusivity gases are most susceptible to error. The parallel tube bed with the hydrogen-nitrogen system would be expected to have most scatter of the experimental results. Unfortunately, there are not enough data points to carry out any form of statistical comparison.

High flow rates of the displacing gas increase the term Q and therefore h, but once again experimental factors will restrict the maximum flow rate because of the turbulence, which can enter the bed packing to some extent, thereby increasing the effective diffusivity and making the result flow dependent. Coupled to this is the effect of pressure gradients from friction losses, or changes in kinetic energy at the entry port, which could cause bulk flow in the bed. Even the parallel tube bed is susceptible to bulk flows as the tubes are not sealed at the blank end.

An increase in the end zone length will have the deleterious effect of increasing k and hence decreasing the RHS. In the experimental apparatus used in this work, k was negligible, so that the end zone depth could probably be doubled without too much influence on the magnitude of α. This depth increase might assist in minimizing another potential source of error, in that the solution to the differential equation assumes perfect mixing in the end zone. The use of a deeper end zone would allow larger

scale eddies to increase the mixing, but at the same time the larger eddies should not be able to penetrate too far into the bed. The millipore filter used to discourage eddy penetration does not show any influence on the results, but this is probably to be expected because the added resistance would not amount to more than 0.3% of the total while the results scatter to ± 10%. The millipore filter may help to reduce the penetration of eddies into the bed but it would not be expected to stop the bulk flow effects discussed earlier.

Finally, the length of the bed, L, may be increased to make α small and hence h/d large. On first inspection this is an obvious improvement, however, there are limitations. The dead time, before the second term of the series may be dropped, is increased four fold by doubling the bed length. In the case of the 0.1 cm^2/sec diffusivity gas the dead time was found to be 232 secs for a 10 cm bed (see introduction). In a 20 cm bed a 15 min dead time would be required.

At the same time the effluent gas concentration must be considered. From equation 2.7, the effluent concentration would change only linearly, with bed length. Thus, at the time when the second term represents 1% of the first, the 10 cm bed after 232 secs would have doubled the concentration of the 20 cm bed after 928 secs. The longer bed thus has the effect of lengthening the time scale, and would allow more gas chromatograph analysis to be carried out before the samples are too dilute, but at the same time would start from a lower concentration.

The use of the three constant equation to fit the curved data would not appear to be responsible for the variations in the results because the data for the butane-nitrogen system as shown in Figure 2.5 for

the tubular bed are not curved, yet the diffusivities calculated are badly scattered. It may be noticed, however, that at a flow rate of 0.903 mls/sec the points at 200 and 300 seconds in Figure 2.5 deviate slightly from the other points, and since the least square equation favours the lower times the scatter may be caused by the small deviations of the first two points.

Nitrogen decay was followed in most of the runs, and so the trace of air in the gas systems appeared as nitrogen, resulting in a curve $Y = Ae^{-Bt} + C$ instead of $Y = Ae^{-Bt}$ (where Y and t are the variables), which can be plotted as a straight line. The use of high purity gases might simplify the interpretation of results.

In summary, there are at least three major sources of error which may influence the diffusivity obtained by this method: (a) eddies from the end zone penetrating the bed to increase the diffusivity (b) bulk flow in the bed caused by pressure gradients in the end zone, which also act to increase the diffusivity and (c) poor mixing in the end zone causing a lowered diffusivity.

There is some indication of the presence of the last of these errors in the large diameter parallel tube bed (see Table 2.II). Examination of the data in Tables 2.II, 2.III and 2.IV shows that for the parallel tube bed (Table 2.II) there was no significant increase in diffusivity with increasing gas flow rate. The other beds used, which were more isotropic in structure, do tend to show such an increase with flow rate. As the range of flow rates used in all beds was comparable, there appears to be a slight effect of the first two sources of error mentioned in all but the parallel tube bed. The results for this latter bed (see Table 2.II) also indicate that there may be some evidence for poor mixing in the end zone.

VII

CONCLUSION

The method as used in the present apparatus is satisfactory for measuring gas molecular diffusivities for binary systems within plus or minus 10%. Analysis of sources of error suggest that by redesigning the apparatus a probable accuracy of 2 1/2% could be readily achieved.

VIII

RECOMMENDATIONS

On the basis of this work, it is apparent that a bed of the following dimensions could minimize the potential sources of error encountered in the present experiments.

Parallel tube packing 1 mm or less OD.

Length 20 to 30 cms.

Diameter 5 cms.

End Zone length 0.25 - 0.5 cms.

The sealing off of the tubes and prevention of bulk flows through the bed is also advisable. It would be advantageous to be able to invert the bed and also much time could be saved if the displaced gas could be purged through the bed, particularly if the dead time is increased to 15 mins. or half an hour by the larger bed.

Further Study

The advantages of the larger bed should be experimentally verified and the magnitude of the flow effects, like bulk flow and turbulence, should be investigated if the larger beds are used to reduce the scatter. The effect of the end zone length on the mixing should also be investigated.

NOMENCLATURE

A, B and C, Constants in least square equation.

A_B	Area of bed, cm^2
A_p	Specific surface area/unit volume of bed, cm^{-1}
A_s	Sample or pulse volume, mls.
C_o	Initial gas concentration in Section II, moles/cm^3
C_n	Concentration in stage n, moles/cm^3
C_1	Concentration in mobile phase, moles/cm^3
C_2	Concentration in stationary phase, moles/cm^3
C_A	Concentration of component A, moles/cm^3
C_{Ao}	End zone concentration, moles/cm^3
C_s	Concentration at pellet surface, moles/cm^3
C_{avg}	Average concentration, moles/cm^3
C'	Initial concentration, moles/$cm.^3$
D	Diffusion coefficient, cm^2/sec
D_B	Molecular diffusion coefficient, cm^2/sec
D_K	Knudsen coefficient, cm^2/sec
D_E	Effective diffusion coefficient, cm^2/sec
D_L	Longitudinal dispersion coefficient (Overall including molecular term contribution), cm^2/sec
D_L*	Eddy diffusion coefficient (excluding molecular diffusion) cm^2/sec
E	Effectiveness factor
F_1	Area fraction of mobile phase = ϵ_B
F_2	Area fraction of stationary phase = $(1 - \epsilon_{B_1})$
H	HETP, cms.
HETP	Height equivalent to a theoretical plant, cms.
K	Constants
L	Length of bed, cms.

N_A	Molar flux, moles/sec of component A per cm^2
$N_A{}^1$	Molar flux per unit geometrical area, moles/$(cm)^2$ sec.
P	Pressure, atm.
Q	Total flux, moles/sec., or gas flow rate, mls./sec. or pellet volume in Appendix IV
R	Gas constant or radius dimension
T	Temperature, °K
U	Volume of gas, mls.
V	Volume of gas phase in theoretical plate, cm^3
V_p	Volume of theoretical plate cms^3
W	Adsorption or partition coefficients.
Z	Coefficient of exponential.
d_p	Pellet diameter, cms.
d_T	Column diameter, cms.
f	Fanning friction factor.
h_D	Hydraulic diameter, cms.
h	Thiele modulus or in section II $h = Q/A_B D_E$
j	$1 + N_A/N_B$
k	First order rate constant, $sec.^{-1}$
k_1	Mass transfer coefficient in mobile phase, cm/sec.
k_2	Mass transfer coefficient in stationary phase, cm/sec.
ℓ	End zone length, cms.
n	Number of theoretical plates, or number of term in series solution.
r	Pore radius, or radius variable in differential equation, cms.
t	Time, seconds
u	Interstitial velocity, cm/sec.
v	Volume of liquid side of theoretical plate, cm^3
$\bar{v}$	Average velocity of a gas molecule, cms/sec.

x	Distance in direction of flux or flow, cms.
y	Mole fraction or peak height.
α	Mass transfer coefficient, sec.$^{-1}$ (Section 1)
α_n	Consecutive roots of equation (2.11) (Section2)
Δ	Error in equality of equation.
ϵ_p	Pellet porosity
ϵ_B	Bed porosity.
ρ_m	Molar density, moles/ml.
ρ	Density, grams/ml.
μ	Viscosity, cps
γ	Eddy diffusivity coefficient.
λ	Tortuosity
σ	Standard deviation.

LITERATURE CITED

1. Thiele, E.W., Ind. Eng. Chem., 31, 916, (1939).

2. Wheeler, A., in "Advances in Catalysis", Vol. 3, 249-327, Academic Press, New York, (1951); Wheeler, A., "Catalysis", Vol. 2, 105-167, P.H. Emmett, Ed., Reinhold Pub. Corp., New York, (1955).

3. Aris, R., Chem. Eng. Sci., 6, 262, (1957).

4. Scott, D. S., Can. J. Chem. Eng., 40, 173, (1962).

5. Scott, D. S. and Dullien, F.A.L., A.I.Ch.E. Journal, 8, 113, (1962).

6. Currie, J.A., Brit. J. App. Phys., 11, 314, (1960).

7. Petersen, E.E., A.I.Ch.E. Journal, 3, 443, (1957); A.I.Ch.E. Journal, 4, 343, (1958).

8. Arnell, J.C., Can. J. Res., 25A, 191, (1947).

9. Rao, M.R. and Smith, J.M., A.I.Ch.E. Journal, 10, 293, (1964).

10. Turner, G.A., Chem. Eng. Sci., 1, 156, (1958).

11. Wakao, N. and Smith, J.M., Chem. Eng. Sci., 17, 825, (1962).

12. Mingle, J.O. and Smith, J.M., A.I.Ch.E. Journal, 7, 243, (1961).

13. Weisz, P.B., A. Phys. Chem., 11, 1, (1957).

14. Scott, D.S. and Cox, K.E., Can. J. Chem. Eng., 38, 201, (1960).

15. McHenry, K.W. and Wilhelm, R.H., A.I.Ch.E. Journal, 3, 83, (1957).

16. Deissler, P.F. and Wilhelm, R.H., Ind. Eng. Chem., 45, 1219, (1953).

17. Van Deemter, J.J., Zuiderweg, F.J. and Klinkenberg, A., Chem. Eng. Sci., 5, 271, (1956).

18. Hougen, J.O., "Experience and Experiments with Process Dynamics", P.13, Chem. Eng. Progress Monograph Series, No.4, 60, A.I.Ch.E., New York, (1964).

19. Klinkenberg, A. and Sjenitzer, F., Chem. Eng. Sci., 5, 285, (1956).

20. Lapidus, L. and Amundson, N.R., J. Phys. Chem., 56, 984, (1952).

21. Engun, S., Chem. Eng. Prog., 48, 227, (1952).

22. Crank, J., "The Mathematics of Diffusion", p. 121, University Press, Oxford, (1965).

23. Carberry, J.J. and Bretton, R.H., A.I.Ch.E. Journal, 4, 367, (1958).

24. Hiby, J.W., "Interaction between Fluids and Particles", Inst. Chem. Eng. Symposium, C 71, London, June (1962).

25. Taylor, G.I., Proc. Roy. Soc., A 225, 473, (1954).

26. Aris, R., Proc. Roy. Soc., A 235, 473, (1956).

27. Turner, J.C.R., Brit. Chem. Eng., 9, 376, (1964).

28. Bischoff, K.B. and Levenspiel, O., Chem. Eng. Sci., 17, 257, (1962), also "Advances in Chemical Engineering", Vol. IV, Academic Press, New York, (1964).

29. Saffman, P.C., Chem. Eng. Sci., 11, 125, (1959), J. Fluid Mech., 6, 321, (1959); 7, 194, (1960); 8, 273, (1960).

30. Harley, J., Nel W., and Pretorius, V., Nature, 181, 177, (1958).

31. Newsome, J.W., Heiser, H.W., Russell, A.S. and Stumpf, H.C., "Alumina Properties", Tech. Paper No. 10, Alcoa Research Laboratories, Aluminum Co. of America, Pitsburgh, (1960).

32. Bird, R.B., Stewart, W.E. and Lightfoot, E.N., "Transport Phenomena", John Wiley and Sons, New York, (1960).

33. Perry, J.H., "Chemical Engineer's Handbook", 3rd Ed., P. 370, McGraw-Hill Book Co., New York, (1950).

34. Cairns, E.J. and Prausnitz, J.M., Chem. Eng. Sci., 12, 20, (1960).

35. Giddings, J.C. and Seager, S.L., Ind. Eng. Chem. Fundamentals, 1, 277, (1962).

36. Kenney, N., Dept. of Chemical Engineering, University of Cambridge, Private communication.

37. Walker, R.E. and Westenberg, A.A., J. Chem. Phys., 29, 1139, (1958).

38. Carslaw, H.S. and Jaeger, J.C., "Conduction of Heat in Solids", 2nd Ed., P. 129, University Press, Oxford, (1959).

39. Ralston, A. and Wilf, H.S., Mathematical Methods for Digital Computers", P. 33, John Wiley and Sons Inc., New York, (1964).

40. Hirschfelder, J.O., Curtiss, C.F. and Bird, R.B., "Molecular Theory of Gases and Liquids", P. 579, John Wiley and Sons Inc., New York(1954).

41. Cox, K.E., MASc. Thesis, "Diffusion of Gases", University of British Columbia, (1959).

42. Bluh, O. and Elder, J.D., "Principles and Applications of Physics", P. 492, Oliver and Boyd Ltd., Edinburgh, (1955).

43. Kipping, P.J., Jeffery, P.C. and Savage, C.A., Research and Development for Industry, No. 39, P. 18, Feb. - March, (1965).

APPENDIX I

DETERMINATION OF THE EFFECTIVE GAS DIFFUSIVITY IN A POROUS SPHERICAL PELLET BY A STEADY STATE METHOD

INTRODUCTION

In order to evaluate the results obtained by the pulse technique an apparatus was constructed to measure the effective gas diffusivity in the test materials by a well established procedure. The steady state method described by Weisz (13) was selected.

THEORY

Different diffusion regimes, Knudsen and bulk, were anticipated in the two samples which were examined and so two solutions are needed for the diffusion equation.

Knudsen Diffusion

The molar flux N_A is given in terms of the Effective Diffusivity D_E and the concentration gradient by Fick's first law,

$$N_A = - D_E \frac{d\,C_A}{dx} \quad \text{at any plane x, moles/sec cm}^2$$

Referring to Figure A I.1,

The total flux Q is given by $Q_A = N_A$ (Area of plane) $= N_A\, \pi\, (R^2 - x^2)$ moles/sec

$$Q_A = D_E\, \pi\, (R^2 - x^2) \frac{dC_A}{dx}$$

$$\int \frac{dx}{R^2 - x^2} = - \int \frac{D_E \pi}{Q_A}\, dC_A$$

$$\frac{1}{2R} \left[\text{Ln} \frac{R + x}{R - x} \right]_{-t}^{+t} = - \frac{D_E \pi}{Q_A} \left[C_A \right]_1^2$$

$$- D_E = \frac{Q_A}{2\pi R} \frac{1}{C_{A_2} - C_{A_1}} \text{Ln} \left[\frac{R + t}{R - t} \right]^2$$

Since $C_A = \rho_m\, y_A$ where y is the mole fraction and ρ_m the molar density

$$D_E = \frac{Q_A}{2\pi R \rho_m} \text{Ln} \left[\frac{R + t}{R - t} \right]^2 \frac{1}{y_{A_1} - y_{A_2}} \quad \text{cm}^2/\text{sec}$$

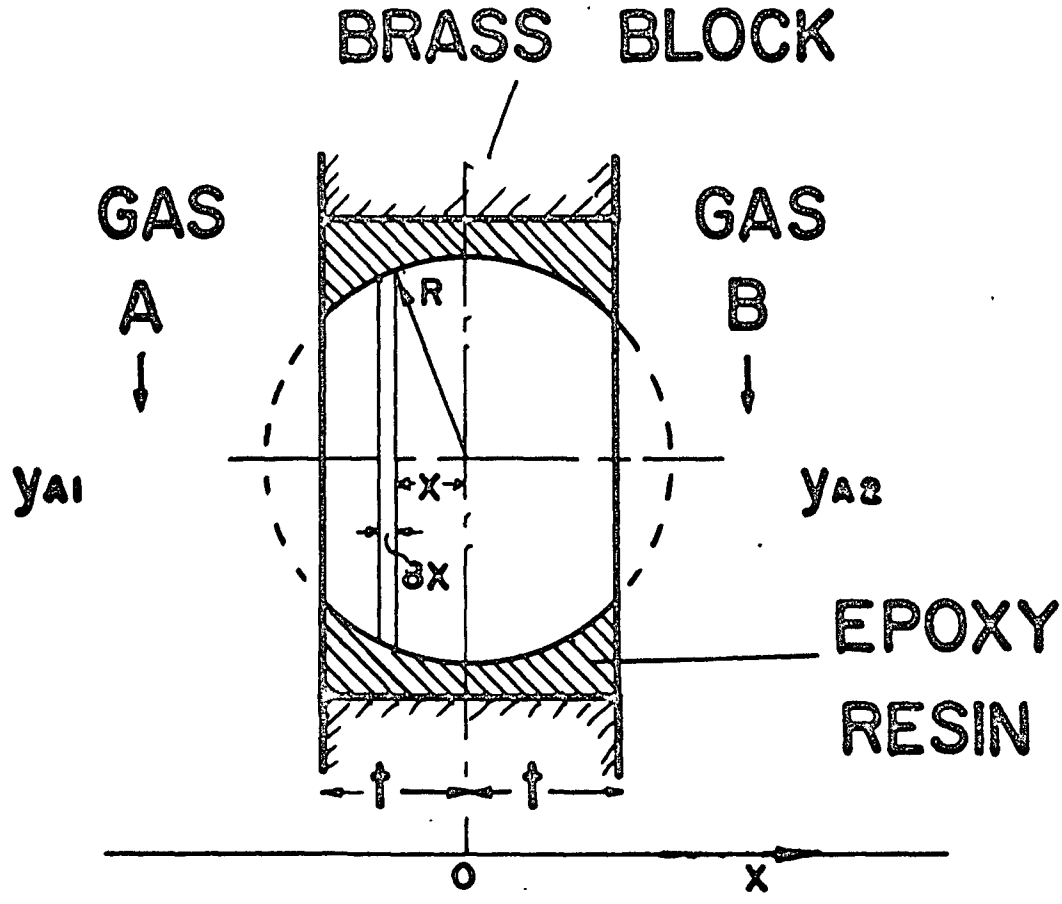

Figure A I.1

Sample Mounting In Steady State Apparatus

Bulk Diffusion

Fick's law is again applied but with a correction for the bulk flow caused by non-equimolar counter diffusion.

$$N_A = - D_E \frac{d\,C_A}{dx} + (N_A + N_B)\, y_A \quad \text{moles/sec cm}^2$$

$$Q_A = N_A\ (\text{Area}) = - D_E \pi (R^2 - x^2) \frac{dC_A}{dx} + (Q_A + Q_B)\, y_A$$

$$D_E\, \pi\, (R^2 - x^2)\, \rho_m \frac{dy_A}{dx} = - Q_A + Q_A y_A + Q_B y_A$$

$$\frac{dy_A}{\left[\left(1 + \frac{Q_B}{Q_A}\right) y_A - 1\right]} = \frac{Q_A\ dx}{D_E \pi \rho_m (R^2 - x^2)}$$

$$\frac{1}{\left(1 + \frac{Q_B}{Q_A}\right)} \left[\operatorname{Ln}\left[y_A\left(1 + \frac{Q_B}{Q_A}\right) - 1\right]\right]_{y_{A_1}}^{y_{A_2}} = \frac{Q_A}{D_E \pi \rho_m} \left[\frac{1}{2R} \operatorname{Ln}\left(\frac{R + x}{R - x}\right)\right]_{-t}^{+t}$$

$$D_B = \frac{Q_A}{2\,\pi\,R\,\rho_m} \left(1 + \frac{Q_B}{Q_A}\right) \frac{\operatorname{Ln}\left(\frac{R + t}{R - t}\right)^2}{\operatorname{Ln}\left[\frac{y_{A_2}\left(1 + \frac{Q_B}{Q_A}\right) - 1}{y_{A_1}\left(1 + \frac{Q_B}{Q_A}\right) - 1}\right]} \quad \text{cm}^2/\text{sec}$$

APPARATUS

The apparatus shown in Figure A I.2 was assembled around a pair of brass blocks between which a third block (shown in Figure A I.1) containing the sample pellet was bolted. The brass blocks were constructed in such a way that two different gases could be flushed through mirror image passages across the two faces of the sample. Streams of hydrogen and nitrogen from their respective cylinders flowed through their respective cylinder pressure regulators and "Moore" constant differential flow controls to the reference sides of a pair of "Gow Mac" NIS model 9220 thermal conductivity cells. From the reference cells the gases could be

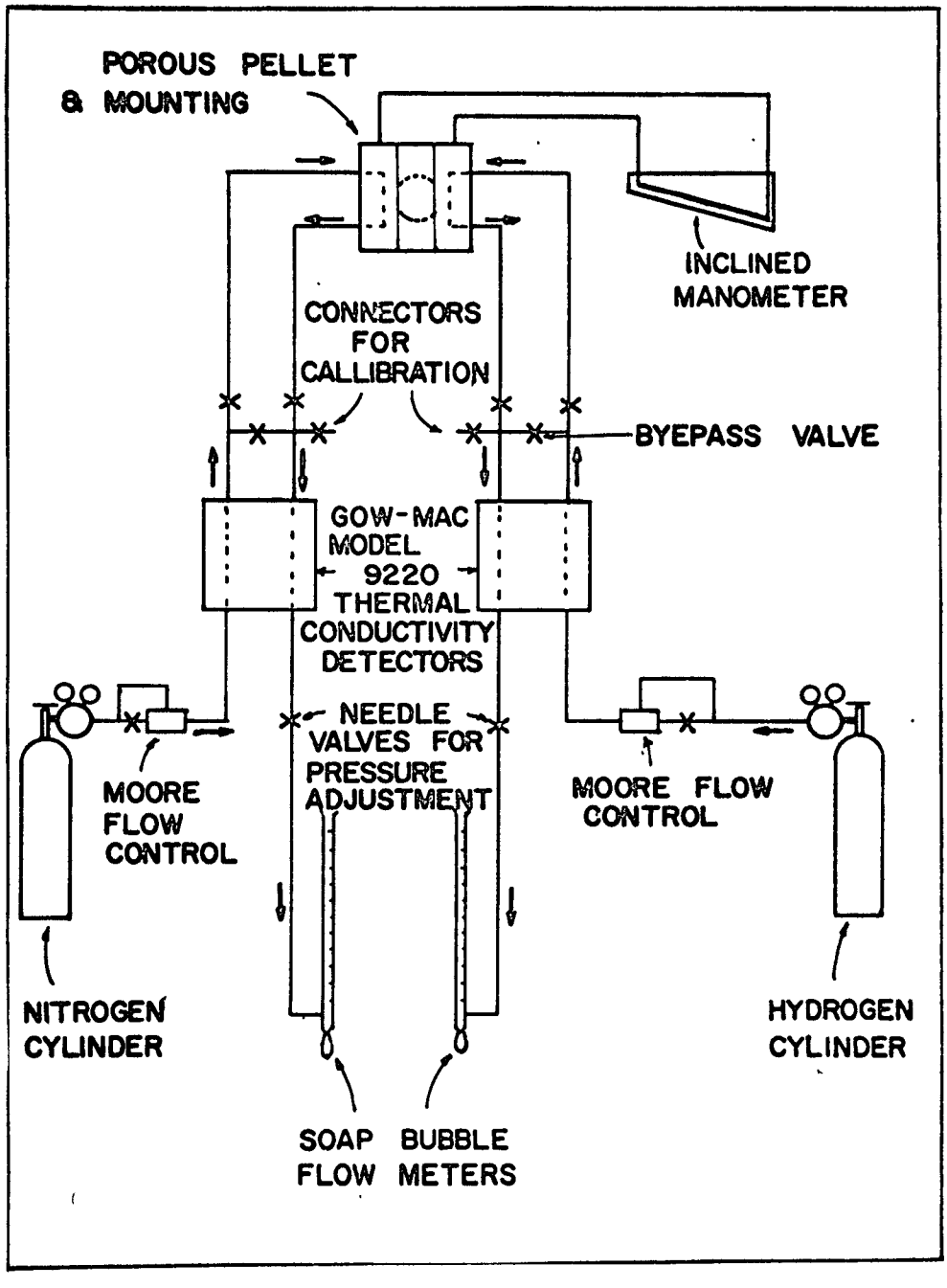

Figure A I.2

Steady State Apparatus

diverted either across the sample faces, or via a by-pass to the measuring side of the cells, and from here the gases were vented to atmosphere through a needle valve and soap bubble flow meter.

Manometer taps in the sample blocks were located opposite the centre of the sample faces and were connected to an inclined oil filled manometer. Polyethylene 1/4" diameter tubing was used for connecting the apparatus, and this allowed flushing of dead end lines by loosening of the fittings.

The test samples were mounted by bathing them in epoxy resin, and then fitting them into the brass block which was drilled with a clearance hole. After the resin had set the faces of the pellet were ground by means of sand paper on a glass plate.

Two "DORION" potentiometers were used to measure the output of the cells which formed part of a conventional bridge circuit.

PROCEDURE

Calibration of Thermal Conductivity Cells

These "diffusion-type" cells have the property of being relatively independent of flow rate, and at low concentrations a linear output with concentration can be assumed. In order to calibrate the nitrogen cell a fairly high flow was set through the cell and sample block by-pass. The nitrogen flow rate was measured with the bubble meter and the cell zero adjusted electrically. A flow of hydrogen was set through its system and measured on the appropriate bubble meter. The polythene tube from the hydrogen was then disconnected and reconnected into a point on the by-pass of the nitrogen system so that the hydrogen now appeared in the measuring

side of the nitrogen cell. The system was allowed to come to equilibrium and the output measured on the potentiometer. The concentration was calculated from the flow rates of the two gases.

Operation

The two gas flows were set to convenient levels and measured while passing through the sample by-pass system. The outputs of the two detectors were set to zero, and then the flows were diverted to pass across the sample faces. The manometer legs were bled and the outlet measuring valves were adjusted to be at maximum opening but maintaining zero pressure difference across the pellet. The system was allowed to come to equilibrium, and then detector outputs were taken at convenient intervals over a period of twenty minutes. The gas streams were set back on the by-pass and the zero drift of the detectors in the course of the experiment recorded along with the flow rates of the gases.

RESULTS

Calibration of thermal conductivity detectors

Nitrogen content in hydrogen cell

Nitrogen flow: 25 mls in 72.0, 72.2 seconds = 0.346 mls/sec.

Hydrogen flow: 50 mls in 8.2, 8.2, 8.6 seconds = 6.1 mls/sec.

$$\text{Mole \% nitrogen} = \frac{0.346}{6.1 + 0.346} \times 100 = 5.37\%$$

Output of detector 9.56 millivolts or 1.78 mv/1% nitrogen

Hydrogen content in nitrogen cell

Nitrogen flow: 50 mls in 7.5, 7.5 seconds = 6.66 mls/sec.

Hydrogen flow: 25 mls in 68.0, 68.5 seconds = 0.367 mls/sec.

$$\text{Mole \% hydrogen} = \frac{0.367}{6.66 + 0.367} \times 100 = 5.22\%$$

Output of detector 11.205 x 5 millivolts or 10.72 mv/1% hydrogen

It is of interest to compare the above result with the calibration of Cox (41)who obtained several points with a similar apparatus and verified the linearity of the response. He obtained a slope of 10.85 mv/1% hydrogen.

Activated Alumina Pellet 1/4" Diameter

Pellet Characteristics

"Alcoa H151 Activated alumina sphere" having 42 A mean pore diameter.

Diameter of pellet used in test = 0.255", 0.262", 0.262"

Average Dia. = 0.66 cms

Thickness of mounting plate, i.e. across flats of pellet = 3/16" = 0.476 cms.

The mean free path of hydrogen at 0°C and 1 atmosphere = 180×10^{-7} cms. (Ref.42) = 1800 A versus 42 A pore size hence Knudsen diffusion will be the predominant mechanism.

The amount of nitrogen which diffused into the hydrogen stream in this experiment was so small that with the lower sensitivity of this detector the output was of the same order as the zero drift during the course of the experiment. For this reason the diffusivity is calculated from the hydrogen flux,

Hydrogen flow rate: 50 mls in 20.5, 20.5 sec. before test
22.0, 22.2 sec. after test

Nitrogen flow rate: 50 mls in 18.8, 18.8 sec. before test
19.0, 19.0 sec. after test

Room temperature 26°C

Atmospheric Pressure 755.6 mm Hg.

Analysis of Streams

Hydrogen in nitrogen mv: 1.47, 1.44, 1.42, 1.41, 1.405, 1.405, 1.405 zero drift add 0.17 mv yielding 1.575 mv.

Nitrogen in hydrogen mv: 0.07, 0.07, 0.07, 0.095, 0.07, 0.08, 0.08 zero drift add 0.045 mv yielding 0.12 mv

Subscript A refers to hydrogen

$$Q_A = \frac{50}{19.0} \times \frac{1.575\,\rho_m}{10.85 \times 100} = .00382\,\rho_m \text{ moles/sec}$$

$$y_{A_1} = 1.0 - \frac{.125 \times .01}{1.78} = 0.9993 \text{ mole fraction}$$

$$y_{A_2} = \frac{1.575}{10.72} = 0.147\% = .00147 \text{ mole fraction}$$

$$D_K = \frac{Q_A}{2\pi R\,\rho_m} \quad \text{Ln}\left(\frac{2R + 2t}{2R - 2t}\right)^2 \quad \frac{1}{y_1 - y_2}$$

$$= \frac{.00382\rho_m}{2\left(\frac{.66}{2}\right)\rho_m} \quad \text{Ln}\left[\frac{.66 + .476}{.66 - .476}\right]^2 - \frac{1}{0.9993 - .00147}$$

$$= 0.0067 \text{ cm}^2/\text{sec}$$

Knudsen diffusivity of hydrogen in pellet = 0.0067 cm^2/sec at 26°C

"Norton" Catalyst Support 1/2" Diameter (Alundum)

Pellet Characteristics

Maximum diameter of pellet = 0.55"

Minimum diameter of pellet = 0.525"

Mean diameter = 0.538" or 1.365 cms.

Thickness of samples plate 0.90 cms.

Pore diameter 90% in range 2 to 40 microns. Hydrogen has a mean free path around 0.18 microns (Ref. 42) so that bulk diffusion will be the predominant mechanism.

Nitrogen flow rate 50 mls in 28.0, 27.0, 27.5 seconds before test

28.1, 28.0 seconds after test

Hydrogen flow rate 50 mls in 27.2, 27.1 seconds before test

29.8, 30.0 seconds after test

Room temperature 23°C

Atmospheric pressure 760.7 mm Hg

Analysis of streams

Hydrogen in nitrogen millivolts		Nitrogen in hydrogen millivolts	
17.495 x 5	17.44 x 5	3.91	4.09
17.485	17.46	3.95	4.10
17.491	17.45	3.97	4.10
17.46	17.44	4.00	4.10
17.47	17.37	4.02	4.13
17.45	17.35	4.04	4.13
17.43	17.39	4.07	4.15
17.39	17.46	4.10	
		4.10	
Average = 17.421 mv		- 4.103 mv	
Zero drift: add 0.0		add 0.22	
17.421 x 5/ 10.72 = 8.11%		4.32/ 1.78 = 2.425%	

Subscript A refers to hydrogen

$y_{A_2} = 0.081$ $\qquad$ $y_{A_1} = 0.97575$

$$Q_A = \frac{50}{28.05} \times .0811\, \rho_m = 0.1445\, \rho_m \text{ moles/sec}$$

$$Q_B = \frac{50}{29.9} \times .02425\, \rho_m = 0.0405\, \rho_m \text{ moles/sec}$$

$$D_{\text{Effective}} = \frac{Q_A}{2\pi R \rho_m}\left(1 + \frac{Q_B}{Q_A}\right) \frac{\left[\frac{2R + 2t}{2R - 2t}\right]^2}{\text{Ln}\left[\frac{y_{A_2}\left(1 + \frac{Q_B}{Q_A}\right) - 1}{y_{A_1}\left(1 + \frac{Q_B}{Q_A}\right) - 1}\right]}$$

$$= \frac{0.1445\, \rho_m}{2\pi \frac{1.365}{2} \rho_m}\left(1 - \frac{0.0405}{0.1445}\right) \frac{\text{Ln}\left(\frac{1.365 + 0.90}{1.365 - 0.90}\right)^2}{\text{Ln}\left(\frac{0.0811\,(.7195) - 1}{0.97575\,(.7191) - 1}\right)}$$

$$= 0.0667 \text{ cm}^2/\text{sec}$$

Effective bulk diffusivity of hydrogen and nitrogen in the 1/2" Norton catalyst supports was found to be 0.0667 cm^2/sec at 23°C and 760.7 mm Hg pressure.

Scott and Dullien (5) pointed out that the ratio of fluxes of two gases diffusing at constant pressure in capillaries should be inversely proportional to the ratio of the square root of their molecular weights. In this experiment a ratio of 3.57 was obtained as compared with a value of 3.74 for the square root of the molecular weights. The difference is probably caused by the difficulty in keeping the pressures identical across the pellet.

No absolute pressure measurements were taken in the test cell and so the actual pressure of the measurement may be expected to be slightly higher than the ambient atmospheric pressure. However, care was taken to operate with the valves wide open except to balance the different pressure drops caused by the difference in viscosity of the gases. Results on other equipment at similar flow rates indicate that a 1/4" tube at flow rates such as used here, the pressure drop is not measurable on a mercury manometer.

CONCLUSION

The diffusion coefficient for the Knudsen diffusion of hydrogen in a 1/4" dia. Alcoa H 151 activated alumina spheres was found to be 0.0067 cm^2/sec at 26°C. The moisture content of the pellet is taken to be 12% by wt from analysis of similar pellets, however, the actual moisture of the test pellet during the test was not obtainable.

The diffusion coefficient for the bulk diffusion of hydrogen and nitrogen in 1/2" dia. Norton SA 203 Alundum catalyst carrier spheres was found to be 0.0667 cm^2/sec at 23°C and 760.7 mm Hg. No moisture adsorption was found in these pellets.

```
ISN        SOURCE STATEMENT

     C     PROGRAM FOR COMPUTATION OF RESULTS FROM NON POROUS PELLET RUNS
   1 85    READ55,NO,CL,CD,DP ,EB ,EP,DOBS
   3 55    FORMAT (I5,3F10.4,2F10.7,F12.9 )
   4       IF (NO) 84,83,84
   5 84    CALL SKIP TO (1)
   6       PRINT 56
   7 56   0FORMAT(8H   RUN  ,2X,6HCOLUMN,3X,6HCOLUMN,4X,6HPELLET,5X,3HBED,6X,
          16HPELLET,4X,11HDIFFUSIVITY   )
  10       PRINT 57
  11 57   0FORMAT(4X,2HNO ,4X,6HLENGTH,2X,8HDIAMETER,2X,8HDIAMETER,2X,8HPOROS
          1ITY,2X,8HPOROSITY  /11X,2HCMS      CMS       CMS  )
  12       READ 81,GM,T,TOBS,P,VISC ,ADS
  13 81    FORMAT(4F12.5,2F12.7 )
  14       D=DOBS*(T/TOBS)**1.7 /P
  15       PRINT 550,NO,CL , CD , DP , EB , EP, D
  16 550   FORMAT(1X,I5,3F10.4,2F10.7,F12.9)
  17       PRINT 65
  20 65    FORMAT(/51H   CARRIER MW   TEMP KELVIN PRESS ATM   VISCOSITY   ,
          1 12H   HYD DIA   ,10H DENSITY                    )
  21       HO =EB*CD/(3.*CD*(1.-EB)/(2.*DP)+1.)
  22       VISC= 0.01709*((273.1+114.)/(T+114.))*(T/273.1)**1.5
  23        RHO=29.*273.*P/(22400.*T)
  24       PRINT 64,GM  , T ,P , VISC   ,HO,RHO
  25 64    FORMAT(1X,3F12.5,3F12.7 // )
  26       N=0
  27       SMS=  0.0
  30       SM =  0.0
  31       SU =  0.0
  32       SUS=  0.0
  33       SW =  0.0
  34       SWS=  0.0
  35       SWU=  0.0
  36       SMW=  0.0
  37       SMWS = 0.0
  40       SMW2 = 0.0
  41       SMW3 = 0.0
  42       SW3  = 0.0
  43       SW4  = 0.0
  44        SG=0.0
  45       SGU=0.0
  46       PRINT 40
  47 40    FORMAT(5X,1H1,9X,1H2,9X,1H3,9X,1H4,7X,1H5,9X,1H6,9X,1H7,9X,1H8,7X,
          11H9,7X,2H10,6X,2H11,6X,2H12,6X,2H13  )
  50       PRINT60
  51 60    FORMAT(74H VELOCITY  HETP      MOLECULAR  PELLET RE    NTU     WID
          1TH      TOTAL     0.43M   EDDY DIFF PECLET EMPTY RE  1/SCH RE HYD /
          228H  CM/SEC    CMS        PECLET,27X,10HCM     CM    ,5X,7HMLS/SEC )
  52       CRE  =  DP*GM *100./(22400.*VISC *T)* 273.*P
  53       CUL  =  CL/(2. * D)
  54 10    READ 99,Q,WIDTH, TOTAL
  55 59    FORMAT(3F12.5 )
  56       IF(Q) 5,6,5
  57 5     HH =(2.36* TOTAL/ WIDTH)**2
  60       H  = CL/HH
  61       U= Q*4./(3.14159*EB*P*CD**2) *T/298.
```

```
 ISN      SOURCE STATEMENT

  62      GAG=H-1.5*D/U
  63      W  = 1./U
  64      RE=CRE*U
  65      NTU= CUL*U
  66      DL=H*U/2.
  67      SC=DL*CRE/DP
  70      REZ=RE*EB
  71      PE=DL*W/DP
  72      PEM =U*DP/D
  73      REM = CRE*U*HD/DP
  74      PRINT52,U,H,PEM,RE,NTU,WIDTH,TOTAL,Q,DL,PE,REZ,SC,REM
  75 52   FORMAT (4F10.5,I8 ,3F10.4 ,5F8.3 )
  76 11   N= N+1
  77      SG=SG+GAG
 100      SGU=SGU+GAG*U
 101      SH  = SH +  H
 102      SU  = SU +  U
 103      SW  = SW +  W
 104      SUS = SUS+  U**2
 105      SWS   = SWS +   W**2
 106      SHU   = SHU +   H*U
 107      SHW   = SHW +   H/U
 110      SHS   = SHS +   H**2
 111      SHWS =SHWS +(H*W)**2
 112      SHW2 =SHW2 + H*W**2
 113      SHW3 =SHW3 + H*W**3
 114      SW3 =SW3 + W**3
 115      SW4 =SW4 + W**4
 116      GOTO  10
 117 6    EN= N
 120      AK =  SU - EN*SUS/ SU
 121      BK =  SU - EN**2/ SW
 122      CK =  SH - EN*SHU/ SU
 123      DK =  SH - EN*SHW/ SW
 124      EK =  SW - EN**2/  SU
 125      FK =  SW - EN*SWS/ SW
 126      C  =  (CK/EK - DK/FK)/ (AK/EK- BK/FK)
 127      B  =  (DK- C*BK)/FK
 130      A  =  (SH - C*SU- B*SW)/EN
 131      CC=(SGU-SG*SU/EN)/(SUS-SU**2/EN)
 132      AA=(SG-CC*SU)/EN
 133 559  PRINT 51
 134 51   FORMAT(/9X,1HA,18X,1HB,17X,1HC,14X,5HSIGMA,9X,1HN)
 135     OSIGMA =SQRT (1./EN*(SHS-2.*A*SH-2.*SHW*B-2.*C*SHU+EN*A**2+2.*A*B*
         1SW + 2.*A*C*SU + B**2*SWS +2.*EN*B*C + C**2*SUS)  )
 136      PRINT 50, A,B, C, SIGMA, N,AA,CC
 137 50   FORMAT(1X,4F18.8,I4//9X,3HAA=,F10.7,5X,3HCC=,F10.7 /  )
 140 558  GAMMA = B/(2.*D)
 141       AMDA = A/(2.*DP)
 142      PRINT 82 ,GAMMA,AMDA
 143 82   FORMAT(/10X,6HGAMMA= ,F10.6,15X,6HLAMDA= ,F10.6   )
 144      GOTO 85
 145 83   STOP
 146      END
```

RUN NO	COLUMN LENGTH CMS	COLUMN DIAMETER CMS	PELLET DIAMETER CMS	BED POROSITY	PELLET POROSITY	DIFFUSIVITY
1	134.6000	2.6100	0.2200	0.3800000	0.	0.102000000

CARRIER MW	TEMP KELVIN	PRESS ATM	VISCOSITY	HYD DIA	DENSITY
28.00000	296.00000	1.00000	0.0182169	0.0824221	0.0011940

1 VELOCITY CM/SEC	2 HETP CMS	3 MOLECULAR PECLET	4 PELLET RE	5 NTU	6 WIDTH CM	7 TOTAL CM	8 Q ML/SEC	9 EDDY DIFF	10 PECLET	11 EMPTY RE	12 1/SCH RE	13 HYD
0.62536	0.46551	1.34882	0.87068	412	2.6800	19.3100	1.2800	0.146	1.058	0.331	0.921	0.326
0.61559	0.46618	1.32774	0.85708	406	2.7500	19.8000	1.2600	0.143	1.060	0.326	0.908	0.321
0.61559	0.45838	1.32774	0.85708	406	2.7200	19.7500	1.2600	0.141	1.042	0.326	0.893	0.321
0.54231	0.49807	1.16968	0.75505	357	3.2100	22.3600	1.1100	0.135	1.132	0.287	0.855	0.283
0.54231	0.49900	1.16968	0.75505	357	3.1900	22.2000	1.1100	0.135	1.134	0.287	0.856	0.283
0.43238	0.59312	0.93258	0.60200	285	4.4100	28.1500	0.8850	0.128	1.348	0.229	0.811	0.226
0.36398	0.65800	0.78506	0.50676	240	5.4700	33.1500	0.7450	0.120	1.495	0.193	0.758	0.190
0.23847	0.89910	0.51424	0.33195	157	2.7100	14.0500	0.4880	0.107	2.043	0.126	0.478	0.124
0.22376	0.97490	0.48262	0.31154	147	1.4200	7.0700	0.4580	0.109	2.216	0.118	0.690	0.117
0.18077	1.11981	0.38989	0.25168	119	3.9500	18.3500	0.3700	0.101	2.545	0.096	0.641	0.094
0.13338	1.47568	0.28768	0.18570	88	2.9900	12.1000	0.2730	0.098	3.354	0.071	0.623	0.370
0.08794	1.99357	0.18968	0.12244	58	10.6700	37.1500	0.1800	0.088	4.531	0.047	0.555	0.046
0.05179	3.63038	0.11170	0.07210	34	11.5500	29.8000	0.1060	0.094	8.251	0.027	0.595	0.027
2.49168	0.37916	5.37420	3.46913	1644	0.6100	4.8700	5.1000	0.472	0.862	1.318	2.989	1.300
1.42172	0.35907	3.06646	1.97944	938	1.0300	8.4500	2.9100	0.255	0.816	0.752	1.615	0.742
0.89407	0.39996	1.92839	1.24480	589	1.7200	13.3700	1.8300	0.179	0.909	0.473	1.132	0.466
1.12858	0.36565	2.43420	1.57131	744	1.3100	10.6500	2.3100	0.206	0.831	0.597	1.306	0.589
0.75239	0.41030	1.62280	1.04754	496	2.0900	16.0400	1.5400	0.154	0.933	0.398	0.977	0.392
0.62536	0.46551	1.34882	0.87068	412	2.6800	19.3100	1.2800	0.146	1.058	0.331	0.921	0.326

A	B	C	SIGMA	N
0.13017484	0.17715220	0.07368439	0.04166462	19

AA= 0.2891281 CC=-0.0333551

GAMMA= 0.868393 LAMDA= 0.295852

END-OF-DATA ENCOUNTERED ON SYSTEM INPUT FILE.

TIME 19HRS 18MIN 59.1SEC

RUN NO	COLUMN LENGTH CMS	COLUMN DIAMETER CMS	PELLET DIAMETER CMS	BED POROSITY	PELLET POROSITY	DIFFUSIVITY
50	111.8000	5.0000	0.2080	0.3660000	0.	0.162381388

CARRIER MW	TEMP KELVIN	PRESS ATM	VISCOSITY	HYD DIA	DENSITY
29.00000	294.70000	1.26900	0.0181546	0.0766955	0.0015219

1 VELOCITY CM/SEC	2 HETP CMS	3 MOLECULAR PECLET	4 PELLET RE	5 NTU	6 WIDTH CM	7 TOTAL CM	8 Q MLS/SEC	9 EDDY DIFF	10 PECLET	11 EMPTY RE	12 1/SCH RE	13 HYD
1.37719	0.25976	1.76410	2.40141	474	2.1500	18.9000	12.7000	0.179	0.624	0.879	1.499	0.885
1.32840	0.26547	1.70159	2.31632	457	0.4600	4.0000	12.2500	0.176	0.638	0.848	1.478	0.856
1.26875	0.28448	1.62519	2.21232	436	0.5000	4.2000	11.7000	0.180	0.684	0.810	1.513	0.815
1.16031	0.34151	1.48629	2.02323	399	0.6000	4.6000	10.7000	0.198	0.821	0.741	1.661	0.745
1.04645	0.35333	1.34044	1.82469	360	0.6700	5.0500	9.6500	0.185	0.849	0.668	1.550	0.673
0.92174	0.38881	1.18069	1.60724	317	0.8100	5.8200	8.5000	0.179	0.935	0.588	1.502	0.593
0.80246	0.44057	1.02790	1.39925	276	1.0000	6.7500	7.4000	0.177	1.059	0.512	1.482	0.515
0.45003	0.66467	0.57646	0.78471	154	2.2200	12.2000	4.1500	0.150	1.598	0.287	1.254	0.289
0.29279	1.15811	0.37504	0.51054	100	4.9000	20.4000	2.7000	0.170	2.784	0.187	1.421	0.188

A	B	C	SIGMA	N
-0.06964026	0.34937887	0.07176007	0.02973078	9

AA= 0.2799876 CC=-0.1502027

GAMMA= 1.063480 LAMDA= -0.167404

RUN NO	COLUMN LENGTH CMS	COLUMN DIAMETER CMS	PELLET DIAMETER CMS	BED POROSITY	PELLET POROSITY	DIFFUSIVITY
51	118.1000	2.6000	0.2080	0.3830000	0.	0.209233964

CARRIER MW	TEMP KELVIN	PRESS ATM	VISCOSITY	HYD DIA	DENSITY
29.00000	296.00000	1.02000	0.0182169	0.0792282	0.0012179

1 VELOCITY CM/SEC	2 HETP CMS	3 MOLECULAR PECLET	4 PELLET RE	5 NTU	6 WIDTH CM	7 TOTAL CM	8 Q ML/SEC	9 EDDY DIFF	10 PECLET	11 EMPTY RE	12 1/SCM RE	13 HYD
4.59739	0.30830	4.57028	6.39324	1297	0.7500	6.2200	9.6000	0.739	0.741	2.449	4.738	2.435
3.56777	0.30534	3.54673	4.96142	1006	0.9000	7.5000	7.4500	0.545	0.734	1.900	3.542	1.893
3.04098	0.29037	3.02305	4.22886	858	1.1000	9.4000	6.3500	0.442	0.698	1.620	2.952	1.611
2.21249	0.30583	2.19945	3.07675	624	1.5000	12.4900	4.6200	0.338	0.735	1.178	2.262	1.172
1.17329	0.41800	1.16637	1.63161	331	3.3500	23.8600	2.4500	0.245	1.005	0.625	1.639	0.621
0.60820	0.59019	0.60461	0.84577	171	6.6500	39.8600	1.2700	0.179	1.419	0.324	1.200	0.322
0.29691	1.08203	0.79516	0.41290	83	4.1000	18.1500	0.6200	0.151	2.631	0.158	1.374	0.157
0.79975	0.49677	0.79504	1.11216	225	1.0500	6.8600	1.6700	0.199	1.194	0.426	1.328	0.424
0.21550	1.48041	0.21423	0.29968	60	6.5000	24.6000	0.4500	0.160	3.559	0.115	1.066	0.114
6.87214	0.45411	6.83161	9.55656	1939	0.6000	4.1000	14.3500	1.550	1.092	3.660	10.432	3.643
11.18220	0.58901	11.11625	15.55022	3155	0.4500	2.7000	23.3500	3.293	1.416	5.956	22.017	5.923
13.88795	0.85824	13.80605	19.31291	3919	1.7000	8.4500	29.0000	5.963	2.063	7.397	39.844	7.356
15.61198	0.89371	15.51990	21.71038	4406	1.5500	7.5500	32.6000	6.976	2.148	8.315	46.541	8.273
18.67690	1.14878	18.56676	25.97254	5270	1.3500	5.8000	39.0000	10.728	2.761	9.947	71.723	9.893
22.26862	1.12923	22.13729	30.96725	6284	1.3500	5.8500	46.5000	12.573	2.714	11.863	84.060	11.796

A	B	C	SIGMA	N
0.04999081	0.30618003	0.05205160	0.04882076	15

AA= 0.0375308 CC= 0.0528450

GAMMA= 0.731669 LANDA= 0.120170

RUN NO	COLUMN LENGTH CMS	COLUMN DIAMETER CMS	PELLET DIAMETER CMS	BED POROSITY	PELLET POROSITY	DIFFUSIVITY
91D	118.1000	2.6000	0.2080	0.3830000	0.	0.209233964

CARRIER MW	TEMP KELVIN	PRESS ATM	VISCOSITY	HYD DIA	DENSITY
29.00000	296.00000	1.02000	0.0182169	0.0792282	0.0012179

1 VELOCITY CM/SEC	2 HETP CMS	3 MOLECULAR PECLET	4 PELLET RE	5 NTU	6 WIDTH CM	7 TOTAL CM	8 Q ML/SEC	9 EDDY DIFF	10 PECLET	11 EMPTY RE	12 1/SCH RE	13 HYD
13.64851	0.69431	13.56801	18.97993	3851	0.3800	2.1000	28.5000	4.738	1.659	7.269	31.678	7.233
17.09655	1.17395	16.99572	23.77486	4824	0.4000	1.7000	35.7000	10.035	2.822	9.106	67.092	9.355
22.02917	1.16293	21.89925	30.63427	6217	1.3700	5.8500	46.0000	12.839	2.796	11.733	85.639	11.669
23.46585	1.64875	23.32746	32.63216	6622	1.4500	5.2000	49.0000	19.345	3.963	12.498	129.333	12.433
8.85956	0.47236	8.80731	12.32031	2500	0.5000	3.3500	18.5000	2.092	1.135	4.719	13.990	4.693
5.26784	0.34159	5.23678	7.32559	1486	0.6600	5.2000	11.0000	0.900	0.821	2.805	5.315	2.793
1.91558	0.31749	1.90428	2.66385	540	1.4500	11.8500	4.0000	0.334	0.763	1.323	2.333	1.315
10.91881	0.58901	10.85441	15.18394	3081	0.4500	2.7000	22.8000	3.216	1.416	5.815	21.499	5.784

A	B	C	SIGMA	N
-0.26517320	0.86951987	0.07300184	0.11659287	8

AA=-0.0705450 CC= 0.0640317

GAMMA= 2.077865 LAMDA= -0.637436

RUN NO	COLUMN LENGTH CMS	COLUMN DIAMETER CMS	PELLET DIAMETER CMS	BED POROSITY	PELLET POROSITY	DIFFUSIVITY
52	111.8000	5.0000	0.2080	0.3720000	0.	0.209233984

CARRIER MW	TEMP KELVIN	PRESS ATM	VISCOSITY	HYD DIA	DENSITY
29.00000	296.00000	1.02000	0.0182169	0.0786661	0.0012179

1 VELOCITY CM/SEC	2 HETP CMS	3 MOLECULAR PECLET	4 PELLET RE	5 NTU	6 WIDTH CM	7 TOTAL CM	8 Q MLS/SEC	9 EDDY DIFF	10 PECLET	11 EMPTY RE	12 1/SCH RE	13 HYD
23.99802	1.04873	23.85649	33.37219	6411	1.2000	5.2500	180.0000	12.594	2.521	12.414	84.130	12.621
21.33157	0.88594	21.20577	29.66417	5699	1.2500	5.9500	160.0000	9.449	2.130	11.035	63.175	11.219
20.33165	0.76573	20.21175	28.27367	5431	1.2500	6.4000	152.5000	7.784	1.841	10.518	52.344	10.593
18.66512	0.84071	18.55504	25.95615	4986	1.3200	6.4500	140.0000	7.846	2.021	9.656	52.456	9.817
17.33190	0.75738	17.22968	24.10214	4630	1.3500	6.9500	130.0000	6.563	1.821	8.966	43.881	9.115
16.39864	0.63871	16.30193	22.80433	4381	1.3200	7.4000	123.0000	5.237	1.535	8.483	35.313	8.625
14.66545	0.54689	14.57896	20.39412	3918	1.3700	8.3000	110.0000	4.010	1.315	7.587	26.811	7.713
10.66578	0.47057	10.60288	14.83209	2849	1.6000	10.4500	80.0000	2.510	1.131	5.518	16.778	5.510
14.33215	0.65127	14.24762	19.93062	3829	1.4500	8.0500	107.5000	4.667	1.556	7.414	31.203	7.538
11.06575	0.50526	11.00049	15.38829	2956	1.6500	10.4000	83.0000	2.796	1.215	5.724	18.690	5.820
8.86593	0.43273	8.81365	12.32917	2368	1.8500	12.6000	66.5000	1.918	1.040	4.586	12.825	4.663
7.86602	0.33131	7.81963	10.93866	2101	1.8500	14.4000	59.0000	1.303	0.795	4.069	8.712	4.137
7.86602	0.37977	7.81963	10.93866	2101	1.8500	13.4500	59.0000	1.434	0.913	4.069	9.986	4.137
7.79935	0.36079	7.75336	10.84596	2083	1.8300	13.6500	58.5000	1.407	0.867	4.035	9.407	4.102
7.26607	0.35437	7.22321	10.10436	1941	1.9000	14.3000	54.5000	1.287	0.852	3.759	8.607	3.921
7.26607	0.34946	7.22321	10.10436	1941	1.9000	14.4000	54.5000	1.270	0.840	3.759	8.488	3.921
6.53279	0.33579	6.49427	9.08465	1745	2.0500	15.8500	49.0000	1.097	0.807	3.379	7.333	3.436
6.13283	0.32216	6.09666	8.52845	1638	2.3500	18.5500	46.0000	0.988	0.774	3.173	6.605	3.225
5.82618	0.29331	5.79182	8.10203	1556	0.5500	4.5500	43.7000	0.854	0.735	3.014	5.712	3.064
5.01292	0.26218	4.98335	6.97108	1339	0.6000	5.2500	37.6000	0.657	0.630	2.593	4.393	2.636
5.01292	0.26218	4.98335	6.97108	1339	0.6000	5.2500	37.6000	0.657	0.630	2.593	4.393	2.536
4.23298	0.26754	4.20802	5.88648	1130	0.7100	6.1500	31.7500	0.566	0.643	2.190	3.786	2.226
3.62637	0.24645	3.60498	5.04291	968	0.8000	7.2200	27.2000	0.447	0.592	1.876	2.988	1.907
2.73311	0.26082	2.71699	3.80072	730	1.1000	9.6500	20.5000	0.356	0.627	1.414	2.383	1.437
1.66653	0.29271	1.65670	2.31751	445	1.8500	15.3200	12.5000	0.244	0.704	0.862	1.631	0.875
1.67986	0.28845	1.66995	2.33605	448	1.9000	15.8500	12.6000	0.242	0.693	0.869	1.620	0.884
1.43988	0.30345	1.43139	2.00233	384	2.2500	18.3000	10.8000	0.218	0.729	0.745	1.461	0.757
1.19990	0.36092	1.19282	1.66861	320	2.9500	22.0000	9.0000	0.217	0.868	0.521	1.448	0.531
0.87993	0.50323	0.87474	1.22365	235	0.9500	6.0000	6.6000	0.221	1.210	0.455	1.480	0.453
0.61995	0.58414	0.61629	0.86212	165	1.4500	8.5000	4.6500	0.181	1.404	0.321	1.211	0.326

A	B	C	SIGMA	N
0.00153686	0.36652558	0.04075336	0.03271169	30

AA= 0.0327542 CC= 0.0389181

GAMMA= 0.875875 LAMDA= 0.003694

RUN NO	COLUMN LENGTH CMS	COLUMN DIAMETER CMS	PELLET DIAMETER CMS	BED POROSITY	PELLET POROSITY	DIFFUSIVITY
53	186.3000	6.2700	1.0300	0.4050000	0.	0.209233364

CARRIER MW	TEMP KELVIN	PRESS ATM	VISCOSITY	HYD DIA	DENSITY
29.00000	296.00000	1.02000	0.0182169	0.3947390	0.0012179

1 VELOCITY CM/SEC	2 HETP CMS	3 MOLECULAR PECLET	4 PELLET RE	5 NTU	6 WIDTH CM	7 TOTAL CM	8 Q ML/SEC	9 EDDY DIFF	10 PECLET	11 EMPTY RE	12 1/SCH RE	13 HYD
0.75928	1.24573	3.73771	5.22858	338	2.2000	11.4000	9.7500	0.473	0.635	2.118	3.162	2.334
1.38227	0.92379	6.80454	9.51869	615	5.7500	34.6000	17.7500	0.638	0.448	3.855	4.269	3.648
2.06368	1.01514	10.15890	14.21101	918	3.8500	22.1000	26.5000	1.047	0.493	5.755	7.003	5.445
2.54650	1.01455	12.53570	17.53585	1133	3.1000	17.8000	32.7000	1.292	0.492	7.102	8.636	6.723
3.05268	0.99830	15.02750	21.02157	1359	2.6000	15.0500	39.2000	1.524	0.485	8.514	10.187	8.356
3.54329	1.12271	17.44264	24.40003	1577	2.4000	13.1000	45.5000	1.989	0.545	9.882	13.298	9.351
3.91320	1.21205	19.26357	26.94729	1742	2.2500	11.8200	50.2500	2.371	0.588	10.914	15.855	10.327
4.36098	1.03526	21.46786	30.03081	1941	1.9000	10.8000	56.0000	2.257	0.503	12.162	15.092	11.509
4.69194	1.08964	23.09712	32.30993	2088	1.8500	10.2500	60.2500	2.556	0.529	13.086	17.090	12.383
3.81585	1.00200	18.78438	26.27696	1698	2.2500	13.0000	49.0000	1.912	0.486	10.542	12.781	10.373
4.59460	1.02629	22.61792	31.63960	2045	1.8900	10.7900	59.0000	2.358	0.498	12.814	15.763	12.126
5.45122	1.10811	26.83482	37.53851	2426	1.7200	9.4500	70.0000	3.020	0.538	15.203	20.193	14.385
6.30784	1.18432	31.05172	43.43742	2808	1.5900	8.4500	81.0000	3.735	0.575	17.592	24.973	16.647

A	B	C	SIGMA	N
0.68256506	0.35607676	0.07115107	0.06606999	13

AA= 0.7240111 CC= 0.0641448

GAMMA= 0.850906 LAMDA= 0.331342

RUN NO	COLUMN LENGTH CMS	COLUMN DIAMETER CMS	PELLET DIAMETER CMS	BED POROSITY	PELLET POROSITY	DIFFUSIVITY
54	185.4000	0.4150	0.2975	0.6300000	0.	0.209233964

CARRIER MW	TEMP KELVIN	PRESS ATM	VISCOSITY	HYD DIA	DENSITY
29.00000	296.00000	1.02000	0.0182169	0.1473621	0.0012179

1 VELOCITY CM/SEC	2 METP CMS	3 MOLECULAR PECLET	4 PELLET RE	5 NTU	6 WIDTH CM	7 TOTAL CM	8 Q MLS/SEC	9 EDDY DIFF	10 PECLET	11 EMPTY RE	12 1/SCM RE	13 HYD
8.34203	0.87373	11.86115	16.59224	3695	1.4500	8.9500	0.7300	3.644	1.458	10.453	24.365	8.219
13.82720	1.12957	19.66026	27.50220	6126	1.0500	5.7000	1.2100	7.809	1.898	17.325	52.211	13.623
17.59826	1.44479	25.02214	35.00280	7796	1.0000	4.8000	1.5400	12.713	2.428	22.052	84.994	17.338
22.74061	1.33151	32.33381	45.23089	10075	0.9200	4.6000	1.9900	19.140	2.238	28.495	101.219	22.404
25.14037	1.86725	35.74592	50.00400	11138	0.9000	3.8000	2.2000	23.472	3.138	31.503	156.925	24.769
29.82562	2.19378	42.40766	59.32293	13214	0.8600	3.3500	2.6100	32.715	3.687	37.373	218.725	29.385
38.28193	2.82904	54.43129	76.14246	16960	0.8600	2.9500	3.3500	54.150	4.755	47.970	362.033	37.715
28.56860	2.53873	40.62036	56.82273	12657	0.9500	3.4400	2.5000	36.264	4.257	35.798	242.449	28.146
21.02649	1.69844	29.89659	41.82153	9315	0.9600	4.2500	1.8400	17.856	2.855	26.348	119.383	23.715
12.79874	1.15076	18.19792	25.45658	5670	1.1100	5.9700	1.1200	7.364	1.934	16.038	49.234	12.613

A	B	C	SIGMA	N
-0.22853924	3.88134199	0.07882725	0.18221123	10

AA= 0.1867108 CC= 0.0688375

GAMMA= 9.275124 LAMDA= -0.384100

RUN NO	COLUMN LENGTH CMS	COLUMN DIAMETER CMS	PELLET DIAMETER CMS	BED POROSITY	PELLET POROSITY	DIFFUSIVITY
55	121.0000	1.1500	1.0050	0.4540000	0.	0.196699211

CARRIER MW	TEMP KELVIN	PRESS ATM	VISCOSITY	HYD DIA	DENSITY
29.00000	296.00000	1.08500	0.0182169	0.2695177	0.0012955

1 VELOCITY CM/SEC	2 HETP CMS	3 MOLECULAR PECLET	4 PELLET RE	5 NTU	6 WIDTH CM	7 TOTAL CM	8 Q MLS/SEC	9 EDDY DIFF	10 PECLET	11 EMPTY RE	12 1/SCH RE	13 HYD
6.67826	1.10204	34.12138	47.73147	2054	1.2500	5.5500	3.4400	3.683	0.548	21.670	26.170	12.803
4.69808	0.81204	24.00399	33.57854	1445	1.4500	7.5000	2.4200	1.908	0.404	15.245	13.566	9.005
4.69808	0.92790	24.00399	33.57854	1445	1.5500	7.5000	2.4200	2.180	0.452	15.245	15.501	9.005
3.57209	0.86016	18.25097	25.53079	1098	1.9500	9.8000	1.8400	1.536	0.428	11.591	10.926	6.347
2.64024	0.79122	13.48985	18.87058	812	2.5000	13.1000	1.3600	1.045	0.394	8.567	7.428	5.361
2.09666	0.75765	10.71253	14.98546	644	3.1000	16.6000	1.0800	0.794	0.377	6.803	5.649	4.319
1.70839	0.79877	8.72872	12.21038	525	3.9500	20.6000	0.8800	0.682	0.397	5.544	4.852	3.275
1.04833	0.88864	5.35626	7.49273	322	7.2000	35.6000	0.5400	0.466	0.442	3.402	3.313	2.009
0.75713	0.91842	3.86841	5.41142	232	2.2000	10.7000	0.3900	0.348	0.457	2.457	2.473	1.451
0.43680	0.93106	2.23178	3.12197	134	5.9000	28.5000	0.2250	0.203	0.453	1.417	1.446	0.837

A	B	C	SIGMA	N
0.60157888	0.15542669	0.06020300	0.05700413	10

AA= 0.4058721 CC= 0.0954678

GAMMA= 0.395087 LAMDA= 0.299293

RUN NO	COLUMN LENGTH CMS	COLUMN DIAMETER CMS	PELLET DIAMETER CMS	BED POROSITY	PELLET POROSITY	DIFFUSIVITY
63	421.0000	0.6600	0.5680	0.4970000	0.	0.761496238

CARRIER MW	TEMP KELVIN	PRESS ATM	VISCOSITY	HYD DIA	DENSITY
29.00000	296.50000	0.98300	0.0182409	0.1747848	0.0011718

1 VELOCITY CM/SEC	2 METP CMS	3 MOLECULAR PECLET	4 PELLET RE	5 NTU	6 WIDTH CM	7 TOTAL CM	8 Q ML/SEC	9 EDDY DIFF	10 PECLET	11 EMPTY RE	12 1/SCM RE	13 HYD
9.46495	0.49963	7.05990	34.53528	2616	1.0000	12.3000	1.5900	2.384	0.440	17.164	15.189	10.627
8.63156	0.49816	6.43828	31.49443	2386	1.1000	13.5500	1.4500	2.150	0.439	15.653	13.811	9.691
7.91722	0.49359	5.90545	28.88800	2188	1.2000	14.8500	1.3300	1.954	0.434	14.357	12.552	8.889
7.20289	0.49283	5.37263	26.28156	1991	1.3000	16.1000	1.2100	1.775	0.434	13.062	11.402	8.087
6.72666	0.49366	5.01742	24.54394	1859	1.3900	17.2000	1.1300	1.660	0.435	12.198	10.666	7.553
5.95280	0.53257	4.44019	21.72030	1645	1.6200	19.3000	1.0000	1.585	0.469	10.795	10.183	6.684
5.29799	0.54366	3.95177	19.33107	1464	1.8700	22.0500	0.8900	1.440	0.479	9.608	9.251	5.949
3.92885	0.64628	2.93053	14.33540	1086	2.7000	29.2000	0.6600	1.270	0.569	7.125	8.156	4.411
2.67876	0.91561	1.99809	9.77413	740	0.9300	8.4500	0.4500	1.226	0.836	4.858	7.878	3.008
1.66678	1.24344	1.24325	6.08168	460	9.3500	72.9000	0.2800	1.036	1.095	3.023	6.657	1.871

A	B	C	SIGMA	N
0.10653326	1.87872805	0.01889421	0.02249600	10

AA= 0.5070601 CC=-0.0209654

GAMMA= 1.233577 LAMDA= 0.093779

RUN NO	COLUMN LENGTH CMS	COLUMN DIAMETER CMS	PELLET DIAMETER CMS	BED POROSITY	PELLET POROSITY	DIFFUSIVITY
64	421.0000	0.6600	0.5680	0.4970000	0.	0.200754303

CARRIER MW	TEMP KELVIN	PRESS ATM	VISCOSITY	HYD DIA	DENSITY
29.00000	297.00000	1.05000	0.0182648	0.1747848	0.0012495

1 VELOCITY CM/SEC	2 HETP CMS	3 MOLECULAR PECLET	4 PELLET RE	5 NTU	6 WIDTH CM	7 TOTAL CM	8 Q MLS/SEC	9 EDDY DIFF	10 PECLET	11 EMPTY RE	12 1/SCH RE	13 HYD
8.37353	0.71677	23.69146	32.53779	8780	1.3000	13.3500	1.5000	3.031	0.631	16.171	20.530	10.313
7.81529	0.67842	22.11203	30.36861	8194	1.3500	14.2500	1.4000	2.651	0.597	15.093	18.136	9.345
7.14541	0.64067	20.21671	27.76558	7492	1.4500	15.7500	1.2800	2.289	0.564	13.799	15.659	8.544
6.36388	0.59639	18.00551	24.72872	6672	1.5500	17.4500	1.1400	1.898	0.525	12.290	12.982	7.613
5.58235	0.52179	15.79431	21.69186	5853	1.6700	20.1000	1.0000	1.456	0.459	10.781	9.964	6.675
4.63335	0.46804	13.10928	18.00424	4858	1.9200	24.4000	0.8300	1.084	0.412	8.948	7.418	5.543
3.62853	0.47013	10.26630	14.09971	3804	2.5000	31.7000	0.6500	0.853	0.414	7.008	5.835	4.339
2.45623	0.47348	6.94950	9.54442	2575	3.7000	46.7500	0.4400	0.581	0.417	4.744	3.978	2.937
1.50723	0.58603	4.26446	5.85680	1580	1.4000	15.9000	0.2700	0.442	0.516	2.911	3.021	1.802

A	B	C	SIGMA	N
-0.05827764	0.79323625	0.08132024	0.01178047	9

AA= 0.2393774 CC= 0.0486056

GAMMA= 1.975639 LAMDA= -0.051301

RUN NO	COLUMN LENGTH CMS	COLUMN DIAMETER CMS	PELLET DIAMETER CMS	BED POROSITY	PELLET POROSITY	DIFFUSIVITY
65	119.5000	2.1750	0.5680	0.4630000-0.		0.196749071

CARRIER MW	TEMP KELVIN	PRESS ATM	VISCOSITY	HYD DIA	DENSITY
29.00000	293.50000	1.05000	0.0180970	0.2465515	0.0012644

1 VELOCITY CM/SEC	2 HETP CMS	3 MOLECULAR PECLET	4 PELLET RE	5 NTU	6 WIDTH CM	7 TOTAL CM	8 Q MLS/SEC	9 EDDY DIFF	10 PECLET	11 EMPTY RE	12 1/SCH RE	13 HYD
7.08854	0.60342	20.46409	28.13152	2152	2.7000	16.1000	13.0000	2.139	0.531	13.025	14.943	12.211
6.78864	0.55490	19.59830	26.94134	2061	2.7500	17.1000	12.4500	1.884	0.488	12.474	13.160	11.694
6.70685	0.54847	19.36218	26.61675	2036	2.7500	17.2000	12.3000	1.839	0.483	12.324	12.851	11.554
6.18884	0.53881	17.86673	24.56098	1879	2.9000	18.3000	11.3500	1.667	0.474	11.372	11.649	10.661
5.61631	0.51662	16.21386	22.28882	1705	3.1500	20.3000	10.3000	1.451	0.455	10.320	10.136	9.575
5.34367	0.48800	15.42678	21.20684	1622	3.2500	21.5500	9.8000	1.304	0.430	9.819	9.110	9.205
4.77113	0.47337	13.77391	18.93468	1448	3.5500	23.9000	8.7500	1.129	0.417	8.767	7.890	8.219
4.49850	0.47137	12.98683	17.85270	1366	3.7500	25.3000	8.2500	1.060	0.415	8.266	7.408	7.749
3.57153	0.42841	10.31075	14.17396	1084	4.5500	32.2000	6.5500	0.765	0.377	6.563	5.345	6.152
2.90085	0.41559	8.37454	11.51228	880	5.4000	38.8000	5.3200	0.633	0.366	5.330	4.212	4.997
2.13747	0.40664	6.17071	8.48274	649	7.2000	52.3000	3.9200	0.435	0.358	3.928	3.036	3.682
2.26288	0.43787	6.53277	8.98045	687	1.6000	11.2000	4.1500	0.495	0.385	4.158	3.462	3.898
1.55403	0.44896	4.48636	6.16729	471	2.3000	15.9000	2.8500	0.349	0.395	2.855	2.437	2.577
0.98149	0.55904	2.83349	3.89513	298	4.1000	25.4000	1.8000	0.274	0.492	1.803	1.917	1.691

A	B	C	SIGMA	N
0.12397321	0.37161307	0.05709327	0.01086156	14

AA= 0.1831935 CC= 0.0491846

GAMMA= 0.944383 LANDA= 0.109131

RUN NO	COLUMN LENGTH CMS	COLUMN DIAMETER CMS	PELLET DIAMETER CMS	BED POROSITY	PELLET POROSITY	DIFFUSIVITY
66	119.5000	2.1750	0.5680	0.4630000	-0.	0.732060581

CARRIER MW	TEMP KELVIN	PRESS ATM	VISCOSITY	HYD DIA	DENSITY
29.00000	293.50000	1.00500	0.0180970	0.2465515	0.0012102

1 VELOCITY CM/SEC	2 HETP CMS	3 MOLECULAR PECLET	4 PELLET RE	5 NTU	6 WIDTH CM	7 TOTAL CM	8 Q MLS/SEC	9 EDDY DIFF	10 PECLET	11 EMPTY RE	12 1/SCH RE	13 HYD
33.04188	1.08620	25.63693	125.50986	2696	0.9000	4.0000	58.0000	17.945	0.956	58.111	120.008	54.483
26.49047	0.95624	20.55375	100.62429	2162	0.9500	4.5000	46.5000	12.666	0.842	46.589	84.701	43.678
21.79055	0.72807	16.90711	82.77159	1778	1.0500	5.7000	38.2500	7.933	0.641	38.323	53.049	35.929
16.09367	0.59599	12.48695	61.13196	1313	1.2000	7.2000	28.2500	4.796	0.525	28.304	32.072	26.536
8.26047	0.37585	6.40923	31.37747	674	1.8000	13.6000	14.5000	1.552	0.331	14.528	10.381	13.520
7.40594	0.37903	5.74621	28.13152	604	2.1000	15.8000	13.0000	1.404	0.334	13.025	9.386	12.211
7.14958	0.40062	5.54730	27.15774	583	2.2000	16.1000	12.5500	1.432	0.353	12.574	9.578	11.789
6.57989	0.37821	5.10529	24.99377	537	2.3500	17.7000	11.5500	1.244	0.333	11.572	8.321	10.849
5.78233	0.39897	4.48646	21.96423	471	2.7000	19.8000	10.1500	1.153	0.351	10.169	7.714	9.534
5.32658	0.39289	4.13285	20.23306	434	2.9500	21.8000	9.3500	1.046	0.346	9.368	6.998	8.783
5.01325	0.40014	3.88974	19.04288	409	3.1000	22.7000	8.8000	1.003	0.352	8.817	6.708	8.265
3.81691	0.42907	2.96151	14.49855	311	4.2000	29.7000	6.7000	0.819	0.378	6.713	5.476	6.293
3.30419	0.45182	2.56369	12.55099	269	5.0500	34.8000	5.8000	0.746	0.398	5.811	4.992	5.448
2.53511	0.52718	1.96697	9.62964	206	6.8500	43.7000	4.4500	0.668	0.464	4.459	4.469	4.183
1.70906	0.71956	1.32605	6.49189	139	12.0500	65.8000	3.0000	0.615	0.633	3.006	4.112	2.818
2.07936	0.54927	1.61336	7.89847	169	2.0000	12.5000	3.6500	0.571	0.484	3.657	3.819	3.428
1.39573	0.82132	1.08294	5.30171	113	3.6000	18.4000	2.4500	0.573	0.723	2.455	3.833	2.301
0.82605	1.36681	0.64092	3.13775	67	7.9000	31.3000	1.4500	0.565	1.233	1.453	3.775	1.362
0.48423	2.11930	0.37571	1.83937	39	3.3000	10.5000	0.8500	0.513	1.866	0.852	3.431	0.798
0.17091	5.09239	0.13260	0.64919	13	13.3000	27.3000	0.3000	0.435	4.483	0.301	2.910	0.282

A	B	C	SIGMA	N
0.12011538	0.86630061	0.02745608	0.07473090	20

AA=-0.1297124 CC= 0.0396874

GAMMA= 0.591686 LAMDA= 0.105735

RUN NO	COLUMN LENGTH CMS	COLUMN DIAMETER CMS	PELLET DIAMETER CMS	BED POROSITY	PELLET POROSITY	DIFFUSIVITY
69	186.3000	6.2700	1.0300	0.4050000	0.	0.209233964

CARRIER MW	TEMP KELVIN	PRESS ATM	VISCOSITY	HYD DIA	DENSITY
29.00000	296.00000	1.02000	0.0182169	0.3947390	0.0012179

1 VELOCITY CM/SEC	2 HETP CMS	3 MOLECULAR PECLET	4 PELLET RE	5 NTU	6 WIDTH CM	7 TOTAL CM	8 Q MLS/SEC	9 EDDY DIFF	10 PECLET	11 EMPTY RE	12 1/SCM RE	13 HYD
26.08798	2.35665	128.42380	179.64859	11614	2.1500	8.1000	335.0000	30.740	1.144	72.758	205.519	68.849
23.90749	2.09059	117.68987	164.63318	10643	2.2500	9.0000	307.0000	24.990	1.015	66.676	167.378	63.394
21.41551	2.08198	105.42252	147.47272	9534	2.4200	9.7000	275.0000	22.293	1.011	59.726	149.046	56.518
18.61202	1.93579	91.62175	128.16720	8285	2.5500	10.6000	239.0000	18.014	0.940	51.908	120.439	49.119
15.57491	1.81694	76.67092	107.25289	6933	2.8900	12.4000	200.0000	14.149	0.882	43.437	94.598	41.104
15.57491	1.65182	76.67092	107.25289	6933	2.8000	12.6000	200.0000	12.864	0.832	43.437	86.301	41.104
12.45993	1.66300	61.33674	85.80231	5547	3.3000	14.8000	160.0000	10.360	0.807	34.750	69.267	32.883
8.72195	1.27502	42.93572	60.06162	3882	4.1000	21.0000	112.0000	5.560	0.619	24.325	37.175	23.318
3.58223	1.00956	17.63431	24.66816	1594	2.0500	11.8300	46.0000	1.808	0.493	9.991	12.089	9.454
4.63354	1.03063	22.80960	31.90773	2062	1.6500	9.4000	59.5000	2.388	0.500	12.923	15.964	12.228
3.95213	1.02574	19.45525	27.21542	1759	1.9000	10.8500	50.7500	2.027	0.498	11.022	13.551	10.433
3.32914	0.92915	16.38841	22.92530	1482	2.2000	13.2000	42.7500	1.547	0.451	9.285	10.340	8.786
2.60880	0.92915	12.84238	17.96486	1161	2.8000	16.8000	33.5000	1.212	0.451	7.276	8.103	6.885
2.12208	0.95168	10.44641	14.61321	944	3.5000	20.7500	27.2500	1.010	0.462	5.918	6.751	5.603
1.46015	1.11456	7.18790	10.05496	650	1.1500	6.3000	18.7500	0.814	0.541	4.072	5.440	3.853
0.79821	1.14091	3.92938	5.49671	355	2.0500	11.1000	10.2500	0.455	0.554	2.226	3.044	2.107

A	B	C	SIGMA	N
0.70091049	0.31824413	0.06312746	0.07078120	16

AA= 0.7032348 CC= 0.0630176

GAMMA= 0.760498 LAMDA= 0.340248

RUN NO	COLUMN LENGTH CMS	COLUMN DIAMETER CMS	PELLET DIAMETER CMS	BED POROSITY	PELLET POROSITY	DIFFUSIVITY
70	186.3000	6.2700	1.0300	0.4050000	0.	0.748550810

CARRIER MW	TEMP KELVIN	PRESS ATM	VISCOSITY	HYD DIA	DENSITY
29.00000	296.50000	1.00000	0.0182409	0.3947390	0.0011920

1 VELOCITY CM/SEC	2 HETP CMS	3 MOLECULAR PECLET	4 PELLET RE	5 NTU	6 WIDTH CM	7 TOTAL CM	8 Q MLS/SEC	9 EDDY DIFF	10 PECLET	11 EMPTY RE	12 1/SCM RE	13 HYD
4.63473	0.92915	6.37736	31.19642	576	1.6000	9.6000	58.2500	2.153	0.451	12.635	14.371	11.956
3.36167	1.00033	4.62564	22.62745	418	2.3000	13.3000	42.2500	1.681	0.486	9.164	10.988	8.672
2.88428	1.00200	3.96874	19.41408	358	2.7000	15.6000	36.2500	1.445	0.486	7.963	9.443	7.445
2.40688	1.10577	3.31185	16.20072	299	3.4000	18.7000	30.2500	1.331	0.537	6.561	8.696	5.209
1.69078	1.19846	2.32650	11.38067	210	5.3000	28.0300	21.2500	1.013	0.582	4.604	6.621	4.362
0.99458	1.58213	1.36853	6.69451	123	10.2000	46.9000	12.5000	0.787	0.768	2.711	5.142	2.565
3.34178	1.01170	4.59827	22.49356	415	2.4000	13.8000	42.0000	1.690	0.491	9.110	11.047	8.620
10.98014	0.98300	15.10859	73.90740	1366	3.0000	17.5000	138.0000	5.397	0.477	29.932	35.268	28.324
14.00366	1.11385	19.26892	94.25871	1742	2.5000	13.7000	176.0000	7.799	0.541	38.175	55.966	36.124
17.82284	1.20315	24.52408	119.96563	2217	2.2000	11.6000	224.0000	10.722	0.584	48.586	70.066	45.976
21.32375	1.12845	29.34131	143.53031	2653	1.8000	9.8000	268.0000	12.031	0.548	58.130	78.625	55.007
24.62575	1.16736	33.88484	165.75609	3064	1.7000	9.1000	309.5000	14.374	0.567	67.131	93.930	63.525
19.41416	1.33798	26.71373	130.67685	2415	2.1000	10.5000	244.0000	12.988	0.650	52.924	84.875	55.381

A	B	C	SIGMA	N
0.67549519	0.85581615	0.02323083	0.06795941	13

AA= 0.5390088 CC= 0.0297571

GAMMA= 0.571649 LAMDA= 0.327910

RUN NO	COLUMN LENGTH CMS	COLUMN DIAMETER CMS	PELLET DIAMETER CMS	BED POROSITY	PELLET POROSITY	DIFFUSIVITY
71	122.0000	1.1500	1.0050	0.4540000	0.	0.725219570

CARRIER MW	TEMP KELVIN	PRESS ATM	VISCOSITY	HYD DIA	DENSITY
29.00000	290.00000	0.99400	0.0179282	0.2695177	0.0012114

1 VELOCITY CM/SEC	2 HETP CMS	3 MOLECULAR PECLET	4 PELLET RE	5 NTU	6 WIDTH CM	7 TOTAL CM	8 Q MLS/SEC	9 EDDY DIFF	10 PECLET	11 EMPTY RE	12 1/SCH RE	13 HYD
26.98967	1.10044	37.40195	183.28539	2270	1.3000	5.8000	13.0000	14.850	0.547	83.212	100.346	49.153
26.47064	1.05343	36.68268	179.76067	2226	1.2500	5.7000	12.7500	13.942	0.524	81.611	94.212	48.208
24.39451	1.04817	33.80560	165.66179	2051	1.4000	6.4000	11.7500	12.785	0.521	75.210	86.389	44.427
20.76129	1.01516	28.77073	140.98876	1746	1.5500	7.2000	10.0000	10.538	0.535	64.009	71.207	37.813
18.16613	0.88690	25.17439	123.36516	1527	1.6500	8.2000	8.7500	8.056	0.441	56.308	54.434	33.384
14.53290	0.80681	20.13951	98.69213	1222	1.9000	9.9000	7.0000	5.863	0.401	44.806	39.615	26.467
11.93774	0.74504	16.54317	81.06854	1004	2.2500	12.2000	5.7500	4.447	0.371	36.835	30.350	21.741
8.82355	0.73362	12.22756	59.92022	742	2.8000	15.3000	4.2500	3.237	0.365	27.204	21.870	16.369
5.70935	0.69510	7.91195	38.77191	480	4.4000	24.7000	2.7500	1.984	0.346	17.602	13.408	13.398
1.55710	1.01222	2.15780	10.57416	130	15.8000	73.5000	0.7500	0.788	0.504	4.801	5.325	2.836
5.50174	0.62926	7.62424	37.36202	462	1.0000	5.9000	2.6500	1.731	0.313	16.962	11.697	10.323
3.32181	0.77561	4.60332	22.55820	279	1.7500	9.3000	1.6000	1.288	0.386	10.241	8.705	6.353
1.45329	1.11689	2.01395	9.86921	122	4.9000	21.7000	0.7000	0.812	0.556	4.481	5.484	2.647
0.57094	2.34615	0.79119	3.87719	48	3.6000	11.0000	0.2750	0.670	1.167	1.760	4.526	1.040

A	B	C	SIGMA	N
0.30983941	1.13807020	0.02831543	0.03608801	14

AA= 0.3436004 CC= 0.0267854

GAMMA= 0.784638 LAMDA= 0.154149

RUN NO	COLUMN LENGTH CMS	COLUMN DIAMETER CMS	PELLET DIAMETER CMS	BED POROSITY	PELLET POROSITY	DIFFUSIVITY
72	122.0000	1.1500	1.0050	0.4540000	0.	0.210973011

CARRIER MW	TEMP KELVIN	PRESS ATM	VISCOSITY	HYD DIA	DENSITY
29.00000	294.00000	1.00000	0.0181210	0.2695177	0.0012022

1 VELOCITY CM/SEC	2 HETP CMS	3 MOLECULAR PECLET	4 PELLET RE	5 NTU	6 WIDTH CM	7 TOTAL CM	8 Q ML/SEC	9 EDDY DIFF	10 PECLET	11 EMPTY RE	12 1/SCH	13 RE HYD
27.19777	2.35064	129.56047	181.33542	7863	1.9000	5.8000	13.0000	31.966	1.169	82.326	212.067	48.633
26.67474	2.13912	127.06892	177.84820	7712	2.0000	6.4000	12.7500	28.530	1.064	80.743	189.273	47.695
25.62867	2.17880	122.08583	170.87376	7410	2.0500	6.5000	12.2500	27.920	1.084	77.577	185.224	45.826
24.05957	2.21762	114.61119	160.41210	6956	2.1000	6.6000	11.5000	26.677	1.103	72.827	176.981	43.019
21.96743	1.93606	104.64500	146.46322	6351	2.2000	7.4000	10.5000	21.265	0.963	66.494	141.375	39.278
19.87530	1.87034	94.67881	132.51434	5746	2.2500	7.7000	9.5000	18.587	0.931	60.162	123.307	35.537
17.78316	1.73712	84.71262	118.56546	5141	2.4500	8.7000	8.5000	15.446	0.864	53.829	102.469	31.797
15.69102	1.57376	74.74643	104.61659	4536	2.6000	9.7000	7.5000	12.347	0.783	47.496	81.911	28.056
12.02978	1.39214	57.30559	80.20605	3478	3.0000	11.9000	5.7500	8.374	0.693	36.414	55.551	21.509
8.36855	1.15284	39.86476	55.79551	2419	3.9000	17.0000	4.0000	4.824	0.574	25.331	32.002	14.963
5.23034	0.99599	24.91548	34.87220	1512	5.8000	27.2000	2.5000	2.605	0.496	15.832	17.280	9.352
1.56910	0.84553	7.47464	10.46166	453	16.7000	85.0000	0.7500	0.663	0.421	4.753	4.401	2.336

A	B	C	SIGMA	N
0.64111141	0.17188688	0.06044230	0.05391870	12

AA= 0.5882264 CC= 0.0625384

GAMMA= 0.407367 LAMDA= 0.318961

TIME 16HRS 41MIN 12.6SEC

```
B DAVES                                   FORTRAN SOURCE LIST GAAA          05/27/69          PAGE  1
        ISN       SOURCE STATEMENT

                C     PROGRAM FOR COMPUTATION OF RESULTS FROM POROUS PELLET RUNS
                1 85  READ55,ND,CL,CD,DP ,EB ,EP,DOBS
                3 55  FORMAT (I5,3F10.4,2F10.7,F12.9 )
                4     IF (ND) 84,83,84
                5 84  CALL SKIP TO (1)
                6     PRINT 56
                7 56 OFORMAT(8H  COLUMN,2X,6HCOLUMN,3X,6HCOLUMN,4X,6HPELLET,5X,3HBED,6X,
                     16HPELLET,4X,11HDIFFUSIVITY  )
               10     PRINT 57
               11 57 OFORMAT(4X,2HNO ,4X,6HLENGTH,2X,8HDIAMETER,2X,8HDIAMETER,2X,8HPOROS
                     1ITY,2X,8HPOROSITY  /11X,2HCMS       CMS       CMS  )
               12     READ 81,GM,T,TOBS,P,VISC ,ADS
               13 81  FORMAT(4F12.5,2F12.7 )
               14     D=DOBS*(T/TOBS)**1.7 /P
               15     PRINT 550,ND,CL , CD , DP , EB , EP, D
               16 550 FORMAT(1X,I5,3F10.4,2F10.7,F12.9)
               17     PRINT 65
               20 65  FORMAT(/51H   CARRIER MW   TEMP KELVIN PRESS ATM   VISCOSITY   ,
                     1 12H   HYD DIA   ,10H DENSITY        )
               21     HD =EB*CD/(3.*CD*(1.-EB)/(2.*DP)+1.)
               22     VISC= 0.01709*((273.1+114.)/(T+114.))*(T/273.)**1.5
               23      RHO=29.*273.*P/(22400.*T)
               24     PRINT 64,GM  , T ,P , VISC   ,HD,RHO
               25 64  FORMAT(1X,3F12.5,3F12.7 // )
               26     N=0
               27     SHS=  0.0
               30     SH =  0.0
               31     SU =  0.0
               32     SUS=  0.0
               33     SW =  0.0
               34     SWS=  0.0
               35     SHU=  0.0
               36     SHW=  0.0
               37     SHWS = 0.0
               40     SHW2 = 0.0
               41     SHW3 = 0.0
               42     SW3  = 0.0
               43     SW4  = 0.0
               44      SG=0.0
               45     SGU=0.0
               46     PRINT60
               47 60  FORMAT(74H VELOCITY  HETP     RECIP VEL    RE          NTU      HID
                     1TH       TOTAL     Q                                          /
                     228H  CM/SEC     CMS        SEC/CM,27X,10HCM      CM    ,7X,6HCC/SEC  )
               50     CRE  =  DP*GM *100./(22400.*VISC *T)* 273.*P
               51     CUL  =  CL/(2. * D)
               52 10  READ 59,Q,WIDTH, TOTAL
               53 59  FORMAT(3F12.5 )
               54     IF(Q) 5,6,5
               55 5   HM =(2.36* TOTAL/ WIDTH)**2
               56     H  = CL/HM
               57     U= Q*4./(3.14159*EB*P*CD**2) *T/298.
               60     W  = 1./U
               61     RE=CRE*U
               62     NTU= CUL*U
```

```
ISN        SOURCE STATEMENT

 63        PRINT 52 ,U,H,W,RE,NTU,WIDTH,TOTAL,Q
 64 52     FORMAT (4F10.5,I5 ,3F10.4 )
 65 11     N= N+1
 66        SH  = SH +  H
 67        SU  = SU +  U
 70        SW  = SW +  W
 71        SUS = SUS+  U**2
 72        SWS   = SWS +   W**2
 73        SHU   = SHU +   H*U
 74        SHW   = SHW +   H/U
 75        SHS   = SHS +   H**2
 76        SHWS =SHWS +(H*W)**2
 77        SHW2 =SHW2 + H*W**2
100        SHW3 =SHW3 + H*W**3
101        SW3 =SW3 + W**3
102        SW4 =SW4 + W**4
103        GOTO  10
104 6      EN= N
105        AK =  SU - EN*SUS/ SU
106        BK =  SU - EN**2/ SW
107        CK =  SH - EN*SHU/ SU
110        DK =  SH - EN*SHW/ SW
111        EK =  SW - EN**2/  SU
112        FK =  SW - EN*SWS/ SW
113        C  =  (CK/EK - DK/FK)/ (AK/EK- BK/FK)
114        B  =  (DK- C*BK)/FK
115        A  =  (SH - C*SU- B*SW)/EN
116 559    PRINT 51
117 51     FORMAT(/9X,1HA,18X,1HB,17X,1HC,14X,5HSIGMA,9X,1HN)
120       0SIGMA =SQRT (1./EN*(SHS-2.*A*SH-2.*SHW*B-2.*C*SHU+EN*A**2+2.*A*B*
          1SW + 2.*A*C*SU + B**2*SWS +2.*EN*B*C + C**2*SUS)  )
121        PRINT 50, A,B, C, SIGMA, N
122 50     FORMAT(1X,4F18.8,I4  )
123        IF(EP)  30,85 ,30
124 30     COR=  0.030*D*HD**.66/8.75*D + .0212*SU*HD/EN)**2
125        C=C-COR
126        DS=(EB/(   C*2.*(1.-EB)))*(DP/(3.14159*(1.+EB/(EP*(1.-EB))))))**2
127        PRINT 63,DS,COR,C
130 63     FORMAT(/25H EFFECTIVE DIFFUSIVITY = ,F10.8/43H CORRECTION OF SLOPE
          1 FOR DIFFUSIVITY TERM =  ,F10.7,19H AND NEW SLOPE C =   ,F10.5 )
131        IF(ADS) 85,85,45
132 45     EA=EP+ADS
133        DS=(EB/(   C*2.*(1.-EB)))*(DP/(3.14159*(1.+EB/(EA*(1.-EB))))))**2
134         TT=D*EP/DS
135        PRINT46,DS,TT ,ADS
136 46     FORMAT(/33H DIFFUSIVITY WITH K=1/(EP+ADS) = ,F10.8/12H TORTUOSITY=
          1,F10.5/15H ADSORPTION =    ,F10.5, 25HMLS GAS/ML OF PELLET      )
137        GOTO 85
140 83     STOP
141        END

        NO MESSAGES FOR ABOVE ASSEMBLY
TIME 17HRS 20MIN 59.6SEC
```

COLUMN NO	COLUMN LENGTH CMS	COLUMN DIAMETER CMS	PELLET DIAMETER CMS	BED POROSITY	PELLET POROSITY	DIFFUSIVITY
56	129.6000	0.6600	0.5970	0.4710000	0.3100000	0.207605682

CARRIER MW	TEMP KELVIN	PRESS ATM	VISCOSITY	HYD DIA	DENSITY
29.00000	296.00000	1.02800	0.0182169	0.1655945	0.0012275

VELOCITY CM/SEC	HETP CMS	RECIP VEL SEC/CM	RE	NTU	WIDTH CM	TOTAL CM	Q CC/SEC
0.95941	0.58797	1.04231	3.85938	299	2.7500	17.3000	0.1600
1.31919	1.00155	0.75804	5.30665	411	2.3900	11.5200	0.2200
2.27860	2.14265	0.43887	9.16602	711	1.7600	5.8000	0.3800
2.87823	2.85963	0.34744	11.57814	898	1.5600	4.4500	0.4800
3.05812	3.46638	0.32700	12.30177	954	7.7000	19.9500	0.5100
4.79705	5.35024	0.20846	19.29689	1497	5.8500	12.2000	0.8000
5.75646	7.57958	0.17372	23.15627	1796	1.1700	2.0500	0.9600
6.17620	7.30867	0.16191	24.84475	1927	5.1000	9.1000	1.0300
7.37546	9.87107	0.13558	29.66898	2302	4.9500	7.6000	1.2300
7.97509	10.41804	0.12539	32.08109	2489	4.5500	6.8000	1.3300
8.63469	12.80894	0.11581	34.73441	2695	4.6000	6.2000	1.4400
8.75461	11.75458	0.11423	35.21683	2732	4.3000	6.0500	1.4600
9.59410	12.69880	0.10423	38.59379	2994	4.1000	5.5500	1.6000
10.31365	12.82180	0.09696	41.48832	3219	3.8600	5.2000	1.7200
11.99262	14.12322	0.08338	48.24224	3743	3.3500	4.3000	2.0000

A	B	C	SIGMA	N
-0.26101748	-0.63914265	1.32167980	0.69283886	15

EFFECTIVE DIFFUSIVITY = 0.00085020
CORRECTION OF SLOPE FOR DIFFUSIVITY TERM = 0.0605318 AND NEW SLOPE C = 1.26115

COLUMN NO	COLUMN LENGTH CMS	COLUMN DIAMETER CMS	PELLET DIAMETER CMS	BED POROSITY	PELLET POROSITY	DIFFUSIVITY
57	421.0000	0.6600	0.5970	0.4710000	0.3100000	0.210264673

CARRIER MW	TEMP KELVIN	PRESS ATM	VISCOSITY	HYD DIA	DENSITY
29.00000	296.00000	1.01500	0.0182169	0.1655945	0.0012120

VELOCITY CM/SEC	HETP CMS	RECIP VEL SEC/CM	RE	NTU	WIDTH CM	TOTAL CM	Q CC/SEC
10.62794	16.53753	0.09409	42.2119610639	8.7000	18.6000	1.7500	
9.53478	15.40599	0.10488	37.87016 9545	9.3000	20.6000	1.5700	
8.32016	13.49911	0.12019	33.04593 8329	10.1000	23.9000	1.3700	
7.28773	11.65843	0.13722	28.94534 7295	10.8000	27.5000	1.2000	
6.07311	9.47155	0.16466	24.12112 6079	12.0000	33.9000	1.0000	
5.22287	8.50542	0.19147	20.74416 5228	2.6500	7.9000	0.8600	
4.12971	6.47520	0.24215	16.40236 4134	3.0000	10.2500	0.6800	
2.97582	4.53345	0.33604	11.81935 2979	3.6000	14.7000	0.4900	
2.00413	3.37384	0.49897	7.95997 2006	4.5000	21.3000	0.3300	
1.21462	2.20735	0.82330	4.82422 1215	1.3500	7.9000	0.2000	
0.48585	1.75714	2.05825	1.92969 486	3.4000	22.3000	0.0800	

A	B	C	SIGMA	N
-0.22380747	0.57967149	1.60895641	0.19640320	11

EFFECTIVE DIFFUSIVITY = 0.00069313
CORRECTION OF SLOPE FOR DIFFUSIVITY TERM = 0.0620292 AND NEW SLOPE C = 1.54693

COLUMN NO	COLUMN LENGTH CMS	COLUMN DIAMETER CMS	PELLET DIAMETER CMS	BED POROSITY	PELLET POROSITY	DIFFUSIVITY
58	421.0000	0.6600	0.5970	0.4710000	0.5000000	0.204915337

CARRIER MW	TEMP KELVIN	PRESS ATM	VISCOSITY	HYD DIA	DENSITY
29.00000	296.00000	1.00790	0.0182169	0.1655945	0.0012035

VELOCITY CM/SEC	HETP CMS	RECIP VEL SEC/CM	RE	NTU	WIDTH CM	TOTAL CM	Q CC/SEC
0.73391	5.41801	1.36257	2.89453	753	21.9000	81.8000	0.1200
2.20172	3.35020	0.45419	8.68360	2261	4.8000	22.8000	0.3600
3.18026	4.78626	0.31444	12.54298	3266	3.8500	15.3000	0.5200
5.32082	8.01792	0.18794	20.98537	5465	2.8400	8.7200	0.8700
6.11589	8.98325	0.16351	24.12112	6282	2.6200	7.6000	1.0000
6.72748	10.17581	0.14864	26.53323	6910	2.5500	6.9500	1.1000
7.33907	11.14604	0.13626	28.94534	7539	2.4000	6.2500	1.2000
8.68456	12.20968	0.11515	34.25199	8921	2.1100	5.2500	1.4200
9.17384	13.47536	0.10901	36.18168	9423	2.0900	4.9500	1.5000
10.76397	17.10708	0.09290	42.4531711057		9.8000	20.6000	1.7600

A	B	C	SIGMA	N
-2.20553330	4.65074056	1.69947962	0.40248025	10

EFFECTIVE DIFFUSIVITY = 0.00126920
CORRECTION OF SLOPE FOR DIFFUSIVITY TERM = 0.0613776 AND NEW SLOPE C = 1.63810

DIFFUSIVITY WITH K=1/(EP+ADS) = 0.00450397
TORTUOSITY= 22.74828
ADSORPTION = 1.37000MLS GAS/ML OF PELLET

COLUMN NO	COLUMN LENGTH CMS	COLUMN DIAMETER CMS	PELLET DIAMETER CMS	BED POROSITY	PELLET POROSITY	DIFFUSIVITY
59	421.0000	0.6600	0.5970	0.4710000	0.5000000	0.211745851

CARRIER MW	TEMP KELVIN	PRESS ATM	VISCOSITY	HYD DIA	DENSITY
29.00000	296.00000	1.00790	0.0182169	0.1655945	0.0012035

VELOCITY CM/SEC	HETP CMS	RECIP VEL SEC/CM	RE	NTU	WIDTH CM	TOTAL CM	Q CC/SEC
11.98715	17.32317	0.08342	47.2773911916	9.0000	18.8000	1.9600	
17.43029	25.13199	0.05737	68.7451917327	7.1500	12.4000	2.8500	
22.93459	30.70657	0.04360	90.4541922799	5.8000	9.1000	3.7500	
27.88846	36.22900	0.03586	109.9923027724	4.9500	7.1500	4.5600	
32.10843	40.22707	0.03114	126.6358731919	4.4500	6.1000	5.2500	
39.44749	42.23292	0.02535	155.5812139215	3.7000	4.9500	6.4500	
47.70395	42.51876	0.02096	188.1447247423	3.0000	4.0000	7.8000	
54.73722	42.09674	0.01827	215.8840154415	2.5000	3.3500	8.9500	
63.91106	35.33998	0.01565	252.0656963535	8.0000	11.7000	10.4500	
72.16751	35.09355	0.01386	284.6291971742	6.9500	10.2000	11.8000	
77.67181	31.52819	0.01287	306.3382077214	6.2000	9.6000	12.7000	
80.72976	35.13947	0.01239	318.3987680254	6.0000	8.8000	13.2000	

A	B	C	SIGMA	N
68.01311398	-592.80078888	-0.33316236	2.48643523	12

INVALID OUTPUT FORMAT. -0.59035632E-02
EFFECTIVE DIFFUSIVITY = XXXXXXXXXX
CORRECTION OF SLOPE FOR DIFFUSIVITY TERM = 0.0190111 AND NEW SLOPE C = -0.35217

COLUMN NO	COLUMN LENGTH CMS	COLUMN DIAMETER CMS	PELLET DIAMETER CMS	BED POROSITY	PELLET POROSITY	DIFFUSIVITY
60	420.0000	1.6000	1.3000	0.5220000	0.3800000	0.205018722

CARRIER MW	TEMP KELVIN	PRESS ATM	VISCOSITY	HYD DIA	DENSITY
29.00000	295.00000	1.03500	0.0181690	0.4436744	0.0012400

VELOCITY CM/SEC	HETP CMS	RECIP VEL SEC/CM	RE	NTU	WIDTH CM	TOTAL CM	Q CC/SEC
0.58324	1.43971	1.71457	5.17474	597	5.9000	42.7000	0.6400
0.95687	1.17827	1.04507	8.48981	980	3.1500	25.2000	1.0500
1.16647	1.20172	0.85728	10.34948	1194	2.5500	20.2000	1.2800
1.52189	1.25354	0.65708	13.50284	1558	2.0500	15.9000	1.6700
1.91375	1.45079	0.52253	16.97962	1960	8.3500	60.2000	2.1000
2.39674	1.59910	0.41723	21.26496	2454	7.1500	49.1000	2.6300
2.73393	1.72312	0.36577	24.25660	2800	6.5000	43.0000	3.0000
3.23515	1.88001	0.30911	28.70365	3313	5.7000	36.1000	3.5500
3.71814	2.01567	0.26895	32.98898	3808	5.1500	31.5000	4.0800
3.71814	2.04571	0.26895	32.98898	3808	5.1800	31.4500	4.0800

A	B	C	SIGMA	N
0.29405186	0.49773393	0.43967650	0.04052734	10

EFFECTIVE DIFFUSIVITY = 0.01938486
CORRECTION OF SLOPE FOR DIFFUSIVITY TERM = 0.1182664 AND NEW SLOPE C = 0.32141

COLUMN NO	COLUMN LENGTH CMS	COLUMN DIAMETER CMS	PELLET DIAMETER CMS	BED POROSITY	PELLET POROSITY	DIFFUSIVITY
61	421.0000	0.6600	0.5970	0.4710000	0.5000000	0.773230240

CARRIER MW	TEMP KELVIN	PRESS ATM	VISCOSITY	HYD DIA	DENSITY
29.00000	299.00000	0.98200	0.0183602	0.1655945	0.0011608

VELOCITY CM/SEC	HETP CMS	RECIP VEL SEC/CM	RE	NTU	WIDTH CM	TOTAL CM	Q CC/SEC
0.95112	1.80907	1.05139	3.58993	258	6.2500	40.4000	0.1500
1.71202	1.48969	0.58411	6.46187	466	2.9200	20.8000	0.2700
2.28269	1.55270	0.43808	8.61583	621	2.2000	15.3500	0.3600
3.42404	1.58861	0.29205	12.92374	932	7.3500	50.7000	0.5400
5.07265	1.87352	0.19714	19.14628	1380	5.4000	34.3000	0.8000
6.15059	2.07753	0.16259	23.21486	1674	4.7000	28.3500	0.9700
7.16512	2.33134	0.13956	27.04412	1950	4.2500	24.2000	1.1300
7.79920	2.57822	0.12822	29.43741	2123	4.1000	22.2000	1.2300
8.94055	2.79545	0.11185	33.74532	2433	3.7500	19.5000	1.4100
10.52575	3.05998	0.09501	39.72853	2865	3.3500	16.6500	1.6600
11.28665	3.42417	0.08860	42.60047	3072	3.1500	14.8000	1.7800
15.78863	4.24708	0.06334	59.59280	4298	2.5600	10.8000	2.4900
25.23645	6.23979	0.03963	95.25274	6870	7.7000	26.8000	3.9800

A	B	C	SIGMA	N
0.64075078	0.87210897	0.22362800	0.07450189	13

EFFECTIVE DIFFUSIVITY = 0.01016580
CORRECTION OF SLOPE FOR DIFFUSIVITY TERM = 0.0191109 AND NEW SLOPE C = 0.20452

COLUMN NO	COLUMN LENGTH CMS	COLUMN DIAMETER CMS	PELLET DIAMETER CMS	BED POROSITY	PELLET POROSITY	DIFFUSIVITY
62	421.0000	0.6600	0.5970	0.4710000	0.3400000	0.767428882

CARRIER MW	TEMP KELVIN	PRESS ATM	VISCOSITY	HYD DIA	DENSITY
29.00000	297.50000	0.98100	0.0182887	0.1655945	0.0011655

VELOCITY CM/SEC	HETP CMS	RECIP VEL SEC/CM	RE	NTU	WIDTH CM	TOTAL CM	Q CC/SEC
1.89463	1.61910	0.52781	7.20795	519	13.1500	89.8500	0.3000
3.41034	1.64960	0.29323	12.97431	935	7.1500	48.4000	0.5400
4.42081	1.76095	0.22620	16.81855	1212	5.8000	38.0000	0.7000
5.36812	1.89269	0.18628	20.42253	1472	4.8500	30.6500	0.8500
6.31544	2.13187	0.15834	24.02650	1732	4.4000	26.2000	1.0000
7.01014	2.20875	0.14265	26.66942	1922	4.0000	23.4000	1.1100
7.83114	2.39186	0.12770	29.79286	2148	3.7000	20.8000	1.2400
7.83114	2.49881	0.12770	29.79286	2148	3.8000	20.9000	1.2400
8.58899	2.56615	0.11643	32.67604	2355	3.5100	19.0500	1.3600
9.34685	2.73856	0.10699	35.55922	2563	3.3500	17.6000	1.4800
10.23101	3.06171	0.09774	38.92293	2806	3.2000	15.9000	1.6200
22.79873	5.85278	0.04386	86.73567	6253	1.9200	6.9000	3.6100

A	B	C	SIGMA	N
0.37897281	1.49184255	0.23788515	0.04411453	12

EFFECTIVE DIFFUSIVITY = 0.00561640
CORRECTION OF SLOPE FOR DIFFUSIVITY TERM = 0.0192997 AND NEW SLOPE C = 0.21859

COLUMN NO	COLUMN LENGTH CMS	COLUMN DIAMETER CMS	PELLET DIAMETER CMS	BED POROSITY	PELLET POROSITY	DIFFUSIVITY
73	119.4000	2.1700	0.3200	0.3900000	0.3100000	0.742124423

CARRIER MW	TEMP KELVIN	PRESS ATM	VISCOSITY	HYD DIA	DENSITY
29.00000	295.00000	1.00000	0.0181690	0.1174626	0.0011981

VELOCITY CM/SEC	HETP CMS	RECIP VEL SEC/CM	RE	NTU	WIDTH CM	TOTAL CM	Q CC/SEC
9.09386	1.01778	0.10996	19.18923	731	4.7500	21.8000	13.2500
8.92227	0.98153	0.11208	18.82717	717	4.9000	22.9000	13.0000
8.40753	0.96925	0.11894	17.74099	676	5.0500	23.7500	12.2500
7.72120	0.89770	0.12951	16.29275	621	5.3000	25.9000	11.2500
7.03487	0.88500	0.14215	14.84450	565	5.7500	28.3000	10.2500
6.00538	0.81740	0.16652	12.67214	483	1.6500	8.4500	8.7500
5.14747	0.72322	0.19427	10.86183	414	1.8000	9.8000	7.5000
4.11797	0.72916	0.24284	8.68946	331	2.2500	12.2000	6.0000
2.91690	0.76273	0.34283	6.15504	234	3.1500	16.7000	4.2500
1.88740	0.92221	0.52983	3.98267	151	5.6000	27.0000	2.7500
0.68633	2.14016	1.45703	1.44824	55	4.8500	15.3500	1.0000

A	B	C	SIGMA	N
-0.01542345	1.43413471	0.09574282	0.01539098	11

EFFECTIVE DIFFUSIVITY = 0.00447061
CORRECTION OF SLOPE FOR DIFFUSIVITY TERM = 0.0166358 AND NEW SLOPE C = 0.07911

TIME 17HRS 21MIN 55.4SEC

TABLE A II.1

	Manometers Inches Oil	Flow Rate cm^3/sec. at 298°K 760 mm Hg
Low Flow (LF)		
	1.8	0.338
	3.65	0.674
	7.9	1.416
	10.7	1.87
	17.5	2.82
	23.7	3.65
	26.1	3.96
High Flow (HF)		
	.91	.811
	1.5	1.31
	2.8	2.37
	4.1	3.21
	5.1	3.91
	7.7	5.88
	7.0	5.38
	10.2	6.90
	15.1	9.46
	8.1	5.85
	14.4	9.00
	18.1	10.50
	21.1	11.70
	24.9	12.68
	24.0	13.45
Very High Flow (VHF)		
	1.65	12.9
	2.35	15.9
	5.3	26.3
	8.7	33.9
	14.4	44.0
	20.05	52.0
	26.1	59.5

Continued....

TABLE A II.1 (Continued)

	Manometers Inches Oil	Flow Rate cm^3/sec. at 298°F 760 mm Hg
Ultra High Flow (UHF)		
	26.7	287.5
	23.3	271
	19.6	246
	17.6	233
	13.9	204
	10.0	171
	6.8	139
	4.35	106
	1.85	64.4
	1.1	48
Extra High Flow (EHF)		
	26.75	348
	23.3	323
	17.6	278
	11.85	221
	8.25	180
	6.35	152
	3.77	112.5
	1.88	73.6
	.95	45.3

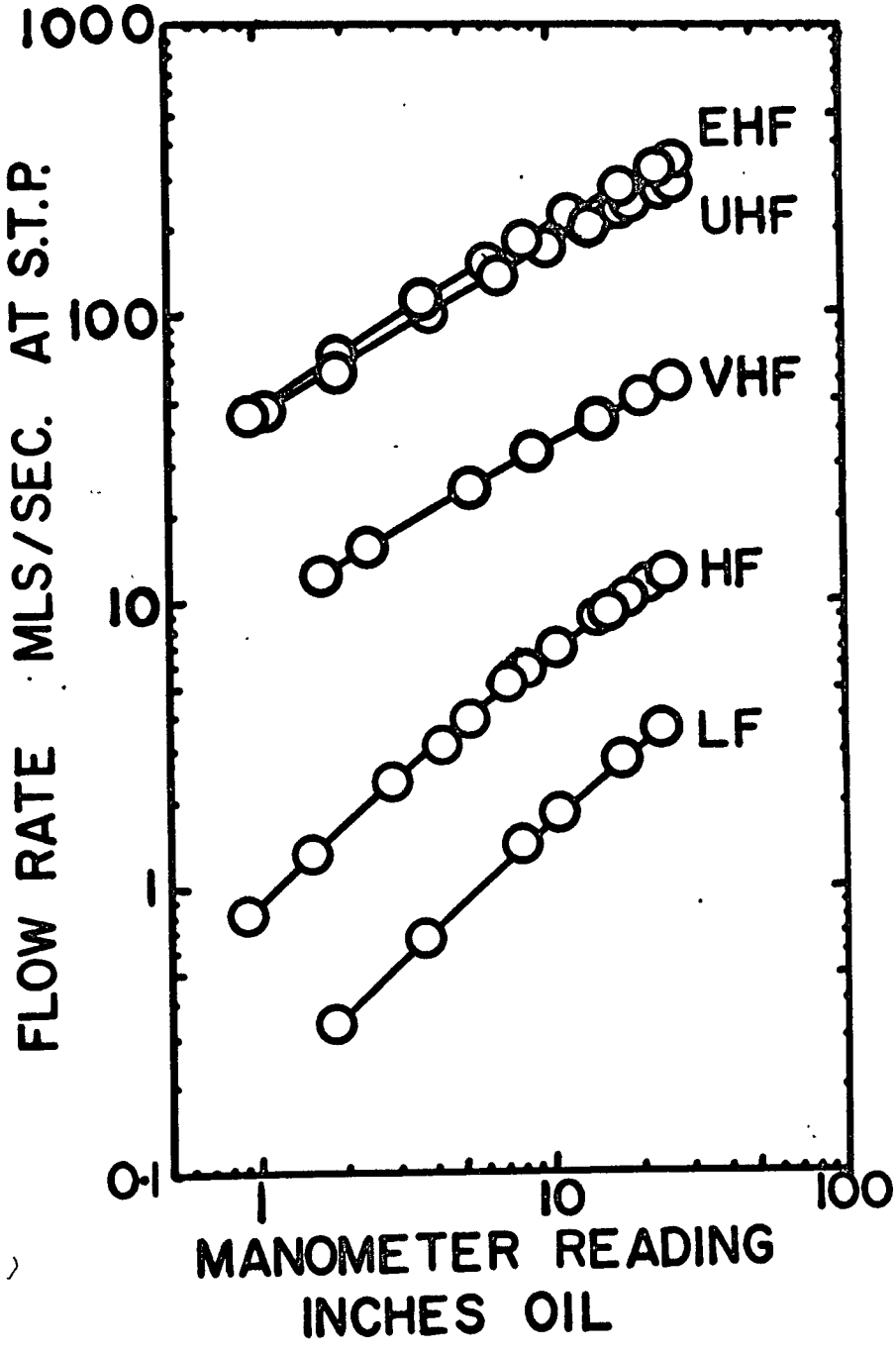

Figure A II.1

Flow Meter Calibration

APPENDIX III

TIME OF DIFFUSION OF A GAS FROM A SPHERICAL PELLET WITH A STEP CHANGE IN SURFACE CONCENTRATION

RATE OF DIFFUSION FROM A SPHERICAL PELLET

The diffusion of a gas from a spherical pellet with a step change in the surface concentration is given by Crank (Ref. 2, page 86).

The amount of gas diffused at time t, (M_t) as compared to the amount of gas diffused at infinite time (M_∞) is given by,

$$\frac{M_t}{M_\infty} = 1 = \frac{6}{\pi^2} \sum_{n=1}^{\infty} \frac{1}{n} \exp\left(- \frac{DEn^2 \pi^2 t}{a^2}\right)$$

where a is the pellet radius.

For the second term in the series to be less than 1% of the first,

$$\exp\left(- \frac{D_E \pi^2 t}{a^2}\right) = \frac{100}{4} \exp\left(- \frac{4\, D_E \pi^2 t}{a^2}\right)$$

$$\mathrm{Ln}\,(25) = \frac{4\pi^2 D_E t}{a^2} - \frac{\pi^2 D_E t}{a^2} = \frac{3\pi^2\, D_E t}{a^2}$$

If D_E = 0.01 cm^2/sec and a = 0.5 cms

$$t = \frac{.25\, \mathrm{Ln}(25)}{3\,\pi^2 \times .01} \simeq 2.82 \text{ seconds}$$

Thus after ten seconds

$$\frac{M_t}{M_\infty} = 1 - \frac{6}{\pi^2}\, e\left(- \frac{.01\ \ ^2 \times 10}{.25}\right) = .9881$$

$$= 98.81\%$$

Thus in ten seconds 98.8% of the gas will diffuse out of a 1 cm diameter pellet if the effective gas diffusivity is 0.01 cm^2/sec

MANUFACTURERS DATA ON POROUS PELLETS (INCLUDING CONTRADICTIONS AND VERIFICATIONS)

Norton Catalyst Supports, 1/2" diameter SA 203 mixture

Information from two sources is summarized below, the first from the manufacturer's general information sheet, and the second from data supplied by the manufacturer in a private communication.

	Manufacturer's Data	Private Communication
Apparent Porosity	0.41	.36 - .40
Water absorption	20%	15 - 19%
Bulk density	2.1 grams/ml	2.1 - 2.3 grams/ml
Apparent Specific Gravity		3.4 - 3.6
Packing Density	75 - 78 lb/ft^3	
Surface Area	less than 1 $meter^2/gram$	
Pore Diameter Range		90% in 2-40 microns

Using the bulk density value of 2.1 and the specific gravity of 3.5, a porosity of 0.382 can be calculated. As a further check on the consistency of the data, if the water adsorbed is assumed to exist as liquid water occupying the pores, then 17% water indicates a porosity of 0.37%. In an experimental check, a pellet was dried by heating to 500°F, and then put in a vacuum which was released by water so that the pellet absorbed as much water as possible. Weighing the pellet between each operation showed that the initial water content was negligible, but the evacuation and saturation procedure yielded a water content of 16.8% which again is an indication of a 37% porosity if the pellet specific gravity of 3.5 is accepted.

In conclusion, a value of 38% porosity has been taken for the pulse apparatus experiments and the information available suggests an error limit of ± 1%.

Activated Alumina Pellets Alcoa H 151 1/4" and 1/8" diameter

Two sources of information were again used to determine the properties of these pellets, but some of these data were contradictory. Because one of these sources was private communication in the form of a letter from the supplied, which differed from the manufacturer's data it was concluded that the supplier had not furnished the correct data. This conclusion is justified in the following paragraphs.

	Manufacturer's Data	Private Communication
Packing Density	52-55 lb/ft^3 51-53 lb/ft^3	
Specific Gravity	3.1-3.3	
Pore Volume	0.3 mls/gm	0.5-0.55 mls/gm
Pore Diameter	50 A°	40 A°
Surface Area (BET)	350 meter^2/gm	390 meter^2/gm
Pore Volume greater than 30A°		0.28 mls/gm
Average Pore Diameter in 90 to 30A° region		42A°
Static Adsorption at 60% RH	22-25%	

A pore volume of 0.3 mls per gram represents a porosity of 50% if the specific gravity of the pellets is taken as 3.2, while a pore volume of 0.5 indicates a porosity of 63%. The problem amounts to deciding which set of data above are consistent.

Placing the pellets in a vacuum and releasing with water to measure the water absorbed showed a porosity of around 50 to 55% which is somewhat indeterminate, lying as it does between the data from the two sources. However, for the 1/8 inch activated alumina pellets the test described below was applied.

The test pellets were placed in the sample loop of a gas chromatograph and a hydrogen purge put on the loop. Air carrier gas was put on the column, which consisted of a 20 ft. length of 1/2" plastic hose to cause dispersion and create a Gaussian pulse distribution. The height of the pulse was proportional to the gas in the pulse, and so by noting the difference in height between the pulse with the pellets in the sample loop, and without, the volume of the solids in the pellets could be determined. The peak heights were calibrated in terms of gas volume by injecting known volumes of hydrogen with a syringe.

The volume of the sample loop was found to be 4.80 mls while the volume of gas when 47 dried pellets occupied the tube was 4.40 mls. From the mean diameter the overall volume of the pellets was calculated to be 0.81 mls and so the porosity is given by (0.81-0.40)/0.81 = 50.5%.

Similarly for 47 wet (12%) pellets, porosities of 28.4 and 33% were obtained.

If the water is assumed to exist as liquid water (31), then the porosity of the wet pellets can be calculated from the moisture content if the dry pellet porosity is known. If a 50% dry pellet porosity is assumed, then for a 12% wet pellet the porosity comes out to be 30.8%. Thus, the manufacturer's data appears to give the best agreement with the observations.

Finally, two individual pellets were weighed and the dimensions of three diameters measured on callipers. This allowed the apparent density of the pellets to be calculated, and if the water content is taken into account, the porosity of the dry pellets can be obtained from a knowledge of the true specific gravity.

0.699 cm pellet weighed 0.3140 grams so density = 1.76 gms/ml

0.617 cm pellet weighed 0.2300 grams so density = 1.87 gms/ml

If 12% water in the pellet is assumed then the densities become 1.57 and 1.67 respectively. In conjunction with the specific gravity the porosities of these two pellets when dried are;

1.57/3.2 = 49% 1.67/3.2 = 52%

The only anomaly left in the manufacturer's data is the claim of 22 to 25% static adsorption of moisture in air of 60% RH. Even with soaking in water only 14% water was adsorbable. However, in an Alcoa product data

bulletin, ("Activated and Catalytic Aluminas", Feb. 1, 1963, Section GB2A, Figure 2, page 8), it is shown that after about six months operation the adsorptive capacity of this material drops to 13 or 14%. The samples used in this work were stored for six months before work was started, and so it is possible that the low moisture contents are to be expected.

The dry pellets were assumed to have a 50% porosity in the pulse apparatus determinations and the porosity of the wet pellets was taken as 31% corresponding to a 12% wet pellet. The 1/4" and 1/8" pellets were assumed to have the same properties.

POROSITY OF PACKED BEDS

Two general methods were used to obtain the porosity of the non porous pellet beds

A.) If the density of the pellet packing was known, the bed was weighed before and after filling and the pellet density used to convert the packing weight to a packing volume. The overall volume of the vessel was calculated from the internal dimensions of the bed.

Example

Run 50: 5 cm. diameter by 111.8 cm. length bed packed with No. 9 lead shot having a density of 10.808 gm/ml.

Weight of column + bungs + screens		= 1051 grams
" " " " + packing		= 35.5 lb.
		= 161028 grams
Weight of packing		= 15,051 grams
Volume of packing	15,051/10.808	= 1392 ml.
Volume of bed	$\frac{\pi(5.0)^2}{4}$ 111.8	= 2195 ml.

$$\text{Bed Porosity} = \frac{2195 - 1392}{2195} = 36.6\%$$

B.) The alternate method of porosity measurement was to weigh the bed, (a) empty, (b) packed, (c) packed and filled with water, (d) unpacked and filled with water. If the density of water is taken as unity the bed porosity is given by (c-b)/(d-a).

Example

Run 54: 1/4" polyethylene tube packed with 2.975 mm glass beads. Column length 184.5 cm and diameter 0.415 cm.

Weight of tube	= 43.0 grams
" " " + packing	= 72.0 grams
" " " " + water	= 89.0 grams
" " " + water	= 70.0 grams

Porosity of bed = (89.0 - 72.0)/(70.0 - 43.0) = 63%

The porosities of the beds of porous pellets are treated individually depending on the reliability of the available manufacturer's data.

Norton Catalyst Support 1/2" diameter SA 203 Mixture, RUN 60

The moisture content of these pellets was found to be negligible and so the manufacturer's pellet density was accepted as a value of 2.05 grams/ml. With the weight of pellets in the bed measured, the porosity of the bed (not including pellet pores) was calculated by method A) above.

Activated Alumina Pellets Alcoa H151 1/4" diameter, RUNS 56,57,58,59,61,62

The bed used for these runs was a single pellet diameter and the porosity was measured as follows. The average diameter was used to calculate the mean pellet volume and then the number of pellets in a measured length of tube was measured. The volume of the pellets is thus known and the volume of the bed over the measured length can be calculated from the internal diameter of the vessel.

Example

Forty-four pellets in line occupy 25.0 cm. making a mean pellet diameter of 0.568 cm. (Note the pellets were graded so that a small pellet was not adjacent to a large pellet, which would introduce an error into the result.)

In the packed bed 18 pellets occupied 10 cm. The volume of the pellets is thus $18\,\pi(0.568)^3/6 = 1.727$ mls. and the volume of the vessel is given by $10\pi(0.66)^2/4 = 3.42$ mls.

The bed porosity is $(3.42 - 1.727)/3.42 = 49.7\%$

Activated Alumina Pellets, Alcoa H 151 1/8" Diameter, RUN 73

The above method could not be applied to a bed of several particle diameters thick. The moisture content of the pellets was determined to be 12%, and weighing the bed before and after filling showed that 467 grams of the wet pellets packed the bed. Thus the weight of dry pellets was 411 grams and since the density of the dry pellets was given as 3.1 to 3.3 gm/cm. by the manufacturer, the volume of solid can be calculated to be 129 ml. The 119.4 cm. long by 2.175 cm. diameter bed contains a volume of 441 ml. and so the porosity of the bed can be evaluated by method A if the dry pellets are assumed to be 50% porous.

The porosity is thus $(441 - 129/0.5)/441 = 41\%$

As a corollary to the above calculation, the porosity of the dry activated alumina pellets is unlikely to be 65% as claimed in the supplier's literature. The assumption of a 65% pellet porosity yields impossible bed porosities, for example, a value of 54% is obtained and a 54% bed porosity is extremely unlikely in a random packed bed of uniform spheres.

Estimation of the Molecular Diffusivity of the Methane Air System Ref (32)

	Mol Wt.	σ	$\bar{K}$	Tc	Pc	V_c
Air	28.97	3.617 Å	97.0	132	36.4	86.6
Methane	16.04	3.822	137.0	190.7	45.8	99.7

$$\sigma_{AB} = 3.7195 \text{ Å}$$

$$\frac{\epsilon_{AB}}{K} = \sqrt{97 \times 137} = 115.4\,°K$$

At 298°K $\quad \frac{KT}{\epsilon_{AB}} = \frac{298}{115.4} = 2.54$

From Table B.2 $\quad \Omega = 0.990$

$$D_{AB} = 0.001858 \sqrt{\frac{(293)^3 \left(\frac{1}{16.04}\right) + \left(\frac{1}{28.97}\right)}{1\ (3.7195)^2\ .990}}$$

$$= \underline{0.212 \text{ cm}^2/\text{sec}}$$

APPENDIX IV

ADSORPTION OF GASES BY ACTIVATED ALUMINA PELLETS

THEORY AND APPARATUS

This experiment was carried out in order to obtain the degree of methane adsorption in dry alumina pellets, adsorption is known to influence the effective diffusivity in a porous pellet (2). The following two assumptions were made,

the adsorption isotherm is linear, i.e. moles adsorbed/gm. solid = W(partial press.)

and the presence of other gases does not affect the adsorption isotherm.

The apparatus is shown in Figure A IV.1. The test chamber BC could be evacuated while the burette zone AB was purged with the test gas. The stop cock A was then turned to shut off the purge gas and open the mercury tube to the burette. The amount of gas used in the test could be adjusted by regulating the burette zone vent at B and adjusting the manometer level.

The vacuum in the test chamber could be shut off at C, and the burette and test chamber connected at B. Thus by knowing the volume of the test chamber and the tube connecting to the burette zero, a series of measurements of the volume and pressure of trapped gas could be made by altering the manometer position. A series of burette readings (volume) and manometer readings (pressure) were taken at corresponding points as well as the atmospheric pressure. The volume of sample solids was also obtained.

Total gas in the system = $\frac{P_oV_o}{RT}$ Moles

A material balance of the trapped gas yields,

$$\frac{P_oV_o}{R\,T} = \frac{P\,V}{R\,T} + WP\rho_pQ$$

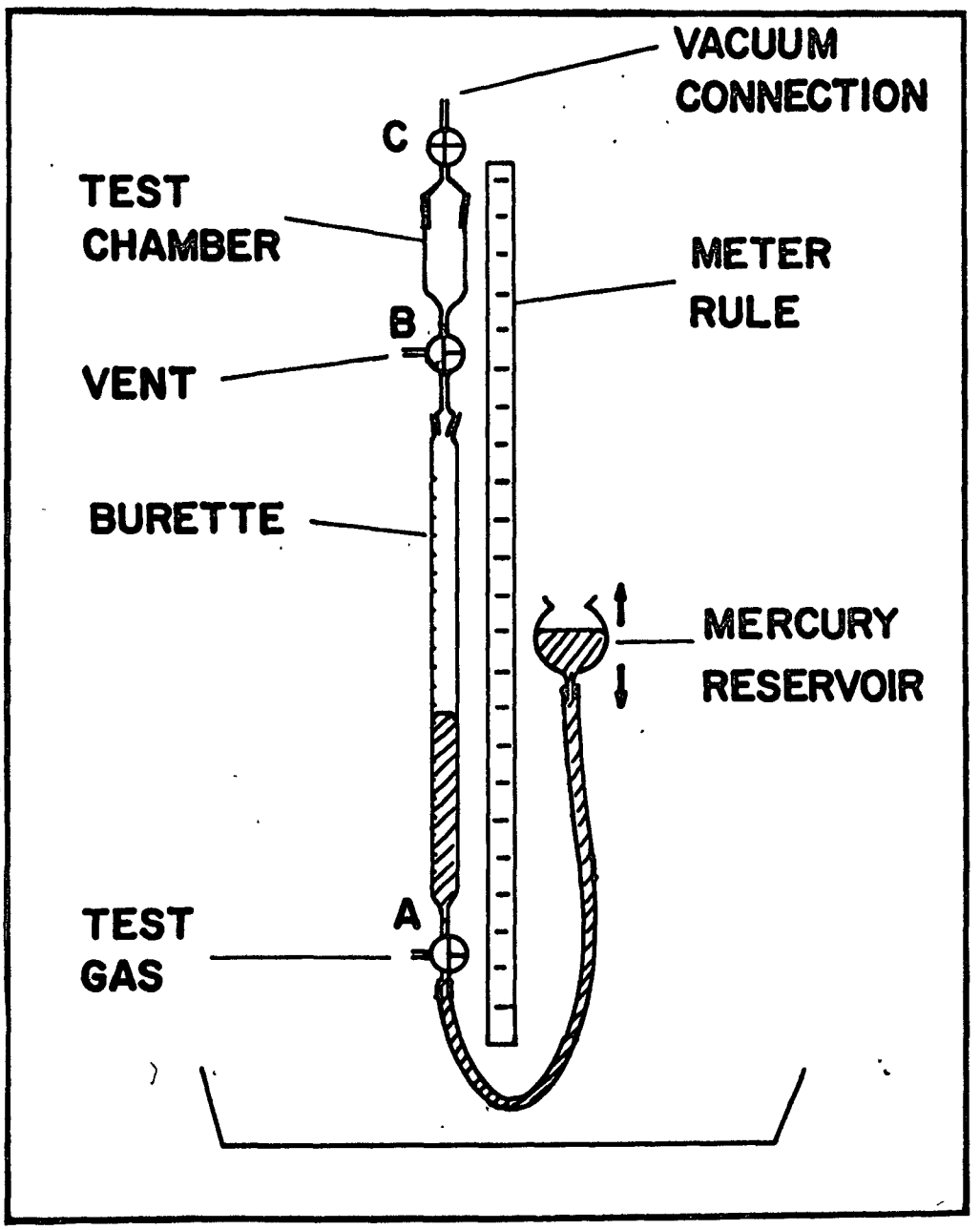

Figure A VI.1

Adsorption Measurement Apparatus

or $V = \frac{P_o V_o}{P} - WRT\,\rho_p Q$

Where ρ_p is the pellet density, and Q the volume of pellets.

Hence a plot of volume V against $\frac{1}{P}$ should yield a straight line having an intercept $WRT\,\rho_p Q$ which is the volume of gas adsorbed. If the overall volume of the pellets (including pores) is known then the volume of adsorbed gas per unit volume of pellets is easily obtained.

RESULTS

Table A IV.I shows the manometer and burette readings along with data in terms of volume and inverse pressure for the methane, hydrogen and nitrogen. Two sets of data are recorded for methane, one assumed atmospheric pressure and the other at about 1/2 atmospheres in order to try and approach the concentration in the pulse apparatus. These points are plotted in Figure A IV.2.

Following are the characteristics of the apparatus which had to be known to prepare Table A IV. 1,

Volume from zero of burette to stop cock B = 6.7 ml.

Volume of empty test chamber = 25.29 ml.

Pellets ALCOA H 151 activated alumina spheres 1/4" diameter.

Weight of dry pellets in sample = 7.68 grams

Volume of solid excluding pores = 7.65/3.2 = 2.4 ml.

Overall volume of pellet (50% porosity) = 4.8 ml.

The overall volume of the pellets was also computed from the dimensions of the pellets and the same result was obtained.

Hence volume to be added to the burette reading = 25.29 + 6.7 - 2.4

= 29.59 ml.

Volume of gas = 29.59 + Burette reading

Pressure in chamber = Atmospheric ± manometer pressure difference

RESULTS AND CONCLUSIONS

The intercept of the hydrogen data is of the order of the accuracy of the experiment, and so it may be concluded that the hydrogen intercept represents zero adsorption. The intercepts were computed by the least squares technique and methane showed 5.22 ml. adsorbed at a half atmosphere and 5.387 ml. at one atmosphere. Since the hydrogen intercept of + 0.316 is taken as zero this must be added to the methane result giving 5.22 + .31 = 5.53 ml. in 4.8 ml. of pellet at a half atmosphere and 6.60 ml. in 4.8 ml. pellet at one atmosphere.

Hence the methane adsorbed per unit volume of pellet material is 1.15 ml. at a half atmosphere and 1.375 ml./ml. pellet at one atmosphere. The results for nitrogen are not particularly of interest but it can be seen from Figure A IV.2 that nitrogen adsorption is slightly higher than that of hydrogen as may be expected. A least squares computation for the nitrogen data was not carried out.

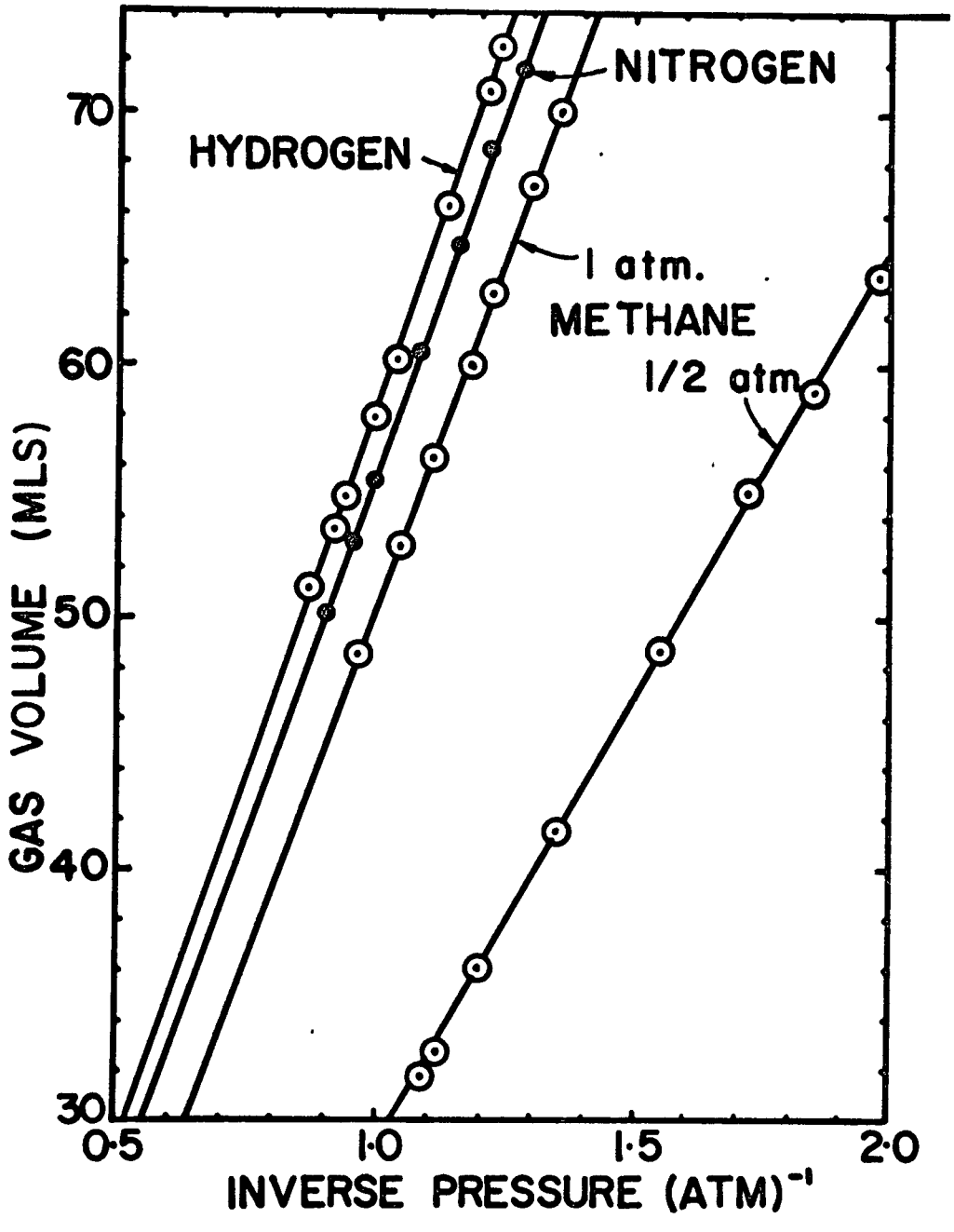

Figure A IV.2

Gas Volume vs. Inverse Pressure For Adsorption Measurement

TABLE A IV.1

RESULTS FOR ADSORPTION APPARATUS

METHANE Low Pressure
Atm. Pressure 759.0 mm Hg
Room Temp. 22°C

Burette mls.	Man. cm.	Press. mm Hg	$atm.^{-1}$	Vol. mls.
0	- 1.5	74.4	1.02	29.59
2.3	- 6.2	69.7	1.09	31.89
4.2	- 8.2	67.7	1.12	33.79
6.5	-12.8	63.1	1.20	36.09
11.9	-19.7	56.2	1.35	41.49
19.1	-26.8	49.1	1.55	48.69
25.4	-31.8	44.1	1.72	54.99
29.4	-35.0	40.9	1.85	58.99
34.01	-37.5	38.4	1.98	63.60
49.0	-45	30.9	2.45	78.59

$\sum \frac{1}{P}^2 = 25.4517$

$\sum \frac{1}{P} = 15.33$

$\sum V = 477.71$

$\sum \frac{V}{P} = 799.7635$

Intercept= -5.2208 mls.

HYDROGEN
765.2 mm Hg
22°C

Burette mls.	Man. cm.	Press. mm Hg	$1/P_{-1}$ atm	Vol. mls.
41.3	-14.0	62.5	1.215	70.89
43.0	-15.4	61.1	1.242	72.59
36.7	- 9.7	66.8	1.138	66.29
30.7	- 3.2	73.3	1.038	60.29
25.3	+ 4.3	80.8	.940	59.89
23.9	+ 6.4	82.9	.917	53.99
21.6	+10.7	87.2	.872	51.19
28.4	0	76.5	.994	57.99

$\sum \frac{1}{P}^2 = 8.86418$

$\sum \frac{1}{P} = 8.356$

$\sum V = 487.62$

$\sum \frac{V}{P} = 517.23384$

Intercept= 0.3167 mls.

TABLE A IV.1 (Continued)

NITROGEN
Atm. Pressure 765.2 mm Hg
Room Temp. 22°C

Burette mls.	Man. cm.	Press. mm Hg	$1/P$ atm.$^{-1}$	Vol. mls.
42.3	-17.0	59.5	1.279	71.89
39.0	-14.0	62.5	1.215	68.59
35.2	-10.5	66.0	1.152	64.79
31.0	- 6.1	70.4	1.08	60.59
25.95	0	76.5	.994	55.54
23.4	+ 3.3	79.8	.953	52.99
20.6	+ 7.7	84.2	.901	50.19

METHANE High Pressure
749.5
22.5°C

Burette mls.	Man. cm.	Press. mm Hg.	$1/P$ atm.$^{-1}$	Vol. mls.
31.0	-10.6	64.3	1.185	60.6
33.3	-12.7	62.2	1.225	62.9
37.55	-16.4	58.5	1.30	67.2
40.8	-18.9	56.0	1.354	70.4
26.8	- 6.5	68.4	1.11	56.4
23.3	- 2.3	72.6	1.045	52.9
21.2	0	74.9	1.018	50.8
19.0	+ 3.3	78.2	0.965	48.6

$\sum \frac{1}{P^2} = 10.71984$

$\sum \frac{1}{P} = 9.202$

$\sum \frac{V}{P} = 548.0431$

$\sum V = 469.8$

$n = 8$

Intercept = -6.387 moles

B DAVIS FORTRAN SOURCE LIST GAAA 04/29/65

```
ISN        SOURCE STATEMENT

 1         PI=3.14159
 2 6       READ 1,DB,EL,ELE,E
 3 1       FORMAT (4F10.5)
 4         IF(DB)70,70,5
 5 5       READ2,S,Q,P,T,TB,DO,J
 7 2       FORMAT(F10.8,5F10.5 ,I2)
10         IF(S)6,6,9
11 9       Q=Q*TB/T
12         CALL SKIP TO (1)
13         I=0
14         IF(J-62)101,102,103
15 101     PRINT61
16 61      FORMAT(20H HYDROGEN-NITROGEN      / )
17         GOTO105
20 102     PRINT62
21 62      FORMAT( 20H NITROGEN-ETHANE      / )
22         GOTO105
23 103     PRINT63
24 63      FORMAT( 20H NITROGEN-BUTANE          /)
25 105     PRINT3,DB,Q,EL,T,ELE,P
26 3       FORMAT(9X,8HBED DATA,50X,8HRUN DATA//
          118H BED DIAMETER CMS   ,F10.5,20X,18HFLOW RATE  CC/SEC= ,F10.5/
          218H BED LENGTH CMS    ,F10.5,20X,18HROOM TEMPERATURE=  ,F10.4/
          318H END ZONE HEIGHT     ,F10.5,20X,18HATM.PRESSURE MM HG     ,F10.1)
27         PRINT31,E,TB
30 31      FORMAT(9H POROSITY     ,F10.5,20X,18HBED TEMPERATURE K=  ,F10.4//)
31         CALLABCD(S)
32         A=1.56/EL
33 20      D=S/A**2
34         H=4.*Q/(D*E*PI*DB**2)
35          EK=ELE/E
36         DEL=H-EK*A**2-A*SIN(A*EL)/COS(A*EL)
37         I=I+1
40         IF(ABS(DEL)-.00001) 51,50,50
41 50      DDEL=-2.*EK*A-A*EL/(COS(A*EL))**2-SIN(A*EL)/COS(A*EL)
42         A=A-DEL/DDEL
43         IF(I-20) 71,71,51
44 71      GOTO20
45 51      D=D*760./P
46         AMDA=DO/D
47         DEF=D*E
50         PRINT52,D,AMDA,DEF,DO,A,I
51 52      FORMAT(10X,15HDIFFUSIVITY=    ,F16.8/10X,7HLAMDA = ,F16.8/10X,25HEF
          1FECTIVE DIFFUSIVITY=    ,F16.8/10X,23HPUBLISHED DIFFUSIVITY=  ,F16.
          28/10X,6HALPHA=  ,F16.8,20X,20H NUMBER ITERATIONS=          ,I2)
52         GOTO6
53 70      STOP
54         END


        NO MESSAGES FOR ABOVE ASSEMBLY
TIME 17HRS 00MIN 06.0SEC
```

```
ISN        SOURCE STATEMENT

 1         SUBROUTINE ABCD(B)
 2         DIMENSION Y(100)
 3         DIMENSION T(100)
 4 2       SY=0.0
 5         N=1
 6         PRINT50
 7 50      FORMAT(20X,30H  TIME SEC.    PEAK HEIGHTS                )
10 26      CONTINUE
11         READ25,T(N),Y(N)
12 25      FORMAT(F10.1,F10.2)
13         IF(T(N))  40,40,41
14 41      PRINT27,T(N),Y(N)
15 27      FORMAT(20X,F10.1,F10.2 )
16         SY=SY+Y(N)
17         N=N+1
20         GOTO26
21 40      NU=N-1
22         DO7IT=1,10
23 11      SEBT=0.0
24         STEBT=0.0
25         SYEBT=0.0
26         SYTEBT=0.0
27         STE2BT=0.0
30         SE2BT=0.0
31         ST2EBT=0.0
32         ST2E2B=0.0
33         SYT2EB =0.0
34         DO12N=1,NU
35         EBT=EXP(-B*T(N))
36         E2BT=EXP(-B*T(N)*2.)
37         SEBT=SEBT+EBT
40         SYTEBT=SYTEBT+Y(N)*T(N)*EBT
41         SYEBT=SYEBT+Y(N)*EBT
42         STEBT=STEBT+T(N)*EBT
43         SYT2EB =SYT2EB +Y(N)*T(N)**2*EBT
44         ST2E2B =ST2E2B +T(N)**2*E2BT
45         ST2EBT =ST2EBT +T(N)**2*EBT
46         STE2BT =STE2BT+T(N)*E2BT
47         SE2BT= SE2BT +E2BT
50 12      CONTINUE
52         EN=NU
53         EROR=  -SYEBT*STEBT*SEBT/EN+SYEBT*STE2BT+STEBT*SY*SE2BT/EN-SYTEBT*
          1SE2BT  -SY*SEBT*STE2BT/EN +SYTEBT*SEBT**2/EN
54 16      DEROR = SYEBT*(STEBT**2 +SEBT*ST2EBT)/EN +STEBT*SEBT*SYTEBT/EN
          1-2.*SYEBT*ST2E2B -STE2BT*SYTEBT-(2.*SY*STEBT*STE2BT+SY* SE2BT*ST2E
          2BT)/EN +2.*SYTEBT*STE2BT +SE2BT*SYT2EB +2.*SY*SEBT*ST2E2B/EN +
          3SY*STE2BT*STEBT/EN -2.*SYTEBT*SEBT*STEBT /EN-SEBT**2*SYT2EB/EN
55 7       B=B-EROR/DEROR
57 15      A= (STEBT*SY/EN-SYTEBT)/(STEBT*SEBT/EN-STE2BT)
60         C=(SY-A*SEBT)/EN
61         PRINT37,A,B,C
62 37      FORMAT(//60H CONSTANTS FOR LEAST SQUARES FIT OF DATA IN Y=C= A*EXP
          1(-BT)      /20X,3HA =,F16.5  /20X,3HB = ,F16.8/20X,3HC =,F16.8 ///
          250H  SUMMATIONS FROM LEAST SQUARES CALCULATION          )
63          PRINT 13,SEBT,SYEBT,        SY,STEBT,STE2BT,SE2BT,ST2EBT,ST2E2B ,
```

```
ISN        SOURCE STATEMENT

           1SYT2EB ,SYTEBT
 64 13      FORMAT(16X,7HSEBT  = ,E12.5/16X,7HSYEBT =    ,E12.5/16X,7HSY    =,
           1E12.5/16X,7HSTEBT =   ,E12.5/16X,7HSTE2BT= ,E12.5/16X,7HSE2BT =  ,
           2E12.5,/16X,7HST2EBT= ,E12.5/16X,7HST2E2B= ,E12.5/16X,7HSYT2EB=,
           3E12.5 /16X,7HSYTEBT=  ,E12.5  )
 65 6       RETURN
 66         END


        NO MESSAGES FOR ABOVE ASSEMBLY
TIME 17HRS 00MIN 39.3SEC
```

PARALLEL TUBE BED

HYDROGEN-NITROGEN

BED DATA

BED DIAMETER CMS 5.03000
BED LENGTH CMS 10.05000
END ZONE HEIGHT 0.27000
POROSITY 0.52000

RUN DATA

FLOW RATE CC/SEC= 0.51029
ROOM TEMPERATURE= 295.5000
ATM.PRESSURE MM HG 757.6
BED TEMPERATURE K= 309.0000

TIME SEC.	PEAK HEIGHTS
200.0	2925.00
300.0	2050.00
400.0	1400.00
500.0	1000.00
600.0	700.00
700.0	480.00

REJECTED POINTS
100 4050

CONSTANTS FOR LEAST SQUARES FIT OF DATA IN Y-C= A*EXP(-BT)

A = 6035.51483
B = 0.00364182
C = 13.98370361

SUMMATIONS FROM LEAST SQUARES CALCULATION

SEBT = 0.14035E 01
SYLBT = 0.27037E 04
SY = 0.85550E 04
STEBT = 0.49346E 03
STE2BT= 0.12702E 03
SE2BT = 0.44471E-00
ST2EBT= 0.20602E 06
ST2E2B= 0.42225E 05
SYT2EB= 0.25773E 09
SYTEBT= 0.77353E 06

DIFFUSIVITY= 0.55121716
LAMDA = 1.48761696
EFFECTIVE DIFFUSIVITY= 0.28663293
PUBLISHED DIFFUSIVITY= 0.82000000
ALPHA= 0.08122977 NUMBER ITERATIONS= 21

HYDROGEN-NITROGEN

BED DATA		RUN DATA	
BED DIAMETER CMS	5.05000	FLOW RATE CC/SEC=	0.54376
BED LENGTH CMS	10.05000	ROOM TEMPERATURE=	295.5000
END ZONE HEIGHT	0.27000	ATM.PRESSURE MM HG	757.6
POROSITY 0.52000		BED TEMPERATURE K=	309.0000

TIME SEC.	PEAK HEIGHTS
300.0	360.00
400.0	245.00
500.0	167.50
600.0	115.00
700.0	82.00
800.0	65.00
1010.0	36.50
1100.0	30.00
1200.0	24.50
1300.0	20.70
1400.0	18.20
1500.0	16.50

REJECTED

800. 490.

CONSTANTS FOR LEAST SQUARES FIT OF DATA IN Y-C= A*EXP(-BT)

A = 1164.03903
B = 0.00406258
C = 15.53300405

SUMMATIONS FROM LEAST SQUARES CALCULATION

SEBT = 0.85436E 00
SYEBT = 0.19530E 03
SY = 0.11809E 04
STEBT = 0.41040E 03
STE2BT= 0.59025E 02
SE2BT = 0.15648E+00
ST2EBT= 0.23771E 06
ST2E2B= 0.24338E 05
SYT2EB= 0.32040E 08
SYTEBT= 0.75092E 05

DIFFUSIVITY= 0.71461010
LAMDA = 1.14747888
EFFECTIVE DIFFUSIVITY= 0.37159725
PUBLISHED DIFFUSIVITY= 0.82000000
ALPHA= 0.07522820 NUMBER ITERATIONS= 21

HYDROGEN-NITROGEN

BED DATA

BED DIAMETER CMS 5.05000
BED LENGTH CMS 10.05000
END ZONE HEIGHT 0.27000
POROSITY 0.52000

RUN DATA

FLOW RATE CC/SEC= 0.56248
ROOM TEMPERATURE= 295.0000
ATM.PRESSURE MM HG 749.8
BED TEMPERATURE K= 309.0000

TIME SEC.	PEAK HEIGHTS	REJECTED POINTS	
150.0	655.00		
200.0	530.00		
250.0	430.00		
300.0	350.00		
400.0	227.50		
700.0	80.00	450.	173.
800.0	58.00	500.	150.
900.0	43.00	600.	104.
1000.0	33.00		
1100.0	26.00		
1200.0	21.50		
1300.0	18.50		

CONSTANTS FOR LEAST SQUARES FIT OF DATA IN Y-C= A*EXP(-BT)

A = 1222.80475
B = 0.00434213
C = 16.91959119

SUMMATIONS FROM LEAST SQUARES CALCULATION

SEBT = 0.18540E 01
SYEBT = 0.85162E 03
SY = 0.24725E 04
STEBT = 0.50833E 03
STE2BT= 0.14210E 03
SE2BT = 0.67076E 00
ST2FBT= 0.19886E 06
ST2E2B= 0.34280E 05
SYT2EB= 0.45377E 08
SYTFBT= 0.18236E 06

DIFFUSIVITY= 0.87263739
LAMDA = 0.93968011
EFFECTIVE DIFFUSIVITY= 0.45377145
PUBLISHED DIFFUSIVITY= 0.82000000
ALPHA= 0.07060957 NUMBER ITERATIONS= 21

HYDROGEN-NITROGEN

BED DATA | RUN DATA

BED DIAMETER CMS 5.03000
BED LENGTH CMS 10.05000
END ZONE HEIGHT 0.27000
POROSITY 0.52000

FLOW RATE CC/SEC= 2.80719
ROOM TEMPERATURE= 295.0000
ATM.PRESSURE MM HG 759.3
BED TEMPERATURE K= 309.0000

TIME SEC.	PEAK HEIGHTS
100.0	33.50
150.0	19.50
200.0	12.00
250.0	7.50
300.0	5.00
350.0	3.50
400.0	3.00

REJECTED POINTS
50. 53.

CONSTANTS FOR LEAST SQUARES FIT OF DATA IN Y-C= A*EXP(-BT)

A = 100.16878
B = 0.01154364
C = 1.89351013

SUMMATIONS FROM LEAST SQUARES CALCULATION

SEBT = 0.70626E 00
SYEBT = 0.15872E 02
SY = 0.84000E 02
STEBT = 0.11141E 03
STE2BT= 0.17635E 02
SE2BT = 0.14510E-00
ST2EBT= 0.21194E 05
ST2E2B= 0.24305E 04
SYT2EB= 0.28352E 06
SYTEBT= 0.19974E 04

DIFFUSIVITY= 0.77602391
LAMDA = 1.05666029
EFFECTIVE DIFFUSIVITY= 0.40353556
PUBLISHED DIFFUSIVITY= 0.82000000
ALPHA= 0.12234301 NUMBER ITERATIONS= 18

NITROGEN-ETHANE

BED DATA

BED DIAMETER CMS 5.03000
BED LENGTH CMS 10.05000
END ZONE HEIGHT 0.27000
POROSITY 0.52000

RUN DATA

FLOW RATE CC/SEC= 0.48497
ROOM TEMPERATURE= 295.0000
ATM.PRESSURE MM HG 749.8
BED TEMPERATURE K= 309.0000

TIME SEC.	PEAK HEIGHTS
300.0	470.00
500.0	318.00
700.0	217.00
900.0	152.00
1050.0	116.00
1200.0	90.00
1350.0	72.50
1500.0	57.00
1650.0	45.50
1800.0	37.00
1950.0	31.00
2100.0	26.00
2300.0	21.50

CONSTANTS FOR LEAST SQUARES FIT OF DATA IN Y-C= A*EXP(-BT)

A = 827.88149
B = 0.00199940
C = 14.53532410

SUMMATIONS FROM LEAST SQUARES CALCULATION

SEBT = 0.17690E 01
SYEBT = 0.48771E 03
SY = 0.16535E 04
STEBT = 0.12777E 04
STE2BT= 0.26591E 03
SE2BT = 0.55805E 00
ST2EBT= 0.12824E 07
ST2E2B= 0.16443E 06
SYT2EB= 0.15489E 09
SYTEBT= 0.23872E 06

DIFFUSIVITY= 0.13564177
LAMDA = 1.11322641
EFFECTIVE DIFFUSIVITY= 0.07054372
PUBLISHED DIFFUSIVITY= 0.15100000
ALPHA= 0.12223252 NUMBER ITERATIONS= 18

NITROGEN-ETHANE

BED DATA

BED DIAMETER CMS 5.03000
BED LENGTH CMS 10.05000
END ZONE HEIGHT 0.27000
POROSITY 0.52000

RUN DATA

FLOW RATE CC/SEC= 1.46170
ROOM TEMPERATURE= 295.0000
ATM.PRESSURE MM HG 755.3
BED TEMPERATURE K= 309.0000

TIME SEC.	PEAK HEIGHTS
200.0	230.00
400.0	130.00
600.0	76.00
700.0	59.00
800.0	46.00
1000.0	28.00
1200.0	19.00

CONSTANTS FOR LEAST SQUARES FIT OF DATA IN Y-C= A*EXP(-BT)

A = 400.67521
B = 0.00294594
C = 7.47580498

SUMMATIONS FROM LEAST SQUARES CALCULATION

SEBT = 0.13359E 01
SYEBT = 0.17447E 03
SY = 0.58830E 03
STEBT = 0.58886E 03
STE2BT= 0.13972E 03
SE2BT = 0.46042E-00
ST2EBT= 0.35038E 06
ST2E2B= 0.55617E 05
SYT2EB= 0.24912E 08
SYTEBT= 0.60145E 05

DIFFUSIVITY= 0.14782405
LAMDA = 1.02148467
EFFECTIVE DIFFUSIVITY= 0.07686850
PUBLISHED DIFFUSIVITY= 0.15100000
ALPHA= 0.14160762 NUMBER ITERATIONS= 12

NITROGEN-ETHANE

BED DATA

BED DIAMETER CMS 5.03000
BED LENGTH CMS 10.05000
END ZONE HEIGHT 0.27000
POROSITY 0.52000

RUN DATA

FLOW RATE CC/SEC= 2.26669
ROOM TEMPERATURE= 296.5000
ATM.PRESSURE MM HG 755.1
BED TEMPERATURE K= 309.0000

TIME SEC.	PEAK HEIGHTS
200.0	150.00
300.0	111.00
400.0	84.00
500.0	62.50
600.0	46.50
700.0	35.50

CONSTANTS FOR LEAST SQUARES FIT OF DATA IN Y-C= A*EXP(-BT)

A = 268.37303
b = 0.00299714
C = 2.44440460

SUMMATIONS FROM LEAST SQUARES CALCULATION

SEBT = 0.17693E 01
SYEBT = 0.17889E 03
SY = 0.48950E 03
STEBT = 0.64948E 03
STE2BT= 0.19830E 03
SE2BT = 0.65044E 00
ST2EBT= 0.28243E 06
ST2E2B= 0.71241E 05
SYT2EB= 0.19810E 08
SYTEBT= 0.54807E 05

DIFFUSIVITY= 0.13953946
LAMDA = 1.08213115
EFFECTIVE DIFFUSIVITY= 0.07256052
PUBLISHED DIFFUSIVITY= 0.15100000
ALPHA= 0.14701164 NUMBER ITERATIONS= 11

NITROGEN-ETHANE

BED DATA

BED DIAMETER CMS 5.03000
BED LENGTH CMS 10.05000
END ZONE HEIGHT 0.27000
POROSITY 0.52000

RUN DATA

FLOW RATE CC/SEC= 2.94336
ROOM TEMPERATURE= 295.0000
ATM.PRESSURE MM HG 752.6
BED TEMPERATURE K= 309.0000

TIME SEC.	PEAK HEIGHTS
200.0	124.00
300.0	88.00
400.0	65.00
500.0	47.50
600.0	35.50
700.0	27.00
800.0	21.50
900.0	17.50
1100.0	12.00

CONSTANTS FOR LEAST SQUARES FIT OF DATA IN Y-C= A*EXP(-BT)

A = 236.84694
B = 0.00356950
C = 7.68526965

SUMMATIONS FROM LEAST SQUARES CALCULATION

SEBT = 0.15573E 01
SYEBT = 0.12301E 03
SY = 0.43800E 03
STEBT = 0.61256E 03
STE2BT= 0.13784E 03
SE2BT = 0.46895E-00
ST2EBT= 0.30660E 06
ST2E2B= 0.48597E 05
SYT2EB= 0.13858E 08
SYTEBT= 0.37354E 05

DIFFUSIVITY= 0.16494461
LAMDA = 0.91545884
EFFECTIVE DIFFUSIVITY= 0.08577120
PUBLISHED DIFFUSIVITY= 0.15100000
ALPHA= 0.14782880 NUMBER ITERATIONS= 10

NITROGEN-ETHANE

BED DATA | RUN DATA

BED DIAMETER CMS 5.03000
BED LENGTH CMS 10.05000
END ZONE HEIGHT 0.27000
POROSITY 0.52000

FLOW RATE CC/SEC= 3.07933
ROOM TEMPERATURE= 295.0000
ATM.PRESSURE MM HG 756.0
BED TEMPERATURE K= 309.0000

TIME SEC.	PEAK HEIGHTS
200.0	115.00
300.0	89.00
400.0	67.00
500.0	52.00
600.0	42.00
700.0	34.00
800.0	29.00
900.0	25.00
1000.0	22.50
1100.0	20.50

100 165

CONSTANTS FOR LEAST SQUARES FIT OF DATA IN Y-C= A*EXP(-BT)

A = 194.37181
B = 0.00328754
C = 14.99706340

SUMMATIONS FROM LEAST SQUARES CALCULATION

SEBT = 0.17802E 01
SYEBT = 0.13444E 03
SY = 0.49600E 03
STEBT = 0.74435E 03
STE2BT= 0.17032E 03
SE2BT = 0.55637E 00
ST2EBT= 0.40273E 06
ST2E2B= 0.63779E 05
SYT2EB= 0.18428E 08
SYTEBT= 0.44269E 05

DIFFUSIVITY= 0.14867555
LAMDA = 1.01563447
EFFECTIVE DIFFUSIVITY= 0.07731129
PUBLISHED DIFFUSIVITY= 0.15100000
ALPHA= 0.14886776 NUMBER ITERATIONS= 10

NITROGEN-ETHANE

BED DATA

BED DIAMETER CMS 5.03000
BED LENGTH CMS 10.03000
END ZONE HEIGHT 0.27000
POROSITY 0.52000

RUN DATA

FLOW RATE CC/SEC= 4.55644
ROOM TEMPERATURE= 295.0000
ATM.PRESSURE MM HG 755.6
BED TEMPERATURE K= 309.0000

TIME SEC.	PEAK HEIGHTS
200.0	78.00
300.0	52.00
400.0	39.00
500.0	28.00
600.0	20.50
700.0	15.50
800.0	12.00

100 118

CONSTANTS FOR LEAST SQUARES FIT OF DATA IN Y-C= A*EXP(-BT)

A = 158.99557
B = 0.00399948
C = 5.92013363

SUMMATIONS FROM LEAST SQUARES CALCULATION

SEBT = 0.12803E 01
SYEBT = 0.65674E 02
SY = 0.24500E 03
STEBT = 0.45836E 03
STE2BT= 0.10195E 03
SE2BT = 0.36539E-00
ST2EBT= 0.19981E 06
ST2E2B= 0.33193E 05
SYT2SB= 0.64644E 07
SYTEBT= 0.18923E 05

DIFFUSIVITY= 0.17814471
LAMDA = 0.34762549
EFFECTIVE DIFFUSIVITY= 0.09263525
PUBLISHED DIFFUSIVITY= 0.15100000
ALPHA= 0.15027141 NUMBER ITERATIONS= 9

NITROGEN-BUTANE

BED DATA | RUN DATA

BED DIAMETER CMS 5.03000
BED LENGTH CMS 10.05000
END ZONE HEIGHT 0.27000
POROSITY 0.52000

FLOW RATE CC/SEC= 0.46141
ROOM TEMPERATURE= 296.0000
ATM.PRESSURE MM HG 761.0
BED TEMPERATURE K= 309.0000

TIME SEC.	PEAK HEIGHTS
300.0	510.00
400.0	440.00
500.0	380.00
600.0	325.00
700.0	285.00
800.0	250.00
900.0	215.00
1000.0	190.00
1200.0	142.00
1400.0	108.00
1600.0	82.00
1800.0	61.00
2000.0	45.00
2200.0	34.00
2400.0	26.00
2600.0	19.00

CONSTANTS FOR LEAST SAUARES FIT OF DATA IN Y-C= A*EXP(-BT)

A = 776.69521
B = 0.00143133
C = 1.50567818

SUMMATIONS FROM LEAST SQUARES CALCULATION

SEBT = 0.39757E 01
SYEBT = 0.12508E 04
SY = 0.31120E 04
STEBT = 0.29702E 04
STE2BT= 0.88801E 03
SE2BT = 0.16027E 01
ST2EBT= 0.30831E 07
ST2E2B= 0.62188E 06
SYT2EB= 0.48802E 09
SYTEBT= 0.69419E 06

DIFFUSIVITY= 0.08172526
LAMDA = 1.16243123
EFFECTIVE DIFFUSIVITY= 0.04249714
PUBLISHED DIFFUSIVITY= 0.09500000
ALPHA= 0.13225333 NUMBER ITERATIONS= 15

NITROGEN-BUTANE

BED DATA		RUN DATA	
BED DIAMETER CMS	5.03000	FLOW RATE CC/SEC=	0.90299
BED LENGTH CMS	10.05000	ROOM TEMPERATURE=	296.0000
END ZONE HEIGHT	0.27000	ATM.PRESSURE MM HG	761.0
POROSITY 0.52000		BED TEMPERATURE K=	309.0000

TIME SEC.	PEAK HEIGHTS
300.0	285.00
400.0	240.00
500.0	205.00
600.0	174.00
700.0	148.00
800.0	126.00
900.0	104.00
1000.0	90.00
1100.0	76.00
1200.0	63.00
1400.0	46.00
1600.0	33.00
1800.0	23.00

CONSTANTS FOR LEAST SAUARES FIT OF DATA IN Y-C= A*EXP(-BT)

A = 466.99112
B = 0.00163191
C = -1.74857622

SUMMATIONS FROM LEAST SQUARES CALCULATION

SEBT = 0.35027E 01
SYEBT = 0.60839E 03
SY = 0.16130E 04
STEBT = 0.23890E 04
STE2BT= 0.70196E 03
SE2BT = 0.13159E 01
ST2EBT= 0.20596E 07
ST2E2B= 0.46022E 06
SYT2EB= 0.21130E 09
SYTEBT= 0.32363E 06

DIFFUSIVITY= 0.07939063
LAMDA = 1.19661468
EFFECTIVE DIFFUSIVITY= 0.04128313
PUBLISHED DIFFUSIVITY= 0.09500000
ALPHA= 0.14327731 NUMBER ITERATIONS= 12

NITROGEN-BUTANE

BED DATA | RUN DATA

BED DIAMETER CMS 5.03000
BED LENGTH CMS 10.05000
END ZONE HEIGHT 0.27000
POROSITY 0.52000

FLOW RATE CC/SEC= 2.04608
ROOM TEMPERATURE= 296.0000
ATM.PRESSURE MM HG 761.0
BED TEMPERATURE K= 309.0000

TIME SEC.	PEAK HEIGHTS
300.0	138.00
400.0	110.00
500.0	92.00
600.0	76.00
700.0	61.00
800.0	51.00
900.0	42.00
1000.0	34.00
1150.0	25.00

CONSTANTS FOR LEAST SQUARES FIT OF DATA IN Y-C= A*EXP(-BT)

A = 249.21826
B = 0.00202606
C = 1.23396216

SUMMATIONS FROM LEAST SQUARES CALCULATION

SEBT = 0.24793E 01
SYEBT = 0.21855E 03
SY = 0.62900E 03
STEBT = 0.14174E 04
STE2BT= 0.41079E 03
SE2BT = 0.86468E 00
ST2EBT= 0.95420E 06
ST2E2B= 0.22771E 06
SYT2EB= 0.57938E 08
SYTEBT= 0.10412E 06

DIFFUSIVITY= 0.09057913
LAMDA = 1.01568647
EFFECTIVE DIFFUSIVITY= 0.04710115
PUBLISHED DIFFUSIVITY= 0.09200000
ALPHA= 0.14946068 NUMBER ITERATIONS= 10

END-OF-DATA ENCOUNTERED ON SYSTEM INPUT FILE.

TIME 17HRS 01MIN 25.3SEC

POROUS SOLID BED

HYDROGEN-NITROGEN

BED DATA		RUN DATA	
BED DIAMETER CMS	2.61000	FLOW RATE CC/SEC=	0.56238
BED LENGTH CMS	7.00000	ROOM TEMPERATURE=	296.0000
END ZONE HEIGHT	0.27000	ATM.PRESSURE MM HG	765.1
POROSITY	0.59000	BED TEMPERATURE K=	306.0000

TIME SEC.	PEAK HEIGHTS
150.0	123.00
200.0	61.00
250.0	34.00
300.0	18.00
350.0	10.00
400.0	6.20
450.0	4.50
500.0	3.20

CONSTANTS FOR LEAST SQUARES FIT OF DATA IN Y-C= A*EXP(-BT)

A = 961.06734
B = 0.01387832
C = 2.63458395

SUMMATIONS FROM LEAST SQUARES CALCULATION

SEBT = 0.24827E-00
SYEBT = 0.20592E 02
SY = 0.25990E 03
STEBT = 0.49247E 02
STE2BT= 0.34536E 01
SE2BT = 0.20727E-01
ST2EBT= 0.10852E 05
ST2E2B= 0.59838E 03
SYT2EB= 0.60443E 06
SYTEBT= 0.34520E 04

DIFFUSIVITY= 0.56476959
LAMDA = 1.45191953
EFFECTIVE DIFFUSIVITY= 0.33321406
PUBLISHED DIFFUSIVITY= 0.82000000
ALPHA= 0.15623251 NUMBER ITERATIONS= 21

HYDROGEN-NITROGEN

BED DATA

BED DIAMETER CMS 2.61000
BED LENGTH CMS 7.00000
END ZONE HEIGHT 0.27000
POROSITY 0.59000

RUN DATA

FLOW RATE CC/SEC= 0.79291
ROOM TEMPERATURE= 296.0000
ATM.PRESSURE MM HG 765.1
BED TEMPERATURE K= 306.0000

TIME SEC.	PEAK HEIGHTS
150.0	66.50
200.0	29.00
250.0	13.50
300.0	6.50
350.0	3.50
400.0	2.20

CONSTANTS FOR LEAST SQUARES FIT OF DATA IN Y-C= A*EXP(-BT)

A = 832.02716
B = 0.01698613
C = 1.35669661

SUMMATIONS FROM LEAST SQUARES CALCULATION

SEBT = 0.13588E-00
SYEBT = 0.64184E 01
SY = 0.12120E 03
STEBT = 0.25209E 02
STE2BT= 0.12077E 01
SE2BT = 0.74926E-02
ST2EBT= 0.50447E 04
ST2E2B= 0.19977E 03
SYT2EB= 0.17307E 06
SYTEBT= 0.10390E 04

DIFFUSIVITY= 0.59620015
LAMDA = 1.37537704
EFFECTIVE DIFFUSIVITY= 0.35175809
PUBLISHED DIFFUSIVITY= 0.82000000
ALPHA= 0.16822422 NUMBER ITERATIONS= 20

HYDROGEN-NITROGEN

BED DATA		RUN DATA	
BED DIAMETER CMS	2.61000	FLOW RATE CC/SEC=	0.92834
BED LENGTH CMS	7.00000	ROOM TEMPERATURE=	296.0000
END ZONE HEIGHT	0.27000	ATM.PRESSURE MM HG	765.1
POROSITY 0.59000		BED TEMPERATURE K= 306.0000	

TIME SEC.	PEAK HEIGHTS
100.0	124.00
150.0	54.00
200.0	23.00
250.0	10.00
300.0	5.00
350.0	3.00
400.0	2.00

CONSTANTS FOR LEAST SQUARES FIT OF DATA IN Y-C= A*EXP(-BT)

A = 673.31601
B = 0.01706416
C = 1.00377709

SUMMATIONS FROM LEAST SQUARES CALCULATION

SEBT = 0.31545E-00
SYEBT = 0.27622E 02
SY = 0.22100E 03
STEBT = 0.42971E 02
STE2BT= 0.44717E 01
SE2BT = 0.40254E-01
ST2EBT= 0.67745E 04
ST2E2B= 0.52398E 03
SYT2EB= 0.36210E 06
SYTEBT= 0.30764E 04

DIFFUSIVITY= 0.53309685
LAMDA = 1.53818204
EFFECTIVE DIFFUSIVITY= 0.31452714
PUBLISHED DIFFUSIVITY= 0.82000000
ALPHA= 0.17831466 NUMBER ITERATIONS= 18

HYDROGEN-NITROGEN

BED DATA		RUN DATA	
BED DIAMETER CMS	2.61000	FLOW RATE CC/SEC=	1.24571
BED LENGTH CMS	7.00000	ROOM TEMPERATURE=	296.0000
END ZONE HEIGHT	0.27000	ATM.PRESSURE MM HG	765.1
POROSITY 0.59000		BED TEMPERATURE K=	306.0000

TIME SEC.	PEAK HEIGHTS
100.0	71.00
150.0	26.00
200.0	10.50
250.0	4.50
300.0	2.20
350.0	1.10

CONSTANTS FOR LEAST SQUARES FIT OF DATA IN Y-C= A*EXP(-BT)

A = 474.73421
B = 0.01905806
C = 0.46243683

SUMMATIONS FROM LEAST SQUARES CALCULATION

SEBT = 0.24124E-00
SYEBT = 0.12443E 02
SY = 0.11730E 03
STCBT = 0.31456E 02
STE2BT= 0.28243E 01
SE2BT = 0.25975E-01
ST2EBT= 0.46459E 04
ST2E2B= 0.32038E 03
SYT2EB= 0.15421E 06
SYTEBT= 0.13553E 04

DIFFUSIVITY= 0.53771282
LAMDA = 1.52497758
EFFECTIVE DIFFUSIVITY= 0.31725056
PUBLISHED DIFFUSIVITY= 0.82000000
ALPHA= 0.18763416 NUMBER ITERATIONS= 16

HYDROGEN-NITROGEN

BED DATA

BED DIAMETER CMS 2.61000
BED LENGTH CMS 7.00000
END ZONE HEIGHT 0.27000
POROSITY 0.59000

RUN DATA

FLOW RATE CC/SEC= 1.83497
ROOM TEMPERATURE= 296.0000
ATM.PRESSURE MM HG 765.1
BED TEMPERATURE K= 306.0000

TIME SEC.	PEAK HEIGHTS
50.0	124.00
100.0	37.00
150.0	14.00
200.0	5.00
250.0	2.00

CONSTANTS FOR LEAST SQUARES FIT OF DATA IN Y-C= A*EXP(-BT)

A = 414.35182
B = 0.02445598
C = 1.89934120

SUMMATIONS FROM LEAST SQUARES CALCULATION

SEBT = 0.41632E-00
SYEBT = 0.40112E 02
SY = 0.18200E 03
STEBT = 0.29271E 02
STE2BT= 0.51951E 01
SE2BT = 0.94899E-01
ST2EBT= 0.26156E 04
ST2E2B= 0.30902E 03
SYT2EB= 0.13315E 06
SYTEBT= 0.22082E 04

DIFFUSIVITY= 0.65093117
LAMDA = 1.25973380
EFFECTIVE DIFFUSIVITY= 0.38404939
PUBLISHED DIFFUSIVITY= 0.82000000
ALPHA= 0.19318470 NUMBER ITERATIONS= 15

NITROGEN-ETHANE

BED DATA		RUN DATA	
BED DIAMETER CMS	2.61000	FLOW RATE CC/SEC=	0.39180
BED LENGTH CMS	7.00000	ROOM TEMPERATURE=	296.0000
END ZONE HEIGHT	0.27000	ATM.PRESSURE MM HG	766.9
POROSITY 0.59000		BED TEMPERATURE K=	306.0000

TIME SEC.	PEAK HEIGHTS
250.0	212.50
400.0	117.00
550.0	68.00
700.0	43.50
850.0	30.50
1000.0	24.50
1150.0	20.50

CONSTANTS FOR LEAST SQUARES FIT OF DATA IN Y-C= A*EXP(-BT)

A = 598.64044
B = 0.00448394
C = 17.36491060

SUMMATIONS FROM LEAST SQUARES CALCULATION

SEBT = 0.65974E 00
SYEBT = 0.97459E 02
SY = 0.51650E 03
STEBT = 0.26179E 03
STE2BT= 0.43494E 02
SE2BT = 0.14366E-00
ST2EBT= 0.12880E 06
ST2E2B= 0.14695E 05
SYT2EB= 0.11034E 08
SYTEBT= 0.30583E 05

DIFFUSIVITY= 0.11308980
LAMDA = 1.33522204
EFFECTIVE DIFFUSIVITY= 0.06672298
PUBLISHED DIFFUSIVITY= 0.15100000
ALPHA= 0.19822370 NUMBER ITERATIONS= 14

NITROGEN-ETHANE

BED DATA

BED DIAMETER CMS 2.61000
BED LENGTH CMS 7.00000
END ZONE HEIGHT 0.27000
POROSITY 0.59000

RUN DATA

FLOW RATE CC/SEC= 0.82082
ROOM TEMPERATURE= 296.0000
ATM.PRESSURE MM HG 766.9
BED TEMPERATURE K= 306.0000

TIME SEC.	PEAK HEIGHTS
200.0	116.00
300.0	77.50
400.0	53.00
500.0	38.50
600.0	29.50
700.0	24.00
1200.0	16.00

CONSTANTS FOR LEAST SQUARES FIT OF DATA IN Y-C= A*EXP(-BT)

A = 267.69002
B = 0.00487665
C = 15.17382121

SUMMATIONS FROM LEAST SQUARES CALCULATION

SEBT = 0.92750E 00
SYEBT = 0.74999E 02
SY = 0.35450E 03
STEBT = 0.30406E 03
STE2BT= 0.58910E 02
SE2BT = 0.22760E-00
ST2EBT= 0.12007E 06
ST2E2B= 0.17230E 05
SYT2EB= 0.64333E 07
SYTEBT= 0.20383E 05

DIFFUSIVITY= 0.10786807
LAMDA = 1.39985816
EFFECTIVE DIFFUSIVITY= 0.06364216
PUBLISHED DIFFUSIVITY= 0.15100000
ALPHA= 0.21166635 NUMBER ITERATIONS= 11

NITROGEN-ETHANE

BED DATA

BED DIAMETER CMS 2.61000
BED LENGTH CMS 7.00000
END ZONE HEIGHT 0.27000
POROSITY 0.59000

RUN DATA

FLOW RATE CC/SEC= 1.32324
ROOM TEMPERATURE= 296.0000
ATM.PRESSURE MM HG 766.9
BED TEMPERATURE K= 306.0000

TIME SEC.	PEAK HEIGHTS
100.0	122.00
200.0	78.50
300.0	53.00
400.0	37.50
500.0	28.50
600.0	23.50

CONSTANTS FOR LEAST SQUARES FIT OF DATA IN Y-C= A*EXP(-BT)

A = 179.89097
B = 0.00525755
C = 15.67274153

SUMMATIONS FROM LEAST SQUARES CALCULATION

SEBT = 0.13840E 01
SYEBT = 0.11813E 03
SY = 0.34300E 03
STEBT = 0.30147E 03
STE2BT= 0.81814E 02
SE2BT = 0.53609E 00
ST2EBT= 0.91409E 05
ST2E2B= 0.16559E 05
SYT2EB= 0.44111E 07
SYTEBT= 0.19442E 05

DIFFUSIVITY= 0.11160270
LAMDA = 1.35301381
EFFECTIVE DIFFUSIVITY= 0.06584559
PUBLISHED DIFFUSIVITY= 0.15100000
ALPHA= 0.21606873 NUMBER ITERATIONS= 10

NITROGEN-ETHANE

BED DATA		RUN DATA	
BED DIAMETER CMS	2.61000	FLOW RATE CC/SEC=	1.90216
BED LENGTH CMS	7.00000	ROOM TEMPERATURE=	296.0000
END ZONE HEIGHT	0.27000	ATM.PRESSURE MM HG	766.9
POROSITY 0.59000		BED TEMPERATURE K=	306.0000

TIME SEC.	PEAK HEIGHTS
100.0	87.50
200.0	58.00
300.0	40.50
400.0	30.00
500.0	24.20
600.0	20.50
700.0	18.00

CONSTANTS FOR LEAST SQUARES FIT OF DATA IN Y-C= A*EXP(-BT)

A = 122.18379
B = 0.00522691
C = 15.04567635

SUMMATIONS FROM LEAST SQUARES CALCULATION

SEBT = 0.14190E 01
SYEBT = 0.87549E 02
SY = 0.27870E 03
STEBT = 0.32232E 03
STE2BT= 0.83302E 02
SE2BT = 0.54180E 00
ST2EBT= 0.10511E 06
ST2E2B= 0.17161E 05
SYT2EB= 0.36787E 07
SYTEBT= 0.15028E 05

DIFFUSIVITY= 0.10828433
LAMDA = 1.39447691
EFFECTIVE DIFFUSIVITY= 0.06388776
PUBLISHED DIFFUSIVITY= 0.15100000
ALPHA= 0.21871432 NUMBER ITERATIONS= 8

NITROGEN-BUTANE

BED DATA		RUN DATA	
BED DIAMETER CMS	2.61000	FLOW RATE CC/SEC=	0.59443
BED LENGTH CMS	7.00000	ROOM TEMPERATURE=	296.0000
END ZONE HEIGHT	0.27000	ATM.PRESSURE MM HG	761.4
POROSITY 0.59000		BED TEMPERATURE K=	306.0000

TIME SEC.	PEAK HEIGHTS
600.0	58.20
700.0	42.00
800.0	30.50
900.0	22.00
1000.0	16.00
1100.0	12.00
1200.0	9.00

CONSTANTS FOR LEAST SQUARES FIT OF DATA IN Y-C= A*EXP(-BT)

A = 429.92207
B = 0.00337326
C = 1.43004961

SUMMATIONS FROM LEAST SQUARES CALCULATION

SEBT = 0.41796E-00
SYEBT = 0.15759E 02
SY = 0.18970E 03
STEBT = 0.32449E 03
STE2BT= 0.24598E 02
SE2BT = 0.35265E-01
ST2EBT= 0.26477E 06
ST2E2B= 0.17748E 05
SYT2EB= 0.80036E 07
SYTEBT= 0.11039E 05

DIFFUSIVITY= 0.07472375
LAMDA = 1.32487999
EFFECTIVE DIFFUSIVITY= 0.04408701
PUBLISHED DIFFUSIVITY= 0.09900000
ALPHA= 0.21227366 NUMBER ITERATIONS= 11

NITROGEN-BUTANE

BED DATA

BED DIAMETER CMS 2.61000
BED LENGTH CMS 7.00000
END ZONE HEIGHT 0.27000
POROSITY 0.59000

RUN DATA

FLOW RATE CC/SEC= 1.14750
ROOM TEMPERATURE= 296.0000
ATM.PRESSURE MM HG 761.4
BED TEMPERATURE K= 306.0000

TIME SEC.	PEAK HEIGHTS
500.0	30.50
600.0	21.00
700.0	15.00
800.0	10.50
900.0	7.50
1000.0	5.50

CONSTANTS FOR LEAST SQUARES FIT OF DATA IN Y-C= A*EXP(-BT)

A = 196.21128
B = 0.00380157
C = 1.12496328

SUMMATIONS FROM LEAST SQUARES CALCULATION

SEBT = 0.42479E-00
SYEBT = 0.86218E 01
SY = 0.90000E 02
STEBT = 0.27490E 03
STE2BT= 0.24136E 02
SE2BT = 0.41500E-01
ST2EBT= 0.18776E 06
ST2E2B= 0.14555E 05
SYT2EB= 0.30630E 07
SYTEBT= 0.50450E 04

DIFFUSIVITY= 0.08021061
LAMDA = 1.23425071
EFFECTIVE DIFFUSIVITY= 0.04732426
PUBLISHED DIFFUSIVITY= 0.09900000
ALPHA= 0.21750321 NUMBER ITERATIONS= 9

NITROGEN-BUTANE

BED DATA

BED DIAMETER CMS 2.61000
BED LENGTH CMS 7.00000
END ZONE HEIGHT 0.27000
POROSITY 0.59000

RUN DATA

FLOW RATE CC/SEC= 2.06757
ROOM TEMPERATURE= 296.0000
ATM.PRESSURE MM HG 761.4
BED TEMPERATURE K= 306.0000

TIME SEC.	PEAK HEIGHTS
300.0	33.00
350.0	27.60
400.0	23.00
450.0	19.50
500.0	16.00

CONSTANTS FOR LEAST SQUARES FIT OF DATA IN Y-C= A*EXP(-BT)

A = 100.53757
B = 0.00400643
C = 2.63222942

SUMMATIONS FROM LEAST SQUARES CALCULATION

SEBT = 0.10478E 01
SYEBT = 0.26568E 02
SY = 0.11850E 03
STEBT = 0.39847E 03
STE2BT= 0.85844E 02
SE2BT = 0.23682E-00
ST2EBT= 0.15652E 06
ST2E2B= 0.32038E 05
SYT2EB= 0.36381E 07
SYTEBT= 0.96794E 04

DIFFUSIVITY= 0.08230689
LAMDA = 1.20281547
EFFECTIVE DIFFUSIVITY= 0.04856106
PUBLISHED DIFFUSIVITY= 0.09900000
ALPHA= 0.22042512 NUMBER ITERATIONS= 8

SPHERICAL PACKING BED

HYDROGEN-NITROGEN

BED DATA

BED DIAMETER CMS 2.61000
BED LENGTH CMS 7.00000
END ZONE HEIGHT 0.27000
POROSITY 0.39300

RUN DATA

FLOW RATE CC/SEC= 0.45564
ROOM TEMPERATURE= 295.0000
ATM.PRESSURE MM HG 742.5
BED TEMPERATURE K= 309.0000

TIME SEC.	PEAK HEIGHTS
50.0	460.00
100.0	207.50
150.0	95.00
200.0	50.50
250.0	28.00
300.0	18.00
350.0	13.00
400.0	11.00
450.0	10.00
500.0	9.00

CONSTANTS FOR LEAST SQUARES FIT OF DATA IN Y-C= A*EXP(-BT)

A = 1023.41085
B = 0.01643952
C = 9.95351410

SUMMATIONS FROM LEAST SQUARES CALCULATION

SEBT = 0.78411E 00
SYEBT = 0.25290E 03
SY = 0.90200E 03
STEBT = 0.69849E 02
STE2BT= 0.14842E 02
SE2BT = 0.23949E-00
ST2EBT= 0.89128E 04
ST2E2B= 0.10975E 04
SYT2EB= 0.12131E 07
SYTEBT= 0.15885E 05

DIFFUSIVITY= 0.68188812
LAMDA = 1.20254330
EFFECTIVE DIFFUSIVITY= 0.26798203
PUBLISHED DIFFUSIVITY= 0.82000000
ALPHA= 0.15708618 NUMBER ITERATIONS= 21

HYDROGEN-NITROGEN

BED DATA

BED DIAMETER CMS 2.61000
BED LENGTH CMS 7.00000
END ZONE HEIGHT 0.27000
POROSITY 0.39300

RUN DATA

FLOW RATE CC/SEC= 0.83168
ROOM TEMPERATURE= 295.0000
ATM.PRESSURE MM HG 742.5
BED TEMPERATURE K= 309.0000

TIME SEC.	PEAK HEIGHTS
50.0	229.00
100.0	80.00
150.0	31.40
200.0	16.00
250.0	9.50
300.0	6.80
350.0	5.80
400.0	5.00

CONSTANTS FOR LEAST SQUARES FIT OF DATA IN Y-C= A*EXP(-BT)

A = 664.12617
B = 0.02184377
C = 6.03381014

SUMMATIONS FROM LEAST SQUARES CALCULATION

SEBT = 0.50477E 00
SYEBT = 0.87271E 02
SY = 0.38350E 03
STEBT = 0.37948E 07
STE2BT= 0.71452E 01
SE2BT = 0.12682E-00
ST2EBT= 0.37986E 04
ST2E2B= 0.44788E 03
SYT2EB= 0.32075E 06
SYTEBT= 0.49743E 04

DIFFUSIVITY= 0.68711584
LAMDA = 1.19339411
EFFECTIVE DIFFUSIVITY= 0.27003652
PUBLISHED DIFFUSIVITY= 0.82000000
ALPHA= 0.18038791 NUMBER ITERATIONS= 17

HYDROGEN-NITROGEN

BED DATA		RUN DATA	
BED DIAMETER CMS	2.61000	FLOW RATE CC/SEC=	1.25171
BED LENGTH CMS	7.00000	ROOM TEMPERATURE=	295.0000
END ZONE HEIGHT	0.27000	ATM.PRESSURE MM HG	742.5
POROSITY 0.39300		BED TEMPERATURE K=	309.0000

TIME SEC.	PEAK HEIGHTS
50.0	122.25
100.0	38.00
150.0	15.00
200.0	6.80
250.0	4.10
300.0	3.20

CONSTANTS FOR LEAST SQUARES FIT OF DATA IN Y-C= A*EXP(-BT)

A = 399.98923.
B = 0.02479557
C = 3.44353834

SUMMATIONS FROM LEAST SQUARES CALCULATION

SEBT = 0.42173E-00
SYEBT = 0.40084E 02
SY = 0.18935E 03
STEBT = 0.29899E 07
STE2BT= 0.52955E 01
SE2BT = 0.96582E-01
ST2EBT= 0.27265E 04
ST2E2B= 0.31592E 03
SYT2EB= 0.13589E 06
SYTEBT= 0.22211E 04

DIFFUSIVITY= 0.66116180
LAMDA = 1.24024105
EFFECTIVE DIFFUSIVITY= 0.25983658
PUBLISHED DIFFUSIVITY= 0.82000000
ALPHA= 0.19394036 NUMBER ITERATIONS= 15

NITROGEN-ETHANE

BED DATA

BED DIAMETER CMS 2.61000
BED LENGTH CMS 7.00000
END ZONE HEIGHT 0.27000
POROSITY 0.39300

RUN DATA

FLOW RATE CC/SEC= 0.60438
ROOM TEMPERATURE= 295.0000
ATM.PRESSURE MM HG 755.5
BED TEMPERATURE K= 309.0000

TIME SEC.	PEAK HEIGHTS
150.0	131.00
300.0	68.00
450.0	40.50
600.0	27.00
700.0	22.50
800.0	20.00
900.0	18.50
1050.0	17.00

CONSTANTS FOR LEAST SQUARES FIT OF DATA IN Y-C= A*EXP(-BT)

A = 251.88520
B = 0.00524220
C = 16.16884971

SUMMATIONS FROM LEAST SQUARES CALCULATION

SEBT = 0.85416E 00
SYEBT = 0.79892E 07
SY = 0.34450E 03
STEBT = 0.24116E 03
STE2BT= 0.49298E 07
SE2BT = 0.26231E-00
ST2EBT= 0.97431E 05
ST2E2B= 0.11567E 05
SYT2EB= 0.44904E 07
SYTEBT= 0.16458E 05

DIFFUSIVITY= 0.11735015
LAMDA = 1.28674738
EFFECTIVE DIFFUSIVITY= 0.04611861
PUBLISHED DIFFUSIVITY= 0.15100000
ALPHA= 0.21198461 NUMBER ITERATIONS= 11

NITROGEN-ETHANE

BED DATA

BED DIAMETER CMS 2.61000
BED LENGTH CMS 7.00000
END ZONE HEIGHT 0.27000
POROSITY 0.39300

RUN DATA

FLOW RATE CC/SEC= 0.91862
ROOM TEMPERATURE= 295.0000
ATM.PRESSURE MM HG 755.5
BED TEMPERATURE K= 309.0000

TIME SEC.	PEAK HEIGHTS
200.0	66.00
300.0	45.50
400.0	32.50
500.0	25.00
600.0	20.50
700.0	18.00
800.0	16.50
900.0	15.80
1000.0	15.20

CONSTANTS FOR LEAST SQUARES FIT OF DATA IN Y-C= A*EXP(-BT)

A = 147.09993
B = 0.00520905
C = 14.26128089

SUMMATIONS FROM LEAST SQUARES CALCULATION

SEBT = 0.86097E 00
SYEBT = 0.40569E 02
SY = 0.25500E 03
STEBT = 0.29095E 03
STE2BT= 0.48934E 02
SE2BT = 0.19242E-00
ST2EBT= 0.12281E 06
ST2E2B= 0.14058E 05
SYT2EB= 0.38177E 07
SYTEBT= 0.11348E 05

DIFFUSIVITY= 0.11182137
LAMDA = 1.35036799
EFFECTIVE DIFFUSIVITY= 0.04394580
PUBLISHED DIFFUSIVITY= 0.15100000
ALPHA= 0.21647434 NUMBER ITERATIONS= 9

NITROGEN-ETHANE

BED DATA		RUN DATA	
BED DIAMETER CMS	2.61000	FLOW RATE CC/SEC=	1.36169
BED LENGTH CMS	7.00000	ROOM TEMPERATURE=	295.0000
END ZONE HEIGHT	0.27000	ATM.PRESSURE MM HG	755.5
POROSITY 0.39300		BED TEMPERATURE K=	309.0000

TIME SEC.	PEAK HEIGHTS
200.0	47.00
300.0	34.00
400.0	25.50
500.0	21.00
600.0	18.00
700.0	16.50
800.0	15.50
900.0	15.00

CONSTANTS FOR LEAST SQUARES FIT OF DATA IN Y-C= A*EXP(-BT)

A = 93.58899
B = 0.00520108
C = 14.02765203

SUMMATIONS FROM LEAST SQUARES CALCULATION

SEBT = 0.85778E 00
SYEBT = 0.30102E 02
SY = 0.19250E 03
STEBT = 0.28642E 03
STE2BT= 0.49129E 02
SE2BT = 0.19307E-00
ST2EBT= 0.11781E 06
ST2E2B= 0.14103E 05
SYT2EB= 0.29717E 07
SYTEBT= 0.86157E 04

DIFFUSIVITY= 0.10895333
LAMDA = 1.38591449
EFFECTIVE DIFFUSIVITY= 0.04281866
PUBLISHED DIFFUSIVITY= 0.15100000
ALPHA= 0.21913726 NUMBER ITERATIONS= 8

NITROGEN-BUTANE

BED DATA		RUN DATA	
BED DIAMETER CMS	2.61000	FLOW RATE CC/SEC=	0.59619
BED LENGTH CMS	7.00000	ROOM TEMPERATURE=	297.5000
END ZONE HEIGHT	0.27000	ATM.PRESSURE MM HG	746.8
POROSITY 0.39300		BED TEMPERATURE K=	309.0000

TIME SEC.	PEAK HEIGHTS
400.0	63.00
500.0	45.00
600.0	32.00
700.0	23.50
800.0	17.00
900.0	13.00
1000.0	10.00
1100.0	8.00

CONSTANTS FOR LEAST SQUARES FIT OF DATA IN Y-C= A*EXP(-BT)

A = 256.29736
B = 0.00363822
C = 3.26159501

SUMMATIONS FROM LEAST SQUARES CALCULATION

SEBT = 0.72341E 00
SYEBT = 0.29272E 02
SY = 0.21150E 03
STEBT = 0.42088E 03
STE2BT= 0.51564E 02
SE2BT = 0.10500E-00
ST2EBT= 0.27074E 06
ST2E2B= 0.27019E 05
SYT2EB= 0.78076E 07
SYTEBT= 0.14588E 05

DIFFUSIVITY= 0.07947453
LAMDA = 1.24568206
EFFECTIVE DIFFUSIVITY= 0.03123349
PUBLISHED DIFFUSIVITY= 0.09900000
ALPHA= 0.21584170 NUMBER ITERATIONS= 10

NITROGEN-BUTANE

BED DATA | RUN DATA

BED DIAMETER CMS 2.61000
BED LENGTH CMS 7.00000
END ZONE HEIGHT 0.27000
POROSITY 0.39300

FLOW RATE CC/SEC= 0.97945
ROOM TEMPERATURE= 297.5000
ATM.PRESSURE MM HG 746.8
BED TEMPERATURE K= 309.0000

TIME SEC.	PEAK HEIGHTS
300.0	55.00
400.0	38.00
500.0	27.50
600.0	20.00
700.0	14.20
800.0	10.70
900.0	8.00
1000.0	6.20

CONSTANTS FOR LEAST SQUARES FIT OF DATA IN Y-C= A*EXP(-BT)

A = 159.15279
B = 0.00370354
C = 2.38304090

SUMMATIONS FROM LEAST SQUARES CALCULATION

SEBT = 0.10087E 01
SYEBT = 0.35282E 02
SY = 0.17960E 03
STEBT = 0.48367E 03
STE2BT= 0.80358E 02
SE2BT = 0.20658E-00
ST2EBT= 0.26753E 06
ST2E2B= 0.34501E 05
SYT2EB= 0.61296E 07
SYTEBT= 0.13942E 05

DIFFUSIVITY= 0.07844734
LAMDA = 1.26199301
EFFECTIVE DIFFUSIVITY= 0.03082981
PUBLISHED DIFFUSIVITY= 0.09900000
ALPHA= 0.21919160 NUMBER ITERATIONS= 8

NITROGEN-BUTANE

BED DATA		RUN DATA	
BED DIAMETER CMS	2.01000	FLOW RATE CC/SEC=	1.23600
BED LENGTH CMS	7.00000	ROOM TEMPERATURE=	297.5000
END ZONE HEIGHT	0.27000	ATM.PRESSURE MM HG	746.8
POROSITY 0.39300		BED TEMPERATURE K=	309.0000

TIME SEC.	PEAK HEIGHTS
350.0	31.00
450.0	22.00
550.0	15.50
650.0	11.00
750.0	8.00
850.0	6.00
950.0	4.60
1050.0	3.50

CONSTANTS FOR LEAST SQUARES FIT OF DATA IN Y-C= A*EXP(-BT)

A = 108.61678
B = 0.00369706
C = 1.28090966

SUMMATIONS FROM LEAST SQUARES CALCULATION

SEBT = 0.84106E 00
SYEBT = 0.16659E 02
SY = 0.10160E 03
STEBT = 0.44553E 03
STE2BT= 0.63004E 02
SE2BT = 0.14346E-00
ST2EBT= 0.26574E 06
ST2E2B= 0.29929E 05
SYT2EB= 0.35909E 07
SYTEBT= 0.74140E 04

DIFFUSIVITY= 0.07752087
LAMDA = 1.27707544
EFFECTIVE DIFFUSIVITY= 0.03046570
PUBLISHED DIFFUSIVITY= 0.09900000
ALPHA= 0.22030460 NUMBER ITERATIONS= 8

TIME 20HRS 58MIN 39.55SEC